Photocatalytic Difluoromethylation and Light-Induced Iron Cross-Coupling in Flow

PROEFSCHRIFT

ter verkrijging van de graad van doctor aan de Technische

Universiteit Eindhoven, op gezag van de rector magnificus

prof.dr.ir. F.P.T. Baaijens, voor een commissie aangewezen door

het College voor Promoties, in het openbaar te verdedigen op

dinsdag 5 november 2019 om 11:00 uur

door

Xiao-Jing Wei

geboren te Henan, China

Dit proefschrift is goedgekeurd door de promotoren en de samenstelling van de promotiecommissie is als volgt:

voorzitter:	prof.dr.ir. J.A.M. Kuipers
promotor:	dr. T. Noël
copromotor(en):	prof.dr. F. Gallucci
leden:	prof.dr. R.P. Sijbesma
	prof.dr. A.J. Minnaard (University of Groningen)
	dr. J. Codée (Leiden University)
	prof.dr. F.P.J.T. Rutjes (Radboud University)
	prof.dr. H. Zuilhof (Wageningen University)

"It is during our darkest moments that we must focus to see the light."---Aristotle

Xiao-Jing Wei

Photocatalytic Difluoromethylation and Light-Induced Iron Cross-Coupling in Flow

Eindhoven University of Technology, 2019

Table of contents

Chapter 1

Introduction to Photocatalytic Difluoromethylation and Iron induced Kumada Cross-Coupling in Continuous Flow

1.1 Photoredox catalysis in Continuous flow

1.1.1 The renaissance of visible light photocatalysis

The area of radical chemistry has been flourished in recent decades and various reaction conditions have been discovered. The traditional method to produce radical intermediates often involves the use of stoichiometric amount of toxic reagents (e.g. Bu_3SnH) at high temperature or using $(Bu_3Sn)_2$ in combination with UV irradiation.[1] The use of such harsh reaction conditions always leads to pollution of the environment and undesired side reactions. On the pursuit of a more sustainable approach to generate radicals, visible light photocatalysis has attracted a lot of attention, as it features with mild reaction conditions (room temperature, avoidance of toxic redox reagents, and selective activation of the photocatalyst with visible light) and great functional group tolerance. Moreover, as visible light is abundantly available in the solar spectrum, solar energy can be used as well to drive photocatalytic reactions forward.[2]

Traditional approaches to radical intermediates
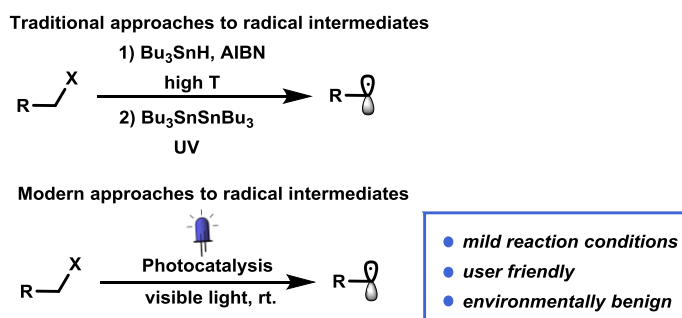
Scheme 1. 1: Traditional and modern approach to radical intermediate

Since the first application of visible light photocatalysis in organic synthesis in 1978 by Kellogg and coworkers,[3] this field has not received enough attention. This changed completely when Macmillan and Nicewicz reported the direct asymmetric alkylation of aldehydes using a combination of organocatalysis and photoredox catalysis in 2008.[4] After that, an exponential growth in research was witnessed within this field allowing the traditional domain of radical processes to be extended.[5] After the seminal work of Macmillan,[4] photo [2 + 2] cycloaddition[6] and dehalogenation reactions[7] were developed subsequently by the Yoon, and Stephenson groups. A lot of catalytic pathways such as decarboxylation,[8] radical C-H functionalization of aromatic compounds,[9] fluoroalkylation reactions[5c] and so on, were shown to proceed through visible light photocatalysis. Moreover, visible light photoredox catalysis has also been used in the total synthesis of complex natural products,[10] serving as an efficient strategy to access structurally complex molecules.

As most organic molecules are transparent for visible light (390-700 nm), visible light can only be harnessed by the transition metal or organic photocatalyst. This feature cannot be underestimated as it minimizes the amount of byproducts formed through overirradiation. Some of the most commonly used photocatalysts in synthetic chemistry are shown in **Scheme 1.2**. The photocatalysts are mainly dominated by highly conjugated systems, which include transition metal complexes with diverse ligands that can tune the properties of the catalyst, functionalized organic dyes and inorganic clusters.

Ru(bpy)₃²⁺   *fac*-Ir(ppy)₃   **Ru(bpz)₃²⁺**

R = H, Fluorescein, R = Br, Eosin Y   **Methylene Blue**   **Rodamine B**

Rose Bengal(RB)   **Acr-Me⁺ (R = H, Ph, mesityl)**   **TBADT**
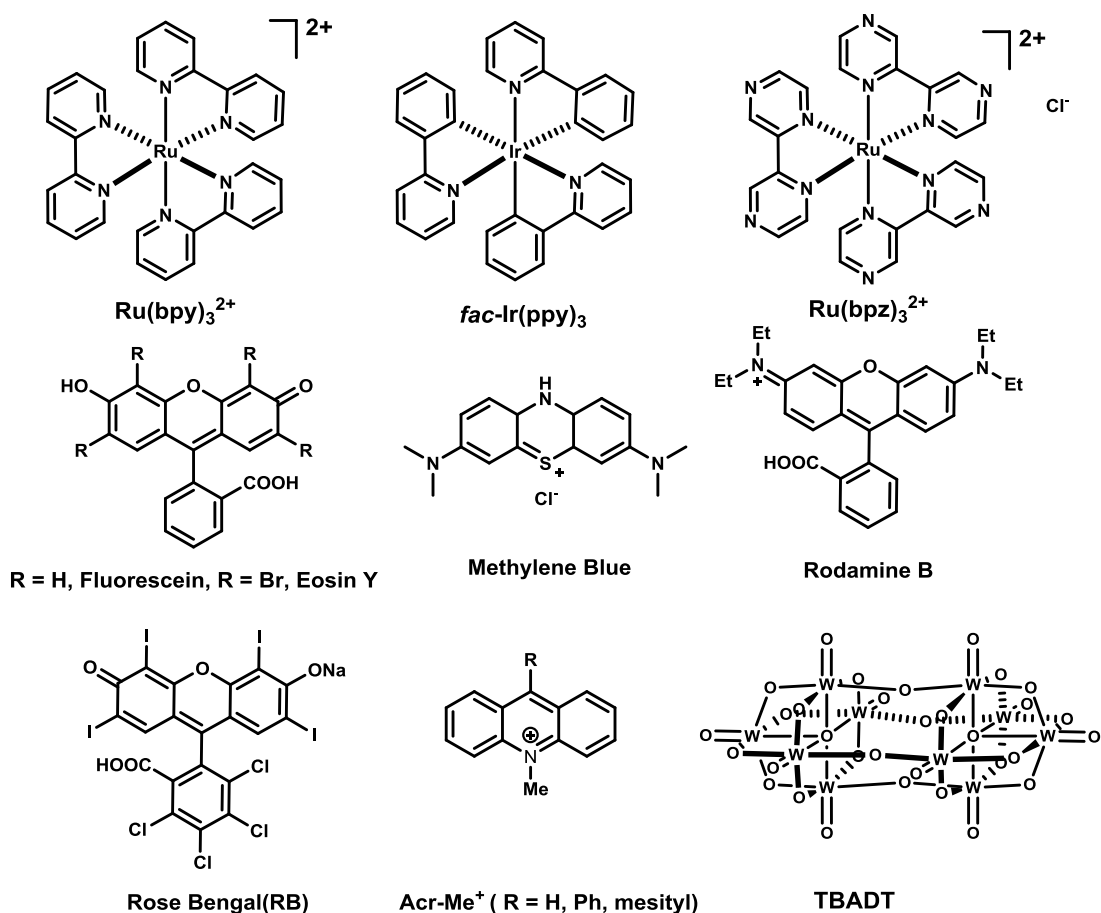
Scheme 1. 2: Examples of commonly used photocatalysts

In the mechanisms, the photocatalysts absorb photons and convert the energy of the photon to chemical potential which can be used in the transformation of the substrates. The interaction between the excited photocatalyst and the substrate could lead to the generation of a different array of reactive intermediates, by which the photocatalysis can be divided into three types: electron transfer, hydrogen atom abstraction and energy transfer, the details are shown in **Scheme 1. 3**:

Mechanisms of homogeneous photocatalysis

i): Electron Transfer

$$[PC^n]^* + sub \longrightarrow PC^{n-1} + sub^{\cdot+}$$

$$[PC^n]^* + sub \longrightarrow PC^{n+1} + sub^{\cdot-}$$

ii): Atom Abstraction

$$[PC]^* + sub\text{-}H \longrightarrow PC\text{-}H + sub^*$$
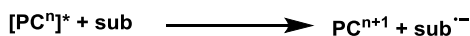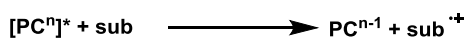
iii): Energy Transfer

$$[PC]^* + sub \longrightarrow PC + sub^*$$

Scheme 1. 3: Three reaction types using visible light photocatalysis

1.1.1.1 Electron transfer (photoredox catalysis)

Much of the recent interest in photocatalysis was focused on photoexcited molecules to participate in electron transfer process (photoredox catalysis). Upon excitation, the photocatalyst can be excited with visible light, producing a stable, long-living photoexcited species $[PC^n]^*$, which can engage in electron transfer process with the substrates. The photo-excited molecule is both a stronger reductant and oxidant compared to the ground state molecule. Thus, this class of photoredox reactions can be involved in single electron oxidation or single electron reduction transformations. The resulting reactive radical ion species, e.g. $A^{\cdot-}$ or $D^{+\cdot}$, can subsequently react further in diverse bond forming reactions. The general photoredox processes are shown in **Scheme 1. 4**:
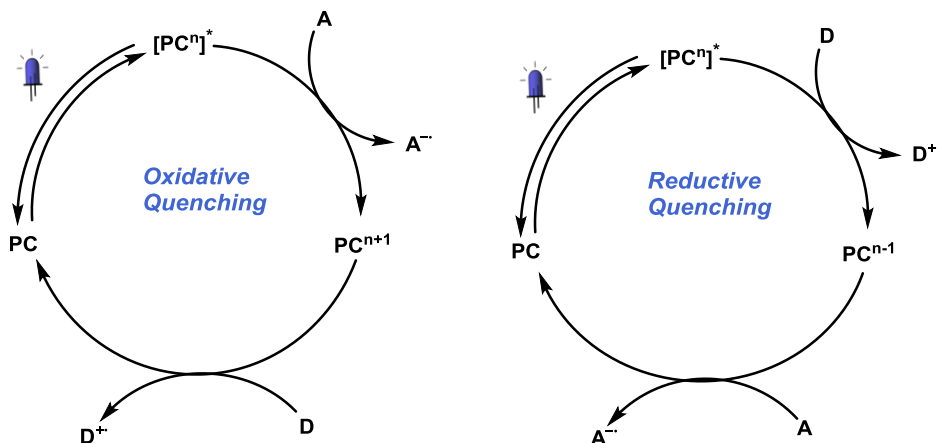
Scheme 1. 4: General mechanism cycle of photoredox catalysis

To verify whether the reaction is proceeding through an oxidative quenching or reductive quenching process, the Stern-Volmer quenching experiment is often employed.[11] This experiment examines the competing two deactivation pathways, quenching via electron transfer or emission. The $I_0/I = 1 + k_q\tau_0[Q]$ is used to explain the relationship between the quencher concentration and emission intensity, the I_0 and I are the emission intensity in the absences and presence of a quencher, k_q is the quenching rate constant, τ_0 is the excited-state lifetime of the photocatalyst, and $[Q]$ is the concentration of quencher. K_{SV} is introduced as Stern-Volmer constant, equal to $k_q\tau_0$, which was shown in the plot of the relationship between I_0/I and the concentration of the quencher $[Q]$.

In 2008, Macmillan and Nicewicz developed a protocol to achieve the asymmetric catalytic α-alkylation of aldehydes via a dual photocatalytic/organocatalytic protocol. The alkyl radicals generated via SET reduction from the corresponding halides coupled in an enantioselective manner with intermediate enamines. Yoon and co-workers reported the intramolecular [2+2] enone cycloaddition reaction by photocatalysis, in this work, Lewis acid was employed to improve the reactivity of the enone substrates.[12] In 2009, the Stephenson group reported the reductive dehalogenation of benzylic and α-acyl halides under a mild reaction condition[13] (**Scheme 1. 5**). These early reports showed the potential of photoredox catalysis in the development of organic reactions, since then, a diverse of Ir and Ru polypyridyl complexes and organic dyes were found to be used as photocatalyst.

Macmillan, 2008, asymmetric catalytic alkylation of aldehyde
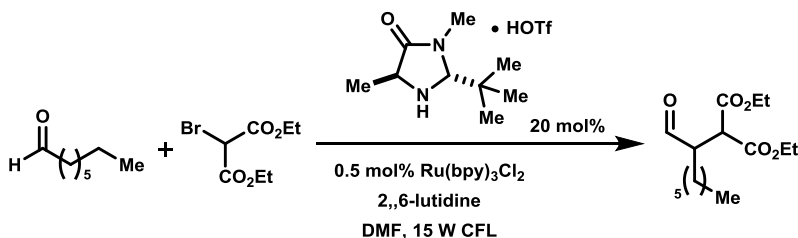
Yoon, 2008, [2+2] photocycloadditions reaction
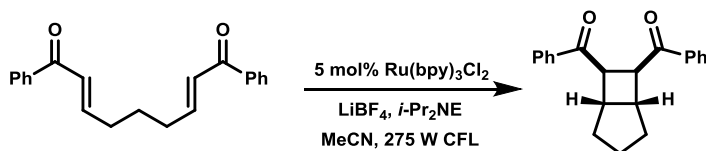
Stephenson, 2009, reductive dehalogenation of activated alkyl halide
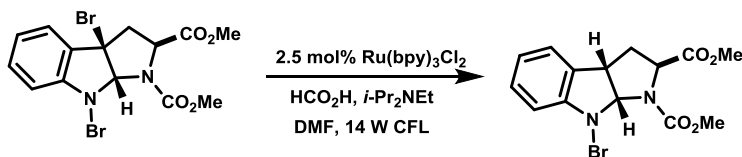
Scheme 1.5: Early examples of photoredox catalysis

1.1.1.2 Energy transfer

Another important reaction mechanism for photocatalysis is energy transfer. Compared to the well-developed single electron transfer photocatalysis, energy transfer has remained largely underdeveloped. With the prosperous development of photocatalysis, there are still a lot of organic substrates which will not engage into the oxidative or reductive processes due to incompatible redox potentials; hence, a single electron transfer process cannot occur. However, the excited photosensitizer has often a relatively high triplet energy, allowing the activation of a substrate with a lower triplet energy (i.e. the energy acceptor; EA) through an energy transfer pathway. Compared with electron transfer processes, the energy transfer process depends on the triplet state energies of the substrate and the photosensitizer, rather than the redox potential.[14] This reaction pathway may provide a complementary approach to photoreactions and provide new opportunities for organic molecule activation.

All visible light mediated energy transfer processes follow a reaction pathway which is shown below. The ground state (S_0) photosensitizer absorbs visible light and reaches a low-lying excited singlet

state S_1. Then an intersystem crossing (ISC) rapidly happens and produces the photosensitizer in the triplet state (T_1). The energy is facial to be transferred from the photosensitizer to the substrate (energy acceptor, EA), affording the substrate (EA) from the ground singlet state (S_0) to the actived triplet state (T_1). The photocatalyzed energy transfer follows a Dexter-type electron transfer.[15] In energy transfer reactions, the triplet energy of the photosensitizer (energy donor) must be higher than those of the substrates (energy acceptor, EA). At the same time, the intersystem crossing rate of the photosensitizer should be high enough to provide an efficient way to obtain the triplet state substrate (EA). Various ruthenium- and iridium-based photosensitizers and organic dyes are good candidates for energy transfer reactions as they possess a relatively high triplet energy and a long lifetime of excited triplet states (**Scheme 1.6**).
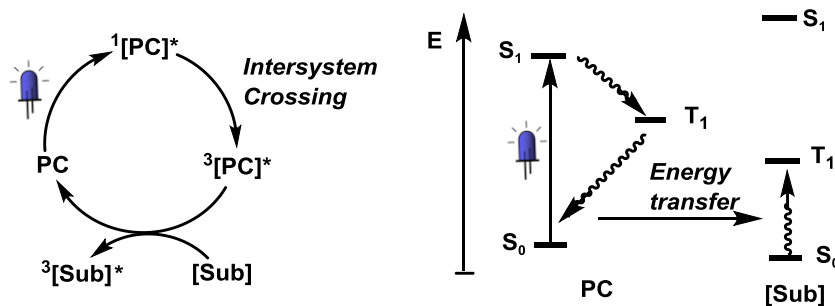
Scheme 1. 6: Reaction process of energy transfer

The **Scheme 1.7** shows the overview of the structure and excited triplet energies of known photosensitizers and selected substrates. It is shown in **Scheme 1.7** that the triplet energy is not related to the structure of the compound, but generally the enlargement of the conjugating system leading to a lower triplet energy. The application of energy transfer processes can be divided major into 4 types: the [2+2] photocycloadditions reactions,[6] the sensitization of azide compounds,[16] the isomerization of alkenes[17] and generation of reactive singlet oxygen[18].

Triplet energies of known photosensitizer and selected substrates (kal/mol)

Scheme 1. 7: Overview of the excited triplet energies of known photosensitizer and selected substrates (kcal/mol)

As an important motif of many natural product, the construction of cyclobutanes always needs to rely on the [2+2] photocycloaddition reaction by UV light. However, with the direct excitation of the alkenes, the reaction suffers from poor selectivity. In 2012, Yoon and co-workers reported the intramolecular [2+2] styrene cycloaddition reaction through use of an Ir-based photocatalyst and visible light (**Scheme 1. 8**). This energy transfer process attracted a lot of interest and many similar [2+2] photocycloadditions reactions were developed afterwards.[6,19]
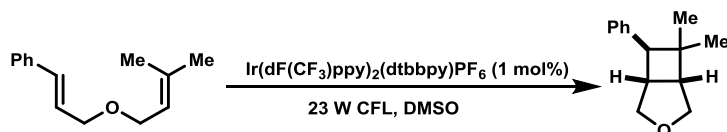
Scheme 1. 8: [2+2] styrene cycloaddition reaction by energy transfer

Azide-containing compounds are commonly used in the synthesis of nitrogen-containing heterocycles. However, azides are very sensitive to heat, light and transition metals. In the conventional protocols, UV light or high temperature are always used.[20] In 2014, Yoon and co-workers discovered the visible light sensitization of aryl and vinyl azides to produce nitrenes with Ru(dtbbpy)$_3$(PF$_6$)$_2$.[16] In the mechanism, the authors proposed that the energy was transferred from the excited-state catalyst to the azides to produce the triplet state intermediate. Next, the nitrene intermediate was formed while nitrogen is released, which is followed by producing the azirine. Finally, the intramolecular cycloaddition results in the formation of the final pyrrole product.
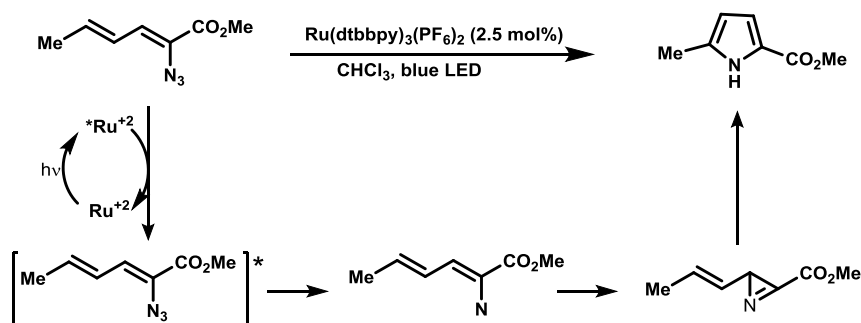
Scheme 1. 9: Synthesis of pyrrole via nitrene intermediate

Another important application of energy transfer in visible light is alkene isomerization. In early studies of photocatalysis, when *fac*-Ir(ppy)$_3$ was used in the C=C bond formation reactions, the *E/Z* selectivity is always an issue.[21] In 2014, Weaver and co-workers found that by irradiation of the more thermodynamically stable *E*-alkene isomer the less stable *Z*-isomer can be obtained.[17] Both an energy transfer and a reductive quenching mechanism were proposed. Two years later, they found that by tuning the size of the ligands of photocatalyst, selectable *E/Z* C−F alkenylation products could be obtained.[22] When a bulky catalyst (i.e. Ir(*t*Buppy)$_3$) was used, the *E*-isomer could be obtained, while the less sterically hindered catalyst (i.e. Ir(dFppy)$_3$)affords the *Z* isomer selectively. They proposed that this reaction proceeds via an energy transfer process and the use of photocatalyst bearing bulkier ligands results into a slower energy transfer.
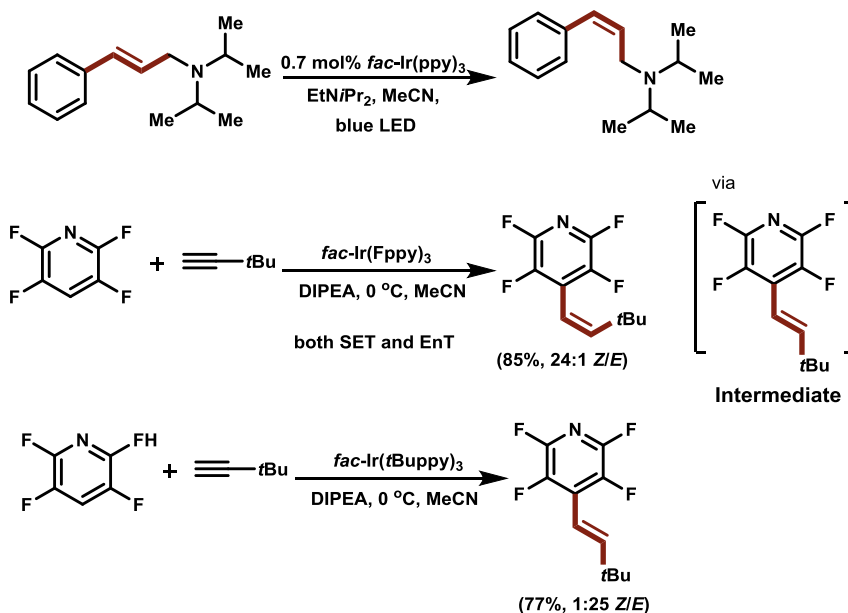
Scheme 1. 10: Reactions of *E*/*Z* selectivity of alkenes

In 2004, a metal-free oxygenation of sulfides to sulfoxides with Rose Bengal as photosensitizer was reported.[23] The mechanism studies show that the singlet oxygen was formed through energy transfer from excited-state of Rose Bengal. This selective aerobic oxidation reaction shows the great promise for the oxygenation of sulfides to sulfoxides through visible-light-induced O₂ sensitization (**Scheme 1. 11**).
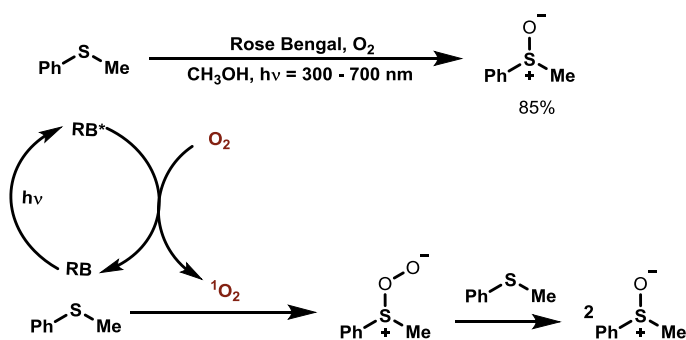
Scheme 1. 11: aerobic oxidation of sulfides with Rose Bengal

1.1.2 The advantages of continuous-flow photochemistry

Despite the great interest in photocatalysis as a synthetic tool, the challenges in scaling photochemical transformations still hampers its widespread adoption in industry. Typically, longer reaction times and low selectivities are observed when scaliong up. As in larger size reactors the radiation distribution is not uniform. The absorption of the light can be explained with a simplified version of the Bouguer-Lambert-Beer law:

$$A = \log_{10} T = \log_{10} \frac{I_0}{I} = \varepsilon c l$$

The equation shows that the light absorbance (A) is influenced by the molar extinction coefficient (ε) of the absorbing compound, the concentration of the absorbing species (c) and the path length to the light source (l). The influence of the dimensions of photoreactors on light absorption is illustrated in **Figure 1.1**.[2b,24] As the high molar extinction coefficient (ε) of the $[Ru(bpy)_3]^{2+}$ photocatalyst, in the first 500 micrometers, 50% of the light irradiation has already been absorbed when the concentration of the photocatalyst is 0.5 mM. But for a traditional batch-type photoreactor, the first fluid layers witnessed a strong intensity light, while the center almost none. Thus longer exposure times are needed to obtain full conversion, resulting in longer reaction times and possibly leading to side reactions due to over-irradiation. This problem can be solved by using microreactors which have smaller dimension. The almost perfect illumination homogeneity can be achieved owing to the narrow width of the capillary or tubing, providing a more efficient performance of the photoreactions.
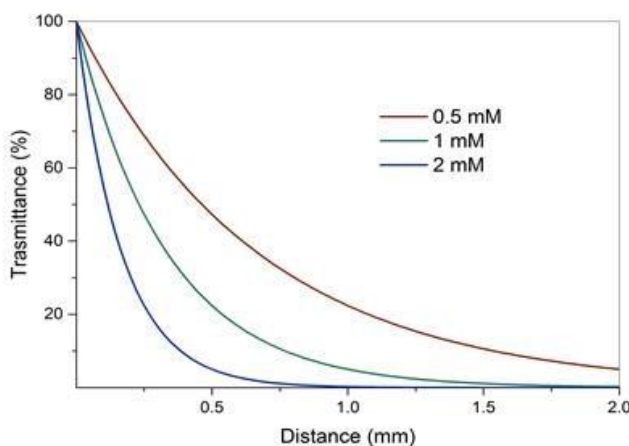
Figure 1. 1: Absorbance of incident light as a function of distance in the reaction medium containing $[Ru(bpy)_3]^{2+}$ as a photocatalyst
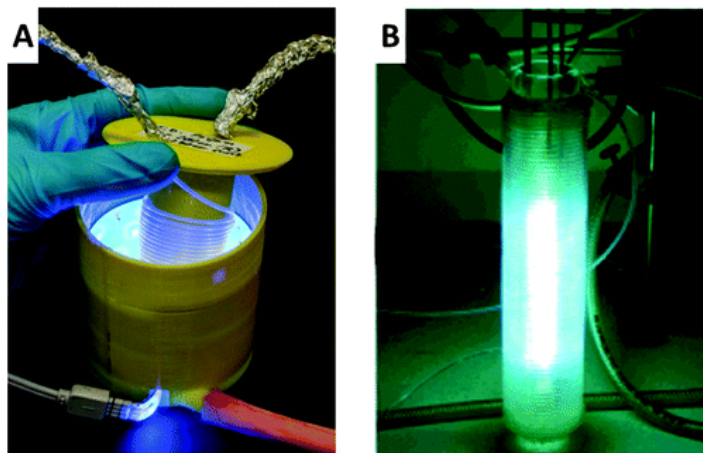
Figure 1. 2: Picture of the set-up for photoreactions

Continuous flow provides a reliable way for the scale up of photoreactions. Moreover, it also provides faster mixing than batch.[2b] The better control on the mixing can result in higher reaction selectivities.[25] Booker-Milburn et al. developed a operationally simple photoreactor consisting of medium pressure Hg lamp with a cooling well with perfluoroethylenepropylene (FEP) tubing wrapped around the lamp (**Figure 1. 2-right**) .[26] The reactor was able to produce 178 g intermolecular [5+2] photocycloaddition product (**Scheme 1. 17**). This system is highly advantageous compared to the traditional batch set up, as it not only ensures a large surface-to volume ratio w, but also avoids over-irradiation by removing the product from the reaction system continuously.

Batch: t = 30 min 66% (0.5 g)
Flow: t = 6 min 64% (38.5 g)
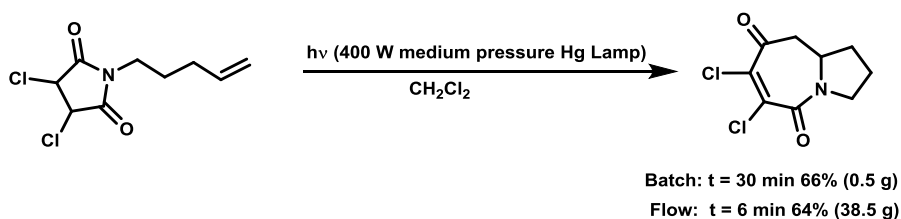
Scheme 1. 17: Large scale synthesis via photocatalysis in flow

Later, our group developed an inexpensive, compact modular photoreactor with commercial available parts (**Figure 1. 2A**).[27] The LED strip was used as a light source which provides visible light at short wavelength range with high intensity. Perfluoroalkoxyalkane (PFA) capillary was used as the reactor material which is transparent for both UV and visible light. This system was successfully used in several photocatalytic transformations, showing reduced reaction times, higher selectivities and lower catalyst loading.[28]

Flow chemistry also provide safe opportunities in case hazardous reagent are used.[29] The nature of specific hazardous reagent can limit their use, especially for large scale production. However,

sometimes the hazardous chemicals show unique reactivity and the alternative routes often need longer reaction steps or are expensive. For example the nitrations, halogenation and lithiation chemistry can be problematic on scale as these reactions are highly exothermic and extremely fast. These reactions tend to accumulate heat and form hot spots, leading to the uncontrollable side product formation. The traditional way to handle these issues is to dilute the solution or add the compound in small portions or by cooling the reaction.

Another advantage of having a high surface-to-volume ratio is that it can provide fast heat transfer, which is the optimal option for the operation of exothermic reaction conditions. For example, organolithium compound have been used in flow by many groups, one pioneering group is the one headed by Yoshida who introduced the concept of 'flash chemistry'.This concept demonstrates the fast generation of the unstable intermediates in a microreactor within milliseconds of residence time by accurate control of the flow rates and the reactor temperature.[30] The application of Grignard reagent in flow have also been reported, notably Jesus Alcazar et al. developed an interesting protocol to produce Grignard reagents and organozinc reagent in flow with an on-column activation of metal powder, thus providing a safe and clean preparation of organometallic reagents in flow.[31]
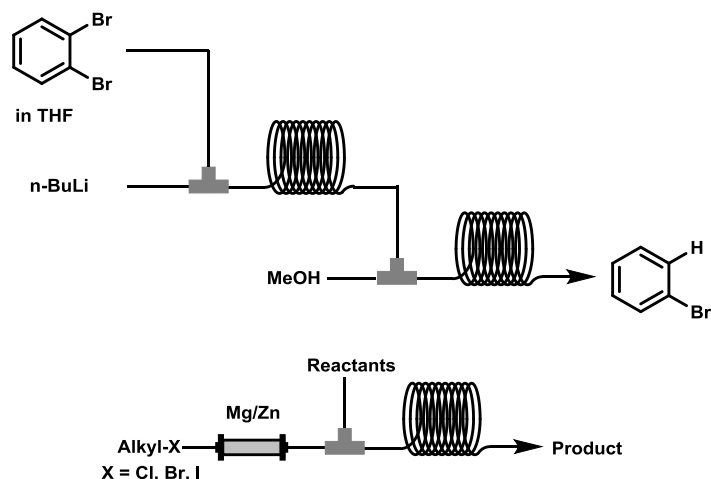
Scheme 1. 18: The use of organic lithium reagent and Grignard reagent in flow

1.2 Photocatalytic Difluoroalkylation Reactions

The introduction of fluorine or fluorinated moieties into organic molecules has attracted lots of attention in recent years since fluorine atoms play a crucial role in improving the ADME properties of drug molecules.[32] As a common fluoroalkyl group, the difluoromethyl group often brings many beneficial effects to the aimed molecules, which are found in many pharmaceuticals and agrochemicals.[33] The hydrogen bond donor properties of the difluoromethyl group increases acidity

of its neighboring group, which increases dipole moments and conformational changes in the molecules, showing superior lipophilicity, binding selectivity, metabolic stability than nonfluoroalkylated analogues.[34] Thus difluoroalkyl group can be found in some pharmaceutical compounds, which is shown in **Scheme 1. 19**.

Pantoprazole

Fluticasone propionate

treating JAK kinase mediated diseases

MCH1 receptor antagonists
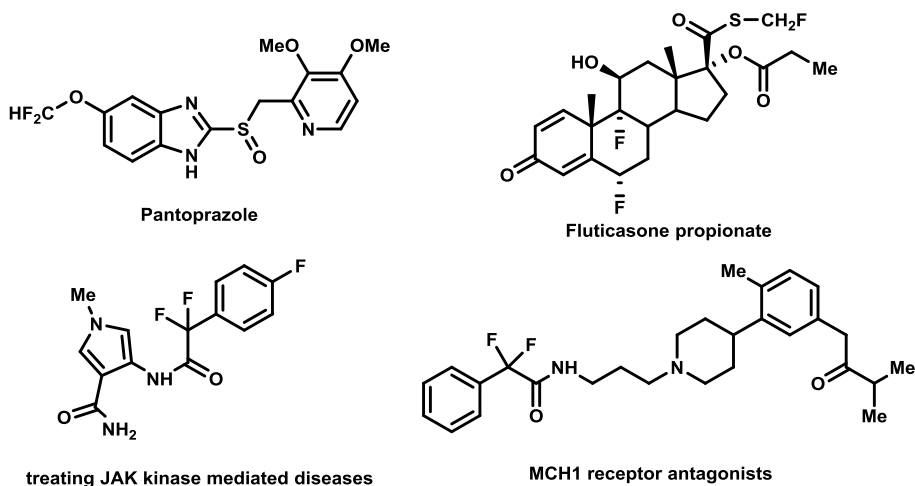
Scheme 1. 19: Examples of difluorinated compounds in drugs

Many strategies to introduce $-CF_2H$ and $-CF_2Y$ (Y $\neq$ H, F) into organic molecules have been developed. Among them, photocatalytic difluoromethylation plays a very important role due to mild conditions and good functional group tolerance. Traditionally, difluoromethylated compounds were prepared with diverse methods, eg. deoxyfluorination of aldehydes with SF_4, DAST (*N, N*-diethylaminosulfur trifluoride), Deoxo-Fluor (bis(2-methoxyethyl)aminosulfur trifluoride).[35] However, harsh reaction conditions are needed and the group tolerance is very poor. In recent years, many protocols on transition metal photocatalytic difluoromethylation have been developed, meanwhile many radical precursors were used to introduce $-CF_2H$ or $-CF_2Y$ (Y $\neq$ H, F), which were shown below in **Scheme 1. 20**:
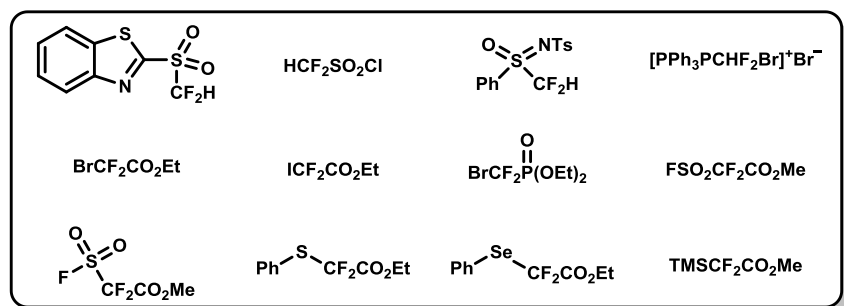
Scheme 1. 20: Radical precursors for difluoroalkylation

The photocatalytic difluoromethylation reactions has already been widely applied into different substrates, like aromatic, alkenes, alkynes and alcohols difluoromethylation.[36]

Since 2014, difluoromethylation was introduced to modify unreactive arenes and heteroarenes by direct C−H functionalization with visible light with *fac*-Ir(ppy)$_3$ at room temperature.[9] This protocol provided a strategy that does not need any prefunctionalization and tolerates a broad substrate scope of arenes and heteroarenes with both electron-rich and electron-poor functional groups. The mechanism was studied with Stern-Volmer quenching experiment, EPR and kinetic isotope effect experiments, which show the photocatalytic pathway proceed via oxidative photocatalytic way and the formation of •CF$_2$CO$_2$Et. However, the reaction suffered from poor regionselectivity. After that the BrCF$_2$PO(OEt)$_2$ was also applied successfully as a reagent for the modification of unreactive arenes and heteroarenes.[37]
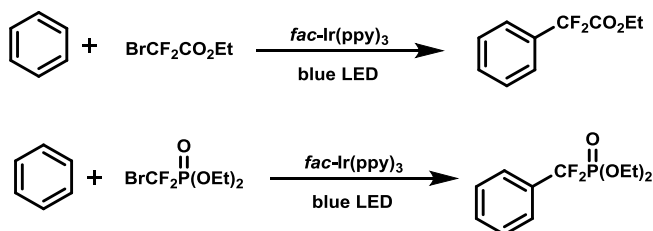
Scheme 1. 21: Difluoroalkyation of unreactive arenes

The alkene difluoromethylation was achieved by visible light photocatalysis with different radical precursors to generate –CF$_2$H and –CF$_2$Y moieties, such as *N*-tosyl-*S*-difluoro-methyl-*S*-phenylsulfoximine,[38] bromodifluoromethylphosphonium bromide,[39] ethyl bromodifluoroacetate and its acetamide derivatives,[40] methyl fluorosulfonyldifluoroacetate[41].
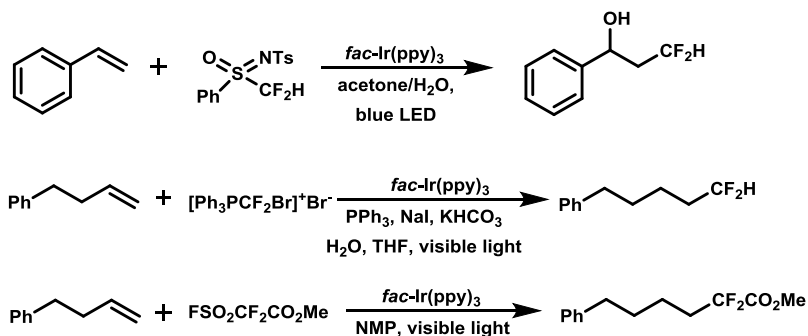
Scheme 1. 22: Difluoroalkylation of alkenes

Difluoromethylation of alkynes with visible light photocatalysis was achieved via a four-component reaction with DABCO•(SO$_2$)$_2$ and hydrazines catalyzed by 9-mes-10-methyl acridinium perchlorate, the (*E*)-ethyl 2,2-difluoro-4-aryl-4-sulfamoylbut-3-enoates were obtained with the insertion of sulfur

dioxide in good yield and stereoselectivity.[42] The direct difluoromethylation of alkynes can be achieved with Platinum(II) complexes,[43] the reaction shows high efficiency and good substrate scope, showing the promise of Pt(II) complex in visible light photocatalysis.

Scheme 1. 23: Difluoroalkylation of alkynes
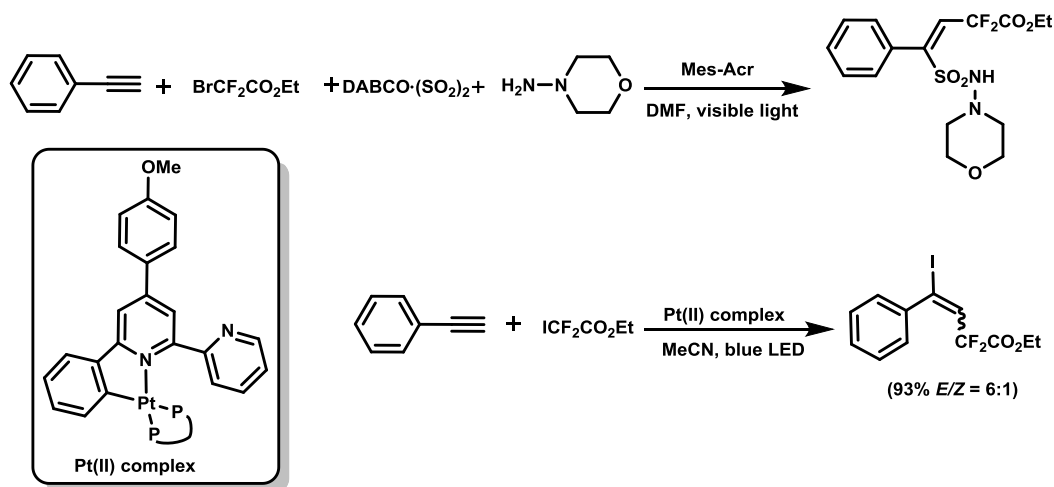
Among the diverse of fluorinated groups, the fluoroalkoxy group such as $-OCF_3$, $-OCF_2H$, $-OCH_2F$ are being increasingly used in a variety of applications. In particular, the difluoromethoxy group ($-OCF_2H$) attracted a lot of attention, as the difluoromethoxy group ($-OCF_2H$) is strong electron withdrawing and able to donate a hydrogen to the target molecule. The latter improves the binding selectivity of the aimed molecule. A general method to achieve this goal is to use $TMSCF_2Br$ in a biphasic system consisting of CH_2Cl_2 and H_2O.[44] This method provides not only a solution to the synthetic problem of the difluoromethylation of alkyl alcohols, but also provides new mechanistic insight to this reaction. Recently, a photocatalytic method of difluoromethylation of phenols and thiophenols was developed with difluorobromoacetic acid.[45] The Cs_2CO_3 and catalytic amount of *fac*-Ir(ppy)$_3$ were used in this system, a variety of aromatic $-OCF_2H$ and $-SCF_2H$ compound were obtained in high yield and good functional group tolerance. The mechanistic study shows that the reaction proceeds through a difluorocarbene generated under visible-light photocatalysis, providing an efficient way to construct the $-OCF_2H$ and $-SCF_2H$ compound.

Scheme 1. 24: Reactions to produce the $-OCF_2H$ and $-SCF_2H$ containing product
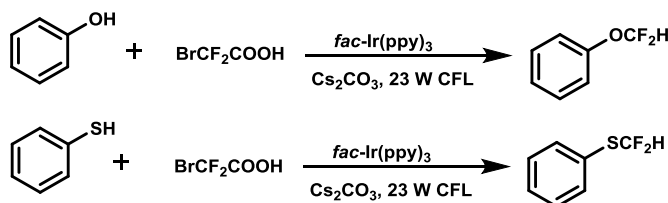
1.3 Iron catalyzed Cross-Coupling reactions

Centered in the d-block, iron is transition metal that belong to the group 8 processing the electron configuration $[Ar]3d^64s^2$, which allowing iron to support oxidative state ranging from −II to +VI. Thus iron based catalyst is expected to provide reductive as well as oxidative ability, holding the promise to be able to achieve the organic synthesis to a large extent. Although the challenges in this field still remain, the effort of the metal in application and synthesis has never been stopped.

From last century, iron-based catalysts have been employed mainly as heterogeneous catalysts.[46] A mile stone was reached when the Haber–Bosch process was patented in 1910, which converted nitrogen and hydrogen into ammonia by the cleavage of the N≡N triple bond. The ammonia obtained from this process plays an important role in the synthesis of fertilizers, building up the chemical basis for increasing the food production. Another important application of iron catalysts is the Fischer-Tropsch process, where a mixture of CO and H_2 ("synthesis gas") is converted to obtain liquid fuel, which plays an important role in providing an energy supply that is independent from raw oil.

In past few years, iron catalyzed homogeneous catalysis also found its application in natural product synthesis[47] and the pharmaceutical industry.[48] In the total synthesis of FTY720 (a promising immune-modulatory agent), the reaction between reaction intermediate triflate and octylmagnesium bromide with catalytic amounts of Fe(acac)$_3$ afforded the key building block in multi gram scale, providing a chemo- and regioselective protocol for the later functionalization. In the total synthesis of muscopyridine and isooncinotine, iron catalysis has been successfully applied in the selective and sequential cross-coupling, affording the key framework in high selectivity and efficiency[47b]. Moreover, a series of medicines were synthesized in the pharmaceutical industry, for example sex pheromone Lobesia botrana, antihypertensive medicines, and treatments for multiple sclerosis and calcimimetics have been successfully prepared on kilogram-scale.
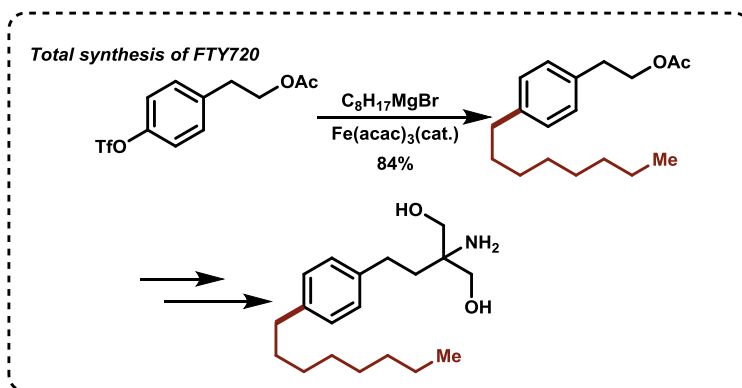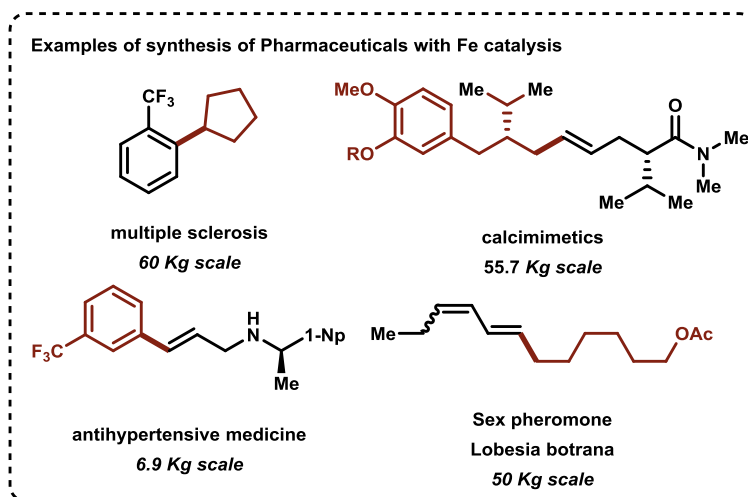
Scheme 1. 25: Examples of application of iron

1.3.1 Why iron catalysis?

Over the past three decades, transition metal catalyzed cross coupling reactions have emerged as one of the most fundamental synthetic transformations to enable efficient carbon-carbon and carbon-heteroatom bond formation.[49] In 1971, Kumada and Corriu first discovered the iron-catalyzed cross coupling of vinyl halides with Grignard reagents.[50] After this promising lead, a prosperous development of the cross coupling reaction between diverse organometallic nucleophiles and organometallic electrophiles was achieved. In addition, a wide variety of transition metals, such as palladium, nickel, copper, iron, were employed in combination with suitable ligands. [51] This category of C−C cross-couplings found essential application both in academia and industry, and was rewarded the Nobel Prize Chemistry in 2010 for Heck, Negishi and Suzuki.
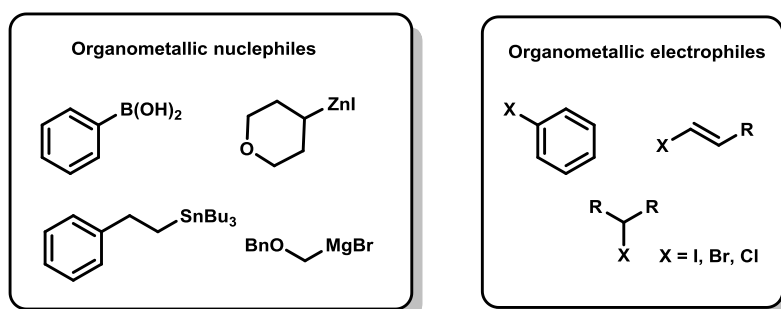
However, it should be noted that iron is nearly not as established as Pd or Ni in the field of cross-coupling. Nevertheless, the potential to use multiple available oxidative states, ranging from −II to +VI, makes iron a promising metal for the cross-coupling field. Moreover, iron got two other major advantages, i.e. its high abundance and relative low toxicity. Besides aluminum (8%), iron is the

second most abundant metal in the earth's crust, comprising around 6% of mass on the surface of the earth. The abundance of iron consequently causes its low cost. Compared to other metals on the world market, the price of iron is very competitive: in May 2019, one gram of palladium cost $42.73 and iridium $47.58, while one ton of iron costs only $86.47.

In addition, iron is recognized as a non-toxic metal to humans. According to the 2007 report by the European Medicines Agency, the residual limit for iron is 1300 ppm in final pharmaceuticals, compared to $\leq$ 10 ppm for most other transition metals like Pd, Pt, Ir, etc.[52] Iron is also present in a large number of biological systems, for example the iron-dependent enzymes, Hemoglobin and Cytochrome P450, which are vital for all forms of life on earth. As an important trace metal for humans, lack of iron will lead to anaemia, behavioral and learning disorders for children.[53] Based on these apparent advantages and due to the increasing demand for sustainable and green chemical processes, catalytic processes based on iron hold great promise for chemical synthesis.

1.3.2 The development of iron catalyzed cross-coupling of Grignard Reagents

1.3.2 .1 Csp^2 electrophiles

In 1941, Kharasch *et al.* were the first to report the iron-mediated homo-coupling of aromatic Grignard reagents in the presence of catalytic amounts of metallic halides (**Scheme 1. 26**).[54] Metallic halides $CoCl_2$, $FeCl_3$, $MnCl_2$ and $NiCl_2$ were proposed to be reduced to a lower oxidation state by the Grignard reagent and the organic halide functioned as the 'oxidant'.
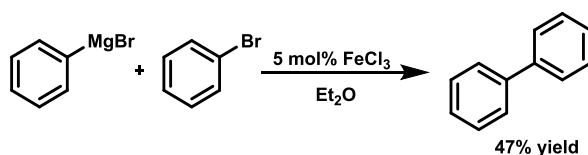
Scheme 1. 26: Kharasch's coupling reaction

After 30 years of these pioneering studies, Kochi and Corriu *et al.* reported the first example of a cross-coupling between alkenyl halides and alkyl Grignard reagents with catalytic amounts of FeX_3.[50b,55] Interestingly, the *E/Z* configuration of the substrate could be kept and (*E*)-alkenyl bromides reacted about 15 times faster than (*Z*)-configured counterparts (**Scheme 1. 27**). By lowering the reaction temperature and changing the solvent, also aryl Grignard reagents were tolerated. However, the alkenyl halides needed to be used in large excess (3 to 5 equiv.) and the yield based on Grignard reagent was always moderate.
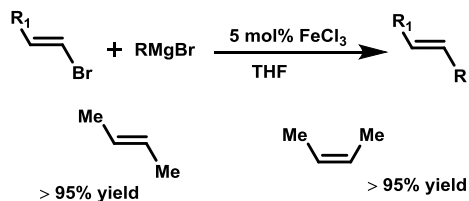
Scheme 1. 27: Kochi and Corriu's pioneering work on Fe-based cross-coupling

This limitation was overcome by addition of NMP as a cosolvent by Cahiez *et al.* in 1998. [56] Under the optimized conditions, alkenyl halides (1.0 equiv., X = I, Br, Cl) reacted stereo- and chemospecifically with Grignard reagents. NMP proved to have a beneficial influence on the reaction especially for substrates that were less reactive (**Scheme 1. 28**). Furthermore, reactive functional groups were better tolerated, such as esters, amides, ketones, alkyl chlorides and phosphates. This finding not only provided an alternative to palladium and nickel catalysis but also provided the possibility for the iron catalysis to synthesize more complex molecules with useful functional groups in the pharmaceutical industry. [48]
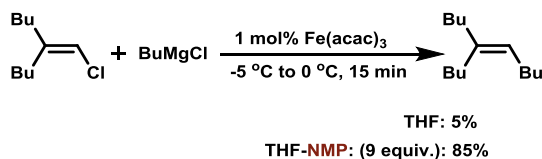
Scheme 1. 28: Cahiez's cross-coupling with NMP as additive

Next, further studies to expand the scope of the alkenyl halides have been carried out.[56-57] Also, alkenyl sulfones, alkenyl bromide, alkenyl phosphate, alkenyl triflate, alkenyl sulfides, alkenyl carboxylates proved to be suitable substrates in iron-based cross coupling chemistry **(Scheme 1. 29)**. The fact that iron could be used in the cross-coupling of alkenyl sulfides with Grignard reagent is remarkable. Cross-coupling takes place exclusively at the alkenyl−S position, which highlights the unique selectivity of iron catalysis. Also alkenyl and aryl carboxylates can be activated with $FeCl_2$.
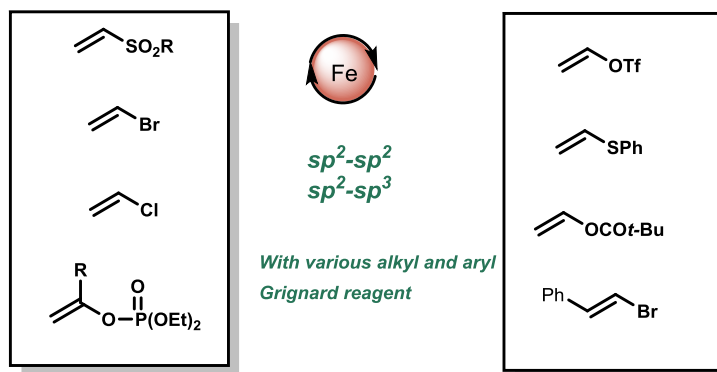
Scheme 1. 29: iron catalysis with various aryl and alkyl halides

In 2002, Fürstner and coworkers developed the first coupling of aryl electrophiles with alkyl Grignard reagents.[58] This report expanded the Csp^2 electrophile substrate scope from alkenyl halides to less reactive aromatic halides. Electron-deficient aryl- and hetero-aromatic chlorides and tosylates, as well as electron rich aryl and hetero aromatic triflates were well tolerated in the protocol developed by Fürstner. Tolerated functional groups comprise for example sulfonates, esters, acetals, ethers, nitriles sulfonamides, thioethers, alkynes and −CF$_3$ groups. As the activation of the aryl chloride is much faster than the attack of Grignard reagent to the polar groups, these functional group remained intact. The high functional group tolerance allows this method for further application in total synthesis and API synthesis.[47a,48] Interestingly, by introducing two different Grignard reagents sequentially, difunctionalized products could be obtained in good yield (**Scheme 1. 30**). The site-selectivity of iron catalysis was further demonstrated in the total synthesis of muscopyridine.[47b] It was found that TMEDA or a simple alkoxide magnesium salt (EtOMgCl) could replace NMP, allowing for the gram-scale synthesis in a cheap and eco-friendly fashion.[59]
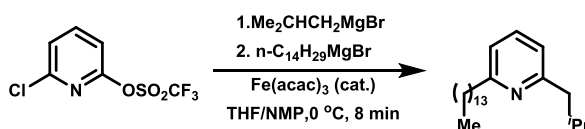
Scheme 1. 30: Difunctionalization with iron catalysis

The combination of aryl Grignard reagents and MeMgBr shows low reactivity in the reaction conditions described above due to the absence of β-hydrogen. This limitation was overcome through combination of FeF$_3$ and saturated *N*-heterocyclic carbene (SIPr-HCl) by the Nakamura group.[60] This procedure allows for the synthesis of various unsymmetrical biaryl compounds starting from aryl chlorides and aryl Grignard reagents in high yield and selectivity. Also, the methylated compound could also be obtained. However, electron rich aryl chlorides remained relatively unreactive in Kumada-type cross-coupling as they could only be activated at high temperature: the aimed product can be obtained at 80 °C after 24 to 84 hours reaction (depending on the reactivity of the Grignard reagent). (**Scheme 1. 31**).[60b,61]
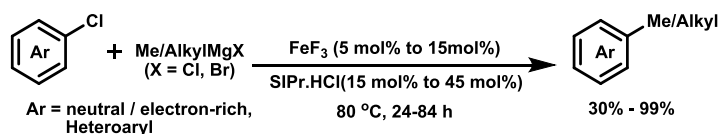
Scheme 1. 31: Kumada cross-coupling with electron-rich aryl chloride

With addition of TMEDA, the Grignard reagent can be generated in situ from the corresponding alkyl or aryl bromide or chloride.[62] The mechanistic study reveals that both aryl and alkyl Grignard reagents were formed during the reaction. The selectivity of this reaction increases with higher loading of

TMEDA, possibly stabilizing the metal complexes (Fe and Mg). The formation of the Grignard reagent is accelerated by FeCl₃, which appears to be the rate-determining step. This protocol provides a good example of a one-pot Kumada cross-coupling protocol which avoids the use of sensitive Grignard reagents (the detail are shown in **Scheme 1. 32**).
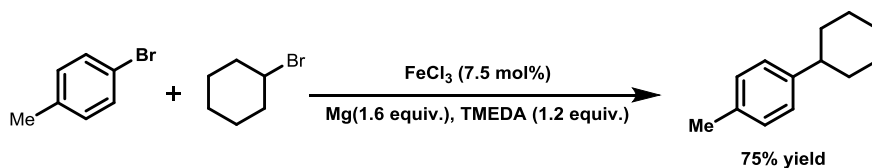
Scheme 1. 32: example of domino reaction with iron catalysis

1.3.2.2 C*sp³* electrophiles

In 2004, the C*sp²*- C*sp³* cross-coupling between alkyl halides and aryl Grignard reagents was achieved with iron catalysis (**Scheme 1. 33**). With FeCl₃ as catalyst, Nakamura[63] *et al.* developed a protocol to couple alkyl halides with aryl Grignard coupling partners. In this reaction, TMEDA works as a bidentate ligand and suppresses side reactions such as *β*-hydrogen elimination. Fürstner *et al.* [64] found that when the low valent iron(−II) complex [Li(TMEDA)]₂[Fe(C₂H₄)₄] was employed, a wide variety of alkyl bromides and iodides could react smoothly with aryl Grignards. Both studies proposed a radical pathway. The Hayashi group found that Fe(acac)₃ could also be used in the cross-coupling of C*sp³* electrophile substrates and aryl Grignard reagents.[65]
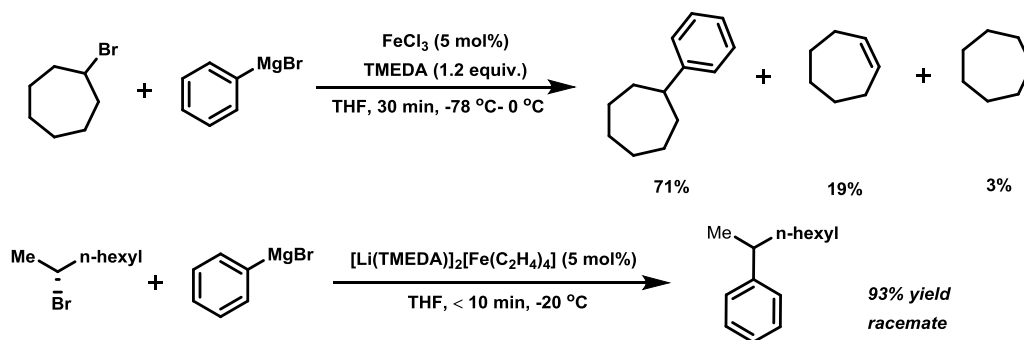
Scheme 1. 33: examples of C*sp²*- C*sp³* cross-coupling

The C*sp³*- C*sp³* cross-coupling is still challenging and the reaction between alkyl halides and alkyl Grignard reagents can be achieved with Fe(OAc)₂ and Xantphos **(Scheme 1. 34)**. The difficulty in the reaction lies in the competitive homocoupling and *β*-hydrogen elimination. The addition of Xantphos could reduce the formation of the side product. A mechanistic study suggested that an alkyl radical was formed from the corresponding alkyl halides**.**
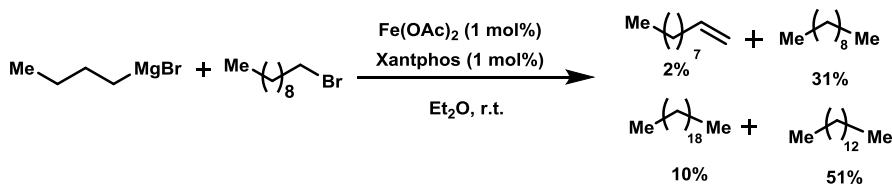
Scheme 1. 34: Examples of C*sp³*- C*sp³* cross-coupling

1.3.3 The mechanism study of Kumada-Corriu Cross-Couplings

Up to now, numerous useful methodologies based on iron catalysis have been developed. However, the precise mechanism of Fe-based cross coupling remains rather unclear, especially in comparison to Pd cross-coupling chemistry. As paramagnetic active species can be formed during the reaction, traditional characterization methods, such as NMR, cannot be used. Also the active paramagnetic intermediate is highly sensitive and short-lived, making the direct characterization of the actual catalytic species a daunting challenge.
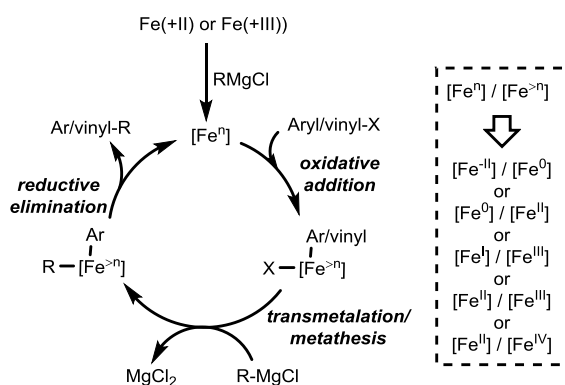
Scheme 1. 35: General Mechanism of iron catalysis

Nevertheless, the understanding of the precise mechanistic details remains a topic of great interest. [66] Generally, iron catalysis follows the well-known catalytic cycle of oxidative addition, transmetalation, and reductive elimination, widely accepted for most metal-catalyzed coupling reactions (**Scheme 1. 35**). Both two-electron and single electron transfer (SET) process can occur in iron catalysis. Moreover, the oxidation state of the catalytic cycle ranges between Fe(−II)/ Fe(0),[67] Fe(0)/ Fe(II),[68] Fe(+I)/ Fe(+III),[69] Fe(II)/Fe(III),[70] Fe(II)/Fe(IV)[71] depending on the reaction conditions. Some important mechanistic studies are discussed below.

In 1976, Kochi and coauthors found that, in the coupling of alkenyl halides with alkyl Grignard reagent, reactive Fe(I) species were formed (S = $^{1}/_{2}$) in situ from the Fe(III) pre-catalyst by addition of Grignard reagent. It was speculated that the oxidative addition of the vinyl halides to Fe(I) was the rate limiting and stereospecific step. Next, the Fe(III) intermediate then undergoes transmetalation

and reductive elimination. A radical pathway is not involved in this Fe(I)/Fe(III) catalytic cycle and was supported by EPR.

In 2008, Fürstner *et al.* carried out a thorough study of the mechanism, operative under their developed protocol,[67] through synthesis of a series of well-defined ferrate complexes, e.g. $[Li(TMEDA)]_2[Fe(C_2H_4)_4]$, $[Fe(cod)_2][Li(dme)]_2$ etc. Although the real catalytic cycle is still difficult to rationalize, after testing various ferrate complexes with different oxidation states, an Fe(−II)/Fe(0) cycle was suggested. Under their reaction conditions, radical intermediates were observed.

In recent years, physical-inorganic spectroscopy analyses, such as Mössbauer, EPR, XAS and MCD at low temperature, under inert atmosphere, were carried out in combination with density functional theory (DFT) and gas chromatography. This proved to be a powerful approach for the identification of in situ formed, reactive iron species.[66c,72]

In 2004, based on the interest in looking for the intermediate in Kochi's study, Neidig's group isolated and characterized an Fe(III) complex, $[MgCl(THF)_5][Me_4Fe]\cdot THF$, from the reaction between $FeCl_3$ and MeMgBr in THF at -80 °C. Upon heating the reaction mixture to room temperature, this $S = {}^3/_2$ species converts to an $S = {}^1/_2$ species, which was observed by Kochi's group.[73] This indicates that this structure is probably the intermediate which originates from the reduction of Fe(III) with Grignard reagents. Two years later, in a combined EPR and MCD study, they succeeded to isolate and characterize the Fe(I) intermediate $[MgCl(THF)_5][Fe_8Me_{12}]^-$.[74] This complex shows low reactivity but, upon addition of Grignard reagent, the cross-coupling product is formed smoothly, suggesting that this structure is indeed an intermediate.

In summary, reaction mechanisms for Fe-based cross-coupling can be divided in two major types, i.e. radical and non-radical pathways. Fe(+I)/Fe(+III) are normally involved in non-radical pathway. Radical-type pathways involve typically Fe(−II), Fe(0), Fe(II) species. When ligands (e.g. TMEDA or diphosphine ligand) are needed in the radical-based cross-coupling, a catalytic cycle of Fe(+II)/Fe(+III) is proposed.[71,75] Evidence for radical pathways could be found mainly through radical clock reactions (e.g. halomethylcyclopropane can be used as a substrate or via the ring-closure of 2-halo acetal derivatives[64]) and the racemization of enantioenriched substrtaes (**Scheme 1. 35**). When no coordinating ligands are involved, active species containing Fe(−II) or Fe(0) are formed depending on the Grignard reagent. With Grignard reagents containing β-hydrogens, an 'inorganic Grignard reagent' $Fe(MgX)_2$ is formed. In contrast, with Grignard reagents, like MeMgBr or PhMgBr, that do not contain β-hydrogens, Fe(0) complex are proposed.[58a,67]
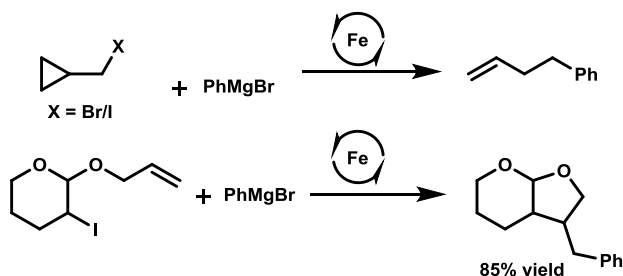
Scheme 1. 36: examples of the radical clock reaction in Kumada cross-coupling

1.4 Research aim and scope

This thesis presents the development of new and useful synthetic methodologies in continuous flow using visible light photocatalysis. Methods to enable the difluoromethylation of cinnamic acid and allylic alcohols were developed. In these reactions, *fac*-Ir(ppy)$_3$ was used as the photocatalyst. Next, we discovered an innovative approach to oxidatively cleave C=C bonds using disulfides as photocatalyst. Herein, an olefin-disulfide charge-transfer complex was found capable to absorb visible light. Finally, earth-abundant iron was used as a catalyst in the visible light promoted Kumada cross-coupling, which allows to overcome the classical limitations of the substrate scope for electron rich aryl chlorides.

The difluoromethylation of cinnamic acids is presented in **Chapter 2**. It represents the first decarboxylative difluoromethylation of cinnamic acids using only visible light photocatalysis without any additional additives to facilitate CO$_2$ extrusion. The *E/Z* selectivity of the difluoromethylated product was studied and the factors that influence the selectivity were examined in detail, e.g. the electron properties and the position of the substituted group. Microflow reactors were used as well and allowed to reduce the reaction time and tune the *E/Z* selectivity. In **Chapter 3**, the difluoromethylation of allylic alcohols followed by a heterocycle migration is presented. Both the synthesis of the starting materials and the transformation itself were carried out in flow.

As the costs of Ir and Ru based transition-metal photocatalysts are generally very high, which makes these catalysts too expensive for industrial application, we next turned our attention to metal-free photocatalysts and the use of earth-abundant first-row transition metals as cheap alternatives. This specific research is shown in **Chapter 4** and **Chapter 5**. In **Chapter 4**, electron-rich aromatic disulfides were employed as photocatalyst. Upon visible-light irradiation, typical mono- and multi-substituted aromatic olefins could be converted to ketones and aldehydes at ambient temperature, hence providing an alternative for the classical ozonolysis process. DFT calculations and NMR analysis were carried out to provide insight in the mechanism. In **Chapter 5**, we focused on the use

of Fe(acac)$_3$ in the Kumada-type cross-coupling for Csp^2-Csp^3 bond formation. We found that unreactive electron-rich aromatic chlorides can be activated using visible light irradiation. A variety of aromatic chlorides bearing electron-rich substituents and heterocycles cross-coupled efficiently under these conditions. DFT calculations and inline UV-Vis studies provided insight in the mechanism, and more specifically in the role of the light activation.

Finally, in **Chapter 6**, using the same catalyst Fe(acac)$_3$, we developed a method to enable the Kumada-type cross coupling reaction of (2-chlorovinyl)benzenes and (chloroethynyl)benzenes with Grignard reagents. The reaction proceeds smoothly under mild reaction conditions with very high efficiency (only minutes of reaction time at room temperature). The preparation of the final product has also been realized in flow by telescoping both the Grignard reagent preparation and the cross coupling reaction.

Reference:

(1) Curran, D. P. *Synthesis* **1988**, *1988*, 417-439.

(2) (a)Cambié, D.; Zhao, F.; Hessel, V.; Debije, M. G.; Noël, T. *Angew. Chem. Int. Ed.* **2017**, *56*, 1050-1054; (b)Cambié, D.; Bottecchia, C.; Straathof, N. J. W.; Hessel, V.; Noël, T. *Chem. Rev.* **2016**, *116*, 10276-10341; (c)Cambié, D.; Noël, T. *Top. Curr. Chem.* **2018**, *376*, 45.

(3) Hedstrand, D. M.; Kruizinga, W. H.; Kellogg, R. M. *Tetrahedron Lett.* **1978**, *19*, 1255-1258.

(4) Nicewicz, D. A.; MacMillan, D. W. C. *Science* **2008**, *322*, 77-80.

(5) (a)Shaw, M. H.; Twilton, J.; MacMillan, D. W. C. *J. Org. Chem.* **2016**, *81*, 6898-6926; (b)Skubi, K. L.; Blum, T. R.; Yoon, T. P. *Chem. Rev.* **2016**, *116*, 10035-10074; (c)Chatterjee, T.; Iqbal, N.; You, Y.; Cho, E. J. *Acc. Chem. Res.* **2016**, *49*, 2284-2294; (d)McAtee, R. C.; McClain, E. J.; Stephenson, C. R. J. *Trends in Chemistry* **2019**, *1*, 111-125.

(6) Lu, Z.; Yoon, T. P. *Angew. Chem. Int. Ed.* **2012**, *51*, 10329-10332.

(7) Narayanam, J. M. R.; Stephenson, C. R. J. *Chem. Soc. Rev.* **2011**, *40*, 102-113.

(8) Huang, H.; Jia, K.; Chen, Y. *Angew. Chem. Int. Ed.* **2015**, *54*, 1881-1884.

(9) Wang, L.; Wei, X. J.; Jia, W. L.; Zhong, J. J.; Wu, L. Z.; Liu, Q. *Org. Lett.* **2014**, *16*, 5842-5845.

(10) (a)Lackner, G. L.; Quasdorf, K. W.; Overman, L. E. In *Visible Light Photocatalysis in Organic Chemistry*; Corey R. J. Stephenson, T. P. Y. D. W. C. M., Ed.; Wiley-VCH Verlag GmbH & Co. KGaA: 2018; Vol. 9, p 283-297; (b)Nicholls, T. P.; Leonori, D.; Bissember, A. C. *Nat. Prod. Rep.* **2016**, *33*, 1248-1254.

(11) Kuijpers, K. P. L.; Bottecchia, C.; Cambié, D.; Drummen, K.; König, N. J.; Noël, T. *Angew. Chem. Int. Ed.* **2018**, *57*, 11278-11282.

(12) Ischay, M. A.; Anzovino, M. E.; Du, J.; Yoon, T. P. *J. Am. Chem. Soc.* **2008**, *130*, 12886-12887.

(13) Narayanam, J. M. R.; Tucker, J. W.; Stephenson, C. R. J. *J. Am. Chem. Soc.* **2009**, *131*, 8756-8757.

(14) (a)Strieth-Kalthoff, F.; James, M. J.; Teders, M.; Pitzer, L.; Glorius, F. *Chem. Soc. Rev.* **2018**, 47, 7190-7202; (b)Xiao, W.-J.; Zhou, Q.-Q.; Zou, Y.-Q.; Lu, L.-Q. *Angew. Chem. Int. Ed.* **2019,** *58,* 1586-1604.

(15) Turro, N. J. *Pure Appl. Chem.* **1977**, *49*, 405-429.

(16) Farney, E. P.; Yoon, T. P. *Angew. Chem. Int. Ed.* **2014**, *53*, 793-797.

(17) Singh, K.; Staig, S. J.; Weaver, J. D. *J. Am. Chem. Soc.* **2014**, *136*, 5275-5278.

(18) Ghogare, A. A.; Greer, A. *Chem. Rev.* **2016**, *116*, 9994-10034.

(19) (a)Wu, L.-L.; Yang, G. H.; Guan, Z.; He, Y.-H. *Tetrahcdron* **2017**, *73*, 1854-1860; (b)Liu, Q.; Zhu, F.-P.; Jin, X.-L.; Wang, X.-J.; Chen, H.; Wu, L.-Z. *Chem. Eur. J.* **2015**, *21*, 10326-10329.

(20) Scheinman, F. *J. Med. Chem.* **1985**, *28*, 686-686.

(21) Iqbal, N.; Jung, J.; Park, S.; Cho, E. J. *Angew. Chem. Int. Ed.* **2014**, *53*, 539-542.

(22) Singh, A.; Fennell, C. J.; Weaver, J. D. *Chem. Sci.* **2016**, *7*, 6796-6802.

(23) Bonesi, S. M.; Fagnoni, M.; Albini, A. *J. Org. Chem.* **2004**, *69*, 928-935.

(24) Su, Y.; Straathof, N. J. W.; Hessel, V.; Noël, T. *Chem. Eur. J.* **2014**, *20*, 10562-10589.

(25) Plutschack, M. B.; Pieber, B.; Gilmore, K.; Seeberger, P. H. *Chem. Rev.* **2017**, *117*, 11796-11893.

(26) Hook, B. D. A.; Dohle, W.; Hirst, P. R.; Pickworth, M.; Berry, M. B.; Booker-Milburn, K. I. *J. Org. Chem.* **2005**, *70*, 7558-7564.

(27) Straathof, N. J. W.; Su, Y.; Hessel, V.; Noël, T. *Nat. Protoc.* **2015**, *11*, 10.

(28) (a)Talla, A.; Driessen, B.; Straathof, N. J. W.; Milroy, L.-G.; Brunsveld, L.; Hessel, V.; Noël, T. *Adv. Synth. Catal.* **2015**, *357*, 2180-2186; (b)Straathof, N. J. W.; Cramer, S. E.; Hessel, V.; Noël, T. *Angew. Chem. Int. Ed.* **2016**, *55*, 15549-15553; (c)Straathof, N. J. W.; Gemoets, H. P. L.; Wang, X.; Schouten, J. C.; Hessel, V.; Noël, T. *ChemSusChem* **2014**, *7*, 1612-1617.

(29) (a)Movsisyan, M.; Delbeke, E. I. P.; Berton, J. K. E. T.; Battilocchio, C.; Ley, S. V.; Stevens, C. V. *Chem. Soc. Rev.* **2016**, *45*, 4892-4928; (b)Gutmann, B.; Cantillo, D.; Kappe, C. O. *Angew. Chem. Int. Ed.* **2015**, *54*, 6688-6728.

(30) Usutani, H.; Tomida, Y.; Nagaki, A.; Okamoto, H.; Nokami, T.; Yoshida, J.-i. *J. Am. Chem. Soc.* **2007**, *129*, 3046-3047.

(31) (a)Huck, L.; de la Hoz, A.; Diaz-Ortiz, A.; Alcazar, J. *Org. Lett.* **2017**, *19*, 3747-3750; (b)Deng, Q.; Shen, R.; Zhao, Z.; Yan, M.; Zhang, L. *Chem. Eng. J.* **2015**, *262,* 1168-1174; (c)Abdiaj, I.; Fontana, A.; Gomez, M. V.; de la Hoz, A.; Alcazar, J. *Angew. Chem. Int. Ed.* **2018**, *57*, 8473-8477.

(32) (a)Yerien, D. E.; Bonesi, S.; Postigo, A. *Org. Biomol. Chem.* **2016**, *14*, 8398-8427; (b)Zhou, Y.; Wang, J.; Gu, Z.; Wang, S.; Zhu, W.; Aceña, J. L.; Soloshonok, V. A.; Izawa, K.; Liu, H. *Chem. Rev.* **2016**, *116*, 422-518.

(33) Hu, J.; Zhang, W.; Wang, F. *Chem Commun* **2009**, *48*, 7465-7478.

28

(34) Erickson, J. A.; McLoughlin, J. I. *J. Org. Chem.* **1995**, *60*, 1626-1631.

(35) (a)Uneyama, K. *Organofluorine chemistry*; John wiley & sons, 2008; (b)Chambers, R. D. *Fluorine in organic chemistry*; CRC press, 2004; (c)O'Hagan, D. *ChemBioChem* **2005**, *6*, 763-763.

(36) Yerien, D. E.; Barata-Vallejo, S.; Postigo, A. *Chemistry Eur. J.* **2017**, *23*, 14676-14701.

(37) Wang, L.; Wei, X.-J.; Lei, W.-L.; Chen, H.; Wu, L.-Z.; Liu, Q. *Chem. Commun.* **2014**, *50*, 15916-15919.

(38) Arai, Y.; Tomita, R.; Ando, G.; Koike, T.; Akita, M. *Chem. Eur. J.* **2016**, *22*, 1262-1265.

(39) Lin, Q.-Y.; Xu, X.-H.; Zhang, K.; Qing, F.-L. *Angew. Chem. Int. Ed.* **2016**, *55*, 1479-1483.

(40) Zhang, M.; Li, W.; Duan, Y.; Xu, P.; Zhang, S.; Zhu, C. *Org. Lett.* **2016**, *18*, 3266-3269.

(41) Yu, W.; Xu, X.-H.; Qing, F.-L. *Org. Lett.* **2016**, *18*, 5130-5133.

(42) Xiang, Y.; Li, Y.; Kuang, Y.; Wu, J. *Chem. Eur. J.* **2017**, *23*, 1032-1035.

(43) Zhong, J.-J.; Yang, C.; Chang, X.-Y.; Zou, C.; Lu, W.; Che, C.-M. *Chem. Commun.* **2017**, *53*, 8948-8951.

(44) Xie, Q.; Ni, C.; Zhang, R.; Li, L.; Rong, J.; Hu, J. *Angew. Chem. Int. Ed.* **2017**, *56*, 3206-3210.

(45) Yang, J.; Jiang, M.; Jin, Y.; Yang, H.; Fu, H. *Org. Lett.* **2017**, *19*, 2758-2761.

(46) Gerhard Ertl, H. K. E., Ferdi Schüth, Jens Weitkamp *Handbook of Heterogeneous Catalysis, 2nd Edition*; Wiley-VCH: Weinheim, 2008; Vol. 1-8.

(47) (a)Seidel, G.; Laurich, D.; Fürstner, A. *J. Org. Chem.* **2004**, *69*, 3950-3952; (b)Fürstner, A.; Leitner, A. *Angew. Chem. Int. Ed.* **2003**, *42*, 308-311; (c)Scheiper, B.; Glorius, F.; Leitner, A.; Fürstner, A. *Proc. Natl. Acad. Sci. U.S.A.* **2004**, *101*, 11960-11965.

(48) Piontek, A.; Bisz, E.; Szostak, M. *Angew. Chem. Int. Ed.* **2018**, *57*, 11116-11128.

(49) Busch, M.; Wodrich, M. D.; Corminboeuf, C. *ACS Catal.* **2017**, *7*, 5643-5653.

(50) (a)Corriu, R. J. P.; Masse, J. P. *J. Chem. Soc., Chem. Commun.* **1972**, 144a-144a; (b)M. Tamura, J. K. *J. Am. Chem. Soc.* **1972**, *94*, 4374-4376.

(51) Heck, R. F. *Organic reactions* **1982**, *27*, 345-390.

(52) Furstner, A. *ACS Cent Sci* **2016**, *2*, 778-789.

(53) Sreedevi, R.; Saranya, S.; Rohit, K. R.; Anilkumar, G. *Adv. Synth. Catal.* **2019**, *361*, 2236-2249.

(54) Kharasch, M. S.; Fields, E. K. *J. Am. Chem. Soc.* **1941**, *63*, 2316-2320.

(55) Tamura, M., Kochi, J. K., *J. Am. Chem. Soc.* **1971**, *93*, 1487-1489.

(56) Cahiez, G.; Avedissian, H. *Synthesis* **1998**, *1998*, 1199-1205.

(57) (a)Li, B.-J.; Xu, L.; Wu, Z.-H.; Guan, B.-T.; Sun, C.-L.; Wang, B.-Q.; Shi, Z.-J. *J. Am. Chem. Soc.* **2009**, *131*, 14656-14657; (b)Fabre, J.-L.; Julia, M.; Verpeaux, J.-N. *Tetrahedron Lett.* **1982**, *23*, 2469-2472; (c)Molander, G. A.; Rahn, B. J.; Shubert, D. C.; Bonde, S. E. *Tetrahedron Lett.* **1983**, *24*, 5449-5452; (d)Scheiper, B.; Bonnekessel, M.; Krause, H.; Fürstner, A. *J. Org. Chem.* **2004**, *69*, 3943-3949; (e)Itami, K.; Higashi, S.; Mineno, M.; Yoshida, J. *Org. Lett.* **2005**, *7*, 1219-1222.

(58) (a)Fürstner, A.; Leitner, A.; Méndez, M.; Krause, H. *J. Am. Chem. Soc.* **2002**, *124*, 13856-13863; (b)Fürstner, A.; Leitner, A. *Angew. Chem. Int. Ed.* **2002**, *41*, 609-612.

(59) (a)Rushworth, P. J.; Hulcoop, D. G.; Fox, D. J. *J. Org. Chem.* **2013**, *78*, 9517-9521; (b)Cahiez, G.; Lefèvre, G.; Moyeux, A.; Guerret, O.; Gayon, E.; Guillonneau, L.; Lefèvre, N.; Gu, Q.; Zhou, E. *Org. Lett.* **2019**, *21*, 2679-2683.

(60) (a)Hatakeyama, T.; Hashimoto, S.; Ishizuka, K.; Nakamura, M. *J. Am. Chem. Soc.* **2009**, *131*, 11949-11963; (b)Nakamura, M.; Agata, R.; Iwamoto, T.; Nakagawa, N.; Isozaki, K.; Hatakeyama, T.; Takaya, H. *Synthesis* **2015**, *47*, 1733-1740.

(61) Perry, M. C.; Gillett, A. N.; Law, T. C. *Tetrahedron Lett.* **2012**, *53*, 4436-4439.

(62) Czaplik, W. M.; Mayer, M.; Jacobi von Wangelin, A. *Angew. Chem. Int. Ed.* **2009**, *48*, 607-610.

(63) Nakamura, M.; Matsuo, K.; Ito, S.; Nakamura, E. *J. Am. Chem. Soc.* **2004**, *126*, 3686-3687.

(64) Martin, R.; Fürstner, A. *Angew. Chem. Int. Ed.* **2004**, *43*, 3955-3957.

(65) Nagano, T.; Hayashi, T. *Org. Lett.* **2004**, *6*, 1297-1299.

(66) (a)Bedford, R. B. *Acc. Chem. Res.* **2015**, *48*, 1485-1493; (b)Kleimark, J.; Hedström, A.; Larsson, P.-F.; Johansson, C.; Norrby, P.-O. *ChemCatChem* **2009**, *1*, 152-161; (c)Sears, J. D.; Neate, P. G. N.; Neidig, M. L. *J. Am. Chem. Soc.* **2018**, *140*, 11872-11883; (d)Cassani, C.; Bergonzini, G.; Wallentin, C.-J. *ACS Catal.* **2016**, *6*, 1640-1648.

(67) Fürstner, A.; Martin, R.; Krause, H.; Seidel, G.; Goddard, R.; Lehmann, C. W. *J. Am. Chem. Soc.* **2008**, *130*, 8773-8787.

(68) Cahiez, G.; Duplais, C.; Moyeux, A. *Org. Lett.* **2007**, *9*, 3253-3254.

(69) Smith, R. S.; Kochi, J. K. *J. Org. Chem.* **1976**, *41*, 502-509.

(70) Przyojski, J. A.; Veggeberg, K. P.; Arman, H. D.; Tonzetich, Z. J. *ACS Catal.* **2015**, *5*, 5938-5946.

(71) Agata, R.; Takaya, H.; Matsuda, H.; Nakatani, N.; Takeuchi, K.; Iwamoto, T.; Hatakeyama, T.; Nakamura, M. *Bull. Chem. Soc. Jpn.* **2019**, *92*, 381-390.

(72) Carpenter, S. H.; Neidig, M. L. *Isr. J. Chem.* **2017**, *57*, 1106-1116.

(73) Al-Afyouni, M. H.; Fillman, K. L.; Brennessel, W. W.; Neidig, M. L. *J. Am. Chem. Soc.* **2014**, *136*, 15457-15460.

(74) Muñoz, S. B.; Daifuku, S. L.; Brennessel, W. W.; Neidig, M. L. *J. Am. Chem. Soc.* **2016**, *138*, 7492-7495.

(75) (a)Noda, D.; Sunada, Y.; Hatakeyama, T.; Nakamura, M.; Nagashima, H. *J. Am. Chem. Soc.* **2009**, *131*, 6078-6079; (b)Takuji, H.; Yu-ichi, F.; Yoshihiro, O.; Takuma, I.; Toru, H.; Shintaro, K.; Kazuki, O.; Hikaru, T.; Masaharu, N. *Chem. Lett.* **2011**, *40*, 1030-1032; (c)Guisán-Ceinos, M.; Tato, F.; Buñuel, E.; Calle, P.; Cárdenas, D. J. *Chem. Sci.* **2013**, *4*, 1098.

Chapter 2

Visible-Light Photocatalytic Decarboxylation of α, β-Unsaturated Carboxylic Acids: Facile access to Stereoselective Difluoromethylated Styrenes in Batch and Flow

Abstract

In the following chapter, a continuous-flow protocol for visible-light photocatalytic decarboxylation of *α, β*-unsaturated carboxylic acids: facile access to stereoselective difluoromethylated styrenes in batch and flow was described. The development of synthetic methodologies which provide access to both stereoisomers of *α, β*-substituted olefins is a challenging undertaking. Herein, we describe the development of an operationally simple and stereoselective synthesis of difluoromethylated styrenes via a visible-light photocatalytic decarboxylation strategy using *fac*-Ir(ppy)$_3$ as the photocatalyst. *Meta* and *para-* substituted cinnamic acids provide the expected *E*-isomer. In contrast, *ortho*-substituted cinnamic acids yield selectively the less stable *Z*-product, whereas the *E*-isomer can be obtained via continuous-flow processing through accurate control of the reaction time. Furthermore, our protocol is amenable to the decarboxylative difluoromethylation of aryl propiolic acids.

Introduction

The introduction of fluorinated moieties into organic compounds has resulted in a dramatic enhancement of their physical, chemical and biological properties, rendering medicinal and agrochemical compounds to be more potent.[1] Nowadays 20-25% of modern drugs contains at least one fluorine atom, consequently, in recent years, a tremendous amount of research effort has been devoted to develop new methods to enable the efficient incorporation of fluorinated moieties into parent molecules.[2] Amongst these, the CF_2 motif plays an increasingly important role, since the hydrogen bond donor properties of the difluoromethyl group increases acidity of its neighboring group, which enhances dipole moments and conformational changes in the molecules.[3] In recent years, great progress has been made with regard to radical difluoroalkylation reactions, especially via visible light photoredox catalysis.[4] Visible light photoredox catalysis has become one of the most powerful tools in organic synthesis wherein both single electron transfer (SET) and triplet-triplet energy transfer (TTET) processes with organic substrates can be facilitated.[5]

With biomass feedstocks of vinyl carboxylic acids abundantly available, these inexpensive and stable compounds have attracted a great deal of attention as substrates for a wide variety of synthetic transformations.[6] Perhaps, the most widely used decarboxylative fluoroalkylation strategy involves transition metal coordination in combination with high temperatures or strong oxidants to facilitate the CO_2 extrusion process (**Figure 2.1A**).[7] It is evident that such harsh reaction conditions have their repercussions on the substrate scope. Photocatalytic strategies have allowed to perform the decarboxylative functionalization process at room temperature but still require stoichiometric amounts of strong oxidants or transition metals (**Figure** 2.**1B**).[8,9] In addition, all these methods give access to the thermodynamically more stable *E*-alkenes,[10] while methods delivering selectively the *Z*-isomers are far less common.[1]

A   **Perfluoroalkylation of olefins via decarboxylative cross-coupling chemistry**

- High reaction temperatures
- Strong oxidants
- High catalyst loadings
- Exclusive *E* isomer

B   **Perfluoroalkylation of olefins via photoredox catalysis:**

- Requires metal cocatalyst or HIR to enable CO_2 extrusion
- Exclusive *E* isomer

C   **This work: Photocatalytic difluoromethylation of cinnamic acids:**

feed stock
starting material

+

EtO_2CF_2C—Br

Inexpensive
CF$_2$ source

visible light
photoredox catalysis

- Practical reaction conditions
- No additional reagents for CO_2 extrusion
- Broad substrate scope
- High *E* selectivity
- High *Z* selectivity in batch and *E* in flow for *o*-substituted substrates

Figure 2.1. (A) Classical decarboxylative cross-coupling strategies. (B) Recent photocatalytic approaches still require the use of metals or hypervalent iodine reagents (HIR) to enable the decarboxylation step. (C) Our strategy for the photocatalytic radical difluoromethylation of cinnamic acids.
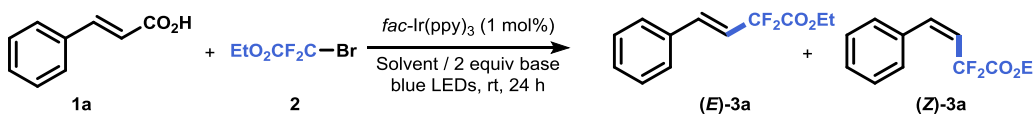
Result and discussion

The strategy we describe here involves a photocatalytic decarboxylation methodology to access difluoroalkenes, which is operationally simple, mild and requires no additional transition metals or oxidants to enable CO_2 extrusion (**Figure 2.1**C). Moreover, with *ortho*-substituted cinnamic acid substrates, *Z*-isomers could be obtained in high selectivity. The corresponding *E*-isomer could be accessed as well via continuous-flow processing through accurate control of the reaction time. To the best of our knowledge, having access to both stereoisomers simply by changing the reactor has never

been reported before and constitutes a powerful approach to tune reaction selectivity for photoredox catalysis.

Building on our recent experience with the direct trifluoromethylation of styrenes,[10a] we commenced our investigations by using *fac*-Ir(ppy)$_3$ as the photocatalyst (**Table 2.1**). The targeted product could be obtained in a 31% yield with an *E/Z* ratio of 52:48 using 3 equivalent of ethyl bromodifluoroacetate **2** and KOAc as a base (**Table 2.1**, entry 1). Interestingly, no metal cocatalyst or hypervalent iodine reagent (HIR) was required to facilitate the CO$_2$ extrusion. The rather poor *E/Z* can be explained due to high triplet energy level of the *fac*-Ir(ppy)$_3$ photocatalyst (E_T = 2.41 eV).[12] Consequently, a triplet-triplet energy transfer occurs leading to an erosion of the stereoselectivity.[11] Various solvents and bases were subsequently screened(**Table 2.1**, Entries 1-6); the best results were obtained using 1,4-dioxane as solvent and NaHCO$_3$ as the base. Addition of water provided an improved yield but a decreased selectivity (**Table 2.1**, Entry 7). Optimal results were obtained when the concentration was reduced to 0.1 M leading to a 68% yield and an excellent *E/Z* selectivity (94:6) (**Table 2.1**, Entry 8). Lastly, control experiments confirmed the photocatalytic nature of our transformation, as no reaction was observed in the absence of photocatalyst and/or light (**Table 2.1**, Entries 9 and 10).

Table 2.1. Reaction discovery and optimization studies for the photocatalytic difluoromethylation of cinnamic acids.[a]

Entry	Base	Solvent	Yield[b]	E/Z[b]
1 [d]	KOAc	0.2 M CH$_3$CN	31 %	52:48
2	KOAc	0.2 M EtOH	44 %	57:43
3	KOAc	0.2 M 1,4-dioxane	60 %	51:49
4	Cs$_2$CO$_3$	0.2 M 1,4-dioxane	46 %	71:29
5	2,6-lutidine	0.2 M 1,4-dioxane	70 %	46:54
6	NaHCO$_3$	0.2 M 1,4-dioxane	75 %	75:25
7[c,d]	NaHCO$_3$	0.2 M 1,4-dioxane	83 %	50:50
8[d]	*NaHCO$_3$*	*0.1 M 1,4-dioxane*	*68 %*	*94:6*
Entry	Change from best conditions (entry 5)		Yield[b]	E/Z[b]
9	No light		0 %	-
10	No Photocatalyst		0 %	-

[a]Reaction conditions: *fac*-Ir(ppy)$_3$ (1 mol%), cinnamic acid **1** (0.2 mmol), NaHCO$_3$ (0.4 mmol), ethyl bromodifluoroacetate **2** (0.6 mmol), solvent (2 mL, 0.1 M), blue LEDs (3.12 W), room temperature, argon atmosphere, stirred for 24 hours. [b]Yield and *E/Z* values are determined with **19F-NMR** using α,α,α-

trifluorotoluene as internal standard. [c]10 equivalents H_2O were added. [d] Reported yields are those of isolated compounds, E/Z values are determined with **¹H-NMR** of isolated products.

Having identified the optimal reaction conditions for the photocatalytic difluoromethylation of cinnamic acid, we aimed to define the reaction scope (**Scheme 2.1**). Our protocol was found to readily accommodate a variety of *para-* and *meta-* substituted cinnamic acids, including electron neutral (**3a-3d**), electron donating (**3e-3g**) and electron withdrawing substituents (**3h-3n**). Overall, the E/Z ratio was good to excellent for all these examples. In addition, the presence of halogens was well tolerated providing opportunities for further decoration of the molecule, e.g. via cross coupling (**3k-3n**). In addition, heterocyclic substrates, such as pyridine (**3o**) and thiophene (**3p**), were found to be competent substrates. The pyridine analogue displayed an excellent E/Z selectivity (99:1), while the thiophene one was obtained with a lower stereoselectivity (61:39). Extended conjugation, e.g. for (2*E*, 4*E*)-5-phenylpenta-2, 4-dienoic acid, was tolerated as well, delivering the corresponding product (**3q**) in good yield and excellent selectivity (81%, 99:1). Also, *β*-substituted cinnamic acids, e.g. 1, 1-diphenylethylene (**3r**), could be successfully subjected to our reaction conditions resulting in a good isolated yield (81% yield). The lower E/Z selectivity in some cases prompted us to evaluate the efficacy of *fac*-Ir(*t*Buppy)₃. This photocatalyst was recently reported by Weaver *et al.* and was shown lower the energy transfer rate due to the increased steric bulk.[11a] However, while an increase in yield was observed, the E/Z selectivity only marginally improved (**Scheme 2.1**, **3b** and **3p**).However, when *ortho*-substituted cinnamic acids were evaluated, a selectivity switch was observed towards the Z product (**Table 2.2**, Entry 1). Interestingly, the use of *fac*-Ir(*t*Buppy)₃ completely altered the selectivity (**Table 2.2**, Entry 2), confirming the observations of Weaver *et al.*[11a] We were delighted to find that an increase in concentration resulted in improvement in both yield and selectivity(**Table 2**, Entry 1 and 3). A further increase in catalyst loading and concentration contributed to an enhancement of the selectivity towards the Z-isomer (**Table 2.2**, Entry 4-6). Kinetic experiments revealed that the thermodynamically more stable E-isomer was formed first, after which the Z-isomer was obtained via a triplet-triplet energy transfer mechanism (TTET) (**Figure 2.6**).[11b] Consequently, it should theoretically be possible to stop the reaction before E/Z isomerization occurs. In order to obtain high conversions in a short amount of time, we turned our attention to the use of continuous-flow microreactors which allow to accelerate photocatalytic reactions due to an improved irradiation profile and enhanced mass transfer characteristics (**Table 2.3**, Entries 1-5).[13, 14]
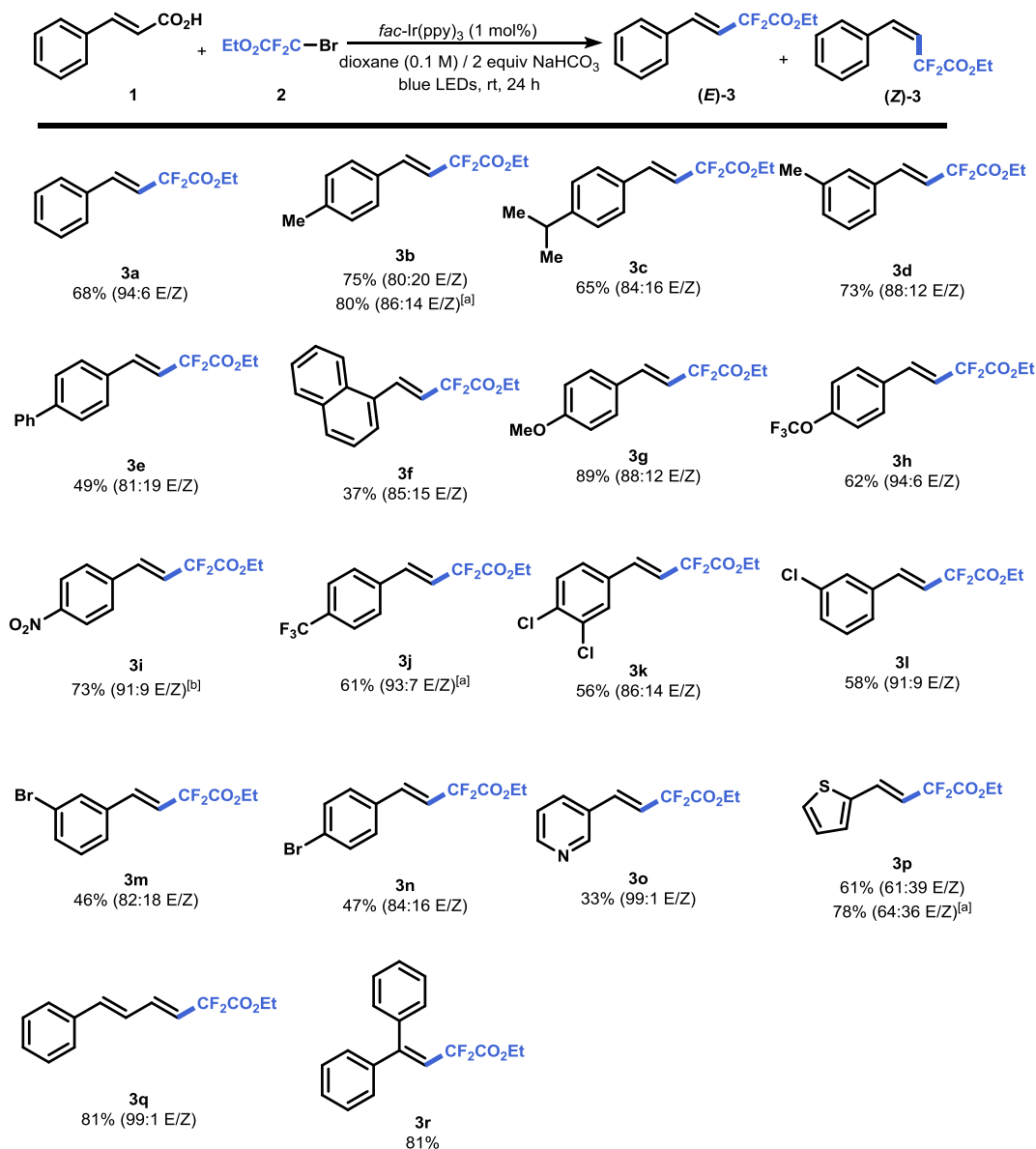
Scheme 2.1. Scope of *meta* and *para* substituted cinnamic Acids. 1) Reaction conditions: cinnamic acid **1** (0.2 mmol, 1.0 equiv), ethyl bromodifluoroacetate **2** (0.6 mmol, 3.0 equiv), *fac*-Ir(ppy)$_3$ (1 mol%), NaHCO$_3$ (0.4 mmol, 2.0 equiv), 1,4-dioxane (2.0 mL), Argon, blue LEDs (3.12 W), 24 h. 2) Reported yields are those of isolated compounds. 3) The ratios in parentheses represent *E*/*Z* ratios, determined by [1]**H-NMR** of isolated products. [a]*fac*-Ir(*t*Buppy)$_3$ was used as the photocatalyst. [b]Reaction time, 30 h.

Table 2.2. Optimization studies for the photocatalytic difluoromethylation of ortho-substituted cinnamic acids in batch [a]
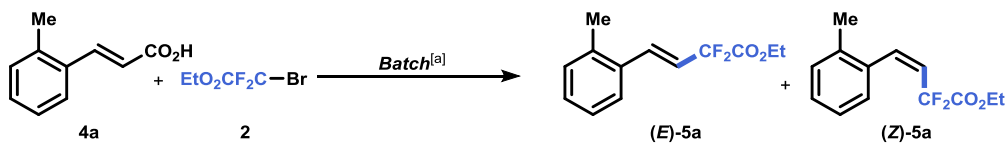
Entry	Conc.	*fac*-Ir(ppy)$_3$	Reaction Time	Yield[b]	E/Z[c]
Batch conditions[a]					
1	0.1 M	1 mol%	24 h	67 %	21:79
2[c]	0.1 M	1 mol%	24 h	60 %	79:21
3	0.2 M	1 mol%	24 h	86 %	15:85
4	0.2 M	3 mol%	24 h	88 %	10:90
5[d]	*0.5 M*	*3 mol%*	*24 h*	*77 %*	*6:94*
6[d]	1.0 M	2 mol%	24 h	57 %	5:95

[a]Reaction conditions in batch: *fac*-Ir(ppy)$_3$, (*E*)-3-(o-tolyl)acrylic acid **4a** (0.2 mmol), ethyl bromodifluoroacetate **2** (0.6 mmol), NaHCO$_3$ (0.4 mmol), H$_2$O(3.0 mmol), 1,4-dioxane, blue LEDs (3.12 W), room temperature, argon atmosphere, stirred for 24 hours; [b]Yield and *E/Z* values are determined with **^{19}F-NMR** using α,α,α-trifluorotoluene as internal standard. [c]*fac*-Ir(*t*Buppy)$_3$ was used as the photocatalyst. [d]Isolated yield and *E/Z* values are determined with ^{1}**H-NMR.**
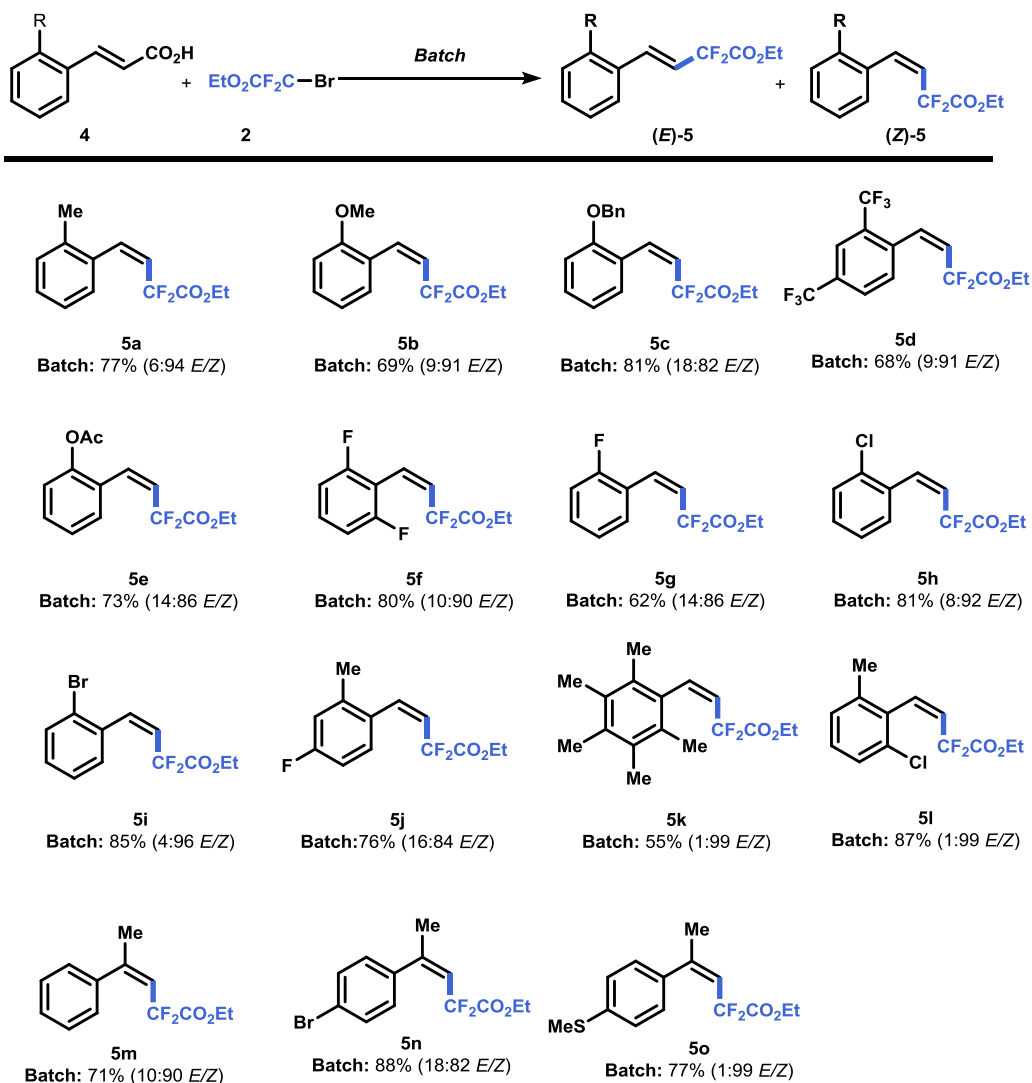
Scheme 2.2. Scope of *ortho* and *beta* substituted cinnamic Acids in batch. 1) Reaction conditions in batch: *fac*-Ir(ppy)$_3$ (3 mol%), *o*-cinnamic acid **4** (0.2 mmol), ethyl bromodifluoroacetate **2** (0.6 mmol), NaHCO$_3$ (0.4 mmol), H$_2$O (3.0 mmol), 1,4-dioxane (0.4 mL, 0.5 M), blue LEDs (3.12 W), room temperature, argon atmosphere, stirred for 24 hours; 2) Isolated yields. 3) The ratios in parentheses represent *E/Z* ratios, determined by **¹H-NMR** of isolated products.

In flow, the reaction time could be reduced significantly resulting in a reverse *E/Z* selectivity (**Table 2.3**, Entry 1). An increase in catalyst loading and concentration could further reduce the reaction time to 15 minutes resulting in an excellent *E* selectivity (62%, 92:8) (**Table 2.3**, Entry 5).[15] Longer residence time lead to an increase in yield but an erosion of the selectivity (**Table 2.3**, Entry 2-3). However, it should be noted that it was possible to recover the starting material quantitatively, which

can be subsequently reintroduced into the flow reactor obtaining higher overall conversions while maintaining a high stereoselectivity (see **Scheme 2.2**, **5g** and **3p**).

Table 2.3. Optimization studies for the photocatalytic difluoromethylation of *ortho*-substituted cinnamic acids continuous-flow[a]
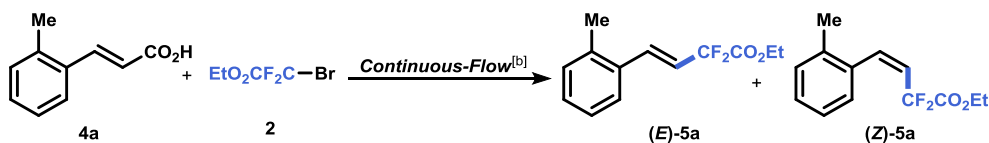
Entry	Conc.	*fac*-Ir(ppy)$_3$	Reaction Time	Yield[b]	E/Z[b]
Continuous-Flow conditions[a]					
1	0.05 M	0.5 mol%	2 h	51 %	75:25
2	0.1 M	0.5 mol%	2 h	68 %	68:32
3	0.1 M	1.0 mol%	2 h	46 %	26:74
4	0.1 M	1.5 mol%	0.5 h	55 %	78:22
5[c]	0.15 M	1.0 mol%	0.25 h	62 %	92:8

[a]Reaction conditions in continuous flow: : *fac*-Ir(ppy)$_3$ (1 mol%), (*E*)-3-(o-tolyl)acrylic acid **4a** (1.0 mmol), ethyl bromodifluoroacetate **2** (3.0 mmol), 2,6-lutidine (2.0 mmol), 1,4-dioxane/EtOH (v/v 5:1, 6.7 mL, 0.15 M), blue LEDs (3.12 W), room temperature, argon atmosphere. [b]Yield and *E/Z* values are determined with **^{19}F-NMR** using α,α,α-trifluorotoluene as internal standard. [c]Isolated yield and *E/Z* values are determined with ^{1}**H-NMR.**

Next, a diverse set of *ortho*-substituted cinnamic acids were examined in batch (**Scheme 2.2**). Cinnamic acids bearing electron-neutral (**5a**), electron-donating (**5b-c**) and electron-withdrawing substituents (**5d-e**) could be difluoromethylated in high *Z*-selectivity in batch, while the corresponding *E*-isomer could be readily accessed via continuous-flow processing (**Scheme 2.3**). Also, *o*-halogenated cinnamic acids were competent substrates (**5f-i**). Enhanced selectivity for the *Z*-isomer was observed with increasing steric bulk (F < Cl < Br). Interestingly, when both *ortho* positions are occupied with bulky groups (e.g. **5k-5l**), a high *Z*-selectivity was observed which could not be revoked via continuous-flow processing.
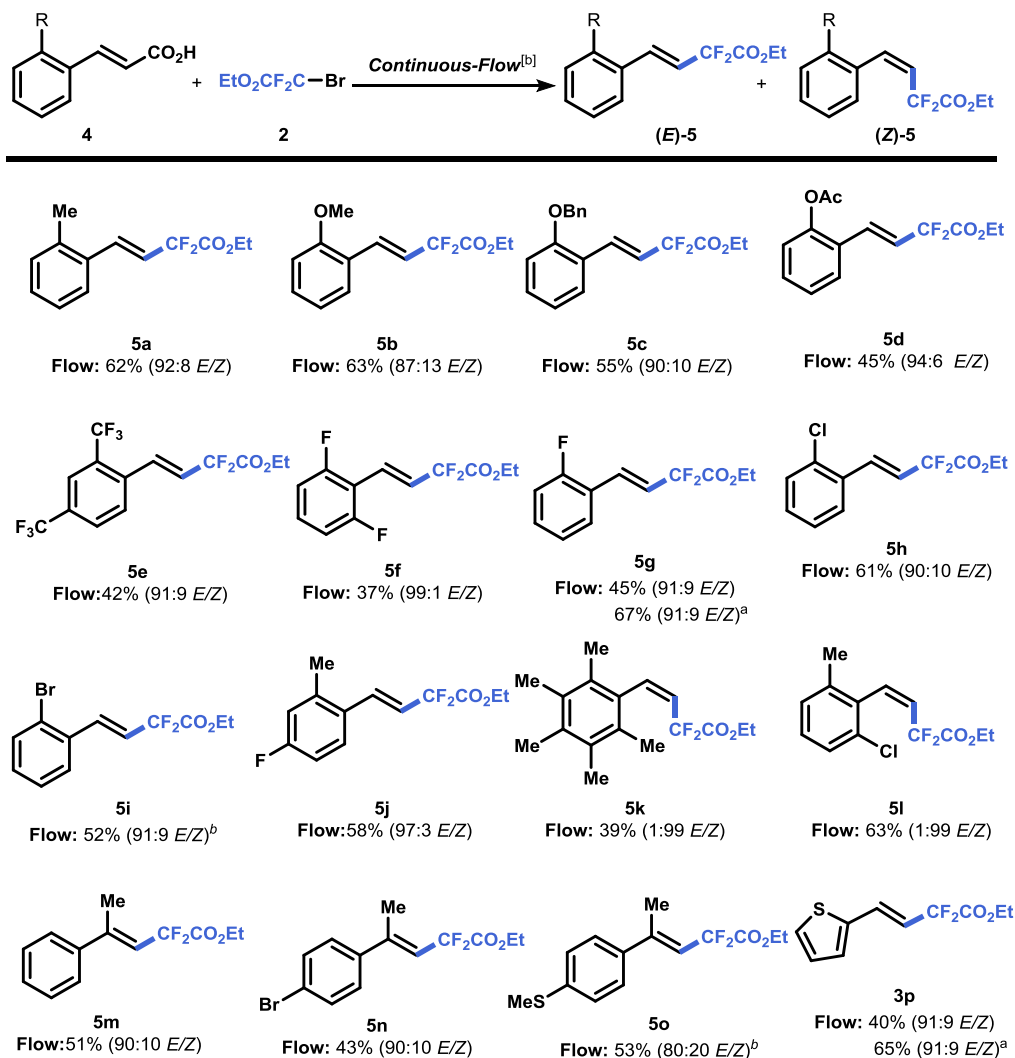
Scheme 2.3. 1) Reaction conditions in continuous flow: *fac*-Ir(ppy)$_3$ (1 mol%), *o*-cinnamic acid **4** (1.0 mmol), ethyl bromodifluoroacetate **2** (3.0 mmol), 2,6-lutidine (2.0 mmol), 1,4-dioxane/EtOH (v/v 5:1, 6.7 mL, 0.15 M), blue LEDs (3.12 W), room temperature, argon atmosphere, residence time: 15 minutes. 2) Isolated yields. 3) The ratios in parentheses represent *E/Z* ratios, determined by **¹H-NMR** of isolated products. [a]yield was based on one time starting material recycle. [b]10 minutes residence time.

This observation highlights the need for sterical bulk in the *ortho*-position to access the *Z*-stereoisomer. Furthermore, in the case of *β*-methyl substituted cinnamic acids, a similar trend in the selectivity was observed due to the steric effect of the *β*-substitutent (**5m**-**5o**). Finally, substrates with a low *E*-selectivity in batch (e.g. substrate **3p**) could be obtained in flow with an improved stereoselectivity.
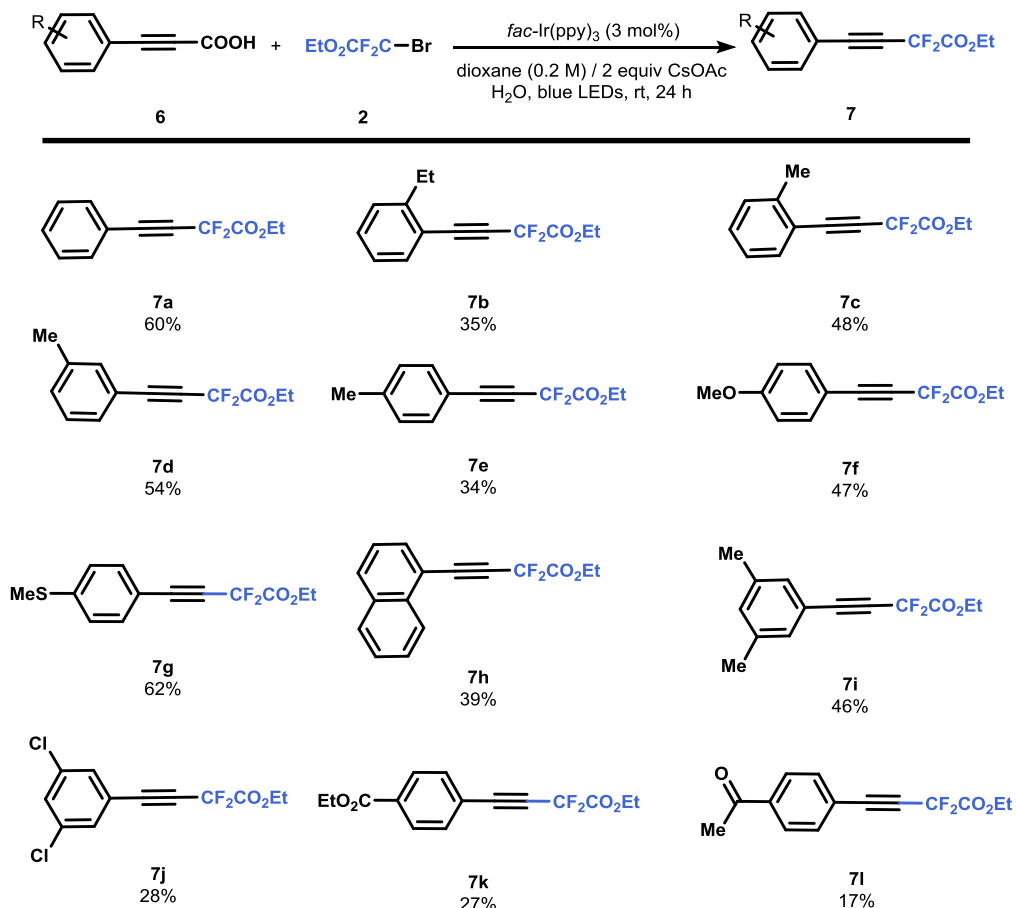
Scheme 2.4. Decarboxylative difluoromethylation of aryl propiolic acids. 1) Reaction conditions: aryl propiolic acid **6** (0.2 mmol, 1.0 equiv), ethyl bromodifluoroacetate **2** (0.6 mmol, 3.0 equiv), *fac*-Ir(ppy)$_3$ (3 mol%), CsOAc (0.4 mmol, 2.0 equiv), H$_2$O (2 mmol, 10 equiv.), 1,4-dioxane (1.0 mL), argon, blue LEDs (3.12 W), 24 h. 2) Reported yields are those of isolated compounds.

To further demonstrate the utility of our protocol, we sought to demonstrate its potential for the decarboxylative difluoromethylation of aryl propiolic acids. A small tweak of the reaction conditions (i.e. CsOAc as a base) resulted in the formation of the desired compounds in modest but synthetically useful yields (**Scheme 2.4**). Our protocol was successfully applied to *ortho-*, *meta-* and *para-*substituted aryl propiolic acids (**7a-7l**). These findings are noteworthy because, to the best of our knowledge, this is the first time that propiolic acids are used as substrates for photocatalytic decarboxylation chemistry.[6a-b]

Mechanistic study

A: UV-Vis absorption spectra:
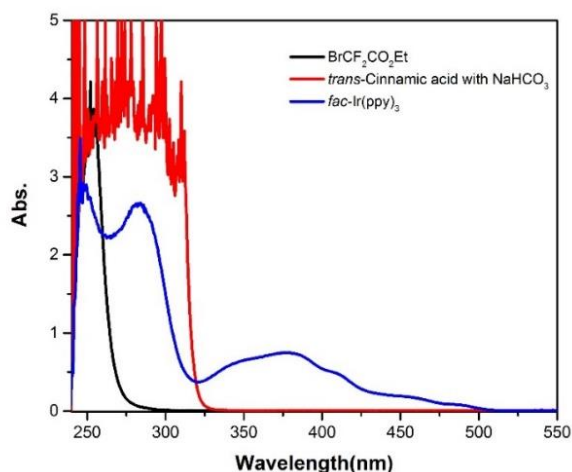
Figure 2.2: UV-Vis absorption spectra: The UV-Vis absorption spectra of ethyl bromodifluoroacetate and basic state of trans-cinnamic acid are below 330 nm in 1,4-dioxane, while *fac*-Ir(ppy)$_3$ exhibits moderate intense MLCT absorption in the range of 320-470 nm. These spectra indicate that the reaction is indeed initiated by photoexcitation of the *fac*-Ir(ppy)$_3$ complex.

B: Stern-Volmer experiments

All solutions were prepared in 1, 4-dioxane, the concentration of the *fac*-Ir(ppy)$_3$ is 7×10^{-6} mol/L, the trans-cinnamic acid 0.01 mol/L with 2.0 equivalent of base NaHCO$_3$, the ethyl bromodifluoroacetate solution 0.0156 mol/L. All samples were bubbled with a stream of argon for 8 hours via a syringe needle prior to use. The *fac*-Ir(ppy)$_3$ solution and the quencher were irradiated at $\lambda = 410$ nm and the emission intensity was recorded between 540-600 nm in a quartz flow cuvette (Hellma analytics, quartz suprasil, art nr. 176-751-85-40). The spectra compose the average data of at least 5 times.

For each quenching experiment, the emission intensity of the solution of *fac*-Ir(ppy)$_3$ with different concentration of quencher, the quencher was: (a) *trans*-cinnamic acid with 2 equivalent of base NaHCO$_3$; (b) ethyl bromodifluoroacetate; (c) *trans*-cinnamic acid.(I$_0$: the intensity without quencher, I: the intensity with quencher, the rate constant was calculated according to K$_{SV}$ = k$_q$τ$_0$, τ$_0$ = 1.9 μs).

Table 2.4: the rate constant of the compound.

Entry	Quencher	Rate Constant(M^{-1} s^{-1})
a	*trans*-cinnamic acid with 2 equiv. of $NaHCO_3$	1.24×10^8
b	ethyl bromodifluoroacetate	1.84×10^8
c	*trans*-cinnamic acid	3.37×10^8

The rate constant of *trans*-cinnamic acid was much reduced by the addition of base (Entry a and c), indicating the necessity of adding base to this reaction. $k_q(a)$ is less than $k_q(b)$, this indicates that the reductive quenching of photoexcited *fac*-Ir(ppy)$_3$ by ethyl bromodifluoroacetate dominate. As the spectral overlap of absorption of ethyl bromodifluoroacetate **2** and photoluminescence of *fac*-Ir(ppy)$_3$ is rather small, the energy transfer from the excited *fac*-Ir(ppy)$_3$ to **2** would be negligible. The photoluminescence quenching is therefore attributed to the electron transfer from the excited *fac*-Ir(ppy)$_3$ to ethyl bromodifluoroacetate **2**.
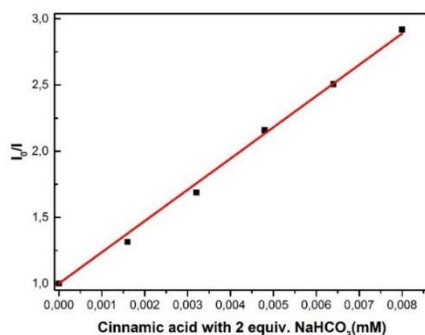
Figure 2.3: The Stern-Volmer plot with cinnamic acid with base. $y = 236.05x+1 (R^2 = 0.999)$
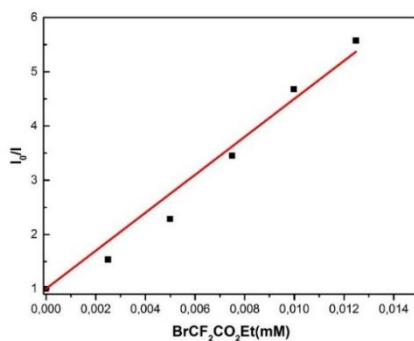
Figure 2.4: The Stern-Volmer plot with $BrCF_2CO_2Et$. $y = 350.05x+1 (R^2 = 0.992)$
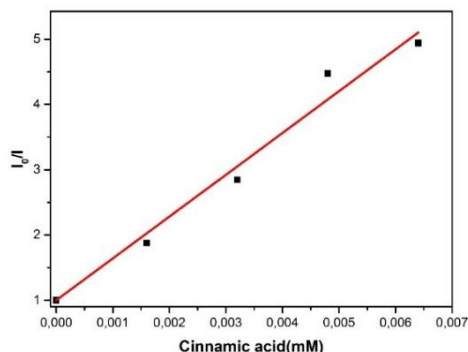
Figure 2.5: The Stern-Volmer plot with cinnamic acid. y= 640.47x+1(R^2= 0.995)

C: Radical Trapping Experiment with TEMPO and BHT

[M+Na]$^+$: 365.1904 (*35% isolated*)
Found: 365.1904

[M+H]$^+$: 280.1724
Found:280.1722
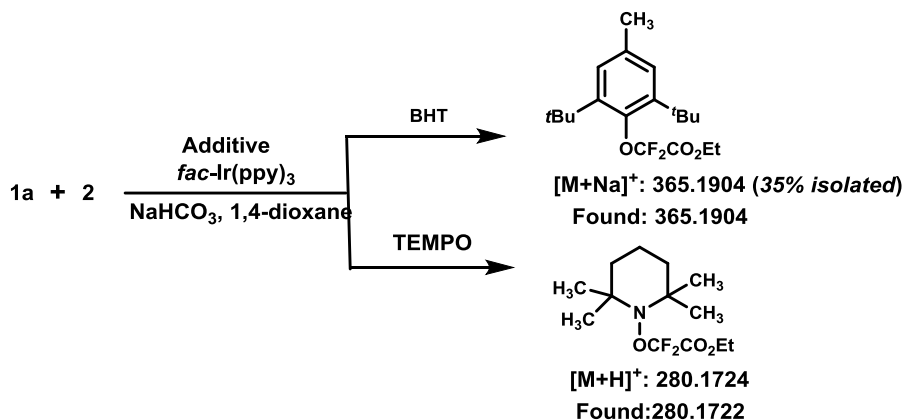
An oven-dried reaction tube (7.5 mL) was charged with cinnamic acid **1a** (0.2 mmol, 1.0 equiv.), diethyl bromodifluoroacetate (0.6 mmol, 3.0 equiv.), *fac*-Ir(ppy)$_3$ (1.3 mg, 1.0 mol%), NaHCO$_3$ (33.6 mg, 0.4 mmol, 2 equiv.), BHT or TEMPO (0.4 mmol, 2 equiv.) and a magnetic stirring bar in 1,4-dioxane (2.0 mL), sealed with a rubber septum. The mixture was subsequently degassed 3 times (freeze-pump-thaw method: cooled to −78 °C and degassed via vacuum evacuation (5 min), backfilled with argon, and warm to room temperature), then irradiated with blue LED (at approximately 1 cm distance from the light source). The temperature in the reactor was kept at room temperature. The reaction was kept for 24 hours. The target product could not be detected by HRMS. Instead the BHT−CF$_2$CO$_2$Et and TEMPO−CF$_2$CO$_2$Et adduct were observed in the HRMS and the BHT−CF$_2$CO$_2$Et was also isolated, which gave a direct evidence for the involvement of •CF$_2$CO$_2$Et radical in the reaction.

D: Time / Isomerization experiments

In order to determine the erosion of the *E*/*Z*-configuration during the decarboxylation reaction, the reaction was monitored by **^{19}F-NMR** over time. Two mixtures were prepared according to General procedure on a 2.0 mmol scale (10 mL) and irradiated with a Blue LED (1.5 × 3.12 W). Samples were collected and analyzed for every 30 minutes by **^{19}F-NMR**.
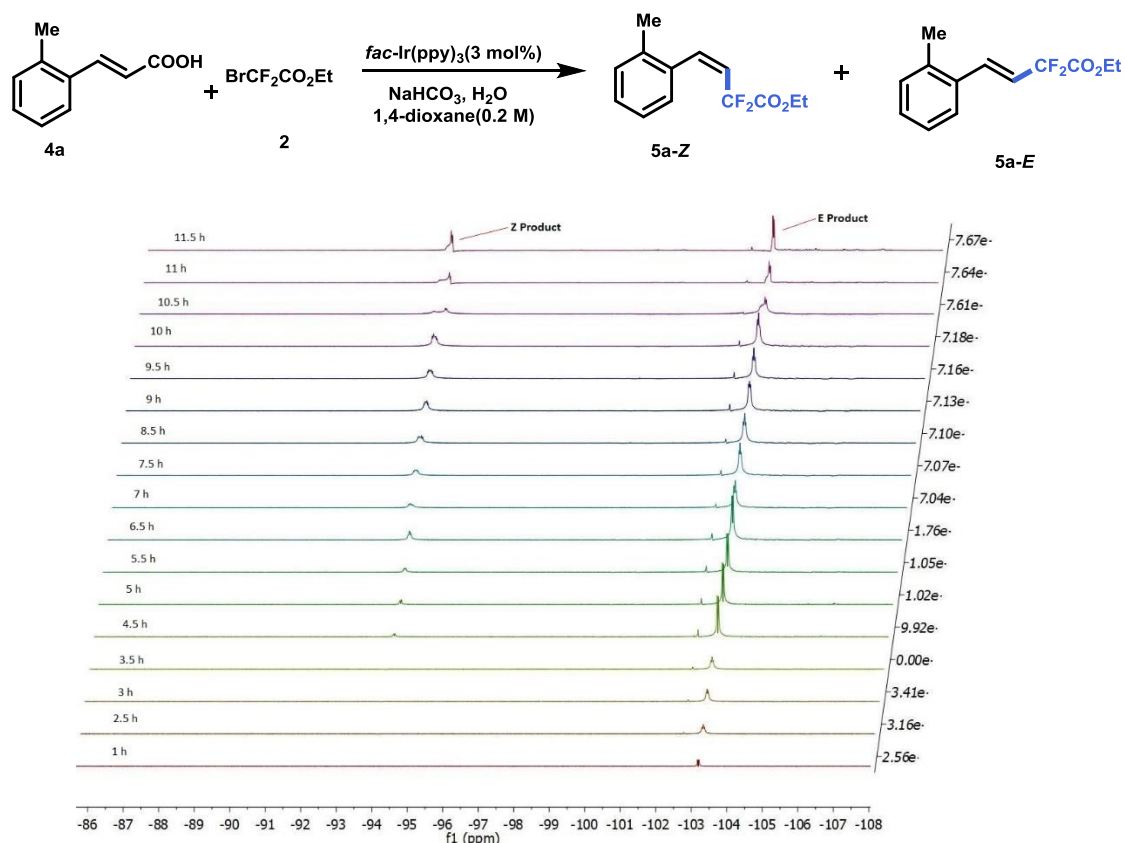
Figure 2.6: **^{19}F-NMR** of the substrates with **4a** and **2**, followed in time with Blue-LEDs light source.

Based on the above results and literature reports, we suggest a plausible mechanism for this visible-Light photocatalyzed decarboxylative difluoroalkylation reactions, which was depicted in **Scheme 2.5**. Photoexcitation of the photocatalyst *fac*-Ir(ppy)$_3$ with blue LEDs undergoes the metal-to-ligand charge transfer (MLCT) excited states of *fac*-[Ir^{3+}(ppy)$_3$]* Photoluminescence quenching experiments shows that the photoexcited *fac*-[Ir^{3+}(ppy)$_3$]* was quenched by **2** at the rate constant of 1.84×10^8 M^{-1} s^{-1}. The luminescence of the photocatalyst can also be quenched by basic state of cinnamic acid A with a lower rate constant at 1.24×10^8 M^{-1} s^{-1}. As the spectral overlap of absorption of ethyl bromodifluoroacetate **2** and photoluminescence of *fac*-Ir(ppy)$_3$ is rather small, the energy transfer from the excited *fac*-Ir(ppy)$_3$ to **2** would be negligible. The photoluminescence quenching is therefore

attributed to the electron transfer from the excited *fac*-Ir(ppy)$_3$ to ethyl bromodifluoroacetate **2**. The addition of base reduce the quenching rate of cinnamic acid from 3.37×10^8 M^{-1} s^{-1} to 1.24×10^8 M^{-1} s^{-1}, resulting in the photocatalyst quenching exclusively initiate by **2**. The key intermediate ·CF$_2$CO$_2$Et along with *fac*-[Ir(ppy)$_3$] $^+$ was produced with the SET process.

The radical was also captured by radical trapping reagent BHT. Then intermolecular π-addition of the radical to A produces a benzylic radical B. Further SET from radical B to *fac*-[Ir(ppy)$_3$]$^+$ affords carbocation C and release the CO$_2$ to regenerates the photocatalyst. As long lifetime (τ_0=1.9 μs)[5a] and high energy (E$_T$ = 2.41 eV)[12a,b] of triplet states of *fac*-[Ir^{3+}(ppy)$_3$]*, the olefinic trans product was excited to reach the lowest-energy triplet state, which will decay to give the mixture of *Z* and *E* alkene. ($E_{1/2}^{red}$ [*Ir^{3+}/Ir^{4+}] = -1.72 V vs SCE), which engages in single-electron reduction with **2** (E^{red}=-0.57 V vs SCE)[12c] to afford the ·CF$_2$CO$_2$Et radical.
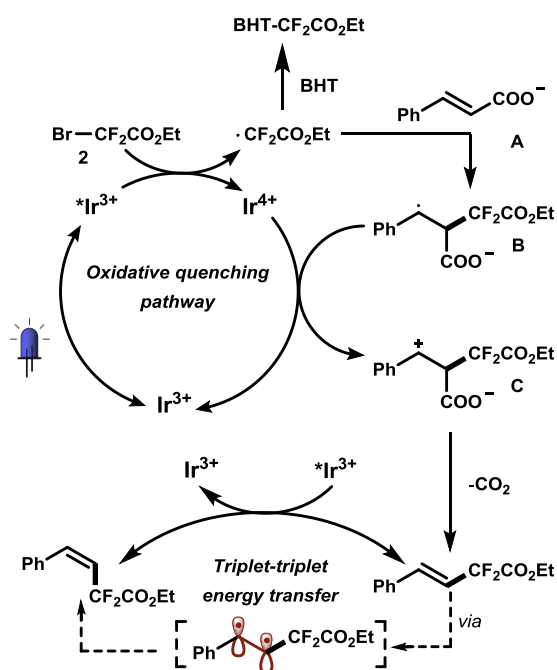
Scheme 2.5. Proposed Catalytic Cycle

Conclusion

In this work, we have introduced a simple yet effective photocatalytic decarboxylative protocol to prepare difluoromethylated styrenes and phenylacetylenes. In contrast to previously described methods, this procedure does not require additional metal catalysts nor hypervalent iodine reagents to facilitate CO_2 extrusion. The generality of our protocol is demonstrated by the broad substrate scope (*difluoromethylated styrenes*: 28 *E*-selective examples and 15 *Z*-selective; & *difluoromethylated phenylacetylenes*: 12 examples). *Ortho*-substituted cinnamic acids give the less stable *Z*-selective products. The thermodynamically favored *E*-stereoisomer could be readily obtained in continuous-flow through accurate control of the reaction time. Having access to both stereoisomers simply by changing the reactor is a unique and powerful approach and provides opportunities for other photocatalytic transformations.

Experimental Section

General procedures for the photocatalytic decarboxylation in batch

An oven-dried reaction tube (7.5 mL) was charged with cinnamic acid (0.2 mmol, 1.0 equiv.), ethyl bromodifluoroacetate (0.6 mmol, 3.0 equiv.), *fac*-Ir(ppy)$_3$ (1.3 mg, 1.0 mol%), NaHCO$_3$ (33.6 mg, 0.4 mmol, 2 equiv.) and a magnetic stirring bar in 1,4-dioxane (2.0 mL), sealed with a rubber septum and subsequently degassed 3 times (freeze-pump-thaw: cooled to −78 °C and degassed via vacuum evacuation (5 min), backfilled with argon, and warm to room temperature). Next the reaction mixture was irradiated with blue LEDs (at approximately 1 cm distance from the light source). The temperature in the reactor was kept at room temperature. After 24 hours, the mixture was transferred to a 50 mL flask with about 20 mL CH$_2$Cl$_2$. The solvent was subsequently removed under reduced pressure and the residue was purified by silica gel column chromatography using petroleum ether/ethyl acetate to give the desired product.

An oven- dried reaction tube (7.5 mL) was charged with *o*-cinnamic acid (0.2 mmol, 1.0 equiv.), ethyl bromodifluoroacetate (0.6 mmol, 3.0 equiv.), *fac*- Ir(ppy)$_3$ (3.9 mg, 3.0 mol%), NaHCO$_3$ (33.6 mg, 0.4 mmol, 2 equiv.), H$_2$O (3.0 mmol, 15 equiv.) and a magnetic stirring bar in 1,4-dioxane (0.4 mL), sealed with a rubber septum and subsequently degassed 3 times (freeze-pump-thaw: cooled to −78 °C and degassed via vacuum evacuation (5 min), backfilled with argon, and warm to room temperature). Next the reaction mixture was irradiated with blue LEDs (at approximately 1 cm distance from the light source). The temperature in the reactor was kept at room temperature. After 24 hours, the mixture was transferred to a 50 mL flask with about 20 mL CH$_2$Cl$_2$, then dried over MgSO$_4$. The solvent was subsequently removed under reduced pressure and the residue was purified by silica gel column chromatography using petroleum ether/ethyl acetate to give the desired product.
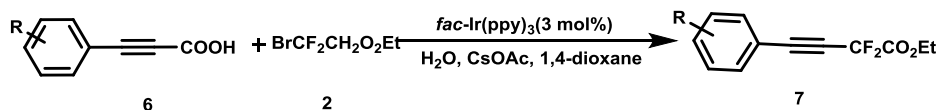
An oven-dried reaction tube (7.5 mL) was charged with aryl propiolic acids (0.2 mmol, 1.0 equiv.), ethyl bromodifluoroacetate (0.6 mmol, 3.0 equiv.), *fac*-Ir(ppy)$_3$ (3.9 mg, 3.0 mol%), CsOAc (76.8 mg, 0.4 mmol, 2 equiv.), H$_2$O (2.0 mmol, 10 equiv.) and a magnetic stirring bar in 1,4-dioxane (1.0 mL), sealed with a rubber septum and subsequently degassed 3 times (freeze-pump-thaw: cooled to −78 °C and degassed via vacuum evacuation (5 min), backfilled with argon, and warm to room temperature. Next the reaction mixture was irradiated with blue LEDs and a balloon with argon was sealed. The temperature in the reactor was kept at room

temperature. After 24 hours, the mixture was transferred to a 50 mL flask with about 20 mL CH_2Cl_2. The solvent was subsequently removed under reduced pressure and the residue was purified by silica gel column chromatography using petroleum ether/ethyl acetate to give the desired product.

B: a: General procedures for the photocatalytic decarboxylation in flow

O-Cinnamic acid (1.0 mmol), *fac*-Ir(ppy)₃ (6.5 mg, 1.0 mol%), $BrCF_2CO_2Et$ (609.0 mg, 3.0 mmol, 3 equiv.), 2,6-lutidine (214 mg, 2.0 mmol, 2 equiv.) was dissolved in 1,4-dioxane/EtOH = 5:1 (v/v, 6.7 mL) and subsequently degassed 3 times (freeze-pump-thaw: cooled to −78 °C and degassed via vacuum evacuation (5 min), backfilled with argon, and warm to room temperature). This reaction mixture was then transferred into a syringe (10 mL) and loaded onto a syringe pump. The reaction mixture was pumped through the microreactor with the desired flow rate (0.053 mL/min). The microreactor assembly was irradiated with a Blue LED array (1.5 × 3.12 Watts) at room temperature. The continuous reaction was allowed to reach steady state prior to collection of the product fractions. A standard residence time of 15 minutes was utilized. The crude product was collected at the end of the reactor. Workup and purification were done following the batch procedure.

b: Procedures for the recycling the starting material for photocatalytic decarboxylation in flow

O-Cinnamic acid (1.5 mmol), *fac*-Ir(ppy)₃ (9.8 mg, 1 mol%), $BrCF_2CO_2Et$ (609.0 mg, 3.0 mmol, 3 equiv.), 2,6-lutidine (321 mg, 2.0 mmol, 2 equiv.) was dissolved in 1,4-dioxane/EtOH = 5:1 (v/v, 10.0 mL) and subsequently degassed 3 times (freeze-pump-thaw: cooled to −78 °C and degassed via vacuum evacuation (5 min), backfilled with argon, and warm to room temperature). This reaction mixture was then transferred into a syringe (10 mL) and loaded onto a syringe pump. The reaction mixture was pumped through the microreactor with the desired flow rate (0.053 mL/min). All the mixture was collected and 15 mL of HCl (1.0 M) was added, the aqueous phase and organic phase are dried separately. The two parts were combined together and purified to get the product and the *o*-cinnamic acid, which was used to be the starting material for the next run of the flow experiment.

C: Set-ups for the flow reactions

All microfluidic fittings were purchased from IDEX Health and Science. The syringes were connected to the capillary using ¼-28 flat-bottom flangeless fittings. A syringe pump (Fusion 200 Classic) equipped with a 10 mL syringe was used to infuse the liquid reagents into a reactor coil fabricated from a high purity perfluoroalkoxyalkane (PFA) capillary tubing (ID = 500 μm). The microreactor assembly was constructed of high purity PFA tubing (IDEX health and science, part no. 1622L) (L = 3.9 meters, ID = 500 μm, V = 0.79 mL) in combination with 1.5 Blue LEDs (3.12 W). The outlet of the microreactor led to the collection vial which is protected by aluminum foil. The reactor was cooled with pressurized air to keep it at room temperature. The detail of the assembling the reactor is based on the literature.

D: Pictures for the set-up.
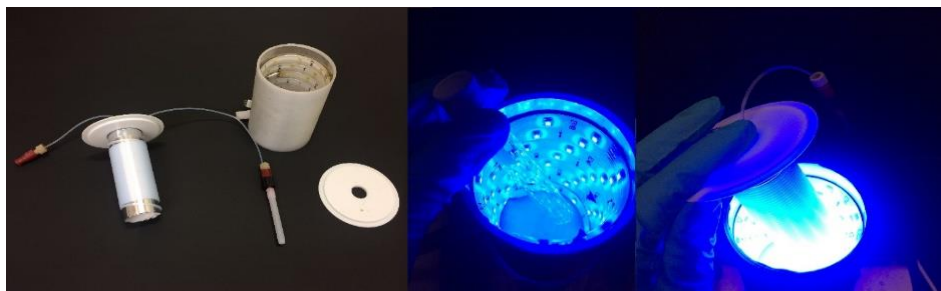
Figure 2.7: Left) pieces for the set-ups for both batch and flow reactor; Middle) inside overview of the batch reactor; Right) inside overview of the flow reactor.
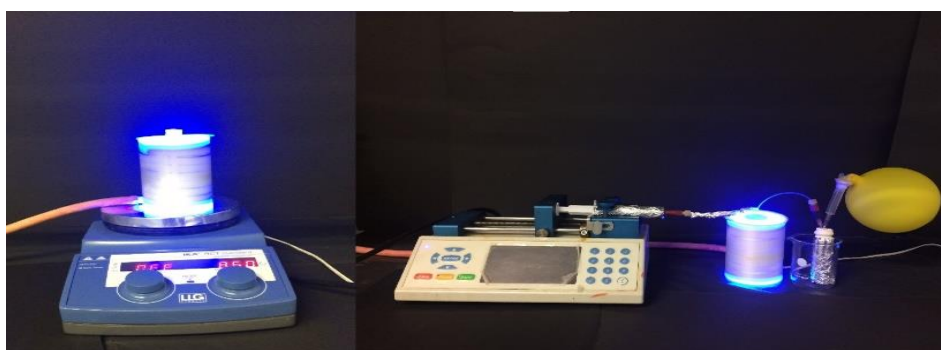
Figure 2.8: Left): Set-up for the batch reaction; 2) Right): Set-up for the flow reaction.
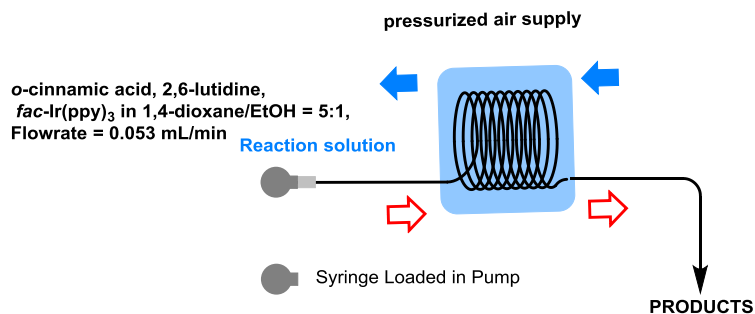
Figure 2.9: Schematic representations of decarboxylation of *ortho*-substituted cinnamic acid in flow.

Compound Characterization

Ethyl 2, 2-difluoro-4-phenylbut-3-enoate(3a)

Purification: Column chromatography (PE/Et$_2$O = 30:1) isolated as a colorless oil (68% yield). E/Z: 94:6.

^{1}H NMR (400 MHz, CDCl$_3$): δ 7.48-7.45(m, 2H), {Z: 7.09 (dt, J = 16.0, 4.0 Hz), E: 6.96 (dt, J = 12.0, 4.0 Hz), 1H}, {E: 6.32 (dt, J = 16.0, 12.0 Hz), Z: 5.77(q, J = 12.0 Hz), 1H}, {E:4.37 (q, J = 8.0 Hz), Z: 4.05(q, J = 8.0 Hz), 2H}, {E: 1.38 (t, J = 8.0 Hz), Z: 1.14 (t, J = 8.0 Hz), 3H}. **^{13}C NMR** (100 MHz, CDCl$_3$): δ 163.9 (t, J = 35.0 Hz), 136.8(t, J = 9.0 Hz), 134.1, 129.6, 128.8, 128.2, 127.4, 118.8 (t, J = 25.0 Hz), 112.7 (t, J = 247.0 Hz), 63.1, 14.0. **^{19}F NMR** (376 MHz, CDCl$_3$): δ -93.99 (d, J = 13.6 Hz), -103.24 (dd, J = 11.5, 2.7 Hz). **IR**: υ (cm^{-1}): 2970, 2927, 1767, 1655, 1454, 1296, 1976, 910, 732. **HRMS** (**ESI**) (m/z): [M+Na]$^+$ calcd. for C$_{12}$H$_{12}$F$_2$NaO$_2$: 249.0703, found: 249.0700.

Ethyl (E)-2, 2-difluoro-4-(p-tolyl)but-3-enoate(3b)

Purification: Column chromatography (PE/Et$_2$O = 30:1) isolated as a colorless oil (75% yield). E/Z: 80:20.

^{1}H NMR (400 MHz, CDCl$_3$): δ 7.42(d, J = 8.0 Hz, 2H), 7.33(d, J = 8.0 Hz, 2H), 7.25-7.22(m, 1H), 7.62-7.60 (m, 2H), {E: 7.57(d, J = 8.0 Hz), Z: 7.48(d, J = 12.0 Hz), 2H}, {E: 7.13 (dt, J = 16.0, 4.0 Hz), Z: 6.98(d, J = 12.0 Hz), 1H}, {E: 7.13 (dt, J = 16.0, 4.0 Hz), Z: 6.98(d, J = 12.0 Hz), 1H}, {E: 6.33 (dt, J = 16.0, 12.0 Hz), Z: 5.90(q, J = 12.0 Hz), 1H}, {E:4.43 (q, J = 8.0 Hz), Z: 4.14(q, J = 8.0 Hz), 2H}, {E:2.45 (s), Z: 2.43(s), 3H}, {E: 1.44 (t, J = 8.0 Hz), Z: 1.22 (t, J = 8.0 Hz), 3H)}. **^{13}C NMR** (100 MHz, CDCl$_3$): δ 164.0 (t, J = 35.0 Hz), 139.9, 138.7 (t, J = 8.0 Hz), 136.7 (t, J = 10.0 Hz), 131.4, 131.3, 129.5, 129.0(t, J = 3.0 Hz), 128.9, 127.4, 121.0 (t, J = 28.0 Hz), 117.7 (t, J = 25.0 Hz), 112.9 (t, J = 247.0 Hz), 63.1, 21.3, 14.0, 13.6. **^{19}F NMR** (376 MHz, CDCl$_3$): δ -94.04, -103.00. **IR**: υ (cm^{-1}) 2924, 1767, 1508, 1296, 1076, 910, 802, 733. **HRMS** (**ESI**) (m/z): [M+Na]$^+$ calcd. for C$_{13}$H$_{14}$F$_2$NaO$_2$: 263.0860, found: 263.0854.

Ethyl (E)-2, 2-difluoro-4-(4-isopropylphenyl)but-3-enoate(3c)

Purification: Column chromatography (PE/Et$_2$O = 30:1) isolated as a colorless oil (65% yield). E/Z: 84:16.

^{1}H NMR (400 MHz, CDCl$_3$): δ {Z: 7.73-7.48(m), E: 7.39(d, J = 8.0 Hz), 2H}, 7.25-7.22(m, 2H), {E: 7.57(dt, J = 16.0, 4.0 Hz), Z: 6.92(d, J = 12.0 Hz), 1H}, {E: 6.26 (dt, J = 16.0, 12.0 Hz), Z: 5.83(q, J = 12.0 Hz), 1H}, {E:4.35(q, J = 8.0 Hz), Z: 4.04(q, J = 8.0 Hz), 2H}, 2.93(heptet, J = 8.0 Hz, 1H), {E: 1.37 (t, J = 8.0 Hz), Z: 1.11 (t, J = 8.0 Hz), 3H}, {E:1.27(s), Z:1.25(s), 3H}. **^{13}C NMR** (100 MHz, CDCl$_3$): δ 150.8, 136.7 (t, J = 9.0 Hz), 131.7, 127.5, 126.9, 126.3, 117.9(t, J = 15.0 Hz), 112.9, 63.1, 34.0, 29.7, 23.8, 14.0. **^{19}F NMR** (376 MHz, CDCl$_3$): δ -94.04, -103.00. **IR**: υ (cm^{-1}) 1697, 1508, 902, 725, 648. **HRMS** (**ESI**) (m/z): [M+Na]$^+$ calcd. for C$_{15}$H$_{18}$F$_2$NaO$_2$: 291.1173, found: 291.1167.

Ethyl (E)-2, 2-difluoro-4-(m-tolyl)but-3-enoate(3d)

Purification: Column chromatography (PE/Et$_2$O = 30:1) isolated as a colorless oil (73% yield). *E/Z*: 88:12.

^{1}H NMR (400 MHz, CDCl$_3$): δ 7.28-7.25 (m, 3H), 7.21-7.17 (m, 1H), {Z: 7.07 (dt, J = 16.0, 4.0 Hz), E: 6.94 (d, J = 12.0 Hz), 1H}, {E: 6.30 (dt, J = 16.0, 12.0 Hz), Z: 5.87 (q, J = 8.0 Hz), 1H}, {E: 4.37 (q, J = 8.0 Hz), Z: 4.03 (q, J = 8.0 Hz), 2H}, {E: 2.38 (s), Z: 2.36 (s), 3H}, {E: 1.38 (t, J = 8.0 Hz), Z: 1.14 (t, J = 8.0 Hz), 3H}. **^{13}C NMR** (100 MHz, CDCl$_3$): δ 164.0 (t, J = 35.0 Hz), 138.8(t, J = 9.0 Hz), 138.5, 137.8, 136.9(t, J = 10.0 Hz),

134.0, 130.4, 129.4, 128.7, 128.1, 128.0, 125.9, 124.6, 121.8(t, J = 28.0 Hz), 118.6 (t, J = 25.0 Hz), 112.8 (t, J = 247.0 Hz), 63.1, 21.3, 14.0. **19F NMR** (376 MHz, CDCl$_3$): δ -93.64 (dd, J = 11.3, 3.7 Hz), -103.18 (dd, J = 11.3, 3.7 Hz). **IR**: υ (cm^{-1}) 2982, 1763, 1655, 1373, 1296, 1219, 1168, 1072, 906, 686. **HRMS** (**ESI**) (m/z): [M+Na]$^+$ calcd. for C$_{13}$H$_{14}$F$_2$NaO$_2$: 263.0860, found: 263.0859.

Ethyl (E)-4-([1, 1'-biphenyl]-4-yl)-2,2-difluorobut-3-enoate(3e)

Purification: Column chromatography (PE/Et$_2$O = 30:1) isolated as a colorless oil (49% yield). E/Z: 81:19.

1H NMR (400 MHz, CDCl$_3$): δ 7.64-7.58 (m, 5H), 7.56-7.53 (m, 2H), 7.49-7.44 (m, 1H), 7.41-7.36 (m, 1H), {E: 7.14 (dt, J = 16.0, 4.0 Hz), Z: 7.00-6.96(m), 1H}, {E: 6.36 (dt, J = 16.0, 12.0 Hz), Z: 5.91 (q, J = 12.0 Hz), 1H}, {E: 4.38 (q, J = 8.0 Hz), Z: 4.10 (d, J = 8.0 Hz), 2H}, {E: 1.39 (t, J = 8.0 Hz), Z: 1.17 (t, J = 7.1 Hz), 3H}. **13C NMR** (100 MHz, CDCl$_3$): δ 163.9 (t, J = 35.0 Hz), 142.4, 141.5, 140.3, 140.2, 138.3, 136.4 (t, J = 10.0 Hz), 129.5 (t, J = 3.0 Hz), 128.9, 128.8, 127.9, 127.7, 127.6, 127.5, 127.0, 126.8, 121.7 (t, J = 28.0 Hz), 118.7 (t, J = 25.0 Hz), 112.8 (t, J = 247.0 Hz), 63.1, 14.0. **19F NMR** (376 MHz, CDCl$_3$): δ -94.26 (d, J = 13.2 Hz), -103.12 (dd, J = 11.4, 2.6 Hz). **IR**: υ (cm^{-1}) 2978, 2885, 1762, 1384, 1153, 1076, 906, 729. **HRMS** (**ESI**) (m/z): [M+Na]$^+$ calcd. for C$_{18}$H$_{16}$F$_2$NaO$_2$: 325.1016, found: 325.1016.

Ethyl (E)-2,2-difluoro-4-(naphthalen-1-yl)but-3-enoate(3f)

Purification: Column chromatography (PE/Et$_2$O = 30:1) isolated as a colorless oil (37% yield). E/Z: 81:19.

1H NMR (400 MHz, CDCl$_3$): δ 8.09 (d, J = 8.0 Hz, 1H), 7.93-7.86 (m, 2H), 7.66 (d, J = 8.0 Hz, 1H), 7.60-7.43 (m, 3H), {E: 6.39 (dt, J = 16.0, 12.0 Hz), Z: 6.21 (q, J = 12.0 Hz), 1H}, {E: 4.40 (q, J = 8.0 Hz), Z: 3.48 (q, J = 8.0 Hz), 2H}, {E: 1.40 (t, J = 8.0 Hz), Z: 0.74 (t, J = 8.0 Hz), 3H}. **13C NMR** (100 MHz, CDCl$_3$): δ 163.9, 134.3(t, J = 10.0 Hz), 131.8, 131.1, 130.9, 129.9, 129.2, 128.7, 128.5, 126.7, 126.2, 125.4, 125.1, 124.7(t, J = 2.0 Hz), 121.9(t, J = 25.0 Hz), 112.6(t, J = 248.0 Hz), 63.2, 14.0. **19F NMR** (376 MHz, CDCl$_3$): δ -92.89(d, J = 11. Hz), -103.12, **IR**: υ (cm^{-1}) 2980, 1800, 1380, 1250, 1080, 906. **HRMS** (**ESI**) (m/z): [M+Na]$^+$ calcd. for C$_{16}$H$_{14}$F$_2$NaO$_2$: 299.0860, found: 299.0859.

Ethyl (E)-2, 2-difluoro-4-(4-methoxyphenyl) but-3-enoate(3g)

Purification: Column chromatography (PE/Et$_2$O = 8:1) isolated as a colorless oil (89% yield). E/Z: 88:12.

1H NMR (400 MHz, CDCl$_3$): δ {E: 7.42-7.38 (m), Z: 7.35-7.33(m), 2H}, 7.03 (dt, J = 16.0, 4.0 Hz, 1H), {Z: 6.94-6.88 (m), E: 6.87-6.82 (m), 2H}, {E: 6.17 (dt, J = 16.0, 12.0 Hz), Z: 5.77(q, J = 12.0 Hz), 1H}, {E:4.36 (q, J = 8.0 Hz), Z: 4.11(q, J = 8.0 Hz), 2H}, {E: 3.84 (s), Z: 3.82 (s), 3H}, {E: 1.37 (t, J = 8.0 Hz), Z: 1.17 (t, J = 8.0 Hz), 3H}. **13C NMR** (100 MHz, CDCl$_3$): δ 164.1 (t, J = 35.0 Hz), 160.8, 160.0, 138.4 (t, J = 9.0 Hz), 136.3(t, J = 9.0 Hz), 130.8, 128.9, 126.8 (t, J = 2.0 Hz), 119.80 (t, J = 28.0 Hz), 116.4 (t, J = 24.0 Hz), 114.2, 113.6, 112.9(t, J = 247.0 Hz), 63.0, 55.4, 14.0, 13.7. **19F NMR** (376 MHz, CDCl$_3$): δ -94.12 (d, J = 13.6 Hz), -102.67 (dd, J = 11.5, 2.7 Hz). **IR**: υ (cm^{-1}) 2978, 1762, 1512, 1253, 1076, 902, 725, 648. **HRMS** (**ESI**) (m/z): [M+Na]$^+$ calcd. for C$_{13}$H$_{14}$F$_2$NaO$_3$: 279.0809, found: 279.0812.

Ethyl (E)-2,2-difluoro-4-(4-(trifluoromethoxy)phenyl)but-3-enoate(3h)

Purification: Column chromatography (PE/Et$_2$O = 30:1) isolated as a colorless oil (62% yield). E/Z: 94:6.

1H NMR (400 MHz, CDCl$_3$): δ {E: 7.51-7.47 (m), Z: 7.41 (d, J = 8.0 Hz), 2H}, {E: 7.25-7.22 (m), Z: 7.20 (d, J = 8.0 Hz), 2H}, {E: 7.08 (dt, J = 16.0, 4.0 Hz), Z: 6.92 (d, J = 12.0 Hz), 1H}, {E: 6.30 (dt, J = 16.0, 12.0 Hz), Z:

5.91 (q, J = 12.0 Hz), 1H}, {E: 4.37 (q, J = 8.0 Hz), Z: 4.12 (d, J = 8.0 Hz), 2H}, {E: 1.38 (t, J = 8.0 Hz), Z: 1.18 (t, J = 8.0 Hz), 3H}. **13C NMR** (100 MHz, CDCl$_3$): δ 163.7 (t, J = 34.0 Hz), 150.0, 135.3(t, J = 10.0 Hz), 132.8, 128.9, 121.2, 120.4(q, J = 257.0 Hz), 119.9 (t, J = 25.0 Hz), 116.5, 112.4 (t, J = 248.0 Hz), 63.2, 14.0. **19F NMR** (376 MHz, CDCl$_3$): δ -57.83, -94.99 (d, J = 16.1 Hz), -103.47 (d, J = 14.9 Hz). **IR**: υ (cm^{-1}) 2978, 1767, 1508, 1257, 1211, 1168, 1076, 910, 733. **HRMS** (**ESI**) (m/z): [M+Na]$^+$ calcd. for C$_{13}$H$_{11}$F$_5$NaO$_3$: 333.0526, found: 333.0521.

Ethyl (E)-2,2-difluoro-4-(4-nitrophenyl)but-3-enoate(3i)

Purification: Column chromatography (PE/Et$_2$O = 30:1) isolated as a colorless oil (73% yield). E/Z: 91:9.

1H NMR (400 MHz, CDCl$_3$): δ {E: 8.26 (d, J = 12.0 Hz), Z: 8.22 (d, J = 8.0 Hz), 2H}, {E: 7.62 (d, J = 8.0 Hz), Z: 7.54 (d, J = 8.0 Hz), 2H}, {E: 7.16 (dt, J = 16.0, 4.0), Z: 6.99 (d, J = 16.0 Hz), 1H}, {E: 6.48 (dt, J = 20.0, 8.0 Hz), Z: 6.09-5.99 (m), 1H}, {E: 4.38 (q, J = 8.0 Hz), Z: 4.21 (q, J = 8.0 Hz), 2H}, {E: 1.39 (t, J = 8.0 Hz), Z: 1.22 (t, J = 8.0 Hz), 3H}. **13C NMR** (100 MHz, CDCl$_3$): δ 163.4 (t, J = 34.0 Hz), 148.3, 140.2, 134.5 (t, J = 10.0 Hz), 129.8, 128.2, 124.2, 123.4, 123.3 (t, J = 25.0 Hz), 112.1 (t, J = 248.0 Hz), 63.5, 14.0. **19F NMR** (376 MHz, CDCl$_3$): δ -96.62 (dd, J = 13.8, 2.3 Hz), -103.95 (dd, J = 11.0, 2.6 Hz). **IR**: υ (cm^{-1}) 1550, 1380, 902, 725, 648. **HRMS** (**ESI**) (m/z): [M+Na]$^+$ calcd. for C$_{12}$H$_{11}$F$_2$NNaO$_4$: 294.0554, found: 294.0548.

Ethyl (E)-2,2-difluoro-4-(4-(trifluoromethyl)phenyl)but-3-enoate(3j)

Purification: Column chromatography (PE/Et$_2$O = 30:1) isolated as a colorless oil (61% yield). E/Z: 93:7.

1H NMR (400 MHz, CDCl$_3$): δ {E: 7.65(d, J = 8.0 Hz), Z: 7.62-7.60 (m), 2H}, {E: 7.57(d, J = 8.0 Hz), Z: 7.48(d, J = 12.0 Hz), 2H}, {E: 7.13 (dt, J = 16.0, 4.0 Hz), Z: 6.03-5.93(m), 1H}, {E: 4.38 (q, J = 8.0 Hz), Z: 4.13(q, J = 8.0 Hz), 2H}, {E: 1.38 (t, J = 8.0 Hz), Z: 1.20 (t, J = 8.0 Hz), 3H}. **13C NMR** (100 MHz, CDCl$_3$): δ 163.6 (t, J = 34.0 Hz), 137.5, 135.4 (t, J = 9.0 Hz), 131.4 (q, J = 32.0 Hz), 129.2, 127.9, 127.7, 125.8(q, J = 4.0 Hz), 125.2, 125.1, 122.5, 121.5 (t, J = 25.0 Hz), 112.3 (t, J = 248.0 Hz), 63.3, 13.9. **19F NMR** (376 MHz, CDCl$_3$): δ -62.84, -95.55, -103.73. **IR**: υ (cm^{-1}) 2978, 2885, 1770, 1458, 1384, 1327, 1153, 1130, 1064, 952. **HRMS** (**ESI**) (m/z): [M+Na]$^+$ calcd. for C$_{13}$H$_{11}$F$_5$NaO$_2$: 317.0577, found: 317.0573.

Ethyl (E)-4-(3,4-dichlorophenyl)-2,2-difluorobut-3-enoate(3k)

Purification: Column chromatography (PE/Et$_2$O = 30:1) isolated as a colorless oil (56% yield). E/Z: 86:14.

1H NMR (400 MHz, CDCl$_3$): δ 7.55 (d, J = 2.0 Hz, 1H), {E: 7.47 (d, J = 8.0 Hz), Z: 7.43 (d, J = 8.0 Hz), 1H}, {E: 7.30-7.27 (m), Z: 7.22 (dd, J = 12.0, 4.0 Hz), 1H}, {E: 7.00 (dt, J = 16.0, 4.0 Hz), Z: 6.83 (dt, J = 16.0, 4.0 Hz), 1H}, {E: 6.23 (dt, J = 16.0, 12.0 Hz), Z: 5.93 (q, J = 12.0 Hz), 1H}, {E: 4.37 (q, J = 8.0 Hz), Z: 4.20(q, J = 8.0 Hz), 2H}, {E: 1.38 (t, J = 8.0 Hz), Z: 1.27 (t, J = 8.0 Hz), 3H}. **13C NMR** (100 MHz, CDCl$_3$): δ 163.6 (t, J = 35.0 Hz), 136.2, 134.4 (t, J = 10.0 Hz), 134.1, 133.6, 133.2, 130.8, 129.1, 128.3, 126.5, 123.4(t, J = 27.0 Hz), 120.8 (t, J = 25.0 Hz), 112.2 (t, J = 248.0 Hz), 63.3, 14.0. **19F NMR** (376 MHz, CDCl$_3$): δ -95.93 (d, J = 13.7 Hz), -103.63 (d, J = 2.6 Hz). **IR**: υ (cm^{-1}) 3649, 2978, 1885, 1766, 1458, 1384, 1149, 1072, 732. **HRMS** (**ESI**) (m/z): [M+Na]$^+$ calcd. for C$_{12}$H$_{10}$Cl$_2$F$_2$NaO$_2$: 316.9924, found: 316.9920.

Ethyl (E)-4-(3-chlorophenyl)-2,2-difluorobut-3-enoate(3l)

Purification: Column chromatography (PE/Et$_2$O = 30:1) isolated as a colorless oil (58% yield). E/Z: 91:9.

¹H NMR (400 MHz, CDCl₃): δ 7.45 (s, 1H), 7.34-7.32 (m, 3H), {E: 7.04 (dt, *J* = 16.0, 4.0 Hz), Z: 6.89 (d, *J* = 12.0 Hz), 1H}, {E: 6.32 (dt, *J* = 16.0, 12.0 Hz), Z: 5.92 (q, *J* = 12.0 Hz), 1H}, {Z: 4.37 (q, *J* = 8.0 Hz), E: 4.13 (q, *J* = 8.0 Hz), 2H}, {E: 1.38 (t, *J* = 8.0 Hz), Z: 1.22 (t, *J* = 8.0 Hz), 3H}. **¹³C NMR** (100 MHz, CDCl₃): δ 163.7 (t, *J* = 35.0 Hz), 137.2, 135.9, 135.4(t, *J* = 10.0 Hz), 134.9, 134.1, 130.1, 129.6, 129.5, 128.8, 128.7, 127.3, 125.7, 123.2(t, *J* = 28.0 Hz), 120.4(t, *J* = 25.0 Hz), 112.4 (t, *J* = 248.0 Hz), 63.2, 14.0. **¹⁹F NMR** (376 MHz, CDCl₃): δ -95.00 (d, *J* = 13.4 Hz), -103.56 (d, *J* = 8.9 Hz). IR: υ (cm⁻¹) 2978, 2885, 1770, 1384, 1315, 1176, 1141, 1087, 906, 725, 651. **HRMS (ESI)** (m/z): [M+Na]⁺ calcd. for $C_{12}H_{11}ClF_2NaO_2$: 283.0313, found: 283.0308.

Ethyl (E)-4-(3-bromophenyl)-2,2-difluorobut-3-enoate(3m)

Purification: Column chromatography (PE/Et₂O = 30:1) isolated as a colorless oil (46% yield). E/Z: 82:18.

¹H NMR (400 MHz, CDCl₃): δ 7.62 (s, 1H), 7.50 (d, *J* = 8.0 Hz, 1H), 7.39 (d, *J* = 8.0 Hz, 1H), 7.32 -7.22 (m, 1H), {E: 7.04 (dt, *J* = 16.0, 4.0 Hz), Z: 6.90 (d, *J* = 12.0 Hz), 1H}, {E: 6.33 (dt, *J* = 16.0, 12.0 Hz), Z: 5.94 (q, *J* = 12.0 Hz), 1H}, {E: 4.38 (q, *J* = 8.0 Hz), Z: 4.14 (q, *J* = 8.0 Hz), 2H}, {E: 1.39 (t, *J* = 8.0 Hz), Z: 1.23 (t, *J* = 8.0 Hz), 3H}. **¹³C NMR** (100 MHz, CDCl₃): δ 163.7 (t, *J* = 35.0 Hz), 137.0(t, *J* = 8.0 Hz), 136.2, 135.3(t, *J* = 10.0 Hz), 132.5, 131.7, 131.6, 130.3, 130.2, 129.7, 127.5, 126.1, 123.5, 123.2, 123.0, 122.2, 120.4(t, *J* = 25.0 Hz), 112.4 (t, *J* = 248.0 Hz), 63.2, 14.0. **¹⁹F NMR** (376 MHz, CDCl₃); δ -95.02 (d, *J* = 13.4 Hz), -103.55 (d, *J* = 9.1 Hz). IR: υ (cm⁻¹) 3645, 2978, 2885, 1766, 1384, 1153, 1076, 906, 729. **HRMS (ESI)** (m/z): [M+Na]⁺ calcd. for $C_{12}H_{11}BrF_2NaO_2$: 326.9808, found: 326.9805.

Ethyl (E)-4-(4-bromophenyl)-2, 2-difluorobut-3-enoate(3n)

Purification: Column chromatography (PE/Et₂O = 30:1) isolated as a colorless oil (47% yield). E/Z: 84:16.

¹H NMR (400 MHz, CDCl₃): δ 7.53-7.47 (m, 2H), {E: 7.33-7.31 (m), Z: 7.25-7.23(m), 2H}, {E: 7.03 (dt, *J* = 16.0, 4.0 Hz), Z: 6.88-6.85(m), 1H}, {E: 6.31 (dt, *J* = 16.0, 8.0 Hz), Z: 5.95-5.85(m), 1H}, {E:4.37 (q, *J* = 8.0 Hz), Z: 4.14(q, *J* = 8.0 Hz), 2H}, {E: 1.38 (t, *J* = 8.0 Hz), Z: 1.21 (t, *J* = 8.0 Hz), 3H}. **¹³C NMR** (100 MHz, CDCl₃): δ 163.8 (t, *J* = 35.0 Hz), 137.5, 135.7 (t, *J* = 10.0 Hz), 133.0, 132.1, 131.4, 130.6(t, *J* = 3.0 Hz), 123.8, 119.6 (t, *J* = 5.0 Hz), 112.5 (t, *J* = 248.0 Hz), 63.2, 14.0. **¹⁹F NMR** (376 MHz, CDCl₃): δ -95.12 (d, *J* = 15.0 Hz), -103.40 (dd, *J* = 11.3, 3.8 Hz). IR: υ (cm⁻¹) 2978, 2885, 1762, 1489, 1072, 906, 729, 651. **HRMS (ESI)** (m/z): [M+Na]⁺ calcd. for $C_{12}H_{11}BrF_2NaO_2$: 326.9808, found: 326.9801.

Ethyl (E)-2, 2-difluoro-4-(pyridin-3-yl)but-3-enoate(3o)

Purification: Column chromatography (PE/Et₂O = 30:1) isolated as a colorless oil (33% yield). E/Z > 99:1.

¹H NMR (400 MHz, CDCl₃): δ 8.68 (d, *J* = 40.0 Hz, 2H), 7.82 (dd, *J* = 8.0, 4.0 Hz, 1H), 7.37 (s, 1H), 7.11 (dt, *J* = 16.0, 4.0 Hz, 1H), 6.41 (dt, *J* = 16.0, 12.0 Hz, 1H), 4.38 (q, *J* = 8.0 Hz, 2H), 1.39 (t, *J* = 8.0 Hz, 3H). **¹³C NMR** (100 MHz, CDCl₃): δ 163.6, 150.2, 148.8, 134.1, 133.3, 133.2, 121.4 (t, *J* = 25.0 Hz), 112.2, 63.4, 14.0. **¹⁹F NMR** (376 MHz, CDCl₃): δ -103.74 (d, *J* = 14.7 Hz). **IR**: υ (cm⁻¹) 2924, 1767, 1458, 1280, 972, 732. **HRMS (ESI)** (m/z): [M+H]⁺ calcd. for $C_{11}H_{12}F_2NO_2$: 228.0836, found: 228.0845.

Ethyl 3-(thiophen-2-yl)acrylate(3p)

Purification: Column chromatography (PE/Et₂O = 30:1) isolated as a pale yellow oil (61% yield). E/Z: 61:39.

¹H NMR (400 MHz, CDCl₃): δ {Z: 7.41(d, *J* = 4.0 Hz), E: 7.32 (d, *J* = 4.0 Hz), 1H},{Z: 7.31 (m), E: 7.17(m), 1H}, {E: 7.20(dt, *J* = 16.0, 4.0 Hz), Z: 6.88(dt, *J* = 12.0, 4.0 Hz), 1H}, {E: 7.34(d, *J* = 4.0 Hz), Z:7.31(d, *J* = 4.0

Hz), 1H}, 7.18-7.16(m, 1H), 7.04-7.02(m, 1H), {Z: 7.07 (dt, J = 16.0, 4.0 Hz), E: 6.94 (d, J = 12.0 Hz), 1H}, {E: 6.12 (dt, J = 16.0, 12.0 Hz), Z: 5.73 (q, J = 8.0 Hz), 1H}, {E: 4.36 (q, J = 8.0 Hz), Z: 4.24 (q, J = 8.0 Hz), 2H}, {E: 1.38 (t, J = 8.0 Hz), Z: 1.25 (t, J = 8.0 Hz), 3H}. **¹³C NMR** (100 MHz, CDCl₃): δ 163.8, 163.3, 138.9, 138.5, 136.3, 131.1(t, J = 4.0 Hz), 130.1(t, J = 9.0 Hz), 129.8(t, J = 10.0 Hz), 129.4, 128.9(t, J = 2.0 Hz), 127.8, 127.6, 127.3, 118.6(t, J = 28.0 Hz), 117.6 (t, J = 25.0 Hz), 112.3, 112.4(t, J = 247.0 Hz), 63.1, 21.3, 14.0. **¹⁹F NMR** (376 MHz, CDCl₃): δ -96.37 (d, J = 15.0 Hz), -102.97 (dd, J = 11.3, 3.7 Hz). **IR**: υ (cm⁻¹) 2986, 1763, 1647, 1307, 1199, 1072, 906, 729, 706. **HRMS** (**ESI**) (m/z): [M+Na]⁺ calcd. for $C_{10}H_{10}F_2NaO_2S$: 255.0267, found: 255.0260.

Ethyl (3E,5E)-2,2-difluoro-6-phenylhexa-3,5-dienoate(3q)

Purification: Column chromatography (PE/Et₂O = 30:1) isolated as a colorless oil (81% yield). E/Z > 99:1.

¹H NMR (400 MHz, CDCl₃): δ 7.46-7.43 (m, 2H), 7.38-7.34 (m, 2H), 7.32-7.28 (m, 1H), 6.90-6.82 (m, 1H), 6.81-6.78 (m, 2H), 5.91 (dt, J = 16.0, 12.0 Hz, 1H), 4.36 (q, J = 8.0 Hz), 2H}, 1.38 (t, J = 8.0 Hz, 3H). **¹³C NMR** (100 MHz, CDCl₃): δ 163.9 (t, J = 35.0 Hz), 138.4 (t, J = 3.0 Hz), 136.8 (t, J = 10.0 Hz), 136.0, 128.8, 128.7, 126.9, 125.7(t, J = 2.0 Hz), 121.6(t, J = 25.0 Hz), 112.5 (t, J = 246.0 Hz), 63.1, 14.0. **¹⁹F NMR** (376 MHz, CDCl₃): δ -98.32(s), -102.94(s). **IR**: υ (cm⁻¹) 3649, 2978, 1766, 1647, 1473, 1384, 1249, 1153, 1072, 952. **HRMS** (**ESI**) (m/z): [M+Na]⁺ calcd. for $C_{14}H_{14}F_2NaO_2$: 275.0860, found: 275.0858.

Ethyl 2,2-difluoro-4,4-diphenylbut-3-enoate(3r)

Purification: Column chromatography (PE/Et₂O = 30:1) isolated as a colorless oil (81% yield).

¹H NMR (400 MHz, CDCl₃): δ 7.30 - 7.27 (m, 3H), 7.26 - 7.22 (m, 3H), 7.20 - 7.17 (m, 2H), 7.14-7.12 (m, 2H), 6.20 (t, J = 12.0 Hz, 1H), 3.84 (q, J = 8.0 Hz, 2H), 1.10 (t, J = 8.0 Hz, 3H). **¹³C NMR** (100 MHz, CDCl₃): δ 163.4 (t, J = 34.0 Hz), 151.0 (t, J = 10.0 Hz), 140.5, 137.1, 129.8(t, J = 2.0 Hz), 129.1, 128.6, 128.4, 128.0, 127.9, 119.5(t, J = 28.0 Hz), 112.5 (t, J = 243.0 Hz), 62.7, 13.7. **¹⁹F NMR** (376 MHz, CDCl₃): δ -90.99. **IR**: υ (cm⁻¹) 2978, 1766, 1103, 1068, 902, 725, 648. **HRMS** (**ESI**) (m/z): [M+Na]⁺ calcd. for $C_{18}H_{16}F_2NaO_2$: 325.1016, found: 325.1008.

Ethyl (Z)-2,2-difluoro-4-(o-tolyl)but-3-enoate(5a)-Z

Purification: Column chromatography (PE/Et₂O = 30:1) isolated as a colorless oil (77% yield). E/Z: 6: 94.

¹H NMR (400 MHz, CDCl₃): δ {E: 7.48(d, J = 8.0 Hz), Z:7.02 (d, J = 8.0 Hz), 1H}, {E: 7.38-7.34(m), Z: 7.26-7.14 (m), 4H}, 7.06 (d, J = 12.0 Hz, 2H), 6.99-6.85(m, 2H), {E: 6.22 (dt, J = 16.0, 12.0 Hz), Z: 5.98 (q, J = 12.0 Hz), 1H}, {E: 4.37 (q, J = 8.0 Hz), Z: 3.88 (q, J = 8.0 Hz), 2H}, {E: 2.40(s), Z: 2.27(s), 3H}, {E: 1.38 (t, J = 8.0 Hz), E: 1.13 (t, J = 8.0 Hz), 3H}. **¹³C NMR** (100 MHz, CDCl₃): δ 163.3 (t, J = 33.0 Hz), 138.1, 136.0 (t, J = 2.0 Hz), 134.7 (t, J = 10.0 Hz), 133.8, 130.7, 129.4(t, J = 5.0 Hz), 129.2(t, J = 3.0 Hz), 128.7, 126.3, 125.5, 123.0 (t, J = 28.0 Hz), 112.3(t, J = 244.0 Hz), 62.8, 19.9, 13.6. **¹⁹F NMR** (376 MHz, CDCl₃): δ -93.78 (d, J = 11.5 Hz), -103.05 (dd, J = 11.5, 2.8 Hz). **IR**: υ (cm⁻¹) 2982, 1766, 1311, 1153, 1095, 1072, 910, 767, 732. **HRMS** (**ESI**) (m/z): [M+Na]⁺ calcd. for $C_{13}H_{14}F_2NaO_2$: 263.0860, found: 263.0861.

Ethyl (E)-2,2-difluoro-4-(o-tolyl)but-3-enoate(5a)-*E*

Purification: Column chromatography (PE/Et₂O = 30:1) isolated as a colorless oil (62% yield). E/Z: 92:8.

¹H NMR (400 MHz, CDCl₃): δ 7.48(d, *J* = 8.0 Hz, 1H), 7.35(dt, *J* = 16.0, 4.0 Hz, 1H}, 7.29-7.19 (m, 3H), {E: 6.22 (dt, *J* = 16.0, 12.0 Hz), Z: 5.98 (q, *J* = 12.0 Hz), 1H}, {E: 4.37 (q, *J* = 8.0 Hz), Z: 3.88 (q, *J* = 8.0 Hz), 2H}, {E: 2.40(s), Z: 2.27(s), 3H}, {E: 1.38 (t, *J* = 8.0 Hz), E: 1.13 (t, *J* = 8.0 Hz), 3H}. **¹³C NMR** (100 MHz, CDCl₃): δ 164.0 (t, *J* = 35.0 Hz), 136.8, 134.7 (t, *J* = 10.0 Hz), 133.2, 130.6, 129.4, 128.7, 126.3, 126.1(t, *J* = 2.0 Hz), 125.5, 120.1(t, *J* = 25.0 Hz), 112.7(t, *J* = 253.0 Hz), 63.1, 19.6, 14.0. **¹⁹F NMR** (376 MHz, CDCl₃): δ -93.80 (d, *J* = 11.5 Hz), -103.05(s). **IR**: υ (cm⁻¹) 1751, 1076, 902, 725, 648.

Ethyl (Z)-2,2-difluoro-4-(2-methoxyphenyl)but-3-enoate(5b)-*Z*

Purification: Column chromatography (PE/Et₂O = 30:1) isolated as a colorless oil (69% yield). E/Z: 9: 91.

¹H NMR (400 MHz, CDCl₃): δ{E: 7.45-7.35 (m), Z: 7.33-7.29 (m), 2H}, 7.06 (d, *J* = 12.0 Hz, 2H), 6.99-6.85(m, 2H), {E: 6.42 (dt, *J* = 16.0, 12.0 Hz), Z: 6.02 (q, *J* = 12.0 Hz), 1H}, {E: 4.36 (q, *J* = 8.0 Hz), Z: 4.01 (q, *J* = 8.0 Hz), 2H}, {E: 3.88(s), Z: 3.83(s), 3H}, {E: 1.37 (t, *J* = 8.0 Hz), Z: 1.15 (t, *J* = 8.0 Hz), 3H}. **¹³C NMR** (100 MHz, CDCl₃): δ 163.4 (t, *J* = 34.0 Hz), 157.8, 156.9, 134.7 (t, *J* = 9.0 Hz), 132.2 (t, *J* = 9.0 Hz), 130.5(t, *J* = 4.0 Hz), 130.3, 128.4, 123.5, 122.0 (t, *J* = 28.0 Hz), 120.7, 120.2, 119.4 (t, *J* = 25.0 Hz), 112.5(t, *J* = 244.0 Hz), 111.0, 63.0, 62.74, 55.40, 13.6. **¹⁹F NMR** (376 MHz, CDCl₃): δ -94.33 (d, *J* = 12.9 Hz), -102.74 (dd, *J* = 11.3, 3.8 Hz). **IR**: υ (cm⁻¹) 2978, 1767, 1462, 1292, 1249, 1072, 906, 725, 648. **HRMS** (**ESI**) (m/z): [M+Na]⁺ calcd. for C₁₃H₁₄F₂NaO₃: 279.0809, found: 279.0808.

Ethyl (E)-2,2-difluoro-4-(2-methoxyphenyl)but-3-enoate(5b)-*E*

Purification: Column chromatography (PE/Et₂O = 30:1) isolated as a colorless oil (63% yield). E/Z: 87:13.

¹H NMR (400 MHz, CDCl₃): δ 7.45-7.26 (m, 3H), 7.08-6.85(m, 2H). 6.99-6.85(m, 2H), {E: 6.42 (dt, *J* = 16.0, 12.0 Hz), Z: 5.90 (q, *J* = 12.0 Hz), 1H}, {E: 4.36 (q, *J* = 8.0 Hz), Z: 4.00 (q, *J* = 8.0 Hz), 2H}, {E: 3.88(s), Z: 3.84(s), 3H}, {E: 1.38 (t, *J* = 8.0 Hz), Z: 1.15 (t, *J* = 8.0 Hz), 3H}. **¹³C NMR** (100 MHz, CDCl₃): δ 164.1 (t, *J* = 35.0 Hz), 157.7, 134.6, 132.2 (t, *J* = 10.0 Hz), 130.8, 130.5(t, *J* = 4.0 Hz), 130.3, 128.3, 123.0, 121.9 (t, *J* = 28.0 Hz), 120.6, 119.6 (t, *J* = 56.0 Hz), 119.3, 113.1 (t, *J* = 247.0 Hz), 111.1, 110.0, 63.0, 55.40, 13.9. **¹⁹F NMR** (376 MHz, CDCl₃): δ -94.32 (d, *J* = 12.9 Hz), -102.90 (dd, *J* = 11.3, 3.8 Hz). **IR**: υ (cm⁻¹) 1763, 1651, 1489, 1458, 1296, 1249, 1076, 903, 725, 648.

Ethyl (Z)-4-(2-(benzyloxy)phenyl)-2,2-difluorobut-3-enoate(5c)-*Z*

Purification: Column chromatography (PE/Et₂O = 30:1) isolated as a colorless oil (81% yield). E/Z: 18: 82.

¹H NMR (400 MHz, CDCl₃): δ 7.50-7.28(m, 7H), 7.16(dd, *J* = 16.0, 4.0 Hz, 1H), 6.99-6.91(m, 2H), {E: 6.46 (dt, *J* = 16.0, 12.0 Hz), Z: 5.92 (q, *J* = 12.0 Hz), 1H}, {E: 5.15(s), Z: 5.12(s), 2H}, {E: 4.33 (q, *J* = 8.0 Hz), Z: 4.01 (q, *J* = 8.0 Hz), 2H}, {Z: 1.33 (t, *J* = 8.0 Hz), E: 1.14 (t, *J* = 8.0 Hz), 3H}. **¹³C NMR** (100 MHz, CDCl₃): δ 163.5 (t, *J* = 34.0 Hz), 156.9, 156.2, 136.8, 136.6, 134.9 (t, *J* = 9.0 Hz), 132.2 (t, *J* = 10.0 Hz), 130.8, 130.7(t, *J* = 4.0 Hz), 130.3, 128.7, 128.6, 128.1, 128.0, 127.3, 127.2, 124.0, 121.8 (t, *J* = 28.0 Hz), 121.1, 120.5, 119.6(t, *J* = 25.0 Hz), 115.0, 112.7, 112.6 (t, *J* = 244.0 Hz), 70.4, 70.2, 63.0, 62.8, 14.0, 13.6. **¹⁹F NMR** (376 MHz, CDCl₃): δ -94.12 (d, *J* = 12.9 Hz), -102.63 (dd, *J* = 11.4, 2.8 Hz). **IR**: υ (cm⁻¹) 2245, 1770, 1273, 1145, 1080, 906, 729, 651. **HRMS** (**ESI**) (m/z): [M+Na]⁺ calcd. for C₁₉H₁₈F₂NaO₃: 355.1122, found: 355.1125.

Ethyl (E)-4-(2-(benzyloxy)phenyl)-2,2-difluorobut-3-enoate(5c)-*E*

Purification: Column chromatography (PE/Et₂O = 30:1) isolated as a colorless oil (55% yield). E/Z: 90:10.

¹H NMR (400 MHz, CDCl₃): δ 7.49-7.29(m, 8H), 7.01-6.97(m, 2H), {E: 6.45 (dt, *J* = 16.0, 12.0 Hz), Z: 5.91 (q, *J* = 12.0 Hz), 1H}, {E: 5.15(s), Z:5.11(s), 2H}, {E: 4.32 (q, *J* = 8.0 Hz), Z: 4.00 (q, *J* = 8.0 Hz), 2H}, {Z: 1.32 (t, *J* = 8.0 Hz), E: 1.14 (t, *J* = 8.0 Hz), 3H}. **¹³C NMR** (100 MHz, CDCl₃): δ 164.0 (t, *J* = 35.0 Hz), 156.8, 134.8, 132.2 (t, *J* = 10.0 Hz), 130.6, 130.2, 128.7, 128.6, 128,5, 128.4, 128.0, 127.9, 127.2, 127.1, 123.4, 121.8, 121.0, 120.4, 119.5(t, *J* = 25.0 Hz), 113.0 (t, *J* = 247.0 Hz), 112.6, 111.6, 70.4, 62.9, 13.9. **¹⁹F NMR** (376 MHz, CDCl₃): δ -94.15 (d, *J* = 12.9 Hz), -102.65 (dd, *J* = 11.4, 2.8 Hz). **IR**: υ (cm⁻¹) 1763, 1296, 1246, 1076, 902, 725, 648.

Ethyl (Z)-4-(2-acetoxyphenyl)-2,2-difluorobut-3-enoate(5d)-Z

Purification: Column chromatography (PE/Et₂O = 30:1) isolated as a colorless oil (73% yield). E/Z: 14: 86.

¹H NMR (400 MHz, CDCl₃): δ {E: 7.57 (dd, *J* = 12.0, 4.0 Hz), Z: 7.40-7.34(m), 2H}, {E: 7.23 (dt, *J* = 8.0, 4.0 Hz), Z: 7.37 (t, *J* = 4.0 Hz), 1H}, 7.13-7.08 (m, 1H), 6.86 (d, *J* = 12.0, 1H), {E: 6.34 (dt, *J* = 16.0, 12.0 Hz), Z: 6.00 (q, *J* = 12.0 Hz), 1H}, {E: 4.36 (q, *J* = 8.0 Hz), Z: 4.06 (q, *J* = 8.0 Hz), 2H}, {E: 2.36 (s), Z: 2.30 (s), 3H}, {E: 1.37 (t, *J* = 8.0 Hz), Z: 1.19 (t, *J* = 8.0 Hz), 3H}. **¹³C NMR** (100 MHz, CDCl₃): δ 168.7, 163.2 (t, *J* = 34.0 Hz), 148.2 (d, *J* = 2.0 Hz), 133.2 (t, *J* = 9.0 Hz), 130.6, 130.4 (t, *J* = 3.0 Hz), 129.9, 127.4, 126.4, 125.7, 124.0 (t, *J* = 28.0 Hz), 123.1, 122.0, 121.2 (t, *J* = 25.0 Hz), 112.0 (t, *J* = 247.0 Hz), 63.1, 20.9, 14.0. **¹⁹F NMR** (376 MHz, CDCl₃): δ -95.46 (d, *J* = 12.8 Hz), -103.71 (dd, *J* = 11.2, 2.9 Hz). IR: υ (cm⁻¹) 1763, 1485, 1450, 1369, 1303, 1203, 1176, 1095, 1072, 1010, 910, 763, 733, 648, 517. **HRMS** (**ESI**) (m/z): [M+Na]⁺ calcd. for C₁₄H₁₄F₂NaO₄: 307.0758, found: 307.0757.

Ethyl (E)-4-(2-acetoxyphenyl)-2,2-difluorobut-3-enoate(5d)-*E*

Purification: Column chromatography (PE/Et₂O = 30:1) isolated as a colorless oil (45% yield). E/Z: 94:6.

¹H NMR (400 MHz, CDCl₃): δ 7.57 (dd, *J* = 8.0, 4.0 Hz), 7.39(t, *J* = 8.0 Hz, 1H), 7.27(t, *J* = 8.0 Hz, 1H), 7.17-7.11 (m, 2H), {E: 6.34 (dt, *J* = 16.0, 12.0 Hz), Z: 5.97 (q, *J* = 12.0 Hz), 1H}, {E: 4.36 (q, *J* = 8.0 Hz), Z: 4.07 (q, *J* = 8.0 Hz), 2H}, {E: 2.36 (s), Z: 2.30 (s), 3H}, {E: 1.38 (t, *J* = 8.0 Hz), Z: 1.19 (t, *J* = 8.0 Hz), 3H}. **¹³C NMR** (100 MHz, CDCl₃): δ 169.0, 163.7 (t, *J* = 34.0 Hz), 148.8, 130.5 (t, *J* = 10.0 Hz), 129.9, 127.4, 126.8, 126.3, 123.0, 121.2(t, *J* = 24.0 Hz), 112.4 (t, *J* = 247.0 Hz), 63.2, 20.9, 13.9. **¹⁹F NMR** (376 MHz, CDCl₃): δ -95.47 (d, *J* = 12.8 Hz), -103.70. **IR**: υ (cm⁻¹) 1763, 1199, 1180, 1076, 906, 729, 648.

Ethyl (Z)-4-(2,4-bis(trifluoromethyl)phenyl)-2,2-difluorobut-3-enoate(5e)-Z

Purification: Column chromatography (PE/Et₂O = 30:1) isolated as a colorless oil (68% yield). E/Z: 9:91.

¹H NMR (400 MHz, CDCl₃): δ 7.86-7.80(m, 1H), 7.72-7.70(m, 2H), 7.15(dd, *J* = 12.0, 4.0 Hz, 1H), {E: 6.39 (dt, *J* = 16.0, 12.0 Hz), Z: 6.09 (q, *J* = 12.0 Hz), 1H}, {E: 4.39 (q, *J* = 8.0 Hz), Z: 4.22 (q, *J* = 8.0 Hz), 2H}, {E: 1.39 (t, *J* = 8.0 Hz), Z: 1.29 (t, *J* = 8.0 Hz), 3H}. **¹³C NMR** (100 MHz, CDCl₃): δ 163.0 (t, *J* = 34.0 Hz), 134.5, 133.7-133.4(m), 131.3, 131.2, 127.9 (q, *J* = 4.0 Hz), 126.3 (q, *J* = 5.0 Hz), 125.6, 125.4(t, *J* = 26.0 Hz), 124.5(d, *J* = 6.0 Hz), 121.8(d, *J* = 4.0 Hz), 119.1, 111.9 (t, *J* = 250.0 Hz), 63.3, 13.7. **¹⁹F NMR** (376 MHz, CDCl₃): δ -93.78 (d, *J* = 11.5 Hz), -103.05 (dd, *J* = 11.5, 2.8 Hz). **IR**: υ (cm⁻¹) 2253, 1766, 1315, 1138, 1088, 906, 652. **HRMS** (**ESI**) (m/z): [M+Na]⁺ calcd. for C₁₄H₁₀F₈NaO₂: 385.0451, found: 385.0456.

Ethyl (E)-4-(2,4-bis(trifluoromethyl)phenyl)-2,2-difluorobut-3-enoate(5e)-*E*

Purification: Column chromatography (PE/Et₂O = 30:1) isolated as a colorless oil (42% yield). E/Z: 91:9.

¹H NMR (400 MHz, CDCl₃): δ 7.96(s, 1H), 7.86-7.83(m, 2H), 7.51-7.46(m, 1H), {E: 6.38 (dt, J = 16.0, 12.0 Hz), Z: 6.10 (q, J = 12.0 Hz), 1H}, {E: 4.39 (q, J = 8.0 Hz), Z: 4.20 (q, J = 12.0 Hz), 2H}, {Z: 1.39 (t, J = 8.0 Hz), E: 0.78 (t, J = 8.0 Hz), 3H}. **¹³C NMR** (100 MHz, CDCl₃): δ 163.2 (t, J = 34.0 Hz), 136.9, 131.9, 131.6, 131.2, 130.9, 129.4, 129.0, 128.7, 125.7 (t, J = 25.0 Hz), 124.5, 123.4, 121.7, 111.8 (t, J = 248.0 Hz), 63.5, 13.9. **¹⁹F NMR** (376 MHz, CDCl₃): δ -94.15 (d, J = 12.9 Hz), -102.65 (dd, J = 11.4, 2.8 Hz). **IR**: υ (cm⁻¹) 2978, 1766, 1346, 1277, 1141, 906, 733.

Ethyl (Z)-3-(2,6-difluorophenyl)acrylate(5f)-*Z*

Purification: Column chromatography (PE/Et₂O = 30:1) isolated as a colorless oil (80% yield). E/Z: 10: 90.
¹H NMR (400 MHz, CDCl₃): δ {E: 7.65-7.45 (m), Z: 6.68-6.78 (m), 2H}, 7.23-7.16(m, 1H), {E: 7.09 (dt, J = 16.0, 4.0 Hz), Z: 6.08 (q, J = 12.0 Hz), 1H}, {E: 4.29 (d, J = 8.0 Hz), Z: 4.20 (q, J = 8.0 Hz), 2H}, {E: 1.29 (t, J = 8.0 Hz), Z: 1.25 (t, J = 8.0 Hz), 3H}. **¹³C NMR** (100 MHz, CDCl₃): δ 163.0 (t, J = 34.0 Hz), 161.0 (dt, J = 7.0, 2.0 Hz), 158.50 (dt, J = 7.0, 2.0 Hz), 130.9, 130.6 (t, J = 11.0 Hz), 130.1 (t, J = 10.0 Hz), 127.0 (t, J = 26.0 Hz), 123.6 (tt, J = 7.0, 2.0 Hz), 112.2, 112.0 (t, J = 244.0 Hz), 111.9 (d, J = 5.0 Hz), 111.7 (d, J = 6.0 Hz), 111.2 (d, J = 6.0 Hz), 111.0 (d, J = 6.0 Hz), 63.0, 13.8. **¹⁹F NMR** (376 MHz, CDCl₃): δ -102.5, -104.5, -111.1. -111.6. **IR**: υ (cm⁻¹) 2978, 1770, 1466, 1307, 1273, 1157, 1076, 906, 729, 648. **HRMS** (**ESI**) (m/z): [M+Na]⁺ calcd. for C₁₂H₁₀F₄NaO₂: 285.0515, found: 285.0510.

Ethyl (E)-4-(2,6-difluorophenyl)-2,2-difluorobut-3-enoate(5f)-*E*

Purification: Column chromatography (PE/Et₂O = 30:1) isolated as a colorless oil (37% yield). E/Z: 99:1.
¹H NMR (400 MHz, CDCl₃): δ 7.34-7.29 (m, 1H), 7.19 (dt, J = 16.0, 4.0 Hz, 1H), 6.99-6.92(m, 2H), 6.69 (dt, J = 16.0, 4.0 Hz, 1H), 4.39 (q, J = 8.0 Hz), 1.39 (t, J = 8.0 Hz), Z: 1.25 (t, J = 8.0 Hz), 3H}. **¹³C NMR** (100 MHz, CDCl₃): δ 163.7 (t, J = 34.0 Hz), 162.6(d, J = 7.0 Hz), 160.1 (d, J = 7.0 Hz), 130.6 (t, J = 11.0 Hz), 125.0 (tt, J = 24.0, 9.0 Hz), 123.3 (tt, J = 11.0, 3.0 Hz), 112.4 (t, J = 248.0 Hz), 112.0, 111.9, 111.8, 111.7, 111.6, 63.2, 13.9. **¹⁹F NMR** (376 MHz, CDCl₃): δ -104.55(dd, J = 11.3, 3.8 Hz), -111.60(t, J = 7.5 Hz). **IR**: υ (cm⁻¹) 1767, 1469, 1300, 1269, 1238, 1199, 1076, 1003, 976, 906, 783, 729, 648.

Ethyl (E)-2,2-difluoro-4-(2-fluorophenyl)but-3-enoate(5g)-*Z*

Purification: Column chromatography (PE/Et₂O = 30:1) isolated as a colorless oil (62% yield). E/Z: 14: 86.
¹H NMR (400 MHz, CDCl₃): δ {E: 7.55-7.46 (m), Z: 7.42-7.29 (m), 2H}, {E: 7.22 (dt, J = 16.0, 4.0 Hz), Z: 7.18-6.96(m), 3H}, {E: 6.45 (dt, J = 16.0, 12.0 Hz), Z: 6.01 (q, J = 12.0 Hz), 1H}, {E: 4.37 (q, J = 8.0 Hz), Z: 4.12 (q, J = 8.0 Hz), 2H}, {E: 1.38 (t, J = 8.0 Hz), Z: 1.21 (t, J = 8.0 Hz), 3H}. **¹³C NMR** (100 MHz, CDCl₃): δ 163.3 (t, J = 34.0 Hz), 159.9 (d, J = 249.0 Hz), 131.4 (td, J = 8.0, 4.0 Hz), 131.1 (d, J = 9.0 Hz), 130.8 (q, J = 4.0 Hz), 130.7 (d, J = 8.0 Hz), 124.0 (dt, J = 28.0, 1.0 Hz), 123.8 (d, J = 4.0 Hz), 122.3 (d, J = 14.0 Hz), 116.1 (d, J = 22.0 Hz), 115.1 (d, J = 21.0 Hz), 112.13 (t, J = 247,0 Hz), 63.0, 13.6. **¹⁹F NMR** (376 MHz, CDCl₃): δ -93.78 (d, J = 11.5 Hz), -103.05 (dd, J = 11.5, 2.8 Hz). **IR**: υ (cm⁻¹) 3649, 2978, 1770, 1458, 1384, 1249, 1072, 952, 732. **HRMS** (**ESI**) (m/z): [M+Na]⁺ calcd. for C₁₂H₁₁F₃NaO₂: 267.0609, found: 267.0609.

Ethyl (E)-2,2-difluoro-4-(2-fluorophenyl)but-3-enoate(5g)-*E*

Purification: Column chromatography (PE/Et₂O = 30:1) isolated as a colorless oil (38% yield). E/Z: 92:8.

¹H NMR (400 MHz, CDCl₃): δ 7.48 (t, *J* = 8.0 Hz, 1H), 7.37-7.30(m, 1H), 7.22(dt, *J* = 16.0, 4.0 Hz, 1H), 7.18-6.97(m, 2H), {E: 6.44 (dt, *J* = 16.0, 12.0 Hz), Z: 6.01 (q, *J* = 12.0 Hz), 1H}, {E: 4.37 (q, *J* = 8.0 Hz), Z: 4.12 (q, *J* = 8.0 Hz), 2H}, {E: 1.38 (t, *J* = 8.0 Hz), Z: 1.21 (t, *J* = 8.0 Hz), 3H}. **¹³C NMR** (100 MHz, CDCl₃): δ 163.8 (t, *J* = 34.0 Hz), 160.9 (d, *J* = 252.0 Hz), 131.1(d, *J* = 7.0 Hz), 129.7(td, *J* = 8.0, 4.0 Hz), 128.6(d, *J* = 2.0 Hz), 124.4 (d, *J* = 3.0 Hz), 123.8(d, *J* = 4.0 Hz), 122.0 (d, *J* = 12.0 Hz), 121.7 (d, *J* = 7.0 Hz), 121.4 (d, *J* = 7.0 Hz), 121.2(t, *J* = 7.0 Hz), 116.1 (d, *J* = 22.0 Hz), 115.0, 112.5, 110.1, 112.5 (t, *J* = 247.0 Hz), 63.2, 13.9. **¹⁹F NMR** (376 MHz, CDCl₃): δ -96.15(d, *J* = 11.5 Hz), -103.68 (dd, *J* = 11.5, 2.8 Hz), -114.0, -115.67-115.78(m). **IR**: υ (cm⁻¹) 1767, 1489, 1458, 1076, 903, 725, 648.

Ethyl (Z)-4-(2-chlorophenyl)-2,2-difluorobut-3-enoate(5h)-*Z*

Purification: Column chromatography (PE/Et₂O = 30:1) isolated as a colorless oil (81% yield). E/Z: 8:92.

¹H NMR (400 MHz, CDCl₃): δ {E: 7.58-7.48 (m), Z: 7.43-7.35 (m), 2H}, 7.32-7.23 (m, 2H), 7.04 (d, *J* = 12.0, 1H), {E: 6.33 (dt, *J* = 16.0, 12.0 Hz), Z: 6.02 (q, *J* = 12.0 Hz), 1H}, {E: 4.38 (q, *J* = 8.0 Hz), Z: 4.03 (q, *J* = 8.0 Hz), 2H}, {E: 1.39 (t, *J* = 8.0 Hz), Z: 1.19 (t, *J* = 8.0 Hz), 3H}. **¹³C NMR** (100 MHz, CDCl₃): δ 163.1 (t, *J* = 34.0 Hz), 135.8 (t, *J* = 9.0 Hz), 134.3, 133.3, 133.2 (t, *J* = 2.0 Hz), 133.0, 131.0(t, *J* = 4.0 Hz), 130.6, 130.0, 129.0, 127.4, 127.1, 126.5, 123.7 (t, *J* = 28.0 Hz), 121.6 (t, *J* = 25.0 Hz), 112.1 (t, *J* = 247.0 Hz), 63.0, 13.6. **¹⁹F NMR** (376 MHz, CDCl₃): δ -94.76 (d, *J* = 12.3 Hz), -103.15 (dd, *J* = 11.3, 3.8 Hz). **IR**: υ (cm⁻¹) 1766, 1473, 1438, 1311, 1157, 1099, 1072, 906, 729, 648. **HRMS** (**ESI**) (m/z): [M+Na]⁺ calcd. for C₁₂H₁₁ClF₂NaO₂: 283.0313, found: 283.0314.

Ethyl (E)-4-(2-chlorophenyl)-2,2-difluorobut-3-enoate(5h)-*E*

Purification: Column chromatography (PE/Et₂O = 30:1) isolated as a colorless oil (61% yield). E/Z: 90:10.

¹H NMR (400 MHz, CDCl₃): δ 7.58-7.48(m, 2H), 7.43-7.37 (m, 1H), {E: 7.32-7.23(m), Z: 7.05 (d, *J* = 12.0), 2H}, {E: 6.33 (dt, *J* = 16.0, 12.0 Hz), Z: 6.02 (q, *J* = 12.0 Hz), 1H}, {E: 4.38 (q, *J* = 8.0 Hz), Z: 4.03 (q, *J* = 8.0 Hz), 2H}, {E: 1.39 (t, *J* = 8.0 Hz), Z: 1.19 (t, *J* = 8.0 Hz), 3H}. **¹³C NMR** (100 MHz, CDCl₃): δ 163.7 (t, *J* = 35.0 Hz), 135.8 (t, *J* = 9.0 Hz), 134.3, 133.2 (t, *J* = 10.0 Hz), 132.4, 131.0(t, *J* = 4.0 Hz), 130.5, 130.0, 129.0, 127.4, 127.3, 126.4, 123.7 (t, *J* = 27.0 Hz), 121.6 (t, *J* = 25.0 Hz), 112.5 (t, *J* = 247.0 Hz), 63.2, 14.0. **¹⁹F NMR** (376 MHz, CDCl₃): δ -94.77 (d, *J* = 12.3 Hz), -103.16 (dd, *J* = 11.3, 3.8 Hz). **IR**: υ (cm⁻¹) 1771, 1697, 1508, 903, 725, 648.

Ethyl (Z)-4-(2-bromophenyl)-2,2-difluorobut-3-enoate(5i)-*Z*

Purification: Column chromatography (PE/Et₂O = 30:1) isolated as a colorless oil (85% yield). E/Z: 6:94.

¹H NMR (400 MHz, CDCl₃): δ 7.58 (dd, *J* = 8.0, 1.2 Hz, 1H), {E: 7.47 (dt, *J* = 16.0, 4.0 Hz), Z: 7.37 (dd, *J* = 8.0, 4.0 Hz), 1H}, 7.30 (td, *J* = 8.0, 4.0 Hz, 1H), 7.20 (t, *J* = 8.0, 1H), 6.98 (d, *J* = 12.0 Hz, 1H), {E: 6.28 (dt, *J* = 16.0, 12.0 Hz), Z: 6.00 (q, *J* = 12.0 Hz), 1H}, {E: 4.38 (q, *J* = 8.0 Hz), Z: 4.02 (q, *J* = 8.0 Hz), 2H}, {E: 1.39 (t, *J* = 8.0 Hz), Z: 1.19 (t, *J* = 8.0 Hz), 3H}. **¹³C NMR** (100 MHz, CDCl₃): δ 163.1 (t, *J* = 34.0 Hz), 137.8 (t, *J* = 9.0 Hz), 134.8, 132.1, 131.0(t, *J* = 3.0 Hz), 130.1, 127.1, 123.4 (t, *J* = 28.0 Hz), 123.0 (t, *J* = 2.0 Hz), 112.0(t, *J* = 245.0 Hz), 63.0, 13.6. **¹⁹F NMR** (376 MHz, CDCl₃): δ -94.60 (d, *J* = 12.2 Hz), -103.08 (d, *J* = 8.3 Hz). **IR**: υ (cm⁻¹) 3649, 2978, 1767, 1392, 1157, 1072, 906, 729, 648. **HRMS** (**ESI**) (m/z): [M+Na]⁺ calcd. for C₁₂H₁₁BrF₂NaO₂: 326.9808, found: 326.9803.

Ethyl (E)-4-(2-bromophenyl)-2,2-difluorobut-3-enoate(5i)-*E*

Purification: Column chromatography (PE/Et$_2$O = 30:1) isolated as a colorless oil (52% yield). E/Z: 91:9.

^{1}H NMR (400 MHz, CDCl$_3$): δ {Z: 7.74-7.71(m), E: 7.47 (dt, *J* = 16.0, 4.0 Hz), 1H}, 7.62-7.53(m, 2H), {E: 7.22(t, *J* = 8.0 Hz), Z: 6.98(d, *J* = 12.0 Hz), 1H}, {E: 6.28 (dt, *J* = 16.0, 12.0 Hz), Z: 6.00 (q, *J* = 12.0 Hz), 1H}, {E: 4.38 (q, *J* = 8.0 Hz), Z: 4.02 (q, *J* = 8.0 Hz), 2H}, {E: 1.39 (t, *J* = 8.0 Hz), Z: 1.19 (t, *J* = 8.0 Hz), 3H}. **^{13}C NMR** (100 MHz, CDCl$_3$): δ 163.1 (t, *J* = 34.0 Hz), 137.8 (t, *J* = 9.0 Hz), 134.8, 132.1, 131.0(t, *J* = 3.0 Hz), 130.1, 127.1, 123.4 (t, *J* = 28.0 Hz), 123.0 (t, *J* = 2.0 Hz), 112.0(t, *J* = 245.0 Hz), 63.0, 13.6. **^{19}F NMR** (376 MHz, CDCl$_3$): δ -94.60 (d, *J* = 12.2 Hz), -103.10 (d, *J* = 8.3 Hz). **IR**: υ (cm^{-1}) 2978, 1766, 1292, 1076, 968, 906, 729.

Ethyl (Z)-2,2-difluoro-4-(4-fluoro-2-methylphenyl)but-3-enoate(5J)-*Z*

Purification: Column chromatography (PE/Et$_2$O = 30:1) isolated as a colorless oil (76% yield). E/Z: 14: 86.

^{1}H NMR (400 MHz, CDCl$_3$): δ {E: 7.47-7.43 (m), Z: 6.94-6.83 (m), 3H}, {E: 7.27(dt, *J* = 12.0, 4.0 Hz), Z: 7.21-7.17(m), 1H}, {E: 6.16 (dt, *J* = 16.0, 12.0 Hz), Z: 5.97 (q, *J* = 12.0 Hz), 1H}, {E: 4.37 (q, *J* = 8.0 Hz), Z: 3.97 (q, *J* = 8.0 Hz), 2H}, {E: 2.38(s), Z: 2.26(s), 3H}, {E: 1.38 (t, *J* = 8.0 Hz), Z: 1.17 (t, *J* = 8.0 Hz), 3H}. **^{13}C NMR** (100 MHz, CDCl$_3$): δ 163.2 (t, *J* = 34.0 Hz), 162.8(d, *J* = 247.0 Hz), 138.7(d, *J* = 8.0 Hz), 137.0 (t, *J* = 9.0 Hz), 130.9 (dt, *J* = 8.0, 3.0 Hz), 123.4 (t, *J* = 28.0 Hz), 117.3(d, *J* = 21.0 Hz), 116.4 (d, *J* = 21.0 Hz), 113.4 (d, *J* = 22.0 Hz), 112.3 (d, *J* = 21.0 Hz), 112.2(t, *J* = 245.0 Hz), 62.9, 20.0, 13.6. **^{19}F NMR** (376 MHz, CDCl$_3$): δ -94.29(d, *J* = 11.4 Hz), -103.03(dd, *J* =11.4, 3.8 Hz), -111.22 -112.15(m), -113.53- -113.44(m). **IR**: υ (cm^{-1}) 2927, 1770, 1492, 1072, 906, 733. **HRMS** (**ESI**) (m/z): [M+Na]$^+$ calcd. for C$_{13}$H$_{13}$F$_3$NaO$_2$: 281.0765, found: 281.0760.

Ethyl (E)-2,2-difluoro-4-(4-fluoro-2-methylphenyl)but-3-enoate(5J)-*E*

Purification: Column chromatography (PE/Et$_2$O = 30:1) isolated as a colorless oil (52% yield). E/Z: 97:3.

^{1}H NMR (400 MHz, CDCl$_3$): δ 7.47-7.43 (m, 1H), 7.28(dt, *J* = 12.0, 4.0 Hz, 1H), 6.94-6.89(m, 2H), {E: 6.16 (dt, *J* = 16.0, 12.0 Hz), Z: 5.97 (q, *J* = 12.0 Hz), 1H}, {E: 4.37 (q, *J* = 8.0 Hz), Z: 3.97 (q, *J* = 8.0 Hz), 2H}, {E: 2.38 (s), Z: 2.26(s), 3H}, {E: 1.38 (t, *J* = 8.0 Hz), Z: 1.17 (t, *J* = 8.0 Hz), 3H}. **^{13}C NMR** (100 MHz, CDCl$_3$): δ 163.9 (t, *J* = 34.0 Hz), 163.2(d, *J* = 249.0 Hz), 139.3(d, *J* = 8.0 Hz), 133.6 (t, *J* = 9.0 Hz), 129.4(t, *J* = 2.0 Hz), 128.0 (dt, *J* = 9.0, 2.0 Hz), 119.8 (dt, *J* = 25.0, 2.0 Hz), 117.2(d, *J* = 21.0 Hz), 113.4 (d, *J* = 22.0 Hz), 112.2, 112.6(t, *J* = 248.0 Hz), 63.1, 19.7, 14.0. **^{19}F NMR** (376 MHz, CDCl$_3$): δ -94.29(d, *J* = 11.4 Hz), -103.01(dd, *J* =11.4, 3.8 Hz), -111.21 -112.14(m). **IR**: υ (cm^{-1}) 2978, 1767, 1651, 1519, 1076, 902, 725, 648.

Ethyl (Z)-2,2-difluoro-4-(2,3,4,5,6-pentamethylphenyl)but-3-enoate(5k)-*Z*

Purification: Column chromatography (PE/Et$_2$O = 30:1) isolated as a colorless oil (55% yield). E/Z: 1: 99.

^{1}H NMR (400 MHz, CDCl$_3$): δ 7.23 (d, *J* = 16.0, 4.0 Hz, 1H), 5.75 (dt, *J* = 16.0, 12.0 Hz, 1H), 4.40 (q, *J* = 8.0 Hz, 2H), 2.27 (s, 3H), 2.24 (s, 6H), 2.21 (s, 6H), 1.39 (t, *J* = 8.0 Hz, 3H). **^{13}C NMR** (100 MHz, CDCl$_3$): δ 164.0 (t, *J* = 35.0 Hz), 138.02 (t, *J* = 10.0 Hz), 134.9, 132.7, 132.3, 131.0 (d, *J* = 1.0 Hz), 124.9 (t, *J* = 25.0 Hz), 112.4 (t, *J* = 248.0 Hz), 63.0, 17.6, 16.8, 16.5, 14.0. **^{19}F NMR** (376 MHz, CDCl$_3$): δ -94.73 (d, *J* = 12.3 Hz), -103.79 (dd, *J* = 11.3, 3.8 Hz). **IR**: υ (cm^{-1}) 2978, 2885, 1766, 1384, 1087, 906, 729, 648. **HRMS** (**ESI**) (m/z): [M+Na]$^+$ calcd. for C$_{17}$H$_{22}$F$_2$NaO$_2$: 319.1486, found: 319.1475.

Ethyl (Z)-4-(2-chloro-6-methylphenyl)-2,2-difluorobut-3-enoate(5l)-*Z*

Purification: Column chromatography (PE/Et$_2$O = 30:1) isolated as a colorless oil (87% yield). E/Z: 1: 99.

¹H NMR (400 MHz, CDCl₃): δ 7.28-7.26 (m, 1H), 7.19-7.12 (m, 3H), 6.14 (dt, J = 16.0, 12.0 Hz, 1H), 4.39 (q, J = 8.0 Hz, 2H), 2.37 (s, 3H), 1.38 (t, J = 8.0 Hz, 3H). **¹³C NMR** (100 MHz, CDCl₃): δ 163.7 (t, J = 35.0 Hz), 138.2, 133.6, 132.9(t, J = 10.0 Hz), 129.0, 127.5, 126.2 (t, J = 25.0 Hz), 112.3 (t, J = 248.0 Hz), 63.1, 21.0, 14.0. **¹⁹F NMR** (376 MHz, CDCl₃): δ -104.38 (dd, J = 11.4, 3.8 Hz). **IR**: υ (cm⁻¹) 2982, 1767, 1261, 1076, 906, 733. **HRMS** (**ESI**) (m/z): [M+Na]⁺ calcd. for $C_{13}H_{13}ClF_2NaO_2$: 297.0470, found: 297.0460.

Ethyl (Z)-2,2-difluoro-4-phenylpent-3-enoate (5m)-*Z*

Purification: Column chromatography (Cyclohexane/EtOAc = 40:1) isolated as a colorless oil (71% yield). *E/Z*: 10:90.

¹H NMR (400 MHz, CDCl₃): δ {E: 7.42-7.41(m), Z: 7.21-7.18(m), 2H}, 7.38-7.30(m, 3H), {E: 5.92 (t, J = 12.0 Hz), Z: 5.81 (t, J = 12.0 Hz), 1H}, {E: 4.38 (q, J = 8.0 Hz), Z: 3.88 (q, J = 8.0 Hz), 2H}, {E: 2.28-2.27(m), Z: 2.18-2.16(m), 3H}, {E: 1.37 (t, J = 8.0 Hz), Z: 1.20 (t, J = 8.0 Hz), 3H}. 3C NMR (100 MHz, CDCl₃): δ 163.6 (t, J = 34.0 Hz), 148.7(t, J = 9.0 Hz), 139.1, 128.1, 128.0, 127.5(t, J = 2.0 Hz), 119.2 (t, J = 28.0 Hz), 112.3(t, J = 244.0 Hz), 62.6, 27.1, 13.6.**¹⁹F NMR** (376 MHz, CDCl₃): δ -91.9 (d, J = 11.3 Hz), -97.7 (d, J = 11.3 Hz). **HRMS** (**ESI**) (m/z): [M+Na]⁺ calcd. for $C_{13}H_{14}F_2NaO_2$: 263.0860, found: 263.0857.

Ethyl (E)-2,2-difluoro-4-phenylpent-3-enoate(5m)-*E*

Purification: Column chromatography (Cyclohexane/EtOAc = 40:1) isolated as a colorless oil (51% yield). *E/Z*: 90: 10.

¹H NMR (400 MHz, CDCl₃): δ {E: 7.45-7.41(m), Z: 7.21-7.19(m), 2H}, 7.40-7.32(m, 3H), {E: 5.93 (dt, J = 12.0, 4.0 Hz), Z: 5.81 (t, J = 12.0, 4.0 Hz), 1H}, {E: 4.37 (q, J = 8.0 Hz), Z: 3.88(q, J = 8.0 Hz), 2H}, {E: 2.29-2.27(m), Z: 2.18-2.16(m), 3H}, {E: 1.37 (t, J = 8.0 Hz), Z: 1.16 (t, J = 8.0 Hz), 3H}. **¹³C NMR** (100 MHz, CDCl₃): δ 164.3 (t, J = 35.0 Hz), 147.7(t, J = 7.0 Hz), 141.6, 128.7, 128.6, 128.0, 127.5(t, J = 2.0 Hz), 126.0, 118.7 (t, J = 27.0 Hz), 113.0(t, J = 247.0 Hz), 63.0, 17.4, 14.0. **¹⁹F NMR** (376 MHz, CDCl₃): δ -91.9 (d, J = 11.3 Hz), -97.7 (d, J = 11.3 Hz).

Ethyl (Z)-4-(4-bromophenyl)-2,2-difluoropent-3-enoate (5n)-*Z*

Purification: Column chromatography (Cyclohexane/EtOAc = 40:1) isolated as a colorless oil (88% yield). E/Z: 18: 82.

¹H NMR (400 MHz, CDCl₃): δ 7.51-7.49(m, 2H), {E: 7.30-7.28(m), Z: 7.09-7.06 (m), 2H}, {E: 5.92 (t, J = 12.0 Hz), Z: 5.81 (t, J = 12.0 Hz), 1H}, {E: 4.37 (q, J = 8.0 Hz), Z: 3.99 (q, J = 8.0 Hz), 2H}, {E: 2.26-2.24(m), Z: 2.15-2.13(m), 3H}, {E: 1.37 (t, J = 8.0 Hz), Z: 1.20 (t, J = 8.0 Hz), 3H}. **¹³C NMR** (100 MHz, CDCl₃): δ 163.6 (t, J = 34.0 Hz), 147.4(t, J = 8.0 Hz), 138.0, 131.6, 131.4, 131.2, 129.4, 129.1, 127.7, 122.9, 122.2, 119.6 (t, J = 27.0 Hz), 119.2, 112.0(t, J = 246.0 Hz), 62.8, 27.0, 13.7. **¹⁹F NMR** (376 MHz, CDCl₃): δ -92.9 (d, J = 11.3 Hz), -97.8 (d, J = 11.3 Hz). **HRMS** (**ESI**) (m/z): [M+Na]⁺ calcd. for $C_{13}H_{13}BrF_2NaO_2$: 340.9965, found: 340.9970.

Ethyl (E)-4-(4-bromophenyl)-2,2-difluoropent-3-enoate(5n)-*E*

Purification: Column chromatography (Cyclohexane/EtOAc = 40:1) isolated as a colorless oil (43% yield). E/Z: 90: 10.

¹H NMR (400 MHz, CDCl₃): δ 7.51-7.46(m, 2H), {E: 7.31-7.27 (m), Z: 7.09-7.07 (m), 2H}, {E: 5.92(t, J = 12.0 Hz), Z: 5.81(t, J = 12.0 Hz), 1H} {E: 4.37 (q, J = 8.0 Hz), Z: 3.99(q, J = 8.0 Hz), 2H}, {E: 2.26-2.24(m), Z: 2.15-

64

2.13(m), 3H}, {E: 1.37 (t, *J* = 8.0 Hz), Z: 1.16 (t, *J* = 8.0 Hz), 3H}. **^{13}C NMR** (100 MHz, CDCl₃): δ 164.1 (t, *J* = 35.0 Hz), 146.6(t, *J* = 7.0 Hz), 140.4, 131.6, 131.2, 129.1(t, *J* = 2.0 Hz), 127.7, 122.8, 122.2, 119.2 (t, *J* = 27.0 Hz), 112.8(t, *J* = 248.0 Hz), 63.1, 17.3, 13.9. **^{19}F NMR** (376 MHz, CDCl₃): δ -92.9 (d, *J* = 11.3 Hz), -97.8 (d, *J* = 11.3 Hz).

Ethyl (Z)-2,2-difluoro-4-(4-(methylthio)phenyl)pent-3-enoate(5o)-*Z*

Purification: Column chromatography (Cyclohexane/EtOAc = 40:1) isolated as a colorless oil (77% yield). *E/Z*: 1: 99.

^{1}H NMR (400 MHz, CDCl₃): δ 7.22-7.20(m, 2H), 7.14-7.11(m, 2H), Z: 5.78 (dt, *J* = 12.0, 4.0 Hz), 1H}, 3.93 (q, *J* = 8.0 Hz), 2H, 2.49(s, 3H), 2.15-2.13(m, 3H), 1.37 (t, *J* = 8.0 Hz). **^{13}C NMR** (100 MHz, CDCl₃): δ 163.7 (t, *J* = 34.0 Hz), 148.1(t, *J* = 10.0 Hz), 138.8, 135.6, 128.0(t, *J* = 2.0 Hz), 125.8, 119.2 (t, *J* = 27.0 Hz), 112.3(t, *J* = 244.0 Hz), 62.87, 26.9, 115.5, 13.6. **^{19}F NMR** (376 MHz, CDCl₃): δ -91.9 (d, *J* = 11.3 Hz), -97.4 (d, *J* = 11.3 Hz). **HRMS** (**ESI**) (m/z): [M+Na]⁺ calcd. for C₁₄H₁₆F₂NaO₂S: 309.0737, found: 309.0737.

Ethyl (E)-2,2-difluoro-4-(4-(methylthio)phenyl)pent-3-enoate (5o)-*E*

Purification: Column chromatography (Cyclohexane/EtOAc = 40:1) isolated as a colorless oil (53% yield). *E/Z*: 80: 20.

^{1}H NMR (400 MHz, CDCl₃): δ {E: 7.37-7.34(m), Z: 7.14-7.12(m), 2H}, 7.25-7.20(m, 2H), {E: 5.96(t, *J* = 12.0 Hz), Z: 5.79(t, *J* = 12.0 Hz), 1H} {E: 4.36 (q, *J* = 8.0 Hz), Z: 3.92(q, *J* = 8.0 Hz), 2H}, {E:2.50(s), Z: 2.49(s), 3H}, {E: 2.26-2.24(m), Z: 2.15-2.13(m), 3H}, {E: 1.37 (t, *J* = 8.0 Hz), Z: 1.17 (t, *J* = 8.0 Hz), 3H}. **^{13}C NMR** (100 MHz, CDCl₃): δ 164.3 (t, *J* = 35.0 Hz), 148.1, 146.9(t, *J* = 7.0 Hz), 139.6, 138.8, 138.0, 135.6, 128.0(t, *J* = 2.0 Hz), 126.4, 126.1, 125.7, 119.2 (t, *J* = 28.0 Hz), 118.0(t, *J* = 26.0 Hz), 113.0(t, *J* = 246.0 Hz), 63.0, 17.1, 13.6. **^{19}F NMR** (376 MHz, CDCl₃): δ -91.9 (d, *J* = 11.3 Hz), -97.4 (d, *J* = 11.3 Hz).

Ethyl (E)-2,2-difluoro-4-(thiophen-2-yl)but-3-enoate(3p)-*E*

Purification: Column chromatography (PE/Et₂O = 30:1) isolated as a pale yellow oil (36% yield). E/Z: 91:9.

^{1}H NMR (400 MHz, CDCl₃): δ 7.39-7.21(m, 3H), {E: 7.09-7.07 (m), Z: 6.94(d, *J* = 12.0 Hz), 1H} {E: 6.17 (dt, *J* = 16.0, 12.0 Hz), Z: 5.78 (q, *J* = 8.0 Hz), 1H}, {E: 4.41 (q, *J* = 8.0 Hz), Z: 4.29 (q, *J* = 8.0 Hz), 2H}, {E: 1.43 (t, *J* = 8.0 Hz), Z: 1.30 (t, *J* = 8.0 Hz), 3H}. **^{13}C NMR** (100 MHz, CDCl₃): δ 163.8(t, *J* = 34.0 Hz), 129.8(t, *J* = 11.0 Hz), 129.4, 127.3, 117.6(t, *J* = 25.0 Hz), 112.4(t, *J* = 248.0 Hz), 63.1, 13.9. **^{19}F NMR** (376 MHz, CDCl₃): δ -96.37 (d, *J* = 15.0 Hz), -102.97 (d, *J* = 11.3 Hz). **IR**: υ (cm⁻¹) 2986, 1763, 1647, 1307, 1199, 1072, 906, 729.

Ethyl 2,2-difluoro-4-phenylbut-3-ynoate(7a)

Purification: Column chromatography (PE/Et₂O = 30:1) isolated as colorless oil (60% yield).

^{1}H NMR (400 MHz, CDCl₃): δ 7.55 (d, *J* = 8.0 Hz, 2H), 7.48-7.44(m, 1H), 7.41-7.36(m, 2H), 4.42 (q, *J* = 8.0 Hz, 2H), 1.41 (t, *J* = 8.0 Hz, 3H). **^{13}C NMR** (100 MHz, CDCl₃): δ 161.6(t, *J* = 35.0 Hz), 132.4(t, *J* = 2.0 Hz), 130.5, 128.5, 119.3(t, *J* = 3.0 Hz), 104.9(t, *J* = 241.0 Hz), 100.0, 89.6(t, *J* = 241.0 Hz), 78.4(t, *J* = 38.0 Hz), 63.8, 13.9. **^{19}F NMR** (376 MHz, CDCl₃): δ -89.96. **IR**(neat): υ (cm⁻¹) 2245, 1770, 1273, 1145, 1080, 906, 729, 652. **HRMS** (**ESI**) (m/z): [M+Na]⁺ calcd. for C₁₂H₁₀F₂NaO₂: 247.0547, found: 247.0541.

Ethyl 4-(2-ethylphenyl)-2,2-difluorobut-3-ynoate(7b)

Purification: Column chromatography (PE/Et$_2$O = 100:1) isolated as a colorless oil (35% yield).

^{1}H NMR (400 MHz, CDCl$_3$): δ 7.51 (d, *J* = 8.0 Hz, 1H), 7.41-7.36 (m, 1H), 7.28-7.26(m, 1H), 4.42 (q, *J* = 8.0 Hz, 2H), 2.82 (q, *J* = 8.0 Hz, 2H), 1.41 (t, *J* = 8.0 Hz, 3H), 1.26 (t, *J* = 8.0 Hz, 3H). **^{13}C NMR** (100 MHz, CDCl$_3$): δ 161.6(t, *J* = 35.0 Hz), 147.8(*J* = 2.0 Hz), 133.0(*J* = 2.0 Hz), 130.7, 128.3, 125.8, 118.4, 105.0(t, *J* = 241.0 Hz), 88.8(t, *J* = 7.0 Hz), 81.6(t, *J* = 38.0 Hz), 63.8, 27.5, 14.8, 13.9. **^{19}F NMR** (376 MHz, CDCl$_3$): δ -89.79. **HRMS** (**ESI**) (m/z): [M+Na]$^+$ calcd. for C$_{14}$H$_{14}$F$_2$NaO$_2$: 275.0860, found: 275.0850.

Ethyl 2,2-difluoro-4-(o-tolyl)but-3-ynoate(7c)

Purification: Column chromatography (PE/Et$_2$O = 50:1) isolated as a colorless oil (48% yield).

^{1}H NMR (400 MHz, CDCl$_3$): δ 7.52-7.49 (m, 1H), 7.37-7.33 (m, 1H), 7.26-7.18(m, 2H), 4.42 (q, *J* = 8.0 Hz, 2H), 2.47(s, 3H), 1.41 (t, *J* = 8.0 Hz, 3H). **^{13}C NMR** (100 MHz, CDCl$_3$): δ 161.6(t, *J* = 35.0 Hz), 141.7, 132.7(t, *J* = 2.0 Hz), 130.5, 129.7, 125.8, 119.1(t, *J* = 3.0 Hz), 105.0(t, *J* = 242.0 Hz), 88.8(t, *J* = 7.0 Hz), 82.1(t, *J* = 38.0 Hz), 63.8, 20.4, 13.9. **^{19}F NMR** (376 MHz, CDCl$_3$): δ -89.70. **IR**(neat): υ (cm^{-1}) 2978, 2241, 1770, 1385, 1269, 1149, 1076, 902, 725. **HRMS** (**ESI**) (m/z): [M+Na]$^+$ calcd. for C$_{13}$H$_{12}$F$_2$NaO$_2$: 261.0703, found: 261.0706.

Ethyl 2,2-difluoro-4-(m-tolyl)but-3-ynoate(7d)

Purification: Column chromatography (PE/Et$_2$O = 30:1) isolated as colorless oil (54% yield).

^{1}H NMR (400 MHz, CDCl$_3$): δ 7.37-7.34(m, 2H), 7.27-7.26(m, 2H), 4.42 (q, *J* = 8.0 Hz, 2H), 2.36(s, 3H), 1.41 (t, *J* = 8.0 Hz, 3H). **^{13}C NMR** (100 MHz, CDCl$_3$): δ 161.6(t, *J* = 34.0 Hz), 138.4, 132.9, 131.4, 129.5(t, *J* = 2.0 Hz), 128.4, 119.1, 104.9(t, *J* = 241.0 Hz), 63.8, 21.1, 13.9. **^{19}F NMR** (376 MHz, CDCl$_3$): δ -89.84. **IR**(neat): υ (cm^{-1}) 2245, 1770, 1508, 1284, 1199, 1134, 1080, 906, 729, 648. **HRMS** (**ESI**) (m/z): [M+Na]$^+$ calcd. for C$_{13}$H$_{12}$F$_2$NaO$_2$: 261.0703, found: 261.0700.

Ethyl 2,2-difluoro-4-(o-tolyl)but-3-ynoate (7e)

Purification: Column chromatography (PE/Et$_2$O = 50:1) isolated as a colorless oil (34% yield).

^{1}H NMR (400 MHz, CDCl$_3$): δ 7.44 (d, *J* = 8.0 Hz, 2H), 7.19 (d, *J* = 8.0 Hz, 2H), 4.42 (q, *J* = 8.0 Hz, 2H), 2.39(s, 3H), 1.41 (t, *J* = 8.0 Hz, 3H). **^{13}C NMR** (100 MHz, CDCl$_3$): δ 141.0, 132.3, 129.3, 116.2, 90.0, 63.8, 29.7, 13.9. **^{19}F NMR** (376 MHz, CDCl$_3$): δ -89.68. **IR**(neat): υ (cm^{-1}) 2978, 1770, 1381, 1145, 1080, 903, 725. **HRMS** (**ESI**) (m/z): [M+Na]$^+$ calcd. for C$_{13}$H$_{12}$F$_2$NaO$_2$: 261.0703, found: 261.0704.

Ethyl 2,2-difluoro-4-(4-methoxyphenyl)but-3-ynoate(7f)

Purification: Column chromatography (cyclohexane/EtOAc = 30:1) isolated as colorless oil (47% yield).

^{1}H NMR (400 MHz, CDCl$_3$): δ 7.49 (d, *J* = 8.0 Hz, 2H), 6.89 (d, *J* = 8.0 Hz, 2H), 4.42 (q, *J* = 8.0 Hz, 2H), 1.41 (t, *J* = 8.0 Hz, 3H). **^{13}C NMR** (100 MHz, CDCl$_3$): δ 161.7(t, *J* = 35.0 Hz), 161.3, 134.1, 130.9, 128.8, 114.2, 111.2, 105.1(t, *J* = 241.0 Hz), 90.1, 63.7, 55.4, 13.9. **^{19}F NMR** (376 MHz, CDCl$_3$): δ -89.40. **HRMS** (**ESI**) (m/z): [M+Na]$^+$ calcd. for C$_{13}$H$_{12}$F$_2$NaO$_3$: 277.0652, found: 277.0647.

Ethyl 2,2-difluoro-4-(4-(methylthio)phenyl)but-3-ynoate(7g)

Purification: Column chromatography (n-hexane/EtOAc = 50:1) isolated as colorless oil (62% yield).

[1H NMR (400 MHz, CDCl$_3$): δ 7.44 (d, *J* = 8.0 Hz, 2H), 7.21 (d, *J* = 8.0 Hz, 2H), 4.42 (q, *J* = 8.0 Hz, 2H), 1.41 (t, *J* = 8.0 Hz, 3H). **13C NMR** (100 MHz, CDCl$_3$): δ 161.6, 142.7, 135.5, 125.4, 115.2(t, *J* = 3.0 Hz), 109.9, 107.2, 105.0(t, *J* = 242.0 Hz), 89.7, 63.8, 31.9, 15.0. **19F NMR** (376 MHz, CDCl$_3$): δ -89.71. **IR**(neat): υ (cm^{-1}) 2253, 902, 721, 648. **HRMS** (**ESI**) (m/z): [M+Na]$^+$ calcd. for C$_{13}$H$_{12}$F$_2$NaO$_2$S: 293.0424, found: 293.0414.

Ethyl 2,2-difluoro-4-(naphthalen-1-yl)but-3-ynoate(7h)

Purification: Column chromatography (n-hexane/EtOAc = 50:1) isolated as colorless oil(39% yield).

1H NMR (400 MHz, CDCl$_3$): δ 8.26 (dd, *J* = 12.0, 4.0 Hz, 1H), 7.96(d, *J* = 8.0 Hz, 1H), 7.90(d, *J* = 8.0 Hz, 1H), 7.81(d, *J* = 8.0 Hz, 1H), 7.66-7.56(m, 2H), 7.50-7.46(m, 1H), 4.47 (q, *J* = 8.0 Hz, 2H), 1.45 (t, *J* = 8.0 Hz, 3H). **13C NMR** (100 MHz, CDCl$_3$): δ 133.0, 132.2, 131.2, 128.5, 127.6, 126.9, 125.5, 123.3, 63.9, 13.9. **19F NMR** (376 MHz, CDCl$_3$): δ -89.65. **IR**(neat): υ (cm^{-1}) 2978, 2885, 2233, 1770, 1384, 1149, 906, 732. **HRMS** (**ESI**) (m/z): [M+Na]$^+$ calcd. for C$_{16}$H$_{12}$F$_2$NaO$_2$: 297.0703, found: 297.0713.

Ethyl 4-(3,5-dimethylphenyl)-2,2-difluorobut-3-ynoate(7i)

Purification: Column chromatography (cyclohexane/EtOAc = 50:1) isolated as colorless oil (46% yield).

1H NMR (400 MHz, CDCl$_3$): δ 7.18 (s, 2H), 7.08(s, 1H), 4.42(q, *J* = 8.0 Hz, 2H), 2.32(s, 6H), 1.41 (t, *J* = 8.0 Hz, 3H). **13C NMR** (100 MHz, CDCl$_3$): δ 161.6, 138.2, 132.4, 130.9, 130.0, 128.8, 118.9, 104.9, 90.2, 63.8, 21.0, 13.9. **19F NMR** (376 MHz, CDCl$_3$): δ -89.73. **HRMS** (**ESI**) (m/z): [M+Na]$^+$ calcd. for C$_{14}$H$_{14}$F$_2$NaO$_2$: 275.0860, found: 275.0850.

Ethyl 4-(3,5-dichlorophenyl)-2,2-difluorobut-3-ynoate(7j)

Purification: Column chromatography (cyclohexane /EtOAc = 100:1) isolated as colorless oil (28% yield).

1H NMR (400 MHz, CDCl$_3$): δ 7.46-7.44 (m, 3H), 4.43(q, *J* = 8.0 Hz, 2H), 1.42 (t, *J* = 8.0 Hz, 3H). **13C NMR** (100 MHz, CDCl$_3$): δ 161.0(t, *J* = 34.0 Hz), 135.4, 131.0, 130.5(t, *J* = 2.0 Hz), 122.1, 104.5(t, *J* = 243.0 Hz), 86.3, 80.2, 64.1, 13.9. **19F NMR** (376 MHz, CDCl$_3$): δ -90.75. **HRMS** (**ESI**) (m/z): [M+Na]$^+$calcd. for C$_{12}$H$_8$Cl$_2$F$_2$NaO$_2$: 314.9767, found: 314.9757.

Ethyl 4-(4-ethoxy-3,3-difluoro-4-oxobut-1-yn-1-yl)benzoate (7k)

Purification: Column chromatography (cyclohexane /EtOAc = 50:1) isolated as colorless oil (27% yield).

1H NMR (400 MHz, CDCl$_3$): δ 8.06 (d, *J* = 8.0 Hz, 2H), 7.62(d, *J* = 8.0 Hz, 2H), 4.42(q, *J* = 8.0 Hz, 2H), 4.41 (q, *J* = 8.0 Hz, 2H), 1.45 (t, *J* = 8.0 Hz, 6H). **13C NMR** (100 MHz, CDCl$_3$): δ 165.6, 161.3(t, *J* = 34.0 Hz), 132.3(t, *J* = 3.0 Hz), 132.1, 129.6, 123.6, 104.7(t, *J* = 242.0 Hz), 88.4(t, *J* = 7.0 Hz), 80.5(t, *J* = 38.0 Hz), 64.0, 61.5, 14.3, 13.9. **19F NMR** (376 MHz, CDCl$_3$): δ -90.41. **HRMS** (**ESI**) (m/z): [M+Na]$^+$calcd. for C$_{15}$H$_{14}$F$_2$NaO$_4$: 319.0758, found: 319.0754.

Ethyl 4-(4-acetylphenyl)-2,2-difluorobut-3-ynoate(7l)

Purification: Column chromatography (cyclohexane/EtOAc = 50:1) isolated as colorless oil (17% yield).

1H NMR (400 MHz, CDCl$_3$): δ 7.97 (d, *J* = 8.0 Hz, 2H), 7.65(d, *J* = 8.0 Hz, 2H), 4.43(q, *J* = 8.0 Hz, 2H), 2.63(s, 3H), 1.42 (t, *J* = 8.0 Hz, 6H). **13C NMR** (100 MHz, CDCl$_3$): δ 197.0, 161.3, 138.1, 132.6(t, *J* = 2.0 Hz), 130.9, 104.7(t, *J* = 242.0 Hz), 88.2(t, *J* = 7.0 Hz), 80.8, 64.0, 26.7, 13.9. **19F NMR** (376 MHz, CDCl$_3$): δ -90.45. **HRMS** (**ESI**) (m/z): [M+Na]$^+$calcd. for C$_{14}$H$_{12}$F$_2$NaO$_3$: 289.0652, found: 289.0649.

Ethyl 2-(2,6-di-tert-butyl-4-methylphenoxy)-2,2-difluoroacetate (BHT-CF$_2$CO$_2$Et)

Purification: Column chromatography (PE/Et$_2$O = 30:1) isolated as a colorless oil (35% yield).

^{1}H NMR (400 MHz, CDCl$_3$): δ 6.55 (s, 2H), 4.16 (q, J = 8.0 Hz, 2H), 1.41 (s, 3H), 1.27 (t, J = 4.0 Hz, 3H), 1.23 (s, 18H). **^{13}C NMR** (100 MHz, CDCl$_3$): δ 185.3, 162.6, 149.1, 137.6, 130.9, 128.8, 116.0. **^{19}F NMR** (376 MHz, CDCl$_3$): δ -113.01. **IR**: υ (cm^{-1}) 2963, 1763, 1647, 1458, 1373, 1307, 1180, 1126, 1030, 906, 733. **HRMS** (**ESI**) (m/z): [M+Na]$^+$ calcd. for C$_{19}$H$_{28}$F$_2$NaO$_3$: 365.1904, found: 365.1904.

Associated Content:

The *Supporting Information* for this article is available on the ACS publication website at DOI: 10.1021/acscatal.7b03019.

Reference:

(1). (a) Zhou, Y.; Wang, J. ; Gu, Z.; Wang, S. ; Zhu, W.; Acena, J. L.; Soloshonok, V. A.; Izawa, K.; Liu, H. *Chem. Rev.* **2016**, *116*, 422-518. (b) Yerien, D. E.; Bonesi, S.; Postigo, A. *Org. Biomol. Chem.* **2016**, *14*, 8398-8427. (c) Gillis, E. P.; Eastman, K. J.; Hill, M. D.; Donnelly, D. J.; Meanwell, N. A. *J. Med. Chem.* **2015**, *58*, 8315-8359. (d) Purser, S.; Moore, P. R.; Swallow, S.; Gouverneur, V. *Chem. Soc. Rev.* **2008**, *37*, 320-330. (e) Mueller, K.; Faeh, C.; Diederich, F. *Science* **2007**, *317*, 1881-1886. (f) Prakash, G. K. S., Wang, F. Chim. Oggi. **2012**, *30*, 30-36.

(2). (a) Alonso, C.; Martínez de Marigorta, E.; Rubiales, G.; Palacios, F. *Chem. Rev.* **2015**, *115*, 1847-1935. (b) Lu, Y.; Liu, C.; Chen, Q.-Y. *Curr. Org. Chem.* **2015**, *19*, 1638-1650. (c) Merino, E.; Nevado, C. *Chem. Soc. Rev.* **2014**, *43*, 6598-6608. (d) Furuya, T.; Kamlet, A. S.; Ritter, T. *Nature* **2011**, *473*, 470-477.

(3). (a) Meanwell, N. A. *J. Med. Chem.* **2011**, *54*, 2529-2591; b) Erickson, J. A.; McLoughlin, J. I. *J. Org. Chem.* **1995**, *60*, 1626-1631.

(4). Chatterjee, T.; Iqbal, N.; You, Y.; Cho, E. J. *Acc. Chem. Res.* **2016**, *49*, 2284-2294.

(5). (a) Prier, C. K.; Rankic, D. A.; MacMillan, D. W. C. *Chem. Rev.* **2013**, *113*, 5322-5363. (b) Lu, Z.; Yoon, T. P. *Angew. Chem. Int. Ed.* **2012**, *51*, 10329-10332.

(6). (a) Wei, Y.; Hu, P.; Zhang, M.; Su, W. *Chem. Rev.* **2017**, DOI: 10.1021/acs.chemrev.6b00516. (b) Jin, Y.; Fu, H. *Asian J. Org. Chem.* **2017**, *6*, 368 −385. (c) Xuan, J.; Zhang, Z.-G.; Xiao, W.-J. *Angew. Chem. Int. Ed.* **2015**, *54*, 15632-15641. (d) Rodriguez, N.; Goossen, L. J. *Chem. Soc. Rev.* **2011**, *40*, 5030-5048.

(7). For selected papers on metal-catalyzed and −mediated decarboxylative synthesis of difluoromethylated olefins: (a) Li, G.; Wang, T.; Fei, F.; Su, Y.-M.; Li, Y.; Lan, Q.; Wang, X.-S. *Angew. Chem. Int. Ed.* **2016**, *55*, 3491-3495. (b) Chen, Q.; Wang, C.; Zhou, J.; Wang, Y.; Xu, Z.; Wang, R. *J. Org. Chem.* **2016**, *81*, 2639-2645. (c) Li, G.; Cao, Y.-X.; Luo, C.-G.; Su, Y.-M.; Li, Y.; Lan, Q.; Wang, X.-S. *Org. Lett.* **2016**, *18*, 4806-4809. (d) Pannecoucke, X.; Poisson, T. *Synlett* **2016**, *27*, 2314-2326. (e) Li, Z.; Cui, Z.; Liu, Z.-Q. *Org. Lett.* **2013**, *15*, 406-409. (f) He, Z.; Luo, T.; Hu, M.; Cao, Y.; Hu, J. *Angew. Chem. Int. Ed.* **2012**, *51*, 3944-3947.

(8). For selected papers on photocatalytic decarboxylative perfluoroalkylation of olefins: (a) Zhang, H.-R.; Chen, D.-Q.; Han, Y.-P.; Qiu, Y.-F.; Jin, D.-P.; Liu, X.-Y. *Chem. Commun.* **2016**, *52*, 11827-11830. (b) Xu, P.; Abdukader, A.; Hu, K.; Cheng, Y.; Zhu, C. *Chem. Commun.* **2014**, *50*, 2308-2310.

(9). For hypervalent iodine-assisted decarboxylation, see: (a) Huang, H.; Jia, K.; Chen, Y. *ACS Catal.*

2016, *6*, 4983-4988. (b) Huang, H.; Jia, K.; Chen, Y. *Angew. Chem. Int. Ed.* **2015**, *54*, 1881-1884. (c) Huang, H.; Zhang, G.; Chen, Y. *Angew. Chem. Int. Ed.* **2015**, *54*, 7872-7876.

(10). While the *Z* isomer is thermodynamically favored, high *Z* selectivies remain challenging via photoredox catalysis, see: (a) Straathof, N. J. W.; Cramer, S. E.; Hessel, V.; Noel, T. *Angew. Chem. Int. Ed.* **2016**, *55*, 15549-15553. (b) Honeker, R.; Garza-Sanchez, R. A.; Hopkinson, M. N.; Glorius, F. *Chem. Eur. J.* **2016**, *22*, 4395-4399. (c) Roh, G.-b.; Iqbal, N.; Cho, E. J. *Chin. J. Chem.* **2016**, *34*, 459-464. (d) Yu, C.; Iqbal, N.; Park, S.; Cho, E. J. *Chem. Commun.* **2014**, *50*, 12884-12887. (e) Iqbal, N.; Jung, J.; Park, S.; Cho, E. J. *Angew. Chem. Int. Ed.* **2014**, *53*, 539-542. (f) Wei, X.-J.; Yang, D.-T.; Wang, L.; Song, T.; Wu, L.-Z.; Liu, Q. *Org. Lett.* **2013**, *15*, 6054-6057. (g) Nguyen, J. D.; D'Amato, E. M.; Narayanam, J. M. R. Stephenson, C. R. J. *Nature Chem.* **2012**, *4*, 854-859.

(11). For photocatalytic Z-selective alkene synthesis, see: (a) Singh, A.; Fennell, C. J.; Weaver, J. D. *Chem. Sci.* **2016**, *7*, 6796-6802. (b) Metternich, J. B.; Gilmour, R. *J. Am. Chem. Soc.* **2016**, *138*, 1040-1045. (c) Fabry, D. C.; Ronge, M. A.; Rueping, M. *Chem. Eur. J.* **2015**, *21*, 5350-5354. (d) Metternich, J. B.; Gilmour, R. *J. Am. Chem. Soc.* **2015**, *137*, 11254-11257. (e) Singh, K.; Staig, S. J.; Weaver, J. D. *J. Am. Chem. Soc.* **2014**, *136*, 5275-5278. (f) Lin, Q.-Y.; Xu, X.-H.; Qing, F.-L. *J. Org. Chem.* **2014**, *79*, 10434-10446. For a recent review on this topic, see: Metternich, J. B.; Gilmour, R. *Synlett* **2016**, *27*, 2541-2552.

(12). (a) Flamigni, L.; Barbieri, A.; Sabatini, C.; Ventura, B.; Barigelletti, F. *Top. Curr. Chem.* **2007**, *281*, 143-203. (b) Chen, F.-C.; He, G.; Yang, Y. *Appl. Phys. Lett.* **2003**, *82*, 1006-1008. (c) Jung, J.; Kim, E.; You, Y.; Cho, E. J. *Adv. Synth. Catal.* **2014**, *356*, 2741-2748.

(13). For selected reviews describing the benefits of flow on photochemistry, see: (a) *Photochemical processes in continuous-flow reactors*, Noel T. Ed., World Scientific Publishing, London, 2017. (b) Cambié, D.; Bottecchia, C.; Straathof, N. J. W.; Hessel, V.; Noel, T. *Chem. Rev.* **2016**, *116*, 10276-10341. (c) Plutschack, M. B.; Correia, C. A.; Seeberger, P. H.; Gilmore, K. *Top. Organomet. Chem.* **2016**, *57*, 43-76.

(14). Y. Su, K. Kuijpers, N. Koenig, M. Shang, V. Hessel, T. Noel, *Chem. Eur. J.* **2016**, *22*, 12295-12300.

(15). For enhanced selectivity in continuous-flow microreactors and the rationale behind it, see: (a) Noel, T.; Su, Y.; Hessel, V. *Top. Organomet. Chem.* **2016**, *57*, 1-42. (b) Hartman, R. L.; McMullen, J. P.; Jensen, K. F. *Angew. Chem. Int. Ed.* **2011**, *50*, 7502-7519. (c) Yoshida, J.-i.; Nagaki, A.; Iwasaki, T.; Suga, S. *Chem. Eng. Technol.* **2005**, *28*, 259-266.

(16): (a): Kelly, C. B.; Patel, N. R.; Primer, D. N.; Jouffroy, M.; Tellis, J. C.& Molander, G. A. *Nat.*

70

*Protoc.***2017**, *12*, 472-492. (B): Sun, J.; Wu, W.; Zhao, J. *Chem. Eur. J.* **2012**, *18*, 8100-8112.

Chapter 3

Visible-Light Photocatalytic Difluoroalkylation-induced 1, 2-Heteroarene Migration of Allylic Alcohols in Batch and Flow

Abstract

A convenient method for the preparation of sp^3-rich heterocycles is reported. The method comprises a photocatalytic difluoroalkylation-induced 1, 2-heteroarene migration of allylic alcohols. Here we describe for the first time the benefits of using flow to facilitate such migration reactions, including shorter reaction times, higher selectivity and opportunities to scale the chemistry.

Introduction

Heteroarenes are widespread in pharmaceuticals, agrochemicals and other bioactive molecules. Hence, the functionalization of heteroarenes remains a contemporary goal within synthetic organic chemistry.[1] In recent years, there is a trend in medicinal chemistry to prepare more sp^3-rich fragments (so-called "escape-from-flatland strategy") to reduce the attrition rate in drug discovery.[2] To achieve this, the sp^3-character of heteroarenes can be enhanced through alkylation via e.g. radical intermediates.[3,4]

An intriguing approach to access synthetically-useful sp^3-rich heteroarenes is the difunctionalization of alkenes initiated by a radical addition followed by a heteroaryl migration.[5,6] Herein, we describe a novel 1,2-heteroarene migration induced by a photocatalytic radical difluoroalkylation. To prepare the target compounds, we developed a two-step protocol which starts from the corresponding heteroaryl ketones and includes a Grignard reaction and subsequent difluoroalkyl radical-induced migration reaction. As shown in this work, both reactions benefited substantially from continuous-flow processing.
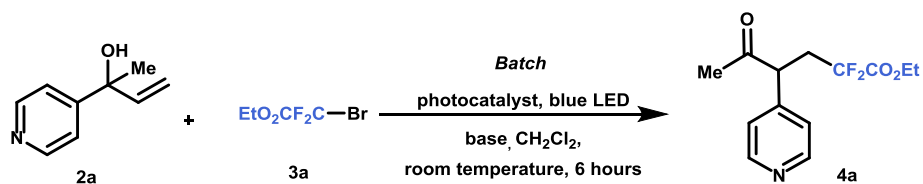
Result and Discussion

Allylic alcohols are typically synthesized via a Grignard reaction between a heteroaryl ketone and vinyl magnesium halide. The reaction is exothermic in nature and requires strict cooling to avoid thermal runaway. Here, we have developed a continuous-flow protocol which allowed us to simultaneously handle the exotherm safely and prepare sufficient starting material for the subsequent photocatalytic migration reaction.[7] The heteroaryl ketone was merged with vinylmagnesium bromide in a T-mixer and subsequently introduced in a capillary microreactor (ID 1.65 mm; 700 μL). To avoid microreactor clogging, the mixer and microreactor were submerged into a sonicated ice bath.[8] A broad variety of heteroaryl allylic alcohols could be prepared in only 5 minutes residence time on a 5-10 mmol scale as shown in **Scheme 3.1**; this includes 4-pyridinyl, 3-pyridinyl, 2-pyridinyl, pyrazinyl, benzothiophenyl, benzofuranyl and thiophenyl bearing allylic alcohols. Notably, the reaction could be carried out at a higher temperature in flow (0 °C vs -78 °C in batch) which resulted in a reduced reaction time (5 min vs 2 h in batch).[9]
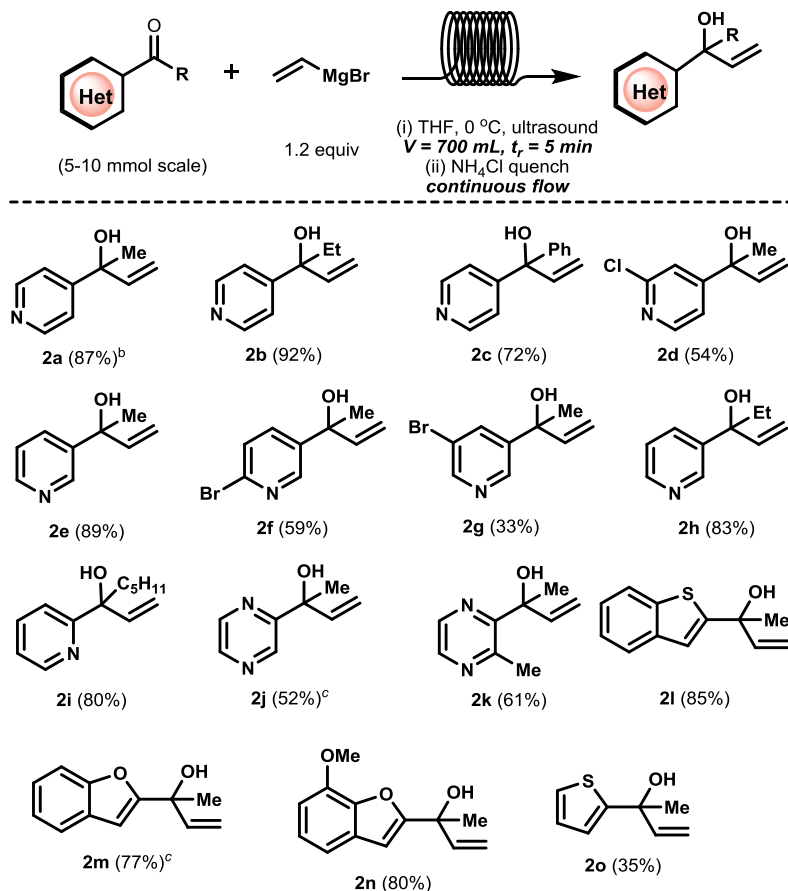
Scheme 3.1: Scope of the continuous-flow Grignard synthesis of allylic alcohols. [a]Reaction conditions: Feed 1 contains **1** (5.0 mmol) in 10 mL THF; Feed 2 contains 10 mL vinylmagnesium bromide (1.67 M in THF). 5 min residence time, 0°C, ultrasound. The reaction is quenched by saturated NH₄Cl at the outlet of the reactor. Reported yields are those obtained after column chromatography. [b]Carried out on a 10 mmol scale, [c]residence time: 2.5 min.

With a diverse set of allylic alcohols in hand, we commenced our investigations toward a broadly applicable difluoroalkylation-induced 1, 2-heteroarene migration with 2-(pyridin-4-yl)but-3-en-2-ol **2a** as the benchmark substrate. Using ethyl bromodifluoroacetate **3a** and Ru(bpy)₃Cl₂·6H₂O as the photocatalyst in the presence of a nitrogen base (**Table 3.1**, Entries 1-3), the target product could be obtained in encouraging yields (15-55%) when the reaction mixture was subjected to blue irradiation. Switching to *fac*-Ir(ppy)₃ as the photocatalyst improved the yield further to 67% (**Table 3.1**, Entry 4). Screening other soluble bases revealed that optimal results could be obtained with imidazole (**Table 3.1**, Entry 6). Several control experiments demonstrate the need for a base, photocatalyst and light (**Table 3.1**, Entries 7-9).

**Table 3.1.** Optimization of the reaction conditions[a]

Entry	Base	Photocatalyst	Yield[b]
1	NEt₃	Ru(bpy)₃Cl₂.6H₂O	31 %
2	iPr₂NEt	Ru(bpy)₃Cl₂.6H₂O	15 %
3	TMEDA	Ru(bpy)₃Cl₂.6H₂O	55 %
4	TMEDA	fac-Ir(ppy)₃	67 %
5	DBU	fac-Ir(ppy)₃	45 %
6	imidazole	fac-Ir(ppy)₃	83 %
7	--	fac-Ir(ppy)₃	57 %
8[c]	imidazole	--	N.D.
9[d]	imidazole	fac-Ir(ppy)₃	N.D.

[a]Reaction Conditions: **2a** (0.2 mmol, 1 equiv.), **3a** (o.6 mmol, 3 equiv.), base (0.4 mmol, 2 equiv.), photocatalyst (1 mol%), dichloromethane(1.0 mL), 12 W blue LEDs ($\lambda = 450$ nm), room temperature, 6 hours. [b] Isolated yield. [c] No photocatalyst. [d] No light.

Having established the optimal reaction conditions, we set out to examine the substrate scope of the developed transformation (**Scheme 3.2**). 4-Pyridine-substituted allylic alcohols bearing various R-groups were subjected to the reaction conditions resulting in the targeted compounds in good yields (R = Me, Et, Ph, **2a-c**). Interestingly, performing the reaction in flow resulted in a substantial reduction (10 min in flow vs. 6 hours in batch) in reaction time and an increase in yield.[10,11] As a consequence of the reduced exposure to light, the reaction mixture was typically cleaner resulting in a more facile purification by column chromatography. Halides on the pyridine moiety were well tolerated providing opportunities for further functionalization via e.g. cross coupling (**4d, 4f, 4g**). Surprisingly, 3-substituted pyridine allylic alcohols (**4e-h**) could also give the aimed product smoothly. However, the yield is probably lower as a result of their lower reactivity in radical processeses.[12] 2-Substituted pyridine allylic alcohol (**4i**) and 2-pyrazine-substituted allylic alcohols (**4j-k**) underwent efficient migration under these photocatalytic conditions. Benzothiophene (**4l**) migrates smoothly as well under our reaction conditons. However, other electron-rich heterocycles, such as benzofuran (**4m-n**) and thiophene (**4o**) are susceptible for a double radical attack yielding the corresponding bifunctionalized compounds in good yield. Also other difluoroalkyl radicals were able to induce the heteroaryl migrations (**Scheme 3.3**) using an analogous reaction protocol where ethyl

bromodifluoroacetate (**3a**) was replaced with bromodifluorophosphonate (yielding compound **5a**), or various bromodifluoroacetamides (yielding compounds **5b-d**).
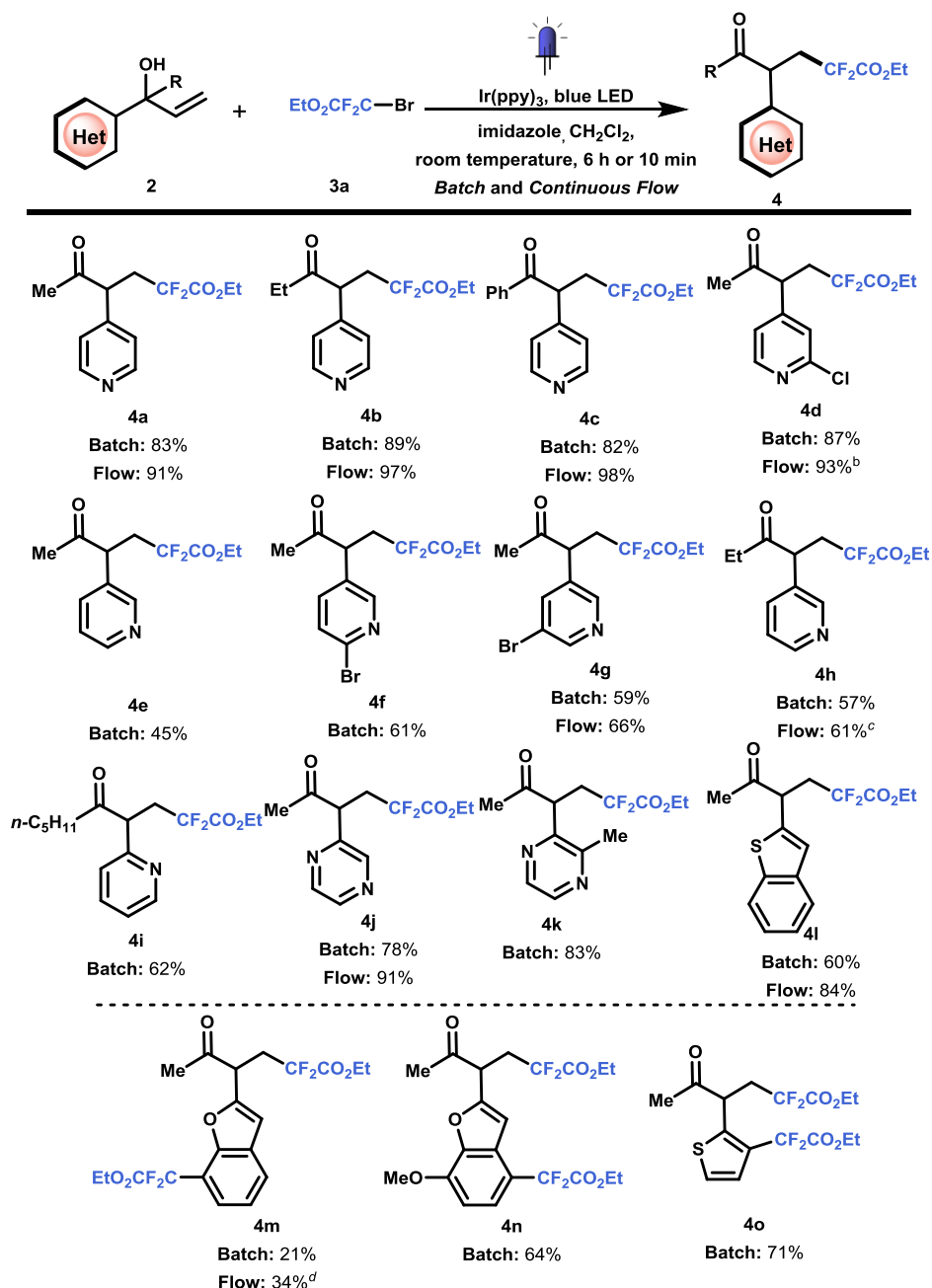
Scheme 3.2: Substrate scope of the photocatalytic radical-induced heterocycle migration – variation of the allylic alcohol substrate. [a]Reaction conditions in batch: **2a** (0.2 mmol), **3a**(o.6 mmol), imidazole (0.4 mmol), Ir(ppy)$_3$ (1 mol%), CH$_2$Cl$_2$ (1.0 mL), 12 W blue LEDs (λ = 450 nm), room temperature, 6 hours. Reaction conditions in flow: **2a** (0.5 mmol), **3a** (1.5 mmol), imidazole (1.0 mmol), Ir(ppy)$_3$ (1 mol%), CH$_2$Cl$_2$ (5.0 mL), 12 W blue

LEDs (λ = 450 nm), room temperature, residence time: 10 minutes. Reported yields are those obtained after column chromatography. [b]Residence time: 15 minutes. [c]Residence time: 20 minutes. [d]Residence time: 5 minutes.
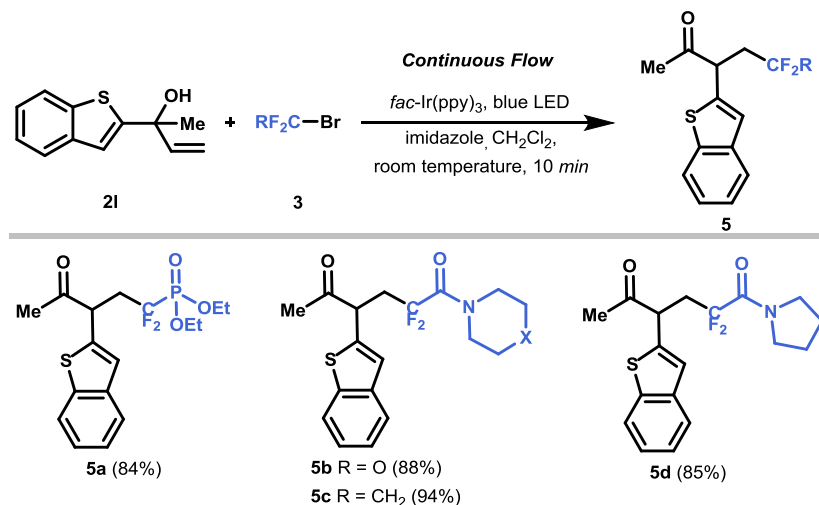
Scheme 3.3: Substrate scope of the photocatalytic radical-induced heterocycle migration – variation of the difluoroalkyl radical precursor. [a]Reaction conditions: **2a** (1.0 mmol), **3a** (3.0 mmol), Ir(ppy)₃ (1 mol%), imidazole (2.0 mmol), CH₂Cl₂ (1.0 mL), 12 W blue LEDs (λ = 450 nm), room temperature, residence time: 10 minutes. Reported yields are those obtained after column chromatography.

Based on the experimental data, a plausible mechanism is suggested in **Figure 3.1**. Upon light excitation, *fac*-[Ir(ppy)₃]* can be oxidatively quenched by ethyl bromodifluoroacetate, generating the corresponding difluoroalkyl radical species.[13] Indeed, radical trapping experiments with BHT (2,6-di-*tert*-butyl-4-methylphenol) showed that this species could be effectively captured (See Supporting Information). The radical subsequently adds to the olefin generating intermediate **A**, which undergoes 1, 2-heterocycle migration via a key spiro radical intermediate **B** to produce **C**. Finally, the intermediate **C** was oxidized to obtain the aimed product **4a**.
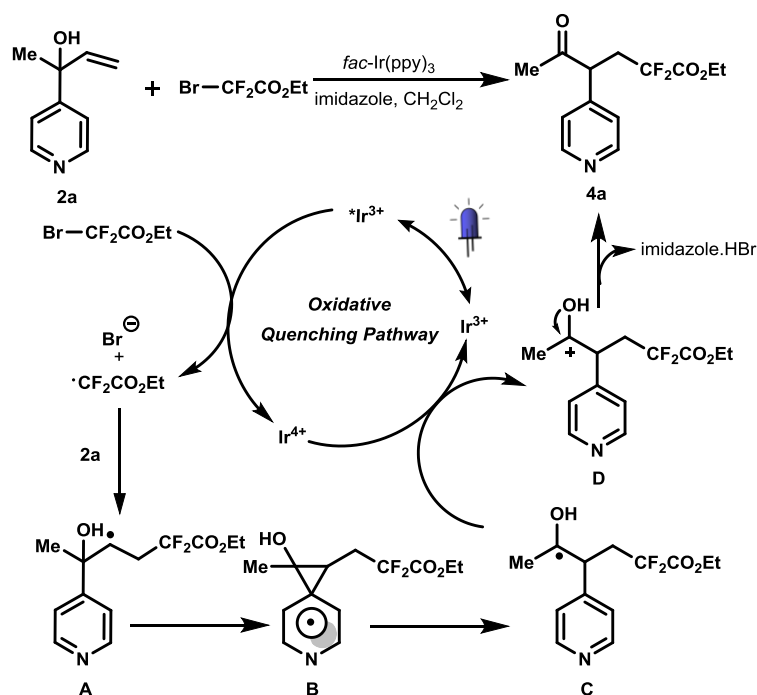
Figure 3.1. Proposed mechanism for the photocatalytic radical-induced heterocycle migration.

Conclusions

In summary, we have developed a novel photocatalytic 1, 2-heterocycle migration method which allows to prepare heterocycles with a *sp³*-enriched character. A variety of synthetically useful *β*-difluorinated α-aryl heterocyclic ketones can be easily prepared under mild reaction conditions with excellent regioselectivity. The application of continuous flow allows to reduce the reaction time (from 6 hours to 10 minutes), provides higher reaction selectivity and potential for scaling the chemistry. Interesting also the allylic alcohol substrates were prepared in flow via a classical Grignard reaction. The flow method enables safe handling of the reaction exotherm and allows to prepare sufficient quantities of starting material for the consecutive migration chemistry.

Experimental Section

General procedure for the preparation of the 2-Heterocycle-but-3-en-2-ol substrates in flow: Heterocyclic ketone (5.0 mmol, 1.0 equiv.) was dissolved in 10 mL THF, which was subsequently degassed 3 times (freeze-pump-thaw: cooled to –78 °C and degassed via vacuum evacuation (5 min), backfilled with argon, and warm to room temperature) and taken up in a first syringe. Next, 6 mL vinylmagnesium bromide (1 M in THF) was dissolved in 4 mL THF and taken up in a second syringe. These two syringes (10 mL) were mounted onto a single syringe pump. The reaction mixture was pumped through the PFA capillary microreactor (ID = 1.65 mm, 65 cm), which was submerged in an ice water bath, which was sonicated to prevent microreactor clogging. The flowrate is 0.14 mL/min, which corresponds to a residence time of 5 min. The quenching solvent is saturated NH_4Cl water solution (Flow rate = 0.21 mL/min). The quenched solution was collected at the end of the reactor and was subsequently extracted by diethyl ether (3×30 mL). The combined organic layers were washed with brine and dried with $MgSO_4$. The product was purified via flash column chromatography using DCM/Acetone or cyclehexane/ EtOAc as eluent.

General procedure for the photocatalytic 1,2-heterocycle migration in batch: An oven- dried reaction tube (7.5 mL) was charged with 2-heterocycle-but-3-en-2-ol **2** (0.2 mmol, 1.0 equiv.), ethyl bromodifluoroacetate (0.6 mmol, 3.0 equiv.), *fac*- Ir(ppy)$_3$ (1.3 mg, 1.0 mol%), imidazole (27.3 mg, 0.4 mmol, 2 equiv.) and a magnetic stirring bar in dichloromethane (1.0 mL), was sealed with a rubber septum and subsequently degassed 3 times (freeze-pump-thaw: cooled to -78 °C and degassed via vacuum evacuation (5 min), backfilled with argon, and warm to room temperature). Next the reaction mixture was irradiated with blue LEDs (at approximately 1 cm distance from the light source). The temperature in the reactor was kept at room temperature using pressurized air. After 6 hours, the reaction mixture was transferred to a 50 mL flask with about 20 mL CH_2Cl_2. The solvent was subsequently removed under reduced pressure and the residue was purified by silica gel column chromatography using dichloromethane/acetone to give the desired product.

General procedure for the photocatalytic 1, 2-heterocycle migration in flow: 2-Heterocycle-but-3-en-2-ol **2** (1.0 mmol, 1.0 equiv.), ethyl bromodifluoroacetate (3.0 mmol, 3.0 equiv.), *fac*- Ir(ppy)$_3$ (6.5 mg, 1.0 mol%), imidazole (136.2 mg, 2.0 mmol, 2 equiv.) and a magnetic stirring bar in dichloromethane (10.0 mL), and was subsequently degassed 3 times (freeze-pump-thaw: cooled to –78 °C and degassed via vacuum evacuation (5 min), backfilled with argon, and warm to room temperature). This reaction mixture was then transferred into a syringe (10 mL) and mounted onto a syringe pump. The reaction mixture was pumped through the microreactor with the desired flow rate (0.053 mL/min). The microreactor assembly was irradiated with a Blue LED array (1.5 $\times$ 3.12 Watts) at room temperature. The continuous reaction was allowed to reach steady state prior to collection of the product fractions. A standard residence time of 10 minutes was utilized. The crude product was collected at the end of the reactor. Workup and purification were done following the batch procedure.

Compound Characterization

2-(pyridin-4-yl)but-3-en-2-ol (2a).

The flow experiment was carried out on a 10.0 mmol scale. Purification: Column chromatography (CH$_2$Cl$_2$/acetone = 30:1), 1.3 g product was isolated as white solid (87% yield). **^{1}H NMR** (400 MHz, CDCl$_3$): δ 8.57 (d, J = 4.0 Hz, 2H), 7.41 (d, J = 4.0 Hz, 2H), 6.17-6.10 (m, 1H), 5.33 (d, J = 16.0 Hz, 1H), 5.22 (d, J = 12.0 Hz, 1H), 2.36 (brs, 1H), 1.65 (s, 3H). **^{13}C NMR** (100 MHz, CDCl$_3$): δ 155.6, 149.5, 149.4, 143.4, 120.4, 113.7, 74.1, 29.1. **HRMS** (**ESI**) m/z: [M+H]$^+$ Calcd for C$_9$H$_{12}$NO: 150.0919; Found: 150.0921.

3-(pyridin-4-yl)pent-1-en-3-ol (2b).

The flow experiment was carried out on a 5.0 mmol scale. Purification: Column chromatography (CH$_2$Cl$_2$/acetone = 30:1), 749.8 mg product was isolated as white solid (92% yield). **^{1}H NMR** (400 MHz, CDCl$_3$): δ 8.49 (d, J = 4.0 Hz, 2H), 7.37 (d, J = 4.0 Hz, 2H), 6.13 (dd, J = 16.0 Hz, 8.0 Hz, 2H), 5.32 (d, J = 16.0 Hz, 1H), 5.20 (d, J = 12.0 Hz, 1H), 2.36 (brs, 1H), 1.92-1.87 (m, 2H), 0.83 (t, J = 8.0 Hz, 3H). **^{13}C NMR** (100 MHz, CDCl$_3$): δ 155.0, 150.7, 149.2, 143.0, 120.8, 113.8, 34.4, 7.6. **HRMS (ESI)** m/z: [M+H]$^+$ Calcd for C$_{10}$H$_{14}$NO: 164.1075; Found: 164.1074.

1-phenyl-1-(pyridin-4-yl)prop-2-en-1-ol (2c).

The flow experiment was carried out on a 5.0 mmol scale. Purification: Column chromatography (CH$_2$Cl$_2$/acetone = 16:1), 759.5 mg product was isolated as white solid (72% yield). **^{1}H NMR** (400 MHz, CDCl$_3$): δ 8.49 (t, J = 4.0 Hz, 2H), 7.36-7.34 (m, 7H), 6.51-6.44 (m, 1H), 5.41-5.34 (m, 2H), 3.10 (brs, 1H). **^{13}C NMR** (100 MHz, CDCl$_3$): δ 155.0, 149.1, 144.5, 142.1, 128.5, 127.9, 126.9, 121.8, 115.5, 78.6. **HRMS (ESI)** m/z: [M+H]$^+$ Calcd for C$_{14}$H$_{14}$NO: 212.1075; Found: 212.1075.

2-(2-chloropyridin-4-yl)but-3-en-2-ol (2d).

The flow experiment was carried out on a 5.0 mmol scale. Purification: Column chromatography (CH$_2$Cl$_2$/acetone = 20:1), 494.1 mg product was isolated as white solid (54% yield). **^{1}H NMR** (400 MHz, CDCl$_3$): δ 8.15(d, J = 4.0 Hz, 1H), 7.39-7.38(m, 1H), 7.23(dd, J = 8.0, 4.0 Hz, 1H), 6.00(m, 1H), 5.24(dd, J = 16.0 Hz, 1H), 5.12(d, J = 12.0 Hz, 1H), 3.64(s, 1H), 1.54(s, 3H). **^{13}C NMR** (100 MHz, CDCl$_3$): δ 159.4, 151.4, 149.0, 142.8, 121.1, 119.4, 114.0, 73.8, 28.8. **HRMS (ESI)** m/z: [M+H]$^+$ Calcd for C$_9$H$_{11}$ClNO: 184.0529; Found: 184.0530.

2-(pyridin-3-yl)but-3-en-2-ol (2e).

The flow experiment was carried out on a 5.0 mmol scale. Purification: Column chromatography (CH$_2$Cl$_2$/acetone = 8:1 to 2:1), 662.8 mg product was isolated as white solid (89% yield). **^{1}H NMR** (400 MHz, CDCl$_3$): δ 8.63 (s, 1H), 8.41-8.39 (m, 1H), 7.76 (dd, J = 16.0, 4.0 Hz, 1H), 7.29-7.26 (m, 1H), 6.20-6.13 (m, 1H), 5.32 (d, J = 16.0 Hz, 1H), 5.20 (d, J = 12.0 Hz, 1H), 2.85 (brs, 1H), 1.68 (s, 3H). **^{13}C NMR** (100 MHz, CDCl$_3$): δ 147.8, 147.0, 144.1, 144.0, 142.0, 133.4, 123.2, 113.4, 113.3, 73.5, 29.4. **HRMS (ESI)** m/z: [M+H]$^+$ Calcd for C$_9$H$_{12}$NO: 150.0919; Found: 150.0918.

2-(6-bromopyridin-3-yl)but-3-en-2-ol (2f).

The flow experiment was carried out on a 5.0 mmol scale. Purification: Column chromatography (CH$_2$Cl$_2$/acetone = 20:1), 669.5 mg product was isolated as yellow oil (59% yield). **^{1}H NMR** (400 MHz, CDCl$_3$): δ 8.55 (s, 1H), 8.50 (s, 1H), 7.99-7.98 (m, 1H), 6.15-6.08 (m, 1H), 5.35-5.20 (m, 2H), 3.21(brs, 1H), 1.66 (s, 3H). **^{13}C NMR** (100 MHz, CDCl$_3$): δ 148.8, 145.2, 144.0, 143.4, 136.1, 120.6, 113.9, 73.0, 29.3. **HRMS (ESI)** m/z: [M+H]$^+$ Calcd for C$_9$H$_{11}$BrNO: 228.0024; Found: 228.0025.

2-(5-bromopyridin-3-yl)but-3-en-2-ol (2g).

The batch experiment was carried out on a 5.0 mmol scale. Purification: Column chromatography (DCM/Acetone = 20:1), 374.0 mg product was isolated as brown oil (33% yield). **^{1}H NMR** (400 MHz, CDCl$_3$): δ 8.44 (s, 1H), 7.67 (dd, J = 8.0, 4.0 Hz, 1H), 7.44 (J = 8.0, 1H), 6.12 (dd, J = 16.0, 8.0 Hz, 1H), 5.33-5.21 (m, 2H), 2.18 (m, 1H), 1.66 (s, 3H). **^{13}C NMR** (100 MHz, CDCl$_3$): δ 147.7, 143.4, 141.2, 140.5, 136.1, 127.5, 113.9, 73.3, 29.4. **HRMS (ESI)** m/z: [M+H]$^+$ Calcd for C$_9$H$_{11}$BrNO: 228.0024; Found: 228.0025.

3-(pyridin-3-yl)pent-1-en-3-ol (2h).

The flow experiment was carried out on a 5.0 mmol scale, residence time: 10 minutes. Purification: Column chromatography (CH$_2$Cl$_2$/acetone = 8:1 to 2:1), 676.4 mg product was isolated as yellow oil (83% yield). **^{1}H NMR** (400 MHz, CDCl$_3$): δ 8.62(s, 1H), 8.42-8.39(m, 1H), 7.78(dd, J = 8.0, 4.0 Hz, 1H), 7.26-7.22 (m, 1H), 6.19-6.12 (m, 1H), 5.32 (d, J = 16.0 Hz, 1H), 5.20 (d, J = 8.0 Hz, 1H), 3.48 (brs, 1H),1.96-1.89 (m, 2H), 0.84 (t, J = 8.0 Hz, 3H). **^{13}C NMR** (100 MHz, CDCl$_3$): δ 147.8, 147.2, 143.3, 141.1, 133.7, 123.0, 113.5, 75.7, 34.6, 7.7. **HRMS (ESI)** m/z: [M+H]$^+$ Calcd for C$_{10}$H$_{14}$NO: 164.1075; Found: 164.1078.

1-(pyridin-2-yl)hexan-1-one (1i).

The compound was made according to a literature procedure.[15] **^{1}H NMR** (400 MHz, CDCl$_3$): δ 8.68 (d, J = 4.0 Hz, 1H), 8.04 (d, J = 4.0 Hz, 1H), 7.82 (t, J = 8.0 Hz, 1H), 7.46 (dd, J = 8.0, 4.0 Hz, 1H), 3.22 (t, J = 8.0 Hz, 2H), 1.73 (t, J = 8.0 Hz, 2H), 1.40-1.36 (m, 4H), 0.92-0.88 (m, 3H). **^{13}C NMR** (100 MHz, CDCl$_3$): δ 202.1, 153.5, 148.8, 136.9, 126.9, 121.8, 37.7, 31.5, 23.6, 22.5, 13.9.

3-(pyridin-4-yl)oct-1-en-3-ol (2i).

The flow experiment was carried out on a 5.0 mmol scale. Purification: Column chromatography (CH$_2$Cl$_2$/acetone = 8:1 to 2:1), 1.0 g mixture of product and starting material (5:1 based on ^{1}HNMR) was obtained as yellow oil (80% yield). **^{1}H NMR** (400 MHz, CDCl$_3$): δ 8.55-8.52 (m, 1H), 7.76-7.73 (m, 1H), 7.39-7.36 (m, 1H), 7.26-7.23 (m, 1H), 6.12 (dd, J = 16.0, 8.0 Hz, 1H), 5.42 (d, J = 16.0 Hz, 1H), 5.34 (brs, 1H), 5.13 (d, J = 16.0 Hz, 1H), 1.92-1.87 (m, 2H), 1.46-1.37 (m, 2H), 1.28-1.20 (m, 4H), 0.84 (t, J = 4.0 Hz, 3H). **^{13}C NMR** (100 MHz, CDCl$_3$): δ 162.5, 148.9, 143.0, 136.8, 126.9, 122.3, 121.7, 120.5, 113.8, 76.3, 41.2, 32.0, 22.9, 14.0. **HRMS (ESI)** m/z: [M+H]$^+$ Calcd for C$_{13}$H$_{20}$NO: 206.1545; Found: 206.1542.

2-(pyrazin-2-yl)but-3-en-2-ol (2j).

The flow experiment was carried out on a 5.0 mmol scale. Purification: Column chromatography (CH$_2$Cl$_2$/acetone = 20:1), 390.0 mg product was isolated as colorless oil (52% yield). **^{1}H NMR** (400 MHz, CDCl$_3$): δ 8.77 (s, 1H), 8.51-8.50 (m, 2H), 6.20-6.12 (m, 1H), 5.42-5.38 (m, 1H), 5.21-5.18 (m, 1H), 3.95 (brs,

1H), 1.69 (s, 3H). **¹³C NMR** (100 MHz, CDCl₃): δ 159.3, 143.0, 142.9, 142.4, 142.3, 113.8, 73.7, 28.1. **HRMS (ESI)** m/z: [M+H]⁺ Calcd for $C_8H_{11}N_2O$: 151.0871; Found: 151.0872.

2-(3-methylpyrazin-2-yl)but-3-en-2-ol (2k).

The flow experiment was carried out on a 5.0 mmol scale. Purification: Column chromatography (CH₂Cl₂/acetone = 30:1), 500.0 mg product was isolated as colorless oil (61% yield). **¹H NMR** (400 MHz, CDCl₃): δ 8.41-8.30 (m, 2H), 6.09-6.01 (m, 1H), 5.66 (brs, 1H), 5.36-5.20 (m, 2H), 2.65-2.64 (m, 3H), 1.67 (s, 3H). **¹³C NMR** (100 MHz, CDCl₃): δ 155.9, 152.1, 142.5, 141.3, 138.8, 114.7, 73.3, 25.7, 25.5. **HRMS (ESI)** m/z: [M+H]⁺ Calcd for $C_9H_{13}N_2O$: 165.1028; Found: 165.1029.

2-(benzo[b]thiophen-2-yl)but-3-en-2-ol (2l).

The flow experiment was carried out on a 5.0 mmol scale. Purification: Column chromatography (Cyclohexane/EtOAc = 20:1), 867.0 mg product was isolated as white solid (85% yield). **¹H NMR** (400 MHz, CDCl₃): δ 7.81-7.69 (m, 2H), 7.35-7.29 (m, 2H), 7.18 (s, 1H), 6.27 (dd, J = 17.2, 10.6 Hz, 1H), 5.42 (dd, J = 17.2, 0.9 Hz, 1H), 5.22 (dd, J = 10.6, 0.9 Hz, 1H), 1.80 (s, 3H). **¹³C NMR** (100 MHz, CDCl₃): δ 152.2, 143.5, 139.7, 139.5, 124.3, 124.1, 123.5, 122.3, 119.7, 113.1, 73.7, 30.0. **HRMS (ESI)** m/z: [M+H]⁺ Calcd for $C_{12}H_{13}SO$: 205.0687; Found: 205.0686.

2-(benzofuran-2-yl)but-3-en-2-ol (2m).

The flow experiment was carried out on a 5.0 mmol scale. Purification: Column chromatography (Cyclohexane/EtOAc = 4:1), 723.8 mg product was isolated as colorless oil (77% yield). **¹H NMR** (400 MHz, CDCl₃): δ 7.56-7.46 (m, 2H), 7.28-7.22 (m, 2H), 6.63(s, 1H), 6.25 (dd, J = 17.3, 10.6 Hz, 1H), 5.41 (dd, J = 17.3, 0.8 Hz, 1H), 5.25 (dd, J = 10.6, 0.9 Hz, 1H), 2.38 (brs, 1H), 1.76 (s, 3H). **¹³C NMR** (100 MHz, CDCl₃): δ 161.0, 145.3, 144.0, 141.7, 129.8, 123.4, 113.8, 113.4, 106.3, 102.2, 71.8, 55.9, 26.9. **HRMS (ESI)** m/z: [M+H]⁺ Calcd for $C_{12}H_{13}O_2$: 189.0916; Found: 189.0916.

2-(7-methoxybenzofuran-2-yl)but-3-en-2-ol (2n).

The flow experiment was carried out on a 5.0 mmol scale. Purification: Column chromatography (Cyclohexane/EtOAc = 4:1), 870 mg product was isolated as colorless oil (80% yield). **¹H NMR** (400 MHz, CDCl₃): δ 7.15-7.14 (m, 2H), 6.79 (dd, J = 5.1, 4.0 Hz, 1H), 6.62 (s, 1H), 6.26 (dd, J = 16.0, 8.0 Hz, 1H), 5.40(d, J = 20.0 Hz, 1H), 5.23(d, J = 8.0 Hz, 1H)), 4.00 (s, 3H), 2.50 (brs, 1H), 1.76 (s, 3H). **¹³C NMR** (100 MHz, CDCl₃): δ 161.0, 145.3, 144.0, 141.7, 129.8, 123.4, 113.8, 113.4, 106.3, 102.2, 71.8, 55.9, 26.9. **HRMS (ESI)** m/z: [M+H]⁺ Calcd for $C_{13}H_{15}O_3$: 219.1021; Found: 219.1021.

2-(thiophen-2-yl)but-3-en-2-ol (2o).

The flow experiment was carried out on a 5.0 mmol scale. Purification: Column chromatography (Cyclohexane/EtOAc = 4:1), 270.0 mg product was isolated as colorless oil (35% yield). **¹H NMR** (400 MHz, CDCl₃): δ 7.24 (dd, J = 4.0, 2.3 Hz, 2H), 6.97-6.96 (m, 2H), 6.23 (d, J = 16.0, 8.0 Hz, 1H), 5.40-5.16 (m, 2H), 2.18 (brs, 1H), 1.75 (s, 3H). **¹³C NMR** (100 MHz, CDCl₃): δ 151.6, 144.0, 126.7, 124.6, 123.2, 112.5, 73.3, 30.2. **HRMS (ESI)** m/z: [M+H]⁺ Calcd for $C_8H_{11}OS$: 155.0531; Found: 155.0529.

Ethyl 2,2-difluoro-5-oxo-4-(pyridin-4-yl)hexanoate (4a).

The batch reaction was carried out on a 0.2 mmol scale and the flow experiment was carried out on a 0.5 mmol scale (2.5 mL liquid was taken), 44.9 mg and 61.7 mg was obtained in batch and flow, the yield is 83%, 91%, the product was yellow oil. Purification: Column chromatography (CH$_2$Cl$_2$/Acetone = 30:1). **^{1}H NMR** (400 MHz, CDCl$_3$): δ 8.53 (t, J = 4.0 Hz, 2H), 7.11-7.09 (m, 2H), 4.13 (dq, J = 8.0, 4.0 Hz, 2H), 3,97 (dd, J = 8.0, 4.0 Hz, 1H), 3.03 (dtd, J = 17.2, 15.3, 5.6 Hz, 1H), 2.27 (dtd, J = 17.2, 15.3, 5.6 Hz, 1H), 2.05 (s, 3H), 1.24 (t, J = 8.0 Hz, 3H). **^{13}C NMR** (100 MHz, CDCl$_3$): δ 203.9, 163.5 (t, J = 33.0 Hz), 150.6, 146.1, 123.3, 114.8 (t, J = 250.0 Hz), 63.1, 51.7 (t, J = 3.0 Hz), 36.2 (t, J = 23.0 Hz), 29.0, 13.7. **^{19}F NMR** (376 MHz, CDCl$_3$): δ -104.67- -104.80(m). **HRMS** (**EI**) m/z: [M+H]$^+$ Calcd for C$_{13}$H$_{16}$F$_2$NO$_3$: 272.1098; Found: 272.1080.

Ethyl 2,2-difluoro-5-oxo-4-(pyridin-4-yl)heptanoate (4b).

The batch reaction was carried out on a 0.2 mmol scale and the flow experiment was carried out on a 0.5 mmol scale (3.2 mL liquid was taken), 50.7 mg, 88.0 mg of product was obtained in batch and flow as a pale yellow oil, the yield is 89%, 97%. Purification: Column chromatography (CH$_2$Cl$_2$/Acetone = 30:1 to 10:1). **^{1}H NMR** (400 MHz, CDCl$_3$): 8.60 (d, J = 4.0 Hz, 2H), 7.20 (d, J = 4.0 Hz, 2H), 4.38-4.15 (m, 2H), 4.06 (dd, J = 7.7, 5.3 Hz, 1H), 3.19-3.05 (m, 1H), 2.61-2.36 (m, 2H), 2.40-2.20 (m, 1H), 1.32 (t, J = 8.0 Hz, 3H), 1.00 (t, J = 8.0 Hz, 3H). **^{13}C NMR** (100 MHz, CDCl$_3$): δ 206.8, 163.5 (t, J = 32.0 Hz), 150.1, 146.9, 123.4, 114.8 (t, J = 250.0 Hz), 63.2, 50.8 (t, J = 3.0 Hz), 36.6 (t, J = 23.0 Hz), 35.3, 13.8. **^{19}F NMR** (376 MHz, CDCl$_3$): δ -104.79(m). **HRMS** (**ESI**) m/z: [M+Na]$^+$ Calcd for C$_{14}$H$_{17}$F$_2$NO$_3$Na: 308.1074; Found: 308.1076.

Ethyl 2,2-difluoro-5-oxo-5-phenyl-4-(pyridin-4-yl)pentanoate (4c).

The batch reaction was carried out on a 0.2 mmol scale and the flow experiment was carried out on a 0.5 mmol scale (3.0 mL liquid was taken), 54.7 mg, 97.7 mg of product was obtained in batch and flow as a yellow oil, the yield is 82%, 98%. Purification: Column chromatography (CH$_2$Cl$_2$/Acetone = 20:1). **^{1}H NMR** (400 MHz, CDCl$_3$): δ 8.55 (brs, 2H), 7.94 (dd, J = 8.0, 4.0 Hz, 2H), 7.55 (t, J = 8.0 Hz, 1H), 7.43 (t, J = 8.0 Hz, 2H), 7.26 (d, J = 8.0 Hz, 2H), 4.98 (t, J = 8.0 Hz, 2H), 4.27-4.10 (m, 2H), 3.28 (dtd, J = 18.2, 15.3, 7.8 Hz), 2.52 (dtd, J = 18.0, 14.9, 5.1 Hz), 1.26 (t, J = 7.2 Hz, 3H). **^{13}C NMR** (100 MHz, CDCl$_3$): δ 196.1, 163.5 (t, J = 33.0 Hz), 150.2, 147.1, 135.2, 133.8, 128.8, 128.7, 123.4, 114.9 (t, J = 250.0 Hz), 63.1, 46.0, 37.8 (t, J = 23.0 Hz), 13.7. **^{19}F NMR** (376 MHz, CDCl$_3$): δ -104.43 (ddd, J = 57.3, 18.0, 15.1 Hz). **HRMS** (**ESI**) m/z: [M+Na]$^+$ Calcd for C$_{18}$H$_{17}$F$_2$NO$_3$Na: 356.1074; Found: 356.1078.

Ethyl 4-(2-chloropyridin-4-yl)-2,2-difluoro-5-oxohexanoate (4d).

The batch reaction was carried out on a 0.2 mmol scale and the flow experiment was carried out on a 0.5 mmol scale (2.5 mL liquid was taken), 53.0 mg was obtained in batch with the yield of 87%, 74.6 mg was obtained in flow with the yield of 93%, product was pale yellow oil. Purification: Column chromatography (CH$_2$Cl$_2$/Acetone = 20:1). **^{1}H NMR** (400 MHz, CDCl$_3$): δ 8.31-8.30 (m, 1H), 7.17 (d, J = 1.5 Hz, 1H), 7.04 (dd, J = 5.1, 1.6 Hz, 1H), 4.17 (dq, J = 7.2, 4.2 Hz, 2H), 3.98 (dd, J = 7.3, 5.7 Hz, 1H), 3.01 (dtd, J = 18.5, 15.2, 7.4 Hz, 1H), 2.26 (dtd, J = 18.1, 14.9, 5.6 Hz, 1H), 2.08 (s, 3H), 1.26 (t, J = 8.0 Hz, 3H). **^{13}C NMR** (100 MHz, CDCl$_3$): δ 203.2, 163.4 (t, J = 32.0 Hz), 152.4, 150.4, 149.2, 123.8, 121.9, 114.7 (t, J = 250.0 Hz), 63.3, 51.3 (t, J = 3.0 Hz), 36.2

(t, J = 23.0 Hz), 29.2, 13.8. **¹⁹F NMR** (376 MHz, CDCl₃): δ -104.70 (dd, J = 47.0, 4.3 Hz). **HRMS (ESI)** m/z: [M+Na]⁺ Calcd for C₁₃H₁₄ClF₂NO₃Na: 328.0528; Found: 328.0520.

Ethyl 2,2-difluoro-5-oxo-4-(pyridin-3-yl)hexanoate (4e).

The batch experiment was carried out on a 0.2 mmol scale. Purification: Column chromatography (CH₂Cl₂/Acetone = 20:1), 24.4 mg product was isolated as yellow oil (45% yield). **¹H NMR** (400 MHz, CDCl₃): δ 8.58 (d, J = 8.0 Hz, 2H), 7.57 (td, J = 8.0, 1.9 Hz, 1H), 7.35-7.32 (m, 1H), 4.21 (dq, J = 7.2, 5.4 Hz, 2H), 4.09 (t, J = 4.0 Hz, 1H), 3.11 (dtd, J = 16.7, 15.1, 7.3 Hz, 1H), 2.37 (dtd, J = 16.4, 15.0, 5.9 Hz, 1H), 2.14 (s, 3H), 1.32 (t, J = 8.0 Hz, 3H). **¹³C NMR** (100 MHz, CDCl₃): δ 204.5, 163.6 (t, J = 32.0 Hz), 149.4, 149.0, 135.7, 133.3, 124.2, 114.9 (t, J = 250.0 Hz), 63.2, 49.7 (t, J = 4.0 Hz), 36.5 (t, J = 24.0 Hz), 29.0, 13.8. **¹⁹F NMR** (376 MHz, CDCl₃): δ -104.67(s). **HRMS (ESI)** m/z: [M+Na]⁺ Calcd for C₁₃H₁₅F₂NO₃Na: 294.0918; Found: 294.0918.

Ethyl 4-(6-bromopyridin-3-yl)-2,2-difluoro-5-oxohexanoate (4f).

The batch reaction was carried out on a 0.2 mmol scale, 42.6 mg of product was obtained as a pale yellow oil, the yield is 61%. Purification: Column chromatography (CH₂Cl₂/Acetone = 30:1). **¹H NMR** (400 MHz, CDCl₃): δ 8.31 (s, 1H), 7.50 (d, J = 8.0 Hz, 1H), 7.40 (d, J = 8.0, 1H), 4.24 (dq, J = 8.0, 4.0 Hz, 2H), 4.06 (t, J = 8.0 Hz, 1H), 3.08 (dtd, J = 17.6, 15.5, 7.3 Hz, 1H), 2.34 (dtd, J = 17.2, 15.3, 5.9 Hz, 1H), 2.15 (s, 3H), 1.33 (t, J = 8.0 Hz, 3H). **¹³C NMR** (100 MHz, CDCl₃): δ 204.1, 163.4 (t, J = 32.0 Hz), 150.0, 141.9, 137.7, 132.4, 128.7, 114.8 (t, J = 250.0 Hz), 63.3, 48.9(t, J = 4.0 Hz), 36.5 (t, J = 24.0 Hz), 29.1, 13.8. **¹⁹F NMR** (376 MHz, CDCl₃): δ -104.68 (s). **HRMS (ESI)** m/z: [M+Na]⁺ Calcd for C₁₃H₁₄BrF₂NO₃Na: 372.0023; Found: 372.0026.

Ethyl 4-(5-bromopyridin-3-yl)-2,2-difluoro-5-oxohexanoate (4g).

The batch reaction was carried out on a 0.2 mmol scale and the flow experiment was carried out on a 0.5 mmol scale (2.7 mL liquid was taken), 41.1 mg, 62.2 mg of product was obtained in batch and flow as a pale yellow oil, the yield is 59%, 66%. Purification: Column chromatography (CH₂Cl₂/Acetone = 30:1). **¹H NMR** (400 MHz, CDCl₃): δ 8.63 (s, 1H), 8.45 (s, 1H), 7.69 (s, 1H), 4.16 (dq, J = 8.0, 4.0 Hz, 2H), 4.00 (t, J = 4.0 Hz, 1H), 3.05-2.97 (m, 1H), 2.28 (dtd, J = 17.2, 15.4, 5.8 Hz, 1H), 2.09 (s, 3H), 1.25 (t, J = 8.0 Hz, 3H). **¹³C NMR** (100 MHz, CDCl₃): δ 203.9, 163.4 (t, J = 32.0 Hz), 150.5, 147.7, 137.8, 134.7, 121.1, 114.7 (t, J = 250.0 Hz), 63.2, 49.1 (t, J = 4.0 Hz), 36.5 (t, J = 24.0 Hz), 29.1, 13.8. **¹⁹F NMR** (376 MHz, CDCl₃): δ -104.70(s). **HRMS (ESI)** m/z: [M+Na]⁺ Calcd for C₁₃H₁₄BrF₂NO₃Na: 372.0023; Found: 372.0026.

Ethyl 2,2-difluoro-5-oxo-4-(pyridin-3-yl)heptanoate (4h).

The batch reaction was carried out on a 0.2 mmol scale and the flow experiment was carried out on a 0.5 mmol scale (3.0 mL liquid was taken), 32.5 mg, 52.1 mg of product was obtained in batch and flow as a pale yellow oil, the yield is 57%, 61%. Purification: Column chromatography (CH₂Cl₂/Acetone = 20:1). **¹H NMR** (400 MHz, CDCl₃): δ 8.58 (d, J = 4.0 Hz, 2H), 7.56 (m, 1H), 7.35-7.32 (m, 1H), 4.20 (dq, J = 7.2, 4.6 Hz, 2H), 4.08 (dd, J = 7.6, 5.6 Hz, 1H), 3.19-3.05 (m, 1H), 2.54-2.37 (m, 1H), 2.36-2.30 (m, 1H), 1.32 (t, J = 7.2 Hz, 3H), 0.99 (t, J = 7.2 Hz, 3H). **¹³C NMR** (100 MHz, CDCl₃): δ 207.5, 163.6 (t, J = 32.0 Hz), 149.5, 149.1, 135.4, 133.5, 124.0, 114.9 (t, J = 250.0 Hz), 63.1, 49.6, 36.8 (t, J = 24.0 Hz), 35.1, 13.8. **¹⁹F NMR** (376 MHz, CDCl₃): δ -104.76 (s). **HRMS (ESI)** m/z: [M+Na]⁺ Calcd for C₁₄H₁₇F₂NO₃Na: 308.1074; Found: 308.1079.

Ethyl 2,2-difluoro-5-oxo-4-(pyridin-2-yl)decanoate (4i).

The batch reaction was carried out on a 0.2 mmol scale, 40.5 mg of product was obtained as a pale yellow oil, the yield is 62%. Purification: Column chromatography (CH_2Cl_2/Acetone = 16:1). **^{1}H NMR** (400 MHz, CDCl$_3$): δ 8.56 (d, J = 4.0 Hz, 1H), 7.67 (td, J = 8.0, 4.0 Hz, 1H), 7.25 (s, 1H), 7.20 (ddd, J = 8.0, 4.0, 1.1 Hz, 1H), 4.26-4.16 (m, 3H), 3.21-3.03 (m, 1H), 2.57 (dtd, J = 18.4, 15.3, 6.1 Hz, 1H), 2.47-2.24 (m, 2H), 1.48 (dtd, J = 14.9, 8.2, 6.7 Hz, 2H), 1.30 (t, J = 8.0 Hz, 3H), 1.24-1.08 (m, 4H), 0.80 (t, J = 7.1 Hz, 3H). **^{13}C NMR** (100 MHz, CDCl$_3$): δ 206.5, 163.8 (t, J = 33.0 Hz), 157.2, 149.6, 137.4, 123.5, 122.6, 115.4 (t, J = 249.0 Hz), 63.0, 53.9, 41.5, 35.6 (t, J = 23.0 Hz), 23.2, 22.3, 13.8. **^{19}F NMR** (376 MHz, CDCl$_3$): δ -104.72 (s). **HRMS (ESI)** m/z: [M+Na]$^+$ Calcd for $C_{17}H_{23}F_2NO_3Na$: 350.1544; Found: 350.1548.

Ethyl 2,2-difluoro-5-oxo-4-(pyrazin-2-yl)hexanoate (4j).

The batch reaction was carried out on a 0.2 mmol scale and the flow experiment was carried out on a 0.5 mmol scale (2.8 mL liquid was taken), 42.5 mg, 69.3 mg of product was obtained in batch and flow as a pale yellow oil, the yield is 78%, 91%. Purification: Column chromatography CH_2Cl_2/Acetone = 20:1). **^{1}H NMR** (400 MHz, CDCl$_3$): δ 8.63 (s, 1H), 8.57-8.54 (m, 2H), 4.30-4.23 (m, 3H), 3.22-3.08 (m, 1H), 2.71-2.57 (m, 1H), 2.13 (s, 3H), 1.33 (t, J = 8.0 Hz, 3H). **^{13}C NMR** (100 MHz, CDCl$_3$): δ 202.9, 163.6 (t, J = 22.0 Hz), 153.1, 144.9, 144.6, 143.7, 115.2 (t, J = 250.0 Hz), 63.2, 52.2, 35.0 (t, J = 23.0 Hz), 28.9, 13.9. **^{19}F NMR** (376 MHz, CDCl$_3$): δ -104.33- -105.72 (m). **HRMS (ESI)** m/z: [M+Na]$^+$ Calcd for $C_{12}H_{14}F_2N_2O_3Na$: 295.0870; Found: 295.0875.

Ethyl 2,2-difluoro-4-(3-methylpyrazin-2-yl)-5-oxohexanoate (4k).

The batch experiment was carried out on a 0.2 mmol scale. Purification: Column chromatography (CH_2Cl_2/Acetone = 16:1), 40.5 mg product was isolated as yellow oil (71% yield). **^{1}H NMR** (400 MHz, CDCl$_3$): 8.62-8.27 (m, 2H), 4.37 (t, J = 8.0 Hz, 1H), 4.23 (dq, J = 7.2, 3.0 Hz, 2H), 3.11 (dtd, J = 20.7, 15.5, 5.3 Hz, 1H), 2.72 (s, 3H), 2.69-2.54 (m, 1H), 2.03 (s, 3H), 1.32 (t, J = 7.2 Hz, 3H). **^{13}C NMR** (100 MHz, CDCl$_3$): δ 202.5, 163.6 (t, J = 32.0 Hz), 152.9, 151.8, 142.7, 142.1, 115.3 (t, J = 250.0 Hz), 63.1, 50.5 (t, J = 2.0 Hz), 34.8 (t, J = 23.0 Hz), 29.7, 28.4, 21.7, 13.8. **^{19}F NMR** (376 MHz, CDCl$_3$): δ -104.97 (ddd, J = 64.6, 20.0, 14.9 Hz). **HRMS (ESI)** m/z: [M+Na]$^+$ Calcd for $C_{13}H_{16}F_2N_2O_3Na$: 309.1027; Found: 309.1034.

Ethyl 4-(benzo[b]thiophen-2-yl)-2,2-difluoro-5-oxohexanoate (4l).

The flow experiment was carried out on a 0.5 mmol scale, 2.2 mL of liquid was collected. Purification: Column chromatography (Cyclohexane/EtOAc = 50:1 to 40:1), 60.2 mg product was isolated as a pale yellow oil (84% yield). **^{1}H NMR** (400 MHz, CDCl$_3$): δ 7.81-7.71 (m, 2H), 7.38-7.31 (m, 2H), 7.17 (s, 1H), 4.37 (dd, J = 7.7, 5.3 Hz, 1H), 4.18 (qq, J = 10.8, 7.2 Hz, 2H), 3.19 (dtd, J = 17.2, 15.4, 7.8 Hz, 1H), 2.55-2.49 (m, 1H), 2.24 (s, 3H), 1.29 (t, J = 8.0 Hz, 3H). **^{13}C NMR** (100 MHz, CDCl$_3$): δ 203.6, 163.6 (t, J = 32.0 Hz), 139.7 (t, J = 23.0 Hz), 124.7, 123.5, 122.3, 114.9 (t, J = 250.0 Hz), 63.1, 47.8, 37.0 (t, J = 24.0 Hz), 28.6, 13.8. **^{19}F NMR** (376 MHz, CDCl$_3$): δ -104.77 (d, J = 40.4 Hz). **HRMS (ESI)** m/z: [M+Na]$^+$ Calcd for $C_{16}H_{16}F_2O_3SNa$: 349.0686; Found: 349.0674.

Ethyl 4-(7-(2-ethoxy-1,1-difluoro-2-oxoethyl)benzofuran-2-yl)-2,2-difluoro-5-oxohexanoate (4m).

The batch reaction was carried out on a 0.2 mmol scale and the flow experiment was carried out on a 0.5 mmol scale (2.2 mL liquid was taken), 18.2 mg, 33.0 mg of product was obtained in batch and flow as a pale yellow

oil, the yield is 21%, 34%. Purification: Column chromatography with (Cyclohexane/EtOAc = 30:1). **^{1}H NMR** (400 MHz, CDCl$_3$): δ 7.58 (d, J = 4.0 Hz, 1H), 7.49 (d, J = 8.0 Hz, 1H), 7.39-7.35(m, 1H), 6.92 (s, 1H), 4.33-4.27 (m, 3H), 4.26-4.14 (m, 2H), 3.26-3.07 (m, 1H), 2.67-2.55 (m, 1H), 2.24 (s, 3H), 1.31-1.29 (m, 6H). **^{13}C NMR** (100 MHz, CDCl$_3$): δ 201.8, 163.5, 155.2, 154.4, 125.5, 124.4, 120.7(t, J = 7.0 Hz), 114.0, 104.9, 62.3, 62.2, 46.4, 34.0, 33.8, 28.6, 22.3, 13.9, 13.8. **^{19}F NMR** (376 MHz, CDCl$_3$): δ -102.95 (d, J = 41.1 Hz), -105.06 (s). **HRMS (ESI)** m/z: [M+Na]$^+$ Calcd for C$_{20}$H$_{20}$F$_4$O$_6$Na: 455.1094; Found: 455.1094.

Ethyl 4-(4-(2-ethoxy-1,1-difluoro-2-oxoethyl)-7-methoxybenzofuran-2-yl)-2,2-difluoro-5-oxohexanoate (4n).

The batch reaction was carried out on a 0.2 mmol scale, 59.0 mg of product was obtained in batch and flow as a pale yellow oil, the yield is 64%. Purification: Column chromatography (Cyclohexane/EtOAc = 30:1). **^{1}H NMR** (400 MHz, CDCl$_3$): δ 7.42 (d, J = 8.0 Hz, 1H), 6.88 (s, 1H), 6.83 (d, J = 8.4 Hz, 1H), 4.32-4.26 (m, 3H), 4.25-4.16 (m, 2H), 4.03 (s, 3H), 3.22-3.08 (m, 1H), 2.69-2.55 (m, 1H), 2.24 (s, 3H), 1.32-1.67 (m, 6H). **^{13}C NMR** (100 MHz, CDCl$_3$): δ 201.7, 164.0 (t, J = 36.0 Hz), 163.5 (t, J = 32.0 Hz), 154.5, 147.2, 144.3, 127.2, 122.1, 117.3 (t, J = 27.0 Hz), 116.2, 114.9 (t, J = 250.0 Hz), 113.7 (t, J = 251.0 Hz), 106.1, 105.2, 70.6, 63.1, 56.2, 46.3 (t, J = 3.0 Hz), 34.0 (t, J = 24.0 Hz), 28.6, 26.5, 23.2, 22.3, 13.9, 13.8. **^{19}F NMR** (376 MHz, CDCl$_3$): δ -102.07 (d, J = 41.1 Hz), -105.06 (s). **HRMS (ESI)** m/z: [M+Na]$^+$ Calcd for C$_{21}$H$_{22}$F$_4$O$_7$Na: 485.1199; Found: 485.1194.

Ethyl 4-(3-(2-ethoxy-1,1-difluoro-2-oxoethyl)thiophen-2-yl)-2,2-difluoro-5-oxohexanoate (4o).

The batch experiment was carried out on a 0.2 mmol scale. Purification: Column chromatography (Cyclohexane/EtOAc = 20:1 to 8:1), 56.5 mg product was isolated as yellow oil (71% yield). **^{1}H NMR** (400 MHz, CDCl$_3$): δ 7.26-7.25 (m, 1H), 6.89-6.87 (m, 1H), 4.37 (q, J = 7.1 Hz, 2H), 4.33-4.30 (m, 1H), 4.27-4.19 (m, 2H), 3.11 (dtd, J = 17.5, 15.2, 8.0 Hz, 1H), 2.51-2.29 (m, 1H), 2.21 (s, 3H), 1.38-1.31 (m, 6H). **^{13}C NMR** (100 MHz, CDCl$_3$): δ 203.3, 163.4 (t, J = 32.0 Hz), 163.0 (t, J = 35.0 Hz), 143.3 (t, J = 2.0 Hz), 134.1 (t, J = 30.0 Hz), 128.7 (t, J = 5.0 Hz), 126.4, 114.6 (t, J = 250.0 Hz), 111.2 (t, J = 250.0 Hz), 63.6, 63.2, 47.0, 37.5 (t, J = 24.0 Hz), 28.6, 13.9, 13.8. **^{19}F NMR** (376 MHz, CDCl$_3$): δ -93.05- -93.13 (m), -104.81- -105.0 (m). **HRMS (ESI)** m/z: [M+Na]$^+$ Calcd for C$_{16}$H$_{18}$F$_4$O$_5$SNa: 421.0709; Found: 421.0713.

Diethyl (3-(benzo[b]thiophen-2-yl)-1,1-difluoro-4-oxopentyl)phosphonate (5a).

The flow experiment was carried out on a 0.5 mmol scale, 2.5 mL of liquid was collected. Purification: Column chromatography (Cyclohexane/EtOAc = 8:1 to 2:1), 81.2 mg product was isolated as a colorless oil (84% yield). **^{1}H NMR** (400 MHz, CDCl$_3$): δ 7.76 (dd, J = 20.0, 8.0 Hz, 2H), 7.37-7.30 (m, 2H), 7.18 (s, 1H), 4.54 (q, J = 4.0 Hz, 1H), 4.32-4.24 (m, 4H), 3.37-3.20 (m, 1H), 2.53-2.40 (m, 1H), 2.27 (s, 3H), 1.39 (q, J = 8.0 Hz, 6H). **^{13}C NMR** (100 MHz, CDCl$_3$): δ 203.8, 140.8, 139.6, 139.5, 124.6, 124.5, 123.4, 122.9, 122.3, 120.7 (t, J = 259.0 Hz), 118.6 (t, J = 260.0 Hz), 64.7 (t, J = 6.0 Hz), 47.0 (q, J = 5.0 Hz), 36.6 (td, J = 20.0, 5.0 Hz), 28.7, 16.4, 16.3. **^{19}F NMR** (376 MHz, CDCl$_3$): δ -111.81-109.54 (m). **HRMS (ESI)** m/z: [M+H]$^+$ Calcd for C$_{17}$H$_{21}$F$_2$O$_4$PS: 391.0944; Found: 391.0945.

4-(benzo[b]thiophen-2-yl)-2,2-difluoro-1-morpholinohexane-1,5-dione (5b).

The flow experiment was carried out on a 0.5 mmol scale, 2.6 mL of liquid was collected. Purification: Column chromatography (Cyclohexane/EtOAc = 30:1 to 16:1), 83.0 mg product was isolated as a colorless oil (88%

88

yield). **¹H NMR** (400 MHz, CDCl₃): δ 7.81-7.71 (m, 2H), 7.38-7.30 (m, 2H), 7.17 (s, 1H), 4.45 (q, J = 4.0 Hz, 1H), 3.74-3.61 (m, 8H), 3.31 (dddd, J = 18.3, 16.8, 15.1, 8.1 Hz, 1H), 2.64-2.50 (m, 1H), 2.25 (s, 3H).**¹³C NMR** (100 MHz, CDCl₃): δ 204.0, 161.5 (t, J = 28.0 Hz), 140.8, 139.6, 139.5, 124.6, 124.5, 123.5, 122.9, 122.3, 118.2 (t, J = 253.0 Hz), 100.0, 66.6, 48.0, 46.5, 43.3, 37.4 (t, J = 22.0 Hz), 28.7, 26.9. **¹⁹F NMR** (376 MHz, CDCl₃): δ -98.02(s). **HRMS (ESI)** m/z: [M+Na]⁺ Calcd for C₁₈H₁₉F₂NO₃SNa: 390.0951; Found: 390.0945.

4-(benzo[b]thiophen-2-yl)-2,2-difluoro-1-(piperidin-1-yl)hexane-1,5-dione (5c).

The flow experiment was carried out on a 0.5 mmol scale, 2.8 mL of liquid was collected. Purification: Column chromatography (Cyclohexane/EtOAc = 30:1 to 16:1), 89.4 mg product was isolated as a colorless oil (94% yield). **¹H NMR** (400 MHz, CDCl₃): δ 7.79-7.70 (m, 2H), 7.36-7.27 (m, 2H), 7.17 (s, 1H), 4.46 (dd, J = 8.0, 4.0 Hz, 1H), 3.57 (td, J = 20.0, 4.0 Hz, 4H), 3.31 (dddd, J = 18.3, 16.8, 15.1, 8.1 Hz, 1H), 2.56 (dddd, J = 18.3, 16.8, 15.1, 8.1 Hz, 1H), 2.24 (s, 3H), 1.65 – 1.56 (m, 6H).**¹³C NMR** (100 MHz, CDCl₃): δ 204.2, 161.1 (t, J = 28.0 Hz), 141.0, 139.6, 139.5, 124.5, 124.3, 123.4, 122.7, 122.2, 118.4 (t, J = 253.0 Hz), 48.1 (t, J = 4.0 Hz), 46.7 (t, J = 6.0 Hz), 44.3, 37.6 (t, J = 23.0 Hz), 28.6, 26.3, 25.5, 24.3. **¹⁹F NMR** (376 MHz, CDCl₃): δ -98.0(s). **HRMS (ESI)** m/z: [M+Na]⁺ Calcd for C₁₉H₂₁F₂NO₂SNa: 388.1159; Found: 388.1155.

4-(benzo[b]thiophen-2-yl)-2,2-difluoro-1-(pyrrolidin-1-yl)hexane-1,5-dione (5d).

The flow experiment was carried out on a 0.5 mmol scale, 2.2 mL of liquid was collected. Purification: Column chromatography (Cyclohexane/EtOAc = 30:1 to 16:1), 65.4 mg product was isolated as a colorless oil (85% yield). **¹H NMR** (400 MHz, CDCl₃): δ 7.79-7.70 (dd, J = 28.0, 8.0 Hz, 2H), 7.36-7.29 (m, 2H), 7.16 (s, 1H), 4.48 (q, J = 4.0 Hz, 1H), 3.64 (q, J = 4.0 Hz, 2H), 3.46 (q, J = 6.8 Hz, 2H), 3.26 (tdd, J = 17.4, 14.9, 8.3 Hz, 1H), 2.55 (qd, J = 16.3, 4.3 Hz, 1H), 2.24(s, 3H), 1.97-1.91 (m, 2H), 1.86-1.78(m, 2H). **¹³C NMR** (100 MHz, CDCl₃): δ 204.2, 161.6 (t, J = 29.0 Hz), 140.8, 139.6, 139.5, 124.5, 124.4, 123.4, 122.8, 122.2, 117.6 (t, J = 252.0 Hz), 48.0 (t, J = 4.0 Hz), 47.4, 46.6 (t, J = 23.0 Hz), 37.0 (t, J = 24.0 Hz), 28.6, 26.9, 26.4, 23.2. **¹⁹F NMR** (376 MHz, CDCl₃): δ -101.50(s). **HRMS (ESI)** m/z: [M+Na]⁺ Calcd for C₁₈H₁₉F₂NO₂SNa: 374.1002; Found: 374.1003.

Associated Content

The *Supporting Information* for this article is available free of charge on the ACS Publications website at DOI: 10.1021/acs.joc.8b01624

References:

(1) (a) Murakami, K; Yamada, S.; Kaneda, T.; Itami, K. *Chem. Rev.* **2017**, *117*, 9302-9332. (b) Yang, Y.; Lan, J.; You, J. *Chem. Rev.* **2017**, *117*, 8787-8863. (c) Boubertakh, O.; Goddard, J.-P. *Eur. J. Org. Chem.* **2017**, *2017*, 2072-2084. (d) Rossi, R.; Bellina, F.; Lessi, M.; Manzini, C. *Adv. Synth. Catal.* **2014**, *356*, 17-117. (e) Vitaku, E.; Smith, D. T.; Njardarson, J. T. *J. Med. Chem.* **2014**, 57, 10257-10274.

(2) (a) Twigg, D. G.; Kondo, N.; Mitchell, S. L.; Galloway, W. R. J. D.; Sore, H. F.; Madin, A.; Spring, D. R. *Angew. Chem. Int. Ed.* **2016**, *55*, 12479-12483. (b) Birudukota, N. V. S.; Ranke, R.; Hover, B. *Org. Biomol. Chem.* **2016**, *14*, 3821-3837. (c) Lovering, F. *Med. Chem. Commun.* **2013**, *4*, 515-519. (d) Lovering, F.; Bikker, J.; Humblet, C. *J. Med. Chem.* **2009**, *52*, 6752-6756.

(3) Duncton, M. A. J. *Med. Chem. Commun.* **2011**, *2*, 1135-1161.

(4) Ackermann, L. *Chem. Commun.* **2010**, *46*, 4866-4877.

(5) For selected reviews on radical aryl migration reactions, see: (a) Zeng, Y.; Ni, C.; Hu, J. *Chem. Eur. J.* **2016**, *22*, 3210-3223. (b) Chen, Z.-M.; Zhang, X.-M.; Tu, Y.-Q. *Chem. Soc. Rev.* **2015**, *44*, 5220-5245. (c) Studer, A.; Bossart, M. *Tetrahedron* **2001**, *57*, 9649-9667.

(6) For some selected recent examples on photocatalytic migration chemistry, see: (a) Wu, X.; Wang, M.; Huan, L.; Wang, D.; Wang, J.; Zhu, C. *Angew. Chem. Int. Ed.* **2018**, *57*, 1640-1644. (b) Tang, X.; Studer, A. *Angew. Chem. Int. Ed.* **2018**, *57*, 814-817. (c) Yu, J.; Wang, D.; Xu, Y.; Wu, Z.; Zhu, C. *Adv. Synth. Catal.* **2018**, *360*, 744-750. (d) Xu, Y.; Wu. Z.; Jiang, J.; Ke, Z.; Zhu, C. *Angew. Chem. Int. Ed.* **2017**, *56*, 4545-4548.

(7) For the handling of exothermic reactions in flow, see: (a) Laudadio, G.; Gemoets, H. P. L.; Hessel, V.; Noël, T. *J. Org. Chem.* **2017**, *82*, 11735-11741. (b) Kockmann, N.; Thenée, P.; Fleischer-Trebes, C.; Laudadio, G. and Noël, T. *React. Chem. Eng.* **2017**, *2*, 258-280. (c) Gutmann, B.; Kappe, C. O. *J. Flow Chem.* **2017**, *7*, 65-71. (d) Movsisyan, M.; Delbeke, E. I. P.; Berton, J. K. E. T.; Battilocchio, C.; Ley, S. V.; Stevens, C. V. *Chem. Soc. Rev.* **2016**, *45*, 4892-4928. (e) Gutmann, B.; Cantillo, D.; Kappe, C. O. *Angew. Chem. Int. Ed.* **2015**, *54*, 6688-6728. (f) Newby, J. A.; Huck, L.; Blaylock, W.; Witt, P. M.; Ley, S. V.; Browne, D. L. *Chem. Eur. J.* **2014**, *20*, 263-271. (g) Newby, J. A.; Blaylock, D. W.; Witt, P. M.; Pastre, J. C.; Zacharova, M. K.; Ley, S. V.; Browne, D. L. *Org. Process Res. Dev.* **2014**, *18*, 1211-1220. (h) Newby, J. A.; Blaylock, D. W.; Witt, P. M.; Turner, R. M.; Heider, P. L.; Harji, B. H.; Browne, D. L.; Ley, S. V. *Org. Process Res. Dev.* **2014**, *18*, 1221-1228. (i) Brodmann, T.; Koos, P.; Metzger, A.; Knochel, P.; Ley, S. V. *Org. Process Res. Dev.* **2012**, *16*, 1102-1113.

(8) For the use of ultrasound to overcome microreactor clogging, see: (a) Chen, Y.; Sabio, J. C.; Hartman, R. L. *J. Flow Chem.* **2015**, *5*, 166-171. (b) Hartman, R. L. *Org. Process Res. Dev.* **2012**, *16*, 870-887. (c) Kuhn, S.; Noel, T.; Gu, L.; Heider, P. L.; Jensen, K. F. Lab Chip **2011**, *11*, 2488–2492. (d) Noel, T.; Naber, J. R.; Hartman, R. L.; McMullen, J. P.; Jensen, K. F.; Buchwald, S. L. *Chem. Sci.* **2011**, *2*, 287–290.

(9) Nagaki, A.; Yoshida, J.-i. *Top. Organomet. Chem.* **2015**, *57*, 137-176.

(10) For the benefits of microreactor technology for photochemistry, see: (a) Noel, T. *J. Flow. Chem.* **2017**, *7*, 87-93. (b) Cambié, D.; Bottecchia, C.; Straathof, N. J. W.; Hessel, V.; Noël, T. *Chem. Rev.* **2016**, *116*, 10276-10341. (c) Loubiere, K.; Oelgemoeller, M.; Aillet, T.; Dechy-Cabaret, O.; Prat, L. *Chem. Eng. Process* **2016**, *104*, 120-132. (d) Mizuno, K.; Nishiyama, Y.; Ogaki, T.; Terao, K.; Ikeda, H.; Kakiuchi, K. *J. Photochem. Photobiol. C* **2016**, *29*, 107-147.

(11) Attempts to connect the two steps in one flow protocol failed. Apparently impurities from the Grignard reaction negatively affect the photocatalytic step. Even using inline purification steps, such as microfluidic extractions, did not solve this issue.

(12) O'Hara, F.; Blackmond, D. G.; Baran, P. S. *J. Am. Chem. Soc.* **2013**, *135*, 12122−12134.

(13) Wei, X.-J.; Boon, W; Hessel, V; Noel, T. *ACS Catal.* **2017**, *7*, 7136-7140.

(14) (a) Straathof, N. J.W.; Su, Y.; Hessel, V.; Noël, T. *Nature Protocols* **2016**, *11*, 10-21. (b) Bottecchia, C.; Wei, X-J.; Kuijpers, K. P. L.; Hessel, V.; Noël, T. *J. Org. Chem.* **2016**, *81*, 7301-7307.

(15) Yang, H.; Huo, N.; Yang, P.; Pei, H.; Lv, H.; Zhang, X. *Org. Lett.* **2015**, *17*, 4144–4147.

Chapter 4

Disulfide-Catalyzed Visible-Light Oxidative Cleavage of C=C Bonds and Evidence of an Olefin-Disulfide Charge-Transfer Complex
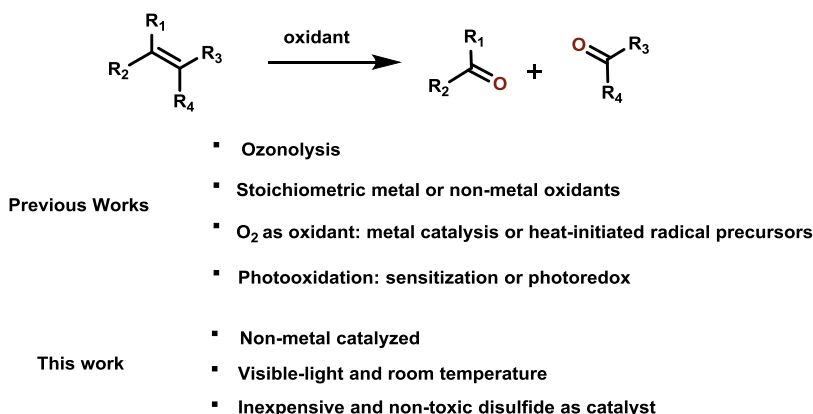
Abstract

A photocatalytic method for the aerobic oxidative cleavage of C=C bonds has been developed. Electron-rich aromatic disulfides were employed as photocatalyst. Upon visible-light irradiation, typical mono- and multi-substituted aromatic olefins could be converted to ketones and aldehydes at ambient temperature. Experimental and computational studies suggest that a disulfide-olefin charge-transfer complex is possibly responsible for the unconventional dissociation of S–S bond under visible-light.

Introduction

The oxidative cleavage of olefins (OCO) is a widely applied transformation in organic synthesis, since it introduces oxygen-containing functional groups such as ketones and aldehydes from inexpensive olefinic feedstock.[1] Despite the simplicity of the reaction, a practical and mild OCO method is still one of the long-sought goals in the development of modern chemical methodologies. One of the most popular methods for this transformation is still the old-fashioned ozonolysis,[2] which requires an ozone generator and displays serious safety issues due to the toxicity of O_3. Modern OCO reactions include methods employing stoichiometric metal or non-metal reagents that are either toxic or strongly oxidizing,[1] or methods that utilizing molecular oxygen as a safer and cleaner oxidant in combination of catalytic amount of transition-metal complexes[3–5] or heat-initiated radical precursors (NHPI,[6] AIBN,[7] etc.). Recently, photochemical OCO methods have been reported with the photon as a traceless reagent and a green source of energy.[8–12] In general, these methods required UV-light, or catalysts that are toxic[8] or metal-based,[9] or a demandingly oxidative photoredox catalyst to be SET-reduced by the olefin.[10–12] Alternatively, it would be attractive to seek a non-metal photocatalyst that functions via a non-redox/sensitization mechanism, and preferably with a reduced cost than most photocatalysts. Herein, we report a visible-light aerobic OCO method that utilizes inexpensive aromatic disulfide as photocatalyst (**Scheme 4.1**).

- Ozonolysis
- Stoichiometric metal or non-metal oxidants
- O_2 as oxidant: metal catalysis or heat-initiated radical precursors
- Photooxidation: sensitization or photoredox

Previous Works

- Non-metal catalyzed
- Visible-light and room temperature
- Inexpensive and non-toxic disulfide as catalyst

This work

Scheme 4.1. Summary of previous OCO methods

Several previously reported radical-catalyzed OCO reactions involved the formation of a dioxetane that decomposes to give the product aldehyde or ketone.[3,6,7] In seeking a photo-initiated radical that could reversibly add to the C=C bond, we envisioned that the thiyl radical generated by the photolysis of disulfide could serve as an ideal catalyst.[13,14] Recently, examples of disulfide-catalyzed photoreactions were reported, in which disulfide undergoes photolysis to catalyze the diboration of terminal alkynes,[15a] or the reduction of a carbon–halide bond with NHC-borane,[15b] or the [3+2]

cycloaddition.[15c] They required light from the UV-region because the dissociation of typical aromatic S–S bond cannot occur under visible-light.[16]

In the hope of establishing a photocatalytic OCO method with visible-light instead of the harmful and equipment-demanding UV light, we were intrigued by the acceleration effect in the thiol-olefin co-oxidation (TOCO) reported and studied in-depth decades ago.[17–21] In the presence of an olefin, the overall rate for the oxidation-addition sequence is significantly faster than the SET oxidation of thiol alone, due to the formation of an olefin-thiol charge-transfer complex (CTC) (**Scheme 4.2**).[17,18] To the best of our knowledge, the same effect between olefin and disulfide has not been reported to date. Recently, photochemical activity of *in situ* formed electron donor-acceptor complex (EDA complex [22–24]) has been reported by Melchiorre,[25] in which two photo-inactive species transiently associate together to form a complex that is photo-active. Therefore, we envisioned that an analogous effect of TOCO/CTC might exist between disulfide and olefin, which could lead to a more feasible S–S bond photolysis by visible-light in the presence of an olefin (**Scheme 4.2**).

Difficulty of photolysis for most diary disulfides under visible light
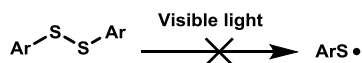
Thiol-olefin co-oxidation(TOCO) via a charge-transfer complex
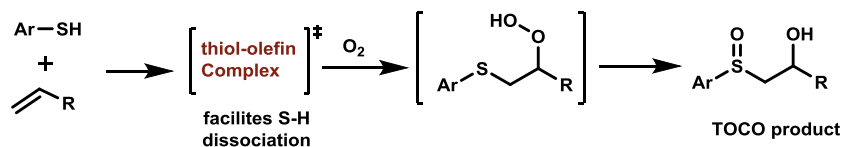
Proposed analogous effect between olefin and disulfide
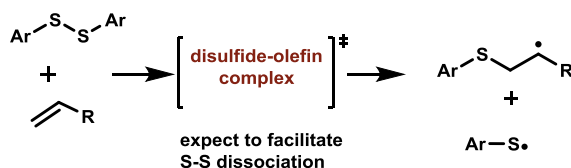
Scheme 4.2. Thiol-olefin co-oxidation (TOCO) and possible analogous effect between olefin and disulfide

Result and Discussion

We initiated our study with a simple experiment, in which the MeCN solution of α-methylstyrene (**1a**) and bis(4-methoxyphenyl) disulfide (**S1**, 5 mol%) was placed under light generated from a white LED lamp and stirred for 16 h with the reaction vial open to air. Gratifyingly, some of the C=C bond was found to be cleaved, and acetophenone (**2a**) was obtained in 18% isolated yield (**Scheme 4.3**).

Like in other radical-mediated OCO methods, we also believed that the key intermediate was the dioxetane (**6**), which was formed from intermediate **5** by the abstraction[26] and substitution of the thiyl radical. Although dioxetane **6** could not be directly observed since it spontaneously decomposed upon formation[6,7] to give product **2a**, several observations were informative to confirm the proposed pathway: 1) The tertiary radical **3** from the thiyl addition underwent α-hydrogen abstraction to give trace amount of compound **4**, which was observed by GC-MS; 2) When the reaction was performed in the presence of methionine (1 equiv.) and water as the trapping reagents for dioxetane,[27] the formation of diol **8** was detected.
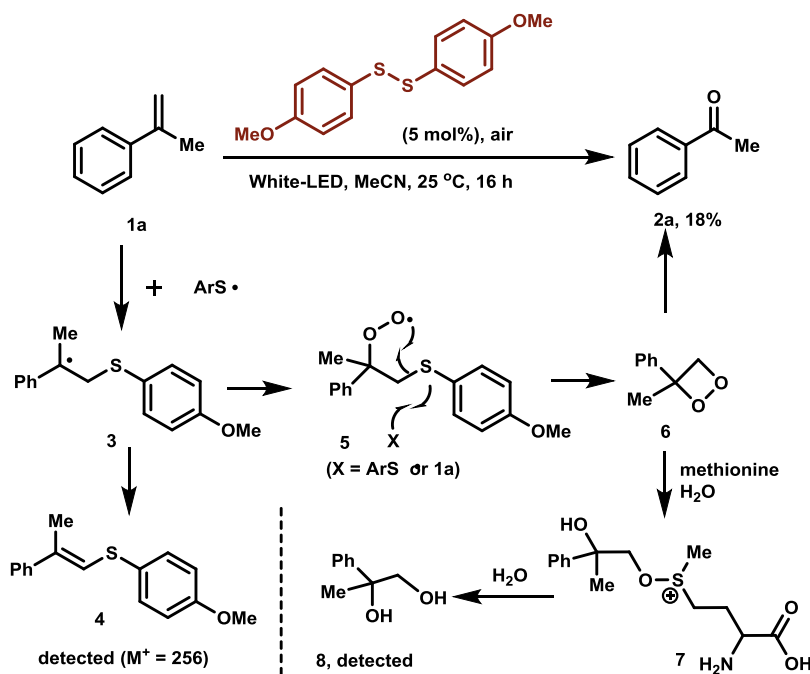
Scheme 4.3. Visible-light oxidative C=C bond cleavage catalyzed by bis(4-methoxyphenyl) disulfide

A set of experiments was performed to confirm the efficacy of disulfides as photo-precatalysts. In the absence of disulfide **S1**, no ketone product was observed (**Table 4.1**, entry 1). The dark reaction in the presence of **S1**, either at ambient temperature (entry 2) or heated to 45 °C (entry 3), afforded no observable product. The reaction in the presence of molecular oxygen (1 bar) gave an elevated yield of 83% (**Table 4.1**, entry 4) compared to the reaction under air. We also examined other disulfides such as bis(phenyl), bis(*p*-tolyl), bis(*p*-chlorophenyl),[28] and bis(2-thiophenyl) disulfides (**S2**–**S5**, entries 5–8), which all gave lower yields than **S1**. Inorganic compounds with S–S bond such as sodium metabisulfite (**S6**) were also examined, however, no ketone **2** was formed in 16 hours (entry 9).

Table 4.1. Exploring reaction conditions.
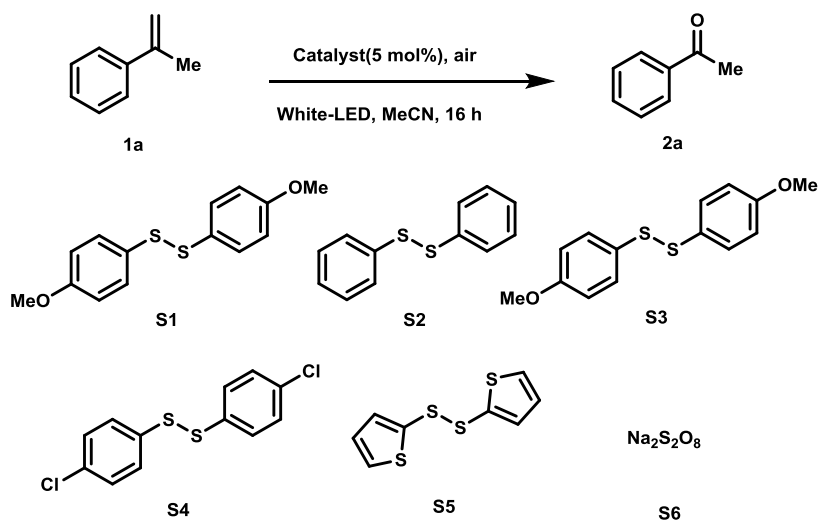
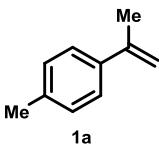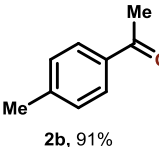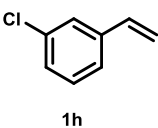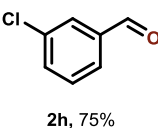**Table 4.2.** Optimization of the reaction conditions[a]
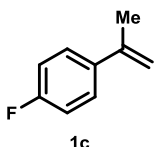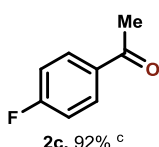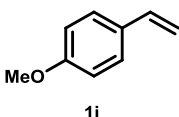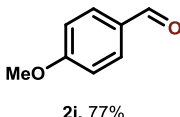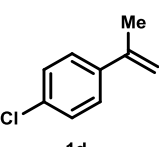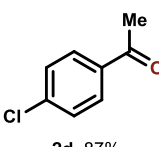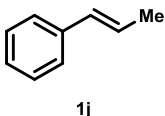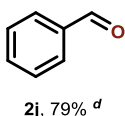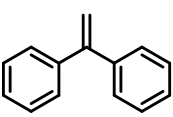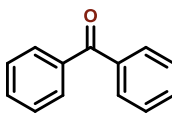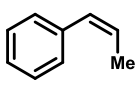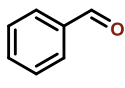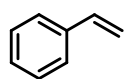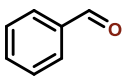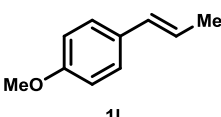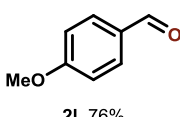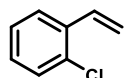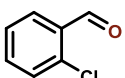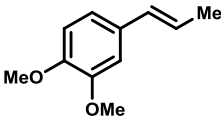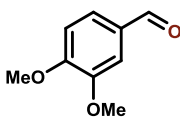
Entry	Catalyst	Oxidant	Light	T/°C	Yield%[a]
1	none	air	white LED	25	0
2	S1	air	dark	25	0
3	S1	air	dark	45	0
4	S1	O_2	white LED	25	83
5	S2	O_2	white LED	25	53
6	S3	O_2	white LED	25	72
7	S4	O_2	white LED	25	70
8	S5	O_2	white LED	25	29
9	S6	O_2	white LED	25	0

[a] Based on isolated product.

With the optimal disulfide confirmed as **S1,** we set out to explore more olefinic substrates. At room temperature, a diverse set of aromatic olefins could be converted to corresponding ketones and aldehydes with 1 bar of O_2 and catalytic amount of **S1** (**Table 4.2**). The reaction with α-methylstyrene analogs (**1b–1d**) all afforded excellent yields of the ketone products (**2b–2d**). Benzophenone (**2e**) could be prepared from 1,1-diphenylethylene (**1e**) in 76% yield, which however required more catalyst (10 mol%). Styrene and its derivatives with *ortho-*, *meta-* and *para-*substituents (**1f–1i**) could all be converted into the aldehyde products in 70–80% yield. In general, the oxidation of 1,2-disubstituted olefins (**1j–1m**) also went smoothly and moderate to good yields were obtained, with

the only exception of the reaction of (Z)-β-methylstyrene (**1k**), in which a part of the starting material either isomerized to the (E)-alkene (**1j**) or was epoxidized.

Table 4.3. Disulfide-catalyzed photo-oxidation of aromatic olefins.

Olefin → Ketone/Aldehyde

S1(5 mol%), O₂(1 bar)

white-LED, MeCN, 25 °C, 16 h

Olefin	Product and Yield [a]	Olefin	Product and Yield [a]
1a	**2b**, 91%	**1h**	**2h**, 75%
1c	**2c**, 92% [c]	**1i**	**2i**, 77%
1d	**2d**, 87%	**1j**	**2j**, 79% [d]
1e	**2e**, 76% [b,c]	**1k**	**2k**, 44% [e]
1f	**2f**, 73% [c]	**1l**	**2l**, 76%
1g	**2g**, 75%	**1m**	**2m**, 60%

[a] Based on yields of isolated product. [b] With 10 mol% catalyst. [c] Acetone as solvent. [d] 1,4-Dioxane as solvent. [e] Methanol as solvent.

 It is commonly believed that the photolysis of most aromatic disulfides requires UV irradiation.[13,15,16] In order to prove that the light from the LED light source was not able to generate the thiyl radical from the disulfide, we carried out two control experiments. Under white LED light, the disulfide-disulfide exchange between bis(4-methoxyphenyl) disulfide (**S1**) and dimethyl disulfide (**S7**) did not take place (**Scheme 4.4**). In contrast, the mixture disulfide formed with 9% yield in 1 hour with irradiation from a medium-pressure Hg lamp. The reason a dialkyl disulfide was chosen for the cross-over experiment was that the exchange between two aromatic disulfides can occur via a concerted mechanism without light.[29–31] The photo-addition of disulfide to terminal alkyne under UV was first observed for dialkyl disulfide by Heiba and Dessau in 1960s.[32] A recent example was reported by Ogawa,[14] in which diphenyl disulfide could be trapped by 1-octyne with light from a medium-pressure Hg lamp. However, under LED irradiation, an equimolar mixture of 1-heptyne and diphenyl disulfide (**S2**) did not undergo any addition reaction. These results suggested that the S–S bond of common aromatic disulfides cannot be cleaved to give thiyl radicals with light from an LED lamp (**Scheme 4.4**).
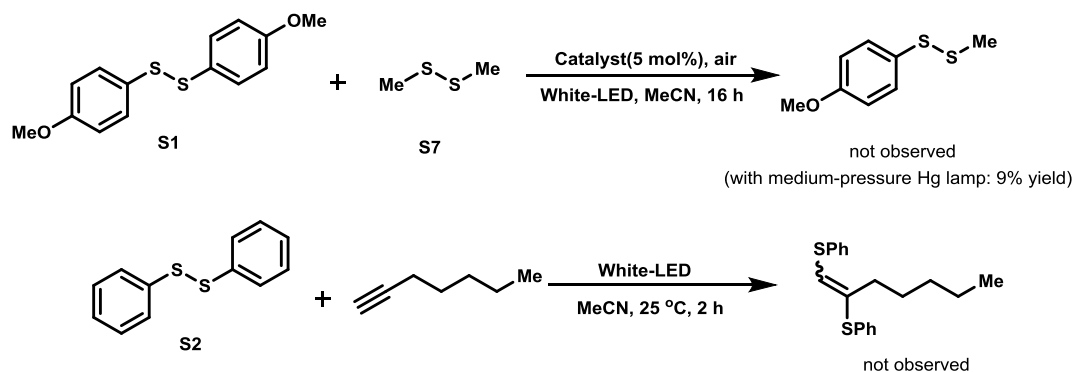
Scheme 4.4. The control experiments

Thus, it is reasonable to assume that the olefin and disulfide have interactions that facilitate the S–S bond photolysis, with the olefin acting as a sensitizer. Following Szmant's procedure to confirm the thiol-olefin charge-transfer complex in the 1980s,[21a] we carried out a set of NMR experiments to seek evidence of the disulfide-olefin complex. By analyzing a series of ^{1}H NMR of a fixed amount of disulfide **S1** mixed with increasing amounts of α-methylstyrene (**1a**), we found that the chemical shift of the disulfide's methoxy group distinctly drifted towards upfield, which indicated that the electron density on the disulfide had increased. This observation could be explained by the electron-donation from the olefin's conjugated π-system to the sulfur atom, based on the same observation and rationalization for the thiol-olefin system.[18–21] The chemical shifts for the olefin remained largely

unchanged. The slope of the curve decreased with the increasing relative concentration of olefin, indicating that the charge-transfer complex was forming towards saturation (**Figure 4.1**).
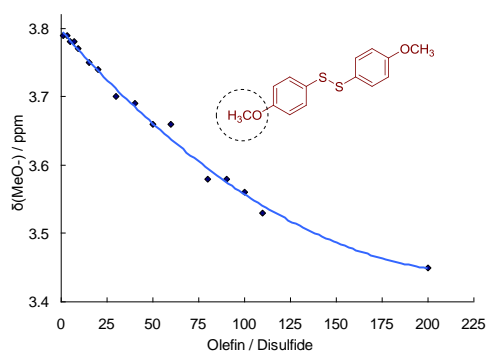

Figure 4.1. Correlation between the chemical shift of –OMe of **S1** and the relative olefin concentration.

In addition to experimental results, computational studies were also performed for the disulfide-olefin charge-transfer complex. The UV-Vis spectra [33,34] of **S1** and the complex **S1-1a** were simulated by DFT calculation at the ωB97x-D/6-31G* level of theory, which was previously used for theoretical studies of the spectroscopic behavior of various disulfides.[35] The energy and UV-Vis spectrum of **S1** were first calculated to confirm the accuracy of the method. The energy gap between HOMO (–7.83 eV) and LUMO (+0.59 eV) was calculated to be 8.42 eV (**Figure 4.2**). The calculated absorption of **S1** fell within the UV region (< 400 nm, **Figure 4.3**) and was in accord with the experimental spectrum.

The structure of the disulfide-olefin complex (**S1-1a**) was proposed based on the results of NMR experiments that the electron density at the disulfide was increased, and also based on Fava[18] and Szmant's[20–21] models that the HOMO of the olefin preferably interacts with the LUMO of the thiol (here it is the LUMO of the disulfide). The complex's geometry was optimized based on the same DFT method (ωB97x-D/6-31G*) for calculating the energy of **S1**. The disulfide-olefin complex (**S1-1a**) displayed a reduced HOMO–LUMO gap of 7.31 eV (HOMO = –6.89 eV, LUMO = +0.42 eV) as compared to that of the free disulfide **S1** (**Figure 4.2**). The reduced HOMO–LUMO gap might be attributed to the elevation of HOMO caused by the electron-donation from the C=C π-orbital to the sulfur (as graphically shown in **Figure 4.2**).[21a] The calculated UV-Vis spectrum of the complex (**S1-1a**) showed that the range of absorption had extended to the visible region (400–440 nm) (**Figure 4.3**). Therefore, the olefin-activated disulfide would lead to a more feasible homolytic S–S bond dissociation under visible-light, and a subsequent thiyl addition to the C=C bond.

HOMO (S1) = –7.83 eV   LUMO (S1) = +0.59 eV

HOMO (S1-1a) = –6.89 eV   LUMO (S1-1a) = +0.42 eV
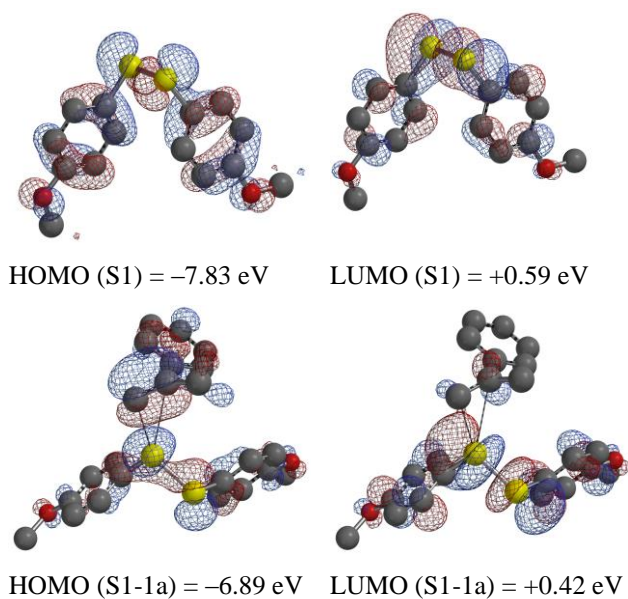
Figure 4.2. Modeling of the disulfide-olefin complex and energy levels by DFT calculation
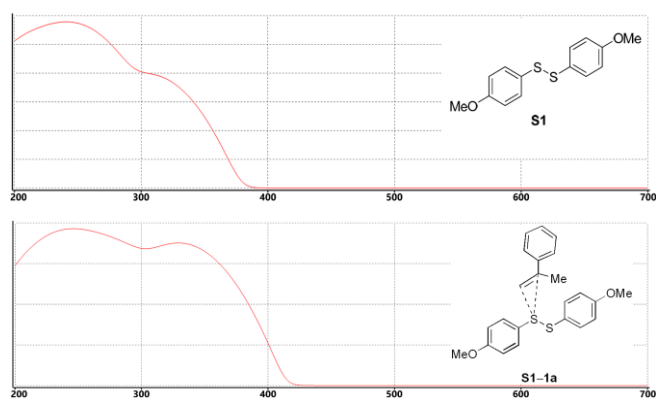
Figure 4.3. The simulated UV-Vis spectra of S1 and the disulfide-olefin complex (S1-1a)

Conclusions

In conclusion, we have developed a mild and non-metal catalyzed method for the aerobic oxidative cleavage the C=C bond under visible-light at room temperature. Bis(4-methoxyphenyl) disulfide was employed as photocatalyst, and typical monosubstituted as well as 1,1- and 1,2-disubstituted aromatic alkenes could be converted to corresponding aldehydes and ketones. Interestingly, we have discovered that the coordinating effect between thiols and olefins might also exist between certain disulfides and olefins. The unconventional homolysis of the aromatic S–S bond by visible-light was rationalized by the olefin-disulfide charge-transfer complex. Mechanistic details of this effect and more synthetic applications are currently being investigated in our lab.

Experimental Section

Procedure for the screening of reaction conditions and catalysts.

In a 7 mL clear glass vial with an O_2 balloon, disulfide catalyst (0.050 mmol) was added to the solution of α-methylstyrene (1.0 mmol) in MeCN (0.3 mL) at room temperature. Under visible-light generated from a white LED lamp (for dark reaction, the vial was wrapped carefully with aluminum foil), the reaction mixture was stirred at indicated temperature for 16 hours. The reaction was monitored by TLC or GC-MS. The product was isolated by flash chromatography eluting with pentane/Et$_2$O (30:1) as a yellowish oil.

General procedure for disulfide-catalyzed photo oxidative cleavage of olefins.

In a 7 mL clear glass vial with an O$_2$ balloon, bis(4-methoxyphenyl) disulfide (0.025–0.050 mmol) was added to the solution of olefin (0.5–1.0 mmol) in MeCN (in some specific cases, 1,4-dioxane, methanol, or acetone was used). Under visible-light generated from a white LED lamp, the reaction mixture was stirred at 25 °C for 16 hours. The reaction was monitored by TLC or GC-MS. The product was isolated by flash chromatography.

Procedure for the disulfide-disulfide exchange reaction.

In a clear glass vial, bis(4-methoxyphenyl) disulfide (28.9 mg, 0.10 mmol) and dimethyl disulfide (9.5 mg, 0.10 mmol) were dissolved in MeCN (1.0 mL) under nitrogen. Under visible-light generated from a white LED lamp, the mixture was stirred at 25 °C for 1 hour. ^{1}H NMR analysis showed no formation of the mixed disulfide. The above procedure was repeated with UV light from a medium-pressure Hg lamp for 1 hour. ^{1}H NMR analysis showed a set of new peak for the formation of mixed disulfide in 9% NMR yield: ^{1}H NMR (500 MHz, CDCl$_3$) δ 7.42 (d, J = 8.7 Hz, 2H), 6.83 (d, J = 8.7 Hz, 2H), 3.76 (s, 3H), 2.38 (s, 3H). MS (EI) m/z [M]$^+$ calcd for C$_8$H$_{10}$OS$_2$: 186.0, found 186.0.
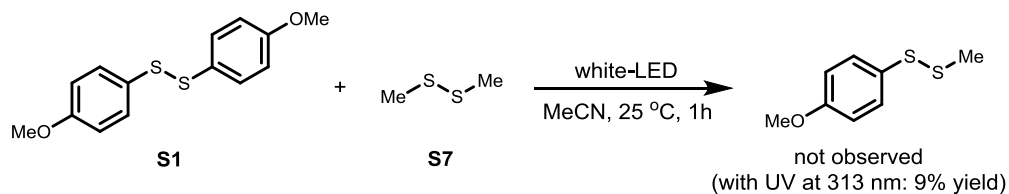
The above procedure was repeated with UV light from a medium-pressure Hg lamp for 1 hour. ^{1}H NMR analysis showed a set of new peak for the formation of mixed disulfide in 9% NMR yield: ^{1}H NMR (500 MHz, CDCl$_3$) δ 7.42 (d, J = 8.7 Hz, 2H), 6.83 (d, J = 8.7 Hz, 2H), 3.76 (s, 3H), 2.38 (s, 3H). MS (EI) m/z [M]$^+$ calcd for C$_8$H$_{10}$OS$_2$: 186.0, found 186.0.

Procedure of mechanistic experiments of the disulfide-catalyzed OCO reaction.

1) TEMPO inhibition experiment:
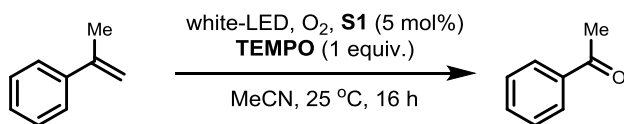
In a 7 mL clear glass vial with an O_2 balloon, bis(4-methoxyphenyl) disulfide (7.3 mg, 0.026 mmol) was added to the solution of α-methylstyrene (61 mg, 0.52 mmol), TEMPO (81 mg, 0.52 mmol) in MeCN (0.3 mL). Under visible-light generated from a white LED lamp, the reaction mixture was stirred at 25 °C for 16 hours. Analysis by NMR and GC-MS showed no product was formed.

2) Dioxetane trapping by methionine:
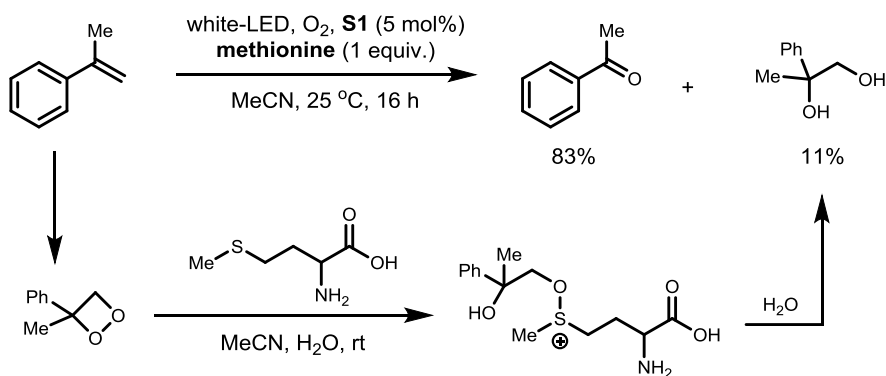
In a 7 mL clear glass vial with an O_2 balloon, bis(4-methoxyphenyl) disulfide (7.3 mg, 0.026 mmol) was added to the solution of α-methylstyrene (61 mg, 0.52 mmol), L-methionine (77 mg, 0.52 mmol) in a mixed solvent of MeCN (0.30 mL) and H_2O (0.15 mL). Under visible-light generated from a white LED lamp, the reaction mixture was stirred at 25 °C for 16 hours. Analysis by NMR and GC-MS showed the formation of 2-phenylpropane-1,2-diol (11% yield). ^{1}H NMR (500 MHz, CDCl_3) δ 7.47–7.18 (m, 5H), 3.79 (d, J = 11.1 Hz, 1H), 3.64 (d, J = 11.1 Hz, 1H), 1.53 (s, 3H). MS (EI): fragmentation pattern was in accord with the one in database for 2-phenylpropane-1, 2-diol.

3) Photosensitizer experiment:
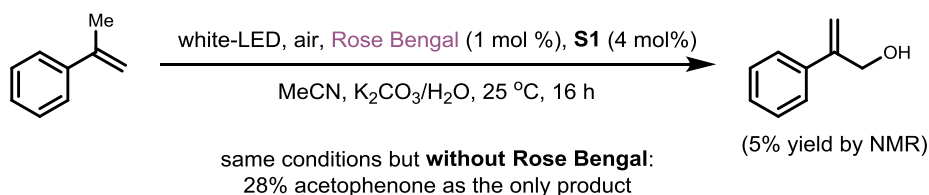
In a 7 mL clear glass vial, bis(4-methoxyphenyl) disulfide (5.0 mg, 0.018 mmol) was added to the solution of α-methylstyrene (52 mg, 0.44 mmol), Rose Bengal (3.0 mg, 0.0029 mmol), K_2CO_3 (12 mg, 0.087 mmol) in a mixed

105

solvent of MeCN (0.80 mL) and H_2O (0.10 mL). The vial was opened to air with a needle on the septum. Under visible-light generated from a white LED lamp, the reaction mixture was stirred at 25 °C for 16 hours. The formation of 2-phenylprop-2-en-1-ol was detected by NMR and GC-MS (with 5% yield by NMR): ^{1}H NMR (500 MHz, DMSO-d[6]) δ: 7.50–7.30 (m, 5H), 5.47 (q, J = 1.3 Hz, 1H), 5.35 (q, J = 1.7 Hz, 1H), 4.27 (t, J = 1.4 Hz, 2H), 2.62 (s, 1H). MS (ESI) m/z $[M+H]^+$ calcd for $C_9H_{11}O$: 135.1, found 135.1. If the above experiment was carried out without Rose Bengal, no formation of 2-phenylprop-2-en-1-ol (or its hydroperoxide form) was detected, and the only product observed was acetophenone (28% yield).

From the above experiments, we believe that the disulfide-catalyzed photo OCO reaction probably proceeds via the dioxetane as the reactive intermediate. A singlet oxygen pathway is less likely.

4) Procedure for the NMR analysis of disulfide-olefin mixtures.

In a set of NMR tubes, a fixed amount of bis(4-methoxyphenyl) disulfide (**S1**) was mixed with varying amount of α-methylstyrene (**1a**) in different ratios. $CDCl_3$ was added as solvent. ^{1}H NMR was taken for each mixture and the chemical shifts were measured relative to the signals for TMS (0.00 ppm). The amounts of **S1** and **1a** in each mixture are listed in the following table.

1a/S1	1a (mg)	S1 (mg)	1a/S1	1a (mg)	S1 (mg)
1	3.8	7.2	40	119.5	7.3
3	9.3	7.3	50	150.4	7.4
5	15.2	7.3	60	180.7	7.2
7	21.6	7.1	80	238.8	7.4
9	27.3	7.3	90	266.9	7.4
15	45.4	7.5	100	294.1	7.3
20	59.8	7.1	110	326.8	7.2
30	88.9	7.2	200	590.9	7.2

Compound Characterization

Acetophenone (2a):

The general procedure was followed by employing α-methylstyrene (119.3 mg, 1.01 mmol) and bis(4-methoxyphenyl) disulfide (14.4 mg, 0.052 mmol, 5.1 mol%) and MeCN (0.3 mL). The reaction was stopped after 16 hours. Purification by flash chromatography eluting with Pentane/Et$_2$O (30:1) afforded the title compound as a yellowish oil (100.8 mg, 83.2%): **^{1}H NMR** (500 MHz, CDCl$_3$) δ 7.98 - 7.94 (m, 2H), 7.58 - 7.54 (m, 1H), 7.48 - 7.44 (m, 2H), 2.60 (s, 3H); **^{13}C NMR** (126 MHz, CDCl$_3$) δ 198.10, 137.08, 133.06, 128.52, 128.25, 26.56; **MS** (EI) m/z [M]$^+$ calcd for C$_8$H$_8$O: 120.15, found 120.0.

1-*p*-Tolylethanone (2b):

The general procedure was followed by employing p,α-dimethylstyrene (68.0 mg, 0.51 mmol) and bis(4-methoxyphenyl) disulfide (7.1 mg, 0.026 mmol, 5.1 mol%) and MeCN (0.3 mL). The reaction was stopped after 16 hours. Purification by flash chromatography eluting with Pentane/Et$_2$O (10:1) afforded the title compound as a colorless oil (62.6 mg, 90.7%): **^{1}H NMR** (500 MHz, CDCl$_3$) δ 7.86 (dt, J = 8.3, 1.7 Hz, 2H), 7.28 - 7.23 (m, 2H), 2.57 (s, 3H), 2.41 (s, 3H); **^{13}C NMR** (126 MHz, CDCl$_3$) δ 197.83, 143.84, 134.69, 129.21, 128.41, 26.50, 21.60; **MS** (EI) m/z [M]$^+$ calcd for C$_9$H$_{10}$O: 134.18, found 134.0.

1-(4-Fluorophenyl)ethanone (2c):

The general procedure was followed by employing 1-fluoro-4-(prop-1-en-2-yl)benzene (78.3 mg, 0.57 mmol) and bis(4-methoxyphenyl) disulfide (7.5 mg, 0.027 mmol, 4.7 mol%) and acetone (0.4 mL). Reaction was stopped after 16 hours. Purification by flash chromatography eluting with Pentane/Et$_2$O (20:1) afforded the title compound as a yellowish oil (73.1 mg, 91.9%): **^{1}H NMR** (500 MHz, CDCl$_3$) δ 7.99 - 7.94 (m, 2H), 7.11 (tt, J = 8.7, 2.0 Hz, 2H), 2.57 (s, 3H); **^{13}C NMR** (126 MHz, CDCl$_3$) δ 196.42, 165.7 (d, J = 255.0 Hz), 133.5 (d, J = 3.0 Hz), 130.9 (d, J = 9.4 Hz), 115.6 (d, J = 21.9 Hz), 26.4; **MS** (EI) m/z [M]$^+$ calcd for C$_8$H$_7$FO: 138.1, found 138.0.

1-(4-Chlorophenyl)ethanone (2d):

The general procedure was followed by employing 4-chloro-α -methylstyrene (77.3 mg, 0.51 mmol) and bis(4-methoxyphenyl) disulfide (7.1 mg, 0.026 mmol, 5.1 mol%). The reaction was stopped after 16 hours. Purification by flash chromatography eluting with Pentane/Et$_2$O (20:1) afforded the title compound as a colorless oil (67.9 mg, 86.7%): **^{1}H NMR** (500 MHz, CDCl$_3$) δ 7.89(dt, J = 8.6, 1.9 Hz, 2H), 7.44 (dt, J = 8.6, 1.9 Hz, 2H), 2.59 (s, 3H); **^{13}C NMR** (126 MHz, CDCl$_3$) δ 196.8, 139.6, 135.4, 129.7, 128.9, 26.5; MS (EI) m/z [M]$^+$ calcd for C$_8$H$_7$ClO: 154.0, found 154.0.

Benzophenone (2e):

The general procedure was followed by employing 1,1-diphenylethylene (95.6 mg, 0.53 mmol) and bis(4-methoxyphenyl) disulfide (14.5 mg, 0.052 mmol, 9.8 mol%) and MeCN (0.4 mL). The reaction was stopped after 16 hours. Purification by flash chromatography eluting with Pentane/Et$_2$O (20:1) afforded the title compound as a yellowish oil (73.3 mg, 75.8%): **^{1}H NMR** (500 MHz, CDCl$_3$) δ 7.81 (d, J = 7.7 Hz, 4H), 7.59 (t,

J = 7.4 Hz, 2H), 7.48 (t, J = 7.7 Hz, 4H); **^{13}C NMR** (126 MHz, CDCl3) δ 196.7, 137.5, 132.4, 130.0, 128.2; **MS** (EI) m/z [M]$^+$ calcd for $C_{13}H_{10}O$: 182.1, found 182.1.

Benzaldehyde (2f):

The general procedure was followed by employing styrene (104.9 mg, 1.01 mmol) and bis(4-methoxyphenyl) disulfide (14.3 mg, 0.051 mmol, 5.0 mol%). The reaction was stopped after 16 hours. Purification by flash chromatography eluting with Pentane/Et$_2$O (40:1) afforded the title compound as a colorless oil (78.3 mg, 73.2%): **^{1}H NMR** (500 MHz, CDCl$_3$) δ 10.01 (s, 1H), 7.87 (d, J = 7.3 Hz, 2H), 7.62 (t, J = 7.4 Hz, 1H), 7.52 (t, J = 7.6 Hz, 2H); **^{13}C NMR** (126 MHz, CDCl$_3$) δ 192.4, 136.3, 134.4, 129.7, 128.9; MS (EI) m/z [M]$^+$ calcd for C_7H_6O: 106.12, found 106.0.

2-Chlorobenzaldehyde (2g):

The general procedure was followed by employing 2-chlorostyrene (68.9 mg, 0.50 mmol) and bis(4-methoxyphenyl) disulfide (7.0 mg, 0.025 mmol, 5.0 mol%) and MeCN (0.3 mL). The reaction was stopped after 16 hours. Purification by flash chromatography eluting with Pentane/Et$_2$O (30:1) afforded the title compound as a yellowish oil (52.5 mg, 75.1%): **^{1}H NMR** (500 MHz, CDCl$_3$) δ 10.50 (s, 1H), 7.93 (dd, J = 7.7, 1.5 Hz, 1H), 7.57 - 7.51 (m, 1H), 7.46 (d, J = 7.9 Hz, 1H), 7.40 (t, J = 7.5 Hz, 1H); **^{13}C NMR** (126 MHz, CDCl$_3$) δ 189.9, 138.0, 135.1, 132.4, 130.6, 129.4, 127.3; MS (EI) m/z [M]$^+$ calcd for C_7H_5ClO: 140.56, found 140.0.

3-Chlorobenzaldehyde (2h):

The general procedure was followed by employing 3-chlorostyrene (70.1 mg, 0.51 mmol) and bis(4-methoxyphenyl) disulfide (7.0 mg, 0.025 mmol, 4.9 mol%) and MeCN (0.3 mL). The reaction was stopped after 16 hours. Purification by flash chromatography eluting with Pentane/Et$_2$O (30:1) afforded the title compound as a yellowish oil (53.1 mg, 74.7%): **^{1}H NMR** (500 MHz, CDCl$_3$) δ 9.98 (s, 1H), 7.86 (t, J = 1.7 Hz, 1H), 7.77 (dt, J = 7.6, 1.1 Hz, 1H), 7.61 (ddd, J = 8.0, 2.1, 1.1 Hz, 1H), 7.49 (t, J = 7.8 Hz, 1H); **^{13}C NMR** (126 MHz, CDCl$_3$) δ 190.9, 137.8, 135.5, 134.4, 130.4, 129.3, 128.0; MS (EI) m/z [M]$^+$ calcd for C_7H_5ClO: 140.0, found 140.0.

4-Methoxybenzaldehyde (2i):

The general procedure was followed by employing 4-methoxystyrene (67.7 mg, 0.50 mmol) and bis(4-methoxyphenyl) disulfide (7.0 mg, 0.025 mmol, 5.0 mol%) and MeCN (0.3 mL). The reaction was stopped after 16 hours. Purification by flash chromatography eluting with Pentane/Et$_2$O (20:1) afforded the title compound as a yellowish oil (52.6 mg, 76.6%): **^{1}H NMR** (500 MHz, CDCl$_3$) δ 9.89 (s, 1H), 7.84 (dt, J = 8.8, 2.0 Hz, 2H), 7.01 (dt, J = 8.7, 1.8 Hz, 2H), 3.89 (s, 3H); **^{13}C NMR** (126 MHz, CDCl$_3$) δ 190.8, 164.6, 132.0, 130.0, 114.3, 55.6; MS (EI) m/z [M]$^+$ calcd for $C_8H_8O_2$: 136.1, found 136.0.

Benzaldehyde (2j):

The general procedure was followed by employing trans-propenylbenzene (69.1mg, 0.50 mmol) and bis(4-methoxyphenyl) disulfide (7.2 mg, 0.026 mmol, 5.2 mol%). The reaction was stopped after 16 hours. Purification by flash chromatography eluting with Pentane/Et$_2$O (50:1) afforded the title compound as a colorless oil (43.2 mg, 78.8%): **^{1}H NMR** (500 MHz, CDCl$_3$) δ 10.02 (s, 1H), 7.87 (d, J = 7.7 Hz, 2H), 7.63 (t, J = 7.4 Hz, 1H), 7.53

(t, J = 7.5 Hz, 2H); **^{13}C NMR** (126 MHz, CDCl$_3$) δ 192.4, 136.3, 134.4, 129.7, 128.9; **MS** (EI) m/z [M]$^+$ calcd for C$_7$H$_6$O: 106.0, found 106.0.

Benzaldehyde (2k):

The general procedure was followed by employing cis-propenylbenzene (60.5 mg, 0.51 mmol) and bis(4-methoxyphenyl) disulfide (7.0 mg, 0.025 mmol, 4.9 mol%) and methanol (0.4 mL). The reaction was stopped after 16 hours. Purification by flash chromatography eluting with Pentane/Et$_2$O (50:1) afforded the title compound as a colorless oil (23.7 mg, 43.6%): **^{1}H NMR** (500 MHz, CDCl$_3$) δ 10.03 (s, 1H), 7.89 (d, J = 7.8 Hz, 2H), 7.64 (t, J = 7.3 Hz, 1H), 7.54 (t, J = 7.5 Hz, 2H); **^{13}C NMR** (126 MHz, CDCl$_3$) δ 192.4, 136.4, 134.5, 129.7, 129.0; **MS** (EI) m/z [M]$^+$ calcd for C$_7$H$_6$O: 106.0, found 106.0.

4-methoxybenzaldehyde (2l):

The general procedure was followed by employing anethole (76.0 mg, 0.51 mmol) and bis(4-methoxyphenyl) disulfide (7.2 mg, 0.026 mmol, 5.1 mol%). The reaction was stopped after 16 hours. Purification by flash chromatography eluting with Pentane/Et$_2$O (20:1) afforded the title compound as a yellowish oil (53.4 mg, 76.4%): **^{1}H NMR** (500 MHz, CDCl$_3$) δ 9.88 (s, 1H), 7.84 (td, J = 8.8, 2.0 Hz, 2H), 7.00 (m, J = 8.8, 1.9 Hz, 2H 2H), 3.89 (s, 3H); **^{13}C NMR** (126 MHz, CDCl$_3$) δ 190.8, 164.6, 132.0, 129.9, 114.3, 55.6; **MS** (EI) m/z [M]$^+$ calcd for C$_8$H$_8$O$_2$: 136.1, found 136.0.

3,4-Dimethoxybenzaldehyde (2m):

The general procedure was followed by employing isoeugenol methyl ether (88.2 mg, 0.49 mmol) and bis(4-methoxyphenyl) disulfide (7.0 mg, 0.025 mmol, 5.1 mol%) and MeCN (0.3 mL). The reaction was stopped after 16 hours. Purification by flash chromatography eluting with Pentane/CH$_3$CO$_2$Et (1:1) afforded the title compound as a yellowish oil (49.6 mg, 60.3%): **^{1}H NMR** (500 MHz, CDCl$_3$) δ 9.85 (s, 1H), 7.47 (d, J = 1.9 Hz, 1H), 7.45 (d, J = 1.9 Hz, 1H), 7.41 (d, J = 1.8 Hz, 1H), 3.96 (s, 3H), 3.94 (s, 3H); **^{13}C NMR** (126 MHz, CDCl$_3$) δ 190.9, 154.4, 149.6, 130.1, 126.9, 110.3, 108.8, 56.2, 56.0; **MS** (EI) m/z [M]$^+$ calcd for C$_9$H$_{10}$O$_3$: 166.1, found 166.1.

Associated Content

The *Supporting Information* for this article is available free of charge on the Wiley Publications website at DOI: 10.1002/anie.201607948.

Reference:

(1) For reviews on oxidative cleavage of olefins, see: (a) Rajagopalan, A.; Lara, M.; Kroutil, W. *Adv. Synth. Catal.* **2013**, *355*, 3321−3335; (b) Wan, J.-P.; Gao, Y.; Wei, L. *Chem. Asian J.* **2016**, *11*, 2092–2102.

(2) Criegee, R. *Angew. Chem. Int. Ed.* **1975**, *87*, 745−752.

(3) Gonzalez-de-Castro, A.; Xiao, J.-L.; *J. Am. Chem. Soc.* **2015**, 137, 8206−8218.

(4) (a) Rubinstein, A.; Jiménez-Lozanao, P.; Carbó, J. J.; Poblet, J. M; Neumann, R. *J. Am. Chem. Soc.* **2014**, *136*, 10941−10948; (b) Hossain, M. M.; Shyu, S.-G. *Tetrahedron* **2014**, *70*, 251−255.

(5) Feng, K.; Zhang, R.-Y.; Wu, L.-Z.; Tu, B.; Peng, M.-L.; Zhang, L.-P.; Zhao, D.; Tung, C.-H. *J. Am. Chem. Soc.* **2006**, *128*, 14685–14690.

(6) Lin, R.; Chen, F.; Jiao, N. *Org. Lett.* **2012**, *14*, 4158−4161.

(7) Wang, G.-Z.; Li, X.-L.; Dai, J.-J.; Xu, H.-J. *J. Org. Chem.* **2014**, *79*, 7220−7225.

(8) Fujiya, A.; Kariya, A.; Nobuta, T.; Tada, N.; Miura, T.; Itoh, A. *Synlett* **2014**, *25*, 0884–0888.

(9) Baucherel, X.; Uziel, J.; Jugé, S. *J. Org. Chem.* **2001**, *66*, 4504−4510.

(10) Murthy, R. S.; Bio, M.; You, Y. *Tetrahedron Lett.* **2009**, *50*, 1041–1044.

(11) Suga, K.; Ohkubo, K.; Fukuzumi, S. *J. Phys. Chem. A* **2003**, *107*, 4339–4346

(12) Singh, A. K.; Chawla, R.; Yadav, L. D. S. *Tetrahedron Lett.* **2015**, *56*, 653−656.

(13) For UV-triggered disulfide homolysis and thiyl addition to olefin, see: (a) Matsuda, O. Ito, M. *J. Am. Chem. Soc*. **1979**, *101*, 1815–1819; (b) Matsuda, O. Ito, M. *J. Am. Chem. Soc*. **1979**, *101*, 5732–5735; (c) Matsuda, O. Ito, M. *J. Am. Chem. Soc*. **1981**, *103*, 5871–5874; (d) Matsuda, O. Ito, M. *J. Am. Chem. Soc*. **1982**, *104*, 1701–1703.

(14) For review on catalysis of radical reactions, see: Studer, A.; Curran, D. P. *Angew. Chem. Int. Ed.* **2016**, *55*, 58–102.

(15) (a) Yoshimura, A.; Takamachi, Y.; Han, L.-B.; Ogawa, A. *Chem. Eur. J.* **2015**, *21*, 13930–13933; (b) Pan, X.; Lalevée, J.; Lacôte, E.; Curran, D. P. *Adv. Synth. Catal.* **2013**, *355*, 3522–3526; (c) Hashimoto, T.; Takino, K.; Hato, K.; Maruoka, K. *Angew. Chem. Int. Ed.* **2016**, *55*, 8081–8085.

(16) For a review on thiyl radical chemistry, see: Dénès, F.; Pichowicz, M.; Povie, G.; Renaud, P. *Chem. Rev.* **2014**, *114*, 2587−2693.

(17) Kharasch, M. S.; Nudenberg, W.; Mantell, G. J. *J. Org. Chem.* **1951**, *16*, 524–532.

(18) Fava, A.; Reichenbach, G.; Peron, U. *J. Am. Chem. Soc.* **1967**, *89*, 6696–6700.

(19) Iriuchijima, S.; Maniwa, K.; Sakakibara, T.; Tsuchihashi, G.-I. *J. Org. Chem.* **1972**, *39*, 1170–1171.

(20) Szmant, H. H.; Mata, A. J.; Namis, A. J.; Panthananickal, A. M. *Tetrahedron* **1976**, *32*, 2665–2680.

(21) (a) D'Souza, V. T.; Nanjundiah, R.; Baeza H., J.; Szmant, H. H. *J. Org. Chem.* **1987**, *52*, 1720–1725; (b) D'Souza, V. T.; Iyer, V. K.; Szmant, H. H. *J. Org. Chem.* **1987**, *52*, 1725–1728; (c) D'Souza, V. T.; Nanjundiah, R.; Baeza H., J.; Szmant, H. H. *J. Org. Chem.* **1987**, *52*, 1729–1740; (d) Chung, M.-I.; D'Souza, V. T.; Szmant, H. H. *J. Org. Chem.* **1987**, *52*, 1741–1744.

(22) Mulliken, R. S. *J. Phys. Chem.* **1952**, *56*, 801–822.

(23) Foster, R. *J. Phys. Chem.* **1980**, *84*, 2135–2141.

(24) Rosokha, S. V.; Kochi, J. K. *Acc. Chem. Res.* **2008**, *41*, 641–653.

(25) (a) Arceo, E.; Jurberg, I. D.; Álvarez-Fernández, A.; Melchiorre, P. *Nat. Chem.* **2013**, *5*, 750–756; (b) Arceo, E.; Montroni, E.; Melchiorre, P. *Angew. Chem. Int. Ed.* **2014**, *53*, 12064–12068; (c) Nappi, M.; Bergonzini, G.; Melchiorre, P. *Angew. Chem. Int. Ed.* **2014**, *53*, 4921–4925.

(26) (a) Liu, W.; Groves, J. T. *Acc. Chem. Res.* **2015**, *48*, 1727−1735; (b) Barrett, A. G. M.; Rys, D. J. *J. Chem. Soc. Chem. Comm.* **1994**, 837−838.

(27) Adam, W.; Bosio, S. G.; Turro, N. J.; Wolff, B. T. *J. Org. Chem.* **2004**, *69*, 1704–1715.

(28) A previous report by Jugé demonstrated a sole example that bis(4-chlorophenyl)disulfide (10–50 mol%), in the presence of a Mn-catalyst and UV-light from a medium-pressure Hg lamp (250 W), was able to initiate the oxidative cleavage of *trans*-methylstilbene (Reference 9). We argue that although the major pathway of Jugé's reaction was initiated with the UV-triggered S–S bond dissociation catalyzed by the Mn-complex, a small portion of the reaction might also follow the visible-light mechanism described in this paper.

(29) Otsuka, H.; Nagano, S.; Kobashi, Y.; Maeda, T.; Takahara, A. *Chem. Commun.* **2010**, *46*, 1150–1152.

(30) Belenguer, A. M.; Friščić, T.; Day, G. M.; Sanders, J. K. M. *Chem. Sci.* **2011**, *2*, 696–700.

(31) Rekondo, A.; Martin, R.; de Luzuriaga, A. R.; Cabañero, G.; Grande, H. J.; Odriozola, I. *Mater. Horiz.* **2014**, *1*, 237–240.

(32) Heiba, E.-A. I.; Dessau, R. M. *J. Org. Chem.* **1967**, *32*, 3837–3840.

(33) No obvious visible absorption of the olefin-disulfide mixture could be observed with an ordinary UV-Vis spectrometer, presumably because the interaction between disulfide and olefin is transient and not significant enough to be in the detectable range.

(34) Barham, J. P.; Coulthard, G.; Emery, K. J.; Doni, E.; Cumine, F.; Nocera, G.; John, M. P.; Berlouis, L. E. A.; McGuire, T.; Tuttle, T.; Murphy, J. A. *J. Am. Chem. Soc.* **2016**, *138*, 7402–7410.

(35) Matxain, J. M.; Asua, J. M.; Ruipérez, F. *Phys. Chem. Chem. Phys*. **2016**, *18*, 1758–1770.

Chapter 5

Visible-Light-Promoted Iron-Catalyzed Csp^2-Csp^3 Kumada Cross-Coupling in Flow

Abstract

A continuous-flow, visible light-promoted method has been developed to overcome the limitations of Fe-catalyzed Kumada-Corriu cross-couplings. A variety of strongly electron-rich aryl chlorides, previously hardly reactive, could be efficiently coupled with aliphatic Grignard reagents at room temperature, in high yields and within a few minutes residence time, considerably enhancing the applicability of this Fe-catalyzed reaction. The robustness of this protocol was demonstrated on the multi-gram scale, providing the potential for future pharmaceutical application.

Introduction

Over the past three decades, transition metal-catalyzed cross-coupling reactions have emerged as one of the most important classes of C-C bond-forming reactions.[1] One of the oldest and most important transformations is the coupling of aryl halides with Grignard reagents. This chemistry has been extensively studied using Pd[2] and Ni[3] catalysis since its first discovery by Kumada and Corriu in 1972.[4]
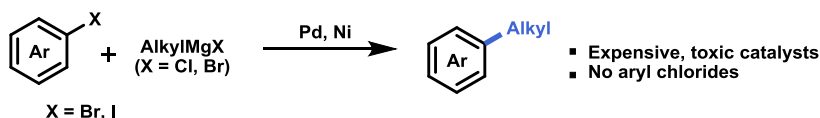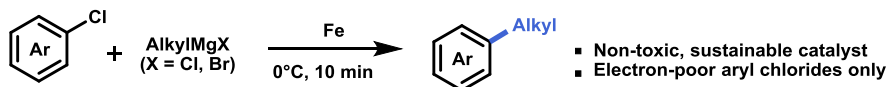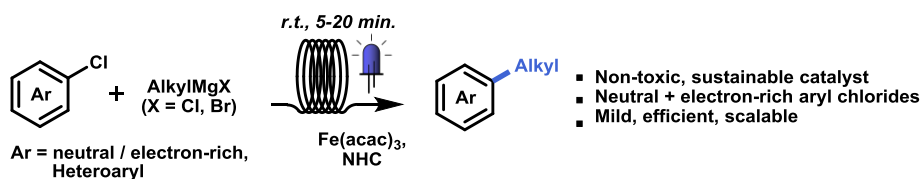
Scheme 5. 1. Csp^2-Csp^3 bond formation *via* Kumada-Corriu cross-couplings

Despite the efficiency of these reactions, these metals are toxic and expensive, and more and more research has been devoted to the development of efficient catalytic methods using cheap, earth-abundant and non-toxic alternative catalysts.[5] In this regard, iron catalysis has been extensively investigated.[6,7] In 2002, based on pioneering studies by, among others, Kharasch,[8] Kochi,[9] and Cahiez,[10] Fürstner developed the first efficient Fe-catalyzed Kumada-Corriu coupling between aryl chlorides and alkyl Grignard reagents.[11] Key to this advancement was the use of *N*-methyl-2-pyrrolidone (NMP) as a co-solvent in the reaction. This method provided a very attractive alternative to the Pd/Ni-catalyzed reaction, as aryl chlorides could be more efficiently employed as starting materials instead of aryl bromides and iodides (**Scheme 5.1**).[12] Nonetheless, this protocol and subsequent ones,[13] are limited to electron-deficient aryl chlorides, triflates, and tosylates, and to primary aliphatic Grignard reagents. Electron-neutral (*e.g.* chlorobenzene) and electron-rich aryl chlorides could only later be successfully employed in the reaction when *N*-heterocyclic carbene

(NHC) ligands were used, but still required high temperatures and/or long reaction times.[14] Despite further notable advancements in the field of Fe-catalyzed cross- couplings,[15] to date the coupling of electron-rich aryl chlorides with aliphatic Grignard reagents remains challenging and the number of reports is still considerably limited.

Very recently, Alcázar and co-workers developed visible light-promoted Pd/Ni-catalyzed Negishi cross-couplings, demonstrating the advantage of irradiation on this type of cross-coupling reaction.[16] Inspired by these results, and following our continuous interest in metal-catalyzed couplings in flow,[17] herein we report a light-promoted Fe-catalyzed Kumada-Corriu coupling for Csp^2-Csp^3 bond-formation in continuous-flow.[18] Considering the present limitations on the scope of aryl chlorides reaction partners typical for this reaction, this method allows the broadening of the substrate scope under very mild and scalable conditions.

Result and Discussion

At the beginning of our study, we treated model substrates chlorobenzene (**1a**) and *n*-propylmagnesium bromide (**2a**) with 1 mol% FeCl$_2$·4H$_2$O and 2 mol% 3-bis(2,6-diisopropyl-phenyl)imidazolinium chloride (SIPr·HCl) as ligand under irradiation of blue LED (450 nm) at 20 °C. To our delight, *n*-propylbenzene **3aa** was obtained in 76% yield using a residence time of 20 minutes, while the reaction without light only furnished 5% of **3aa** (**Table 5.1**, entries 1-2). This shows that visible light indeed significantly accelerates the Kumada cross-coupling. At 25 °C the reaction proceeded more efficiently, giving 84% yield (entry 3). Different iron halides such as FeF$_3$ or FeCl$_3$ gave moderate to good yield, while the use of Fe(acac)$_3$ (acac = acetylacetonate) resulted in an excellent 89% yield of **3aa** (entries 4-6). Increasing the catalyst loading (2%) and concentration resulted in 98% yield within only 15 minutes residence time (entry 7). Control experiments in the absence of Fe or NHC gave no product, while the reaction in the dark under these conditions only produced 11% of **3aa** (entries 8-10). Interestingly, when cyclohexylmagnesium chloride (CyMgCl) **2b** was employed in the reaction, full conversion was achieved within only 5 minutes residence time (entry 11). This reagent was thus selected for further studies.

Table 5.1. Optimization of reaction conditions.[a]
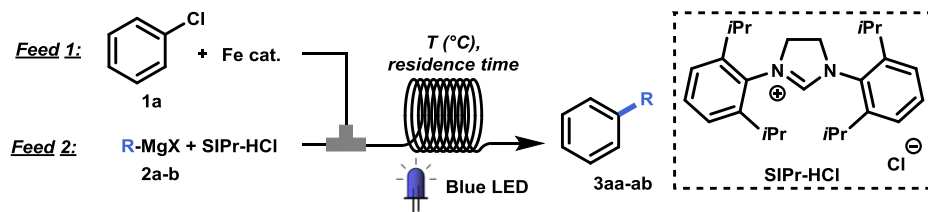
Entry	Cat.	R	RT (min)	Yield (%)
1[b,c]	FeCl₂.4H₂O	*n*-Propyl (**2a**)	20	76 (**3aa**)
2[b,c,d]	FeCl₂.4H₂O	*n*-Propyl (**2a**)	20	5 (**3aa**)
3[b]	FeCl₂.4H₂O	*n*-Propyl (**2a**)	20	84 (**3aa**)
4[b]	FeF₃	*n*-Propyl (**2a**)	20	45 (**3aa**)
5[b]	FeCl₃	*n*-Propyl (**2a**)	20	73 (**3aa**)
6[b]	Fe(acac)₃	*n*-Propyl (**2a**)	20	89 (**3aa**)
7	Fe(acac)₃	*n*-Propyl (**2a**)	15	98 (**3aa**)
8	/	*n*-Propyl (**2a**)	15	0 (**3aa**)
9[e]	Fe(acac)₃	*n*-Propyl (**2a**)	15	0 (**3aa**)
10[d]	Fe(acac)₃	*n*-Propyl (**2a**)	15	11 (**3aa**)
11	Fe(acac)₃	Cyclohexyl (**2b**)	5	96 (**3ab**)

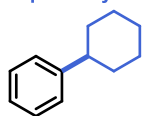[a]Reaction conditions: Feed 1: Chlorobenzene **1a** (2 mmol), Fe(acac)₃ (0.04 mmol), tetrahydrofuran (THF, 5 mL). Feed 2: Grignard reagent (3 mmol), SIPr·HCl (0.08 mmol), THF, 25 °C, 24 W blue LED. RT = residence time. GC yields are reported. [b] Fe(acac)₃ (0.02 mmol), SIPr·HCl (0.04 mmol), [c]T = 20 ºC. [d] No light; [e] No ligand.

With the optimal conditions in hand, the scope of this trans-formation was investigated (**Scheme 5.2**). Unfunctionalized aryl chlorides in the coupling with Grignard **2b** already show large differences in yields between irradiation and non-irradiation conditions (**3ab-3cb**, 83-91% *vs* 27-51%). Substrates containing a fluorine or methyl moiety also reacted smoothly, giving 88-99% yield under irradiation (**3db-3eb**). Furthermore, functionalization with one or two strongly electron-donating methoxy groups, including at very challenging *ortho* positions, also resulted in high isolated yields of compounds **3fb-3jb** (61-93%). It has to be noted that for compounds **3ib** and **3jb**, 5% Fe(acac)₃ and 10% NHC were required to reach full conversion within 20 minutes residence time. The strong electron-donating groups –NMe₂ and –NHMe were also tolerated in the reaction and furnished **3kb** and **3lb** in high yields (82-96%). The presence of a free NH moiety in **3lb** is particularly noteworthy, as it avoids the introduction of protecting groups. Unprotected NH functionalities in medicinally relevant[7c] indoles and pyrrolopyridines were also successfully tolerated (**3mb-3nb**, 91%). Other functionalized heterocyclic chlorides, such as 2-methylquinoline, 2-methoxypyridine, 2-methyltiopyrimidine, and benzofuran chlorides were reacted with **2b** in modest to good yields (**3ob-3rb**, 45-84%).

Scope of aryl chlorides

3ab
hν: 99% (91%)
no hν: 39%

3bb
hν: 83% (83%)
no hν: 51%

3cb
hν: 91% (90%)
no hν: 27%

3db
hν: 91% (88%)[a]
no hν: 34%

3eb
hν: 100% (99%)
no hν: 35%

3fb
hν: 93% (89%)
no hν: 2%

3gb
hν: 98% (85%)
no hν: 34%

3hb
hν: 99% (93%)
no hν: 21%

3ib
hν: 72% (72%)[b,f]
no hν: 61%

3jb
hν: 85% (61%)[b,f]
no hν: 58%

3kb
hν: 100% (96%)
no hν: 2%

3lb
hν: 90% (82%)[c,f]
no hν: 2%

3mb
hν: 98% (91%)[c,d]
no hν: 0%

3nb
hν: 100% (91%)[c,d]
no hν: 23%

3ob
hν: 74% (68%)
no hν: 45%

3pb
hν: 45% (45%)[d]
no hν: 13%

3qb
hν: 100% (84%)[e]
no hν: 100%

3rb
hν: 78% (75%)[b,d]
no hν: 68%

Scope of Grignard reagents

3ha
hν: 96% (95%)[f,g]
no hν: (41%)

3ra
hν: 62% (55%)
no hν: (28%)

3hc
hν: 76% (73%)[h]
no hν: 0%

3nc
hν: 80% (75%)[c,h]
no hν: 0%

3hd
hν: 75% (70%)
no hν: 4%

3nd
hν: 74% (70%)[i,k]
no hν: 10%

3od
hν: 86% (78%)[c,j]
no hν: 0%

3sd
hν: 100% (95%)[j]
no hν: 69%

3he
hν: 100% (85%)[j]
no hν: 9%
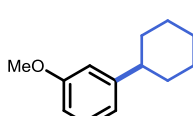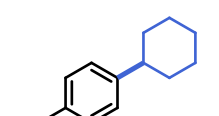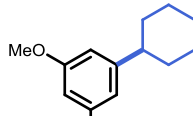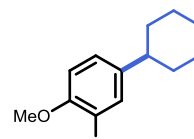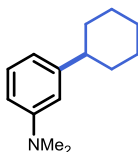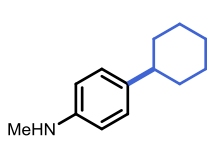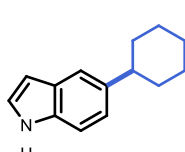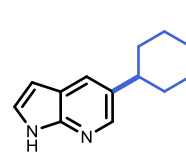
Scheme 5.2. Substrate scope. Reaction conditions: Feed 1: 1 (2 mmol, 1.0 equiv.), Fe(acac)₃ (0.04 mmol), THF 5 mL. Feed 2: 2b (1.5 equiv.), SIPr·HCl (0.08 mmol), 25 °C, RT: 5 minutes, 24 W blue LED. GC/LC yield. Isolated yield reported in brackets. [a] RT = 2 min; [b] Fe(acac)₃ (5 mol%), SIPr·HCl (10 mol%); [c] Grignard reagent (2.5 equiv.); [d] RT = 15 min; [e] RT = 1 min; [f] RT = 20 min. Scope of Grignard reagents, reaction conditions: Feed 1: 1 (2 mmol, 1.0 equiv.), Fe(acac)₃ (5 mol%). Feed 2: 3 (1.5 equiv.), SIPr·HCl (15 mol%), 25 °C, RT: 20 minutes, [g]Fe(acac)₃ (2 mol%), SIPr·HCl (4 mol%), [h] Fe(acac)₃ (10 mol%), SIPr·HCl (30 mol%) in batch with 34 W blue LED irradiation at 45 °C for 4 hours; [i]40 °C. [j] 0.3 equiv. of *i*PrMgBr was added as additive in Feed 2 in advance. [k] 2d (2.0 equiv.).

Next, we studied the reactivity of different Grignard reagents. A few generally less reactive alkyl Grignard reagents, such as *n*-propylmagnesium and (trimethylsily)methylmagnesium chlorides,[19] were successfully employed in the coupling with electron-rich or heterocyclic aryl chlorides, affording good isolated yields of the coupling products **3ha-3nc** (55-95%). Encouraged by these results, some new Grignard reagents decorated with medicinally important moieties, such as tetrahydropyrane and *N*-methylpiperidine[20] were prepared[21] and tested in the reaction. Compounds **3hd-3he**, featuring electron-rich or heteroaromatic moieties, were obtained under mild reaction conditions in 70-95% yield.[22] As expected, most of these compounds were only obtained in trace amounts in the absence of light. Finally, the scalability of this protocol was demonstrated on a multi-gram scale synthesis of unprotected indole **3mb** (**Scheme 5.3**). With only 5 minutes residence time, after running continuously for 2.5 hours, 11.36 gram of **3mb** were isolated (95%), with the space-time yield reaching 454 mg/h·mL.
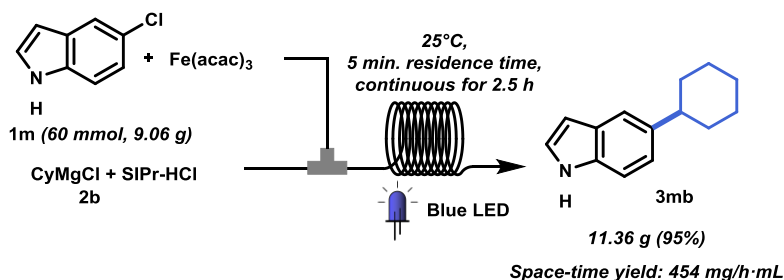
Scheme 5.3. Reaction scale-up. Feed 1: **1m** (9.06 g, 60 mmol), Fe(acac)$_3$ (423.6 mg, 2 mol%), THF (150 mL); Feed 2: **2b** (150 mL, 1.0 M in THF, 2.5 equiv.), SIPr·HCl, (1.02 g, 4 mol%); 25 ºC, residence time = 5 minutes..

Mechanistic study

Despite the recent interest in Fe-catalyzed cross-couplings, the elucidation of their mechanism is not straightforward.[23] The current mechanistic understanding of Fe-catalyzed Kumada coupling using β-hydrogen-containing Grignard reagents[24] supports an initial reduction of Fe(III) to a lower oxidation states species [Fe^{red}] by the Grignard, leading to FeX$_n$ or Fe(MgX)$_n$ intermediates. Different oxidation states for [Fe^{red}] have been suggested, ranging from Fe(-II) to Fe(+I).[15d,24-25] This initial necessary step is followed by a rate-determining oxidative addition of the aryl chloride, and a transmetalation with further Grignard reagent, or *vice versa*. The final reductive elimination is suggested to be fast and restore the [Fe^{red}] species.[11b,25]

We performed some experiments to understand the effect of irradiation in this reaction. Kinetic profiles for the coupling of chlorobenzene **1a** and *p*-chloroanisole **1h** with CyMgCl **2b** with and without irradiation showed a clear beneficial effect of light on the rate of the reaction. In particular, the effect of irradiation is much more pronounced for the coupling of electron-rich **1h** than for chlorobenzene **1a** (**Figure 5.1** a-b).This might suggest an effect of light in facilitating the oxidative addition, although other effects cannot as yet be excluded. A strong effect of light was also observed for the coupling with chloroindole **1m**, which results in almost no reaction in the absence of light. Light on/off experiments on this reaction show that light is needed during the whole process (**Figure 5.1**c), so its role in the mere generation of an active catalytic species (off-cycle) can be excluded.
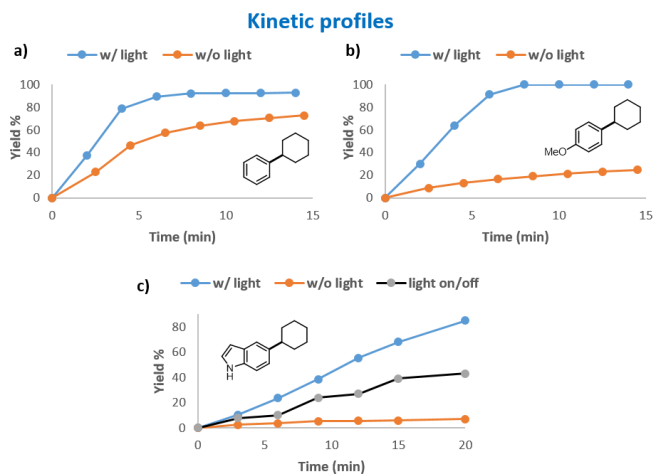
Figure 5.1. a) Batch reaction profiles for the coupling of CyMgCl **2b** with chlorobenzene **1a** and b) *p*-chloroanisole **1h** with or without blue light irradiation; c) reaction profiles for the coupling with chloroindole **1m** with or without light, and in light on/off experiment
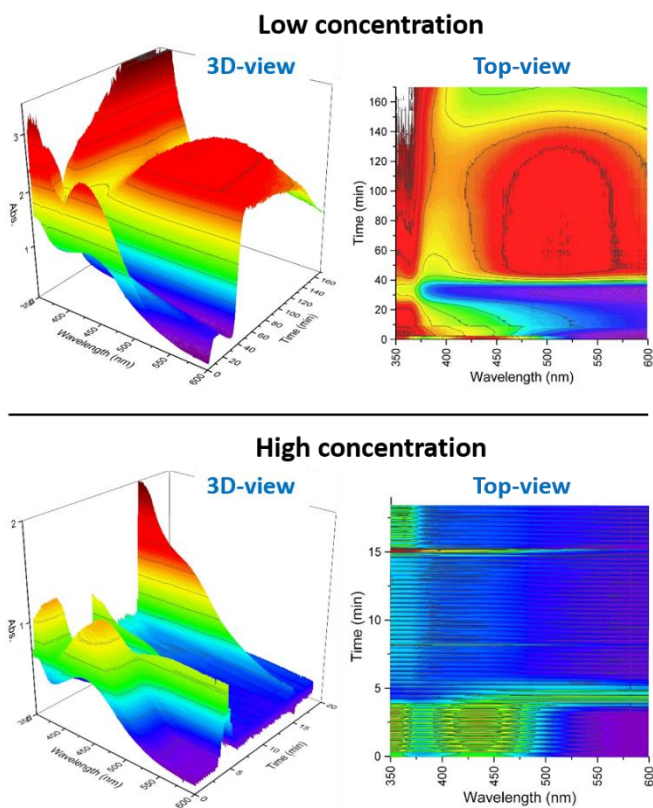
Figure 5.2: In-line UV-Vis analysis of the reaction between CyMgCl **2b** and chloroindole **1m**; Top: 0.01 M in THF, Bottom: 0.1 M.

In-line UV-Vis analysis of the reaction between CyMgCl **2b** and chloroindole **1m** (under irradiation) was performed at low concentration (0.01 M) to study the first step of the reaction (**Figure 5.2**, top). Upon addition of **2b** and **1m** to a solution of Fe/NHC in THF, the characteristic absorption band of Fe(acac)$_3$ (ca. 450 nm) immediately disappeared, and a broad, stable band in the visible range (450-600 nm) appears after ca. 30 min. This band remained almost unchanged for the following 100 min. Similar results were obtained without irradiation.

The same experiment under more concentrated conditions (0.1 M, **Figure 5.2**, bottom) also showed the disappearance of Fe(acac)$_3$ and the formation of the large band at 450-600 nm upon addition of Grignard and chloroindole. Under such conditions, this band appeared and disappeared quickly, and a new weak band at ≈ 450 nm briefly appeared after a short time. After turning the light on, the same band appeared with a much higher intensity. Full conversion was observed within several minutes from this event.

Density functional theory (DFT) calculations suggest the broad band at 450-600 nm might be related to a Fe(I) species, while the one at 450 to a Fe(III) species. Therefore, we propose a catalytic cycle where an Fe(I) intermediate is formed upon reduction of the precatalyst by the Grignard reagents at the beginning of the reaction, followed by a slow oxidative addition to give a Fe(III) species (**Scheme 5.4**). The higher intensity of the sudden peak at 450 nm upon irradiation suggest an effect of light in promoting an aerobic oxidation process (or analogous) yielding the Fe(III) species. This would be in agreement with the kinetic measurements shown in **Figure 5.1**. As almost no difference was observed in the dark and light experiments at low concentration, it seems the initial formation of the reduced Fe(I) species (off-cycle process) is not particularly influenced by light, which is instead essential during the real catalytic process (**Figure 5.1c**).
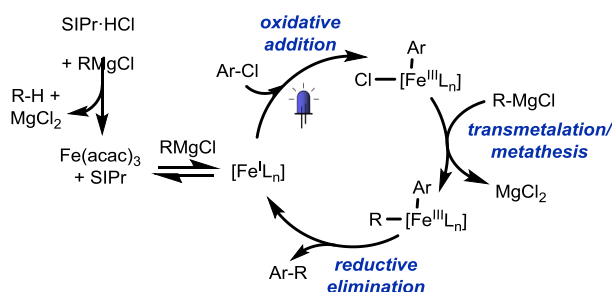
Scheme 5.4: Proposed mechanism.

Conclusion

We have reported a scalable, visible light-accelerated coupling of unactivated and electron-rich aryl chlorides with alkylmagnesium compounds in continuous-flow conditions. The use of blue light was demonstrated to considerably accelerate the coupling reaction, and allowed the use of mild conditions and very short reaction times even for previously very stubborn substrates, and makes a competitive alternative to the commonly used Pd or Ni catalysts for this transformation. Preliminary mechanistic studies suggested an Fe(I)/Fe(III) catalytic cycle.[26] Further mechanistic studies are being undertaken in our laboratory.

Experiment section

Kinetic measurements, general procedure

Measurements of reaction profiles were performed in batch in 7 ml vials under irradiation of blue LED light (4.5 W), using the setup shown in **Figure 5.3**. Reactions with or without light were performed at the same time to ensure reproducibility. One of the vial was exposed to light during the reaction, while the second was covered with aluminum foil for the whole time.
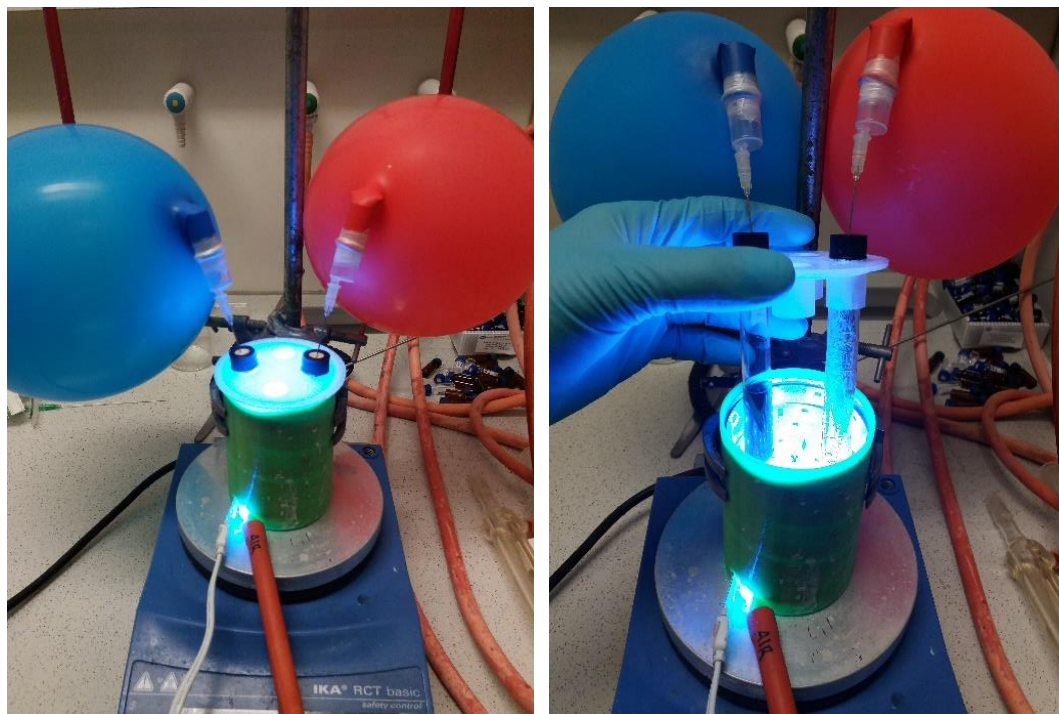
Figure 5.3: Batch setup used for kinetic measurements

SIPr·HCl (17 mg, 0.04 mmol) was charged into each of the two vials, the vials were flushed with Ar, and closed with a screw-cap with an Ar balloon attached. A stock solution of Fe(acac)$_3$ (14 mg, 0.04 mmol), aryl chloride (2.0 mmol), and decane (internal standard, 80 µL, 0.4 mmol) in 6 mL dry THF was prepared, and half of this was added, under Ar, into each of the vials. Cyclohexylmagnesium chloride (1.5 mL of a 1.0 M solution in 2-MeTHF, 1.5 mmol) was then added into each vial, and the vials were placed into the reactor and stirred (1000 rpm) at room temperature. Samples of 0.2 mL were then taken at different times from each vial and transferred into a 1.5 mL GC vial, the excess Grignard reagent was quenched with acetone, and the solid formed was filtered over celite before injecting the samples into GC-FID.

Light on/off reaction
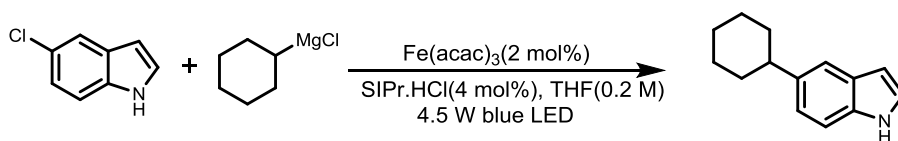
Scheme 5.5: Light on/off experiments with 5-Clindole and CyMgCl in batch

SIPr·HCl (17 mg, 0.04 mmol) was charged into three vials, the vials were flushed with Ar, and closed with a screw-cap with an Ar balloon. Cyclohexyl magnesium chloride (2.5 mL of a 1.0 M solution in 2-MeTHF, 2.5 mmol) was then added into each vial, and the vials were placed into the reactor and stirred at room temperature for 10 minutes. A stock solution of Fe(acac)₃ (21.2 mg, 0.06 mmol), 5-chloroindole (3.0 mmol), and decane (internal standard, 256 mg) in 7.5 mL THF was prepared. 2.5 mL of the stock solution was added under Ar into each of the three vials. Samples of 0.1 mL were taken at different times from each vial and transferred into a 1.5 mL GC vial, the excess Grignard reagent was quenched with acetone, and the solid formed was filtered over celite before injecting the samples into GC-FID. The result was shown in **Figure 5.1** c).

Radical clock experiments

The reaction between *o*-butenylchlorobenzene and cyclohexylmagnesium chloride mainly resulted in the formation of the expected coupling product, but a broad array of side products was observed, including some possibly deriving from a radical pathways. GC-MS data for the identified compounds are shown below.
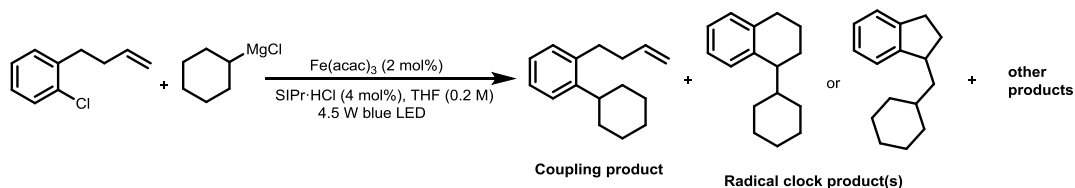
Scheme 5.6: Intramolecular radical clock experiment

Apart from dehalogenation of the aryl chloride, isomerization (loss of -CH₃ fragments in some of the peaks, only possible from isomerized alkenyl chains) and hydrogenation of the alkenyl chain (both in the aryl chloride and the dehalogenated derivative) was observed. Reductive dehalogenation and hydrogenation might come from a Fe hydride intermediate formed upon β-hydrogen elimination of the Fe-alkyl species. The formation of bi(cyclohexane) from homocoupling of the Grignard reagent was also observed here, as in other examples in the scope.

Besides the formation of the expected coupling product (RT 10.81min), other products are observed with the same m/z values (RT 10.93, 11.20), but considerably different fragmentation patterns. The expected coupling product is recognizable by the loss of a –CH₂CH=CH₂ fragment (m/z 173, M-41, similar fragmentation in the starting aryl chloride), and a cyclohexyl (m/z 131). These peaks are not observed in the other products, which instead show the peak at m/z 117 (M-43, -CH₂CH₂CH₃). This suggests that the butenyl chain in no longer present in the product and the fragmentation might be due to the (fused) alkylic residue (radical clock products). As these

are minor compounds, we do not believe a free radical mechanism to be predominant under the reaction conditions.
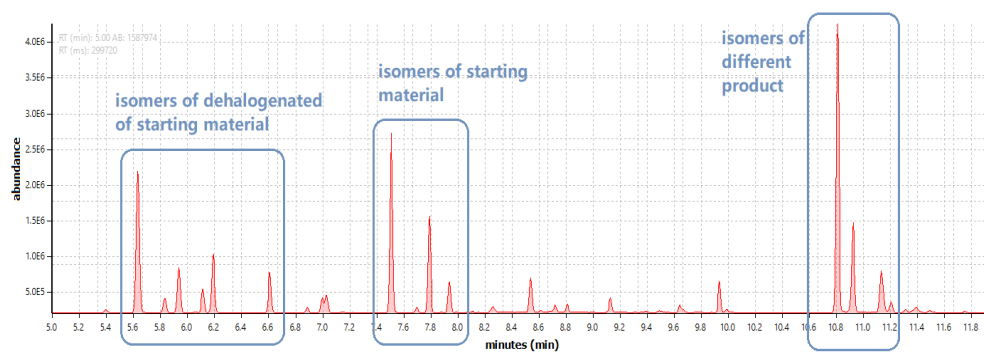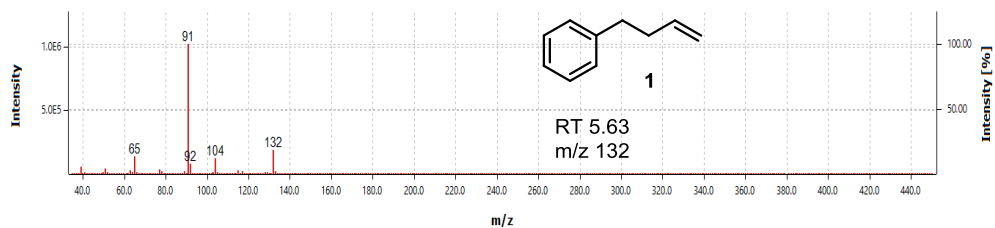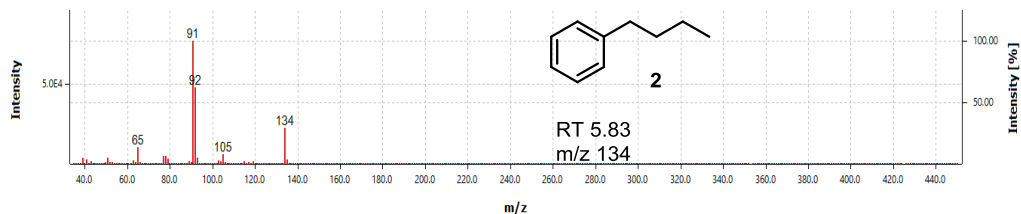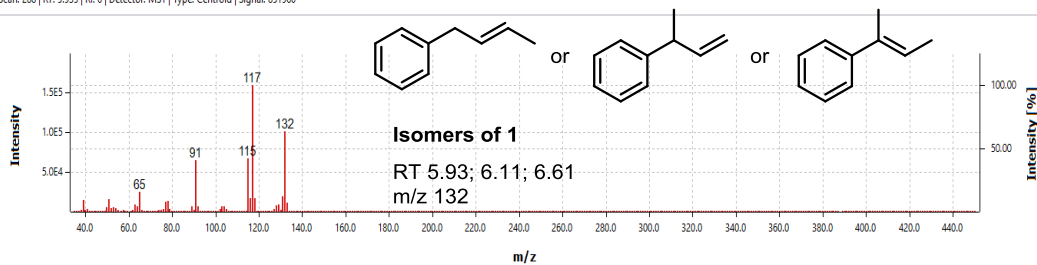
Scan: 324 | RT: 6.115 | RI: 0 | Detector: MS1 | Type: Centroid | Signal: 546881

Isomers of 1

RT 5.93; 6.11; 6.61
m/z 132
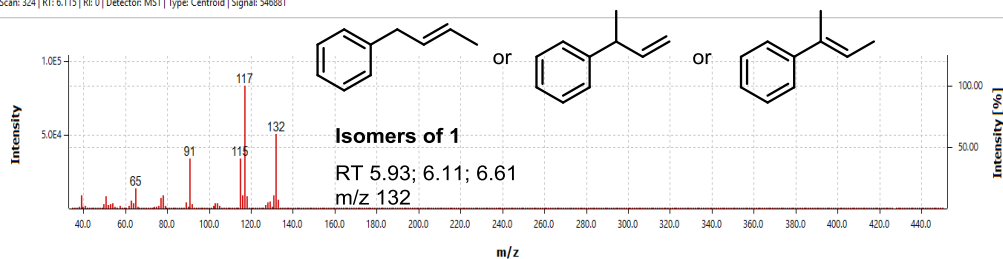
Scan: 423 | RT: 6.61 | RI: 0 | Detector: MS1 | Type: Centroid | Signal: 785193

Isomers of 1

RT 5.93; 6.11; 6.61
m/z 132
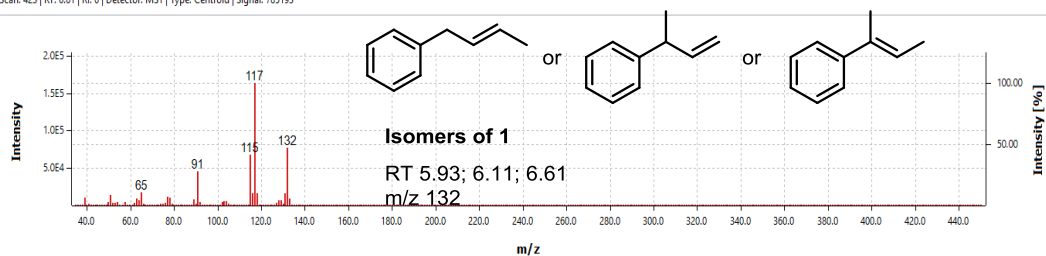
Scan: 602 | RT: 7.505 | RI: 0 | Detector: MS1 | Type: Centroid | Signal: 2767464

3

RT 7.50
m/z 166
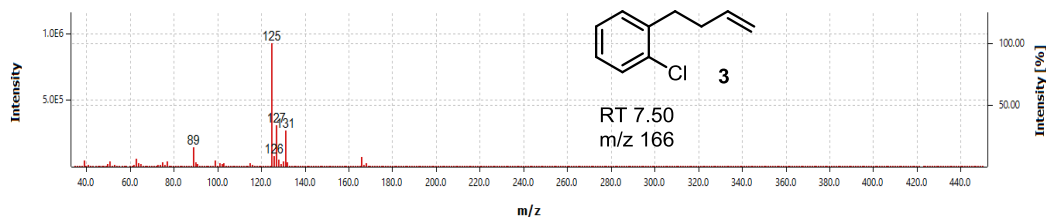
Scan: 640 | RT: 7.695 | RI: 0 | Detector: MS1 | Type: Centroid | Signal: 289008

4

RT 7.70
m/z 168
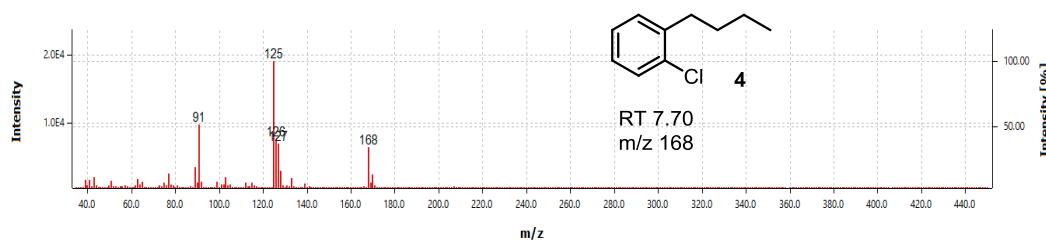
Scan: 659 | RT: 7.79 | RI: 0 | Detector: MS1 | Type: Centroid | Signal: 1577139
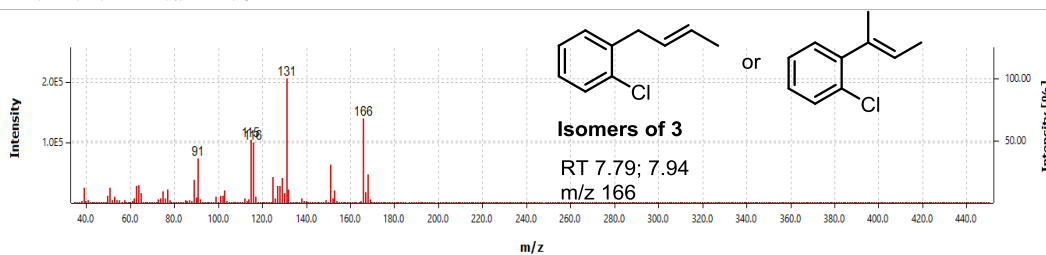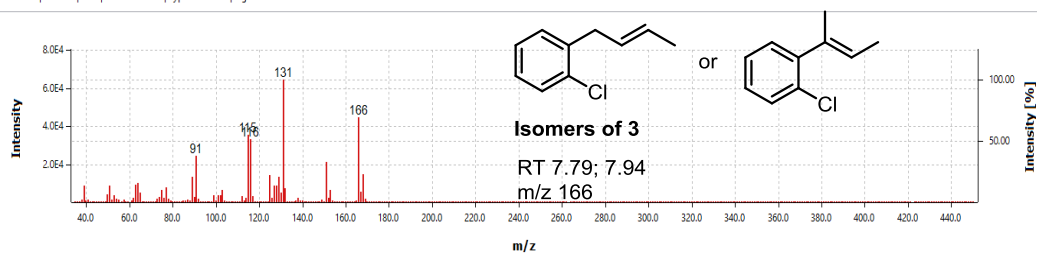
Isomers of 3

RT 7.79; 7.94
m/z 166

127
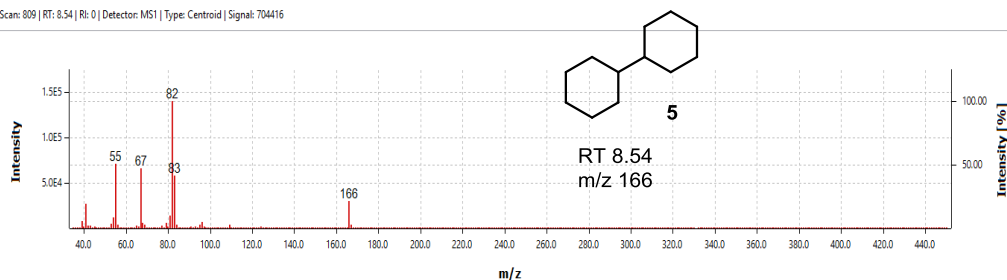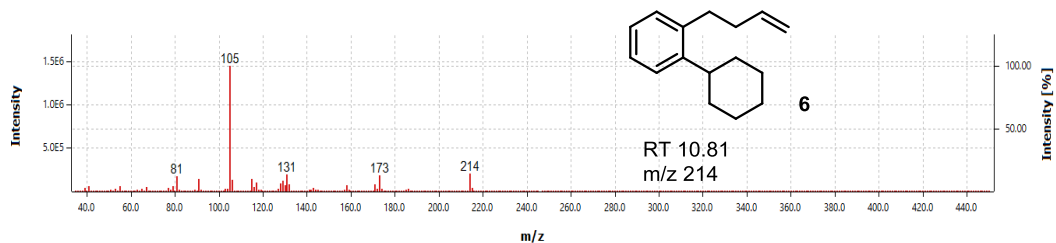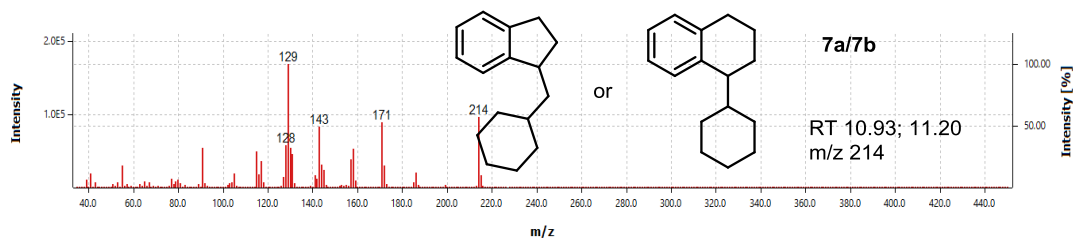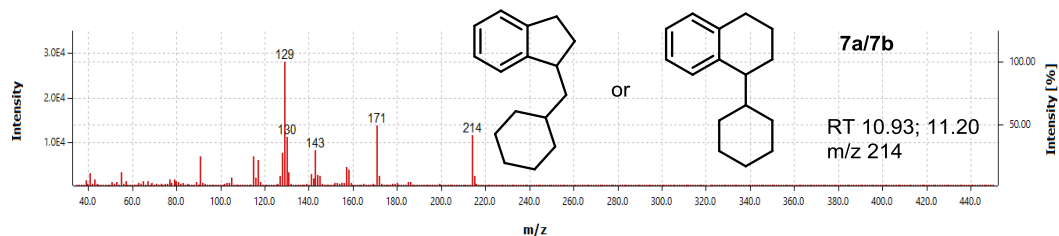
Figure 5.4: Fragments of the peaks on GC-MS spectra

In-line UV-Vis measurements

UV-Vis spectra for the reaction components are shown in **Figure 5.5**:
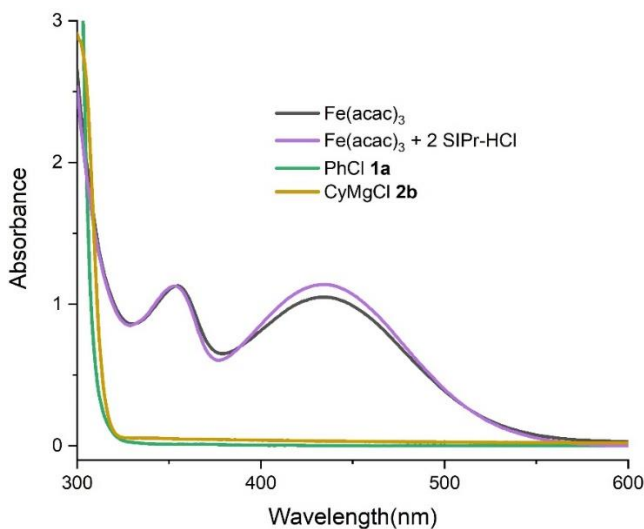
Figure 5.5: UV-Vis spectra for the reaction components in THF

General procedure of in-line UV-Vis analysis to test the importance of ligand: A solution of Fe(acac)₃ (5 mg, 0.014 mmol) [and SIPr-HCl (12 mg, 0.028 mmol)] in dry THF (20 mL) was charged into a round-bottom flask and stirred under Ar. The solution was continuously analyzed by in-line UV-Vis spectrophotometry (300-600 nm range) using the apparatus shown in **Figure 5.6**, collecting one measurement per second. After approximately 2 minutes, slow additions of chlorobenzene (PhCl, **1a**) (250 µL of a 1.0 M solution in THF, 0.25 mmol) and/or cyclohexylmagnesium chloride (CyMgCl, **2b**) (250 µL of a 1.0 M solution in 2-MeTHF, 0.25 mmol) were performed via a syringe pump (20 µL/min for **2b** and 28 µL/min for **1a**). These experiments were performed in the absence of blue light irradiation.
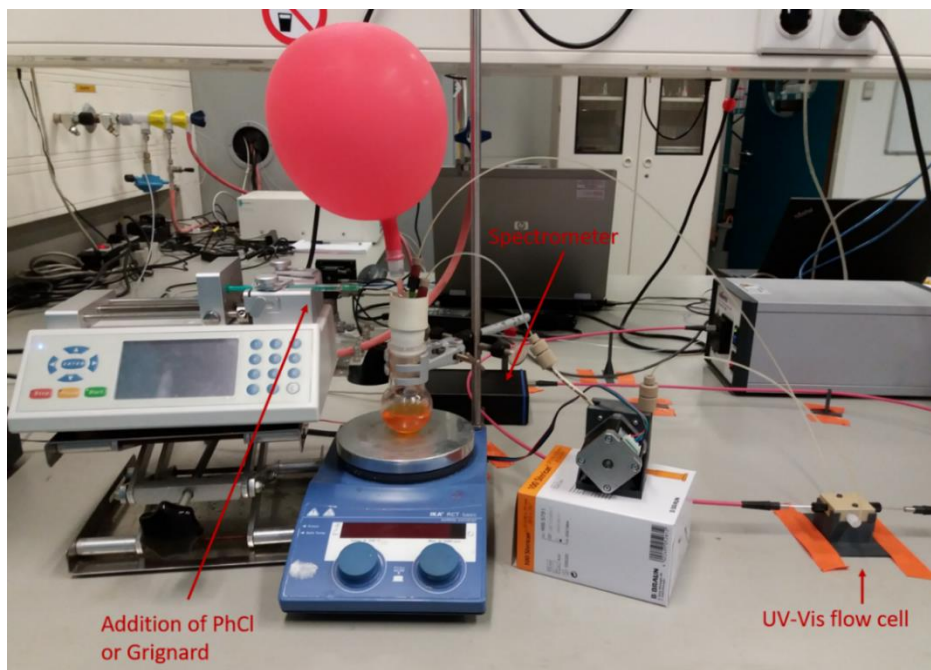
Figure 5.6: In-line UV-Vis setup

Results: THF solutions of either Fe(acac)$_3$ or Fe(acac)$_3$/SIPr-HCl show absorption maxima at around 350 and 445 nm.

In the absence of the NHC ligand, the absorption in the area between 400 and 500 nm decreases upon addition of Grignard reagent (**Figure 5.7**). In contrast, in the presence of the ligand, the addition of Grignard results only in a slight initial decrease in absorption in this area, which increases again upon further addition of Grignard (**Figure 5.8**). The slight decrease observed might be related to the role of the initial aliquots of Grignard as a base for the NHC precursor.

The difference between the two cases suggests that the NHC-coordinated reduced iron species [Fe^{red}] formed upon reaction with Grignard is more strongly absorbing in the blue light region than the non-coordinated one. This might explain the crucial role of the ligand in the reaction.

A similar behavior is observed when PhCl is added to the solution before the Grignard reagent (**Figures 5.9-5.10**). The addition of the aryl chloride has no effect on the absorption spectra, suggesting that no interaction between the Fe(III) catalyst and the aryl chloride takes place. Subsequent addition of Grignard reagent induces the same effects as described above for **Figures 5.7**-**5.8**. This behavior suggests that Fe(III) species alone cannot interact with the aryl chloride in the absence of Grignard. The Grignard reagent then has a role in generating the active species [Fe^{red}] before the catalytic cycle begins.
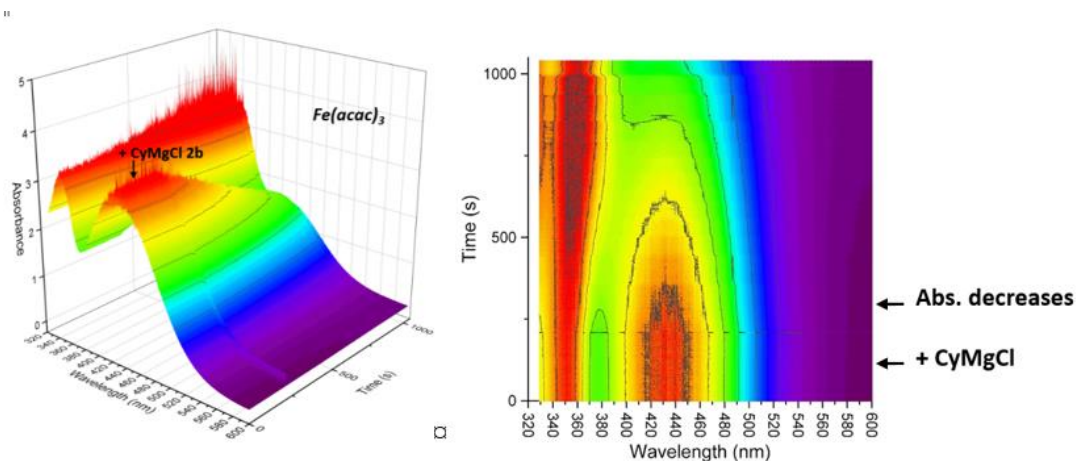
Figure 5.7: In-line UV-Vis measurements for the addition of cyclohexylmagnesium chloride **2b** to Fe(acac)₃
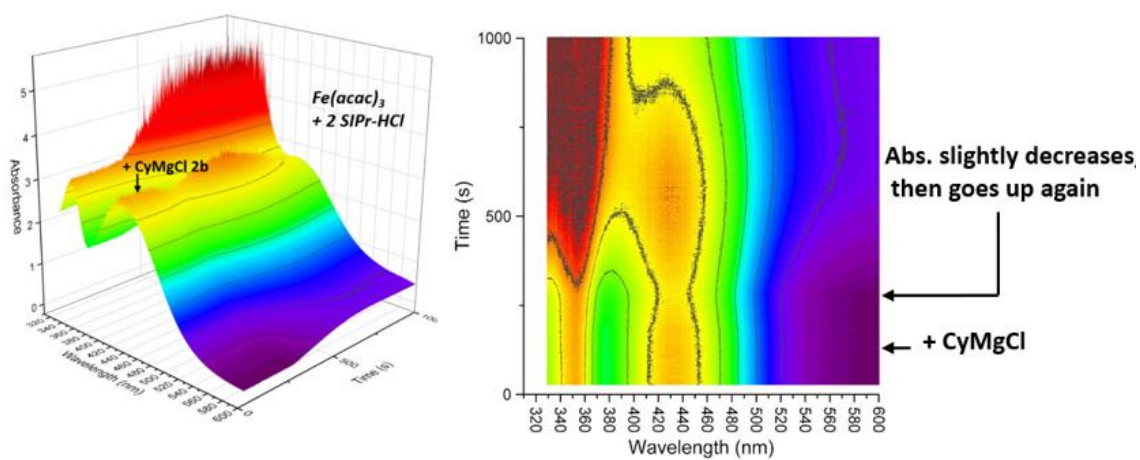
Figure 5.8: In-line UV-Vis measurements for the addition of cyclohexylmagnesium chloride **2b** to Fe(acac)₃/SIPr·HCl
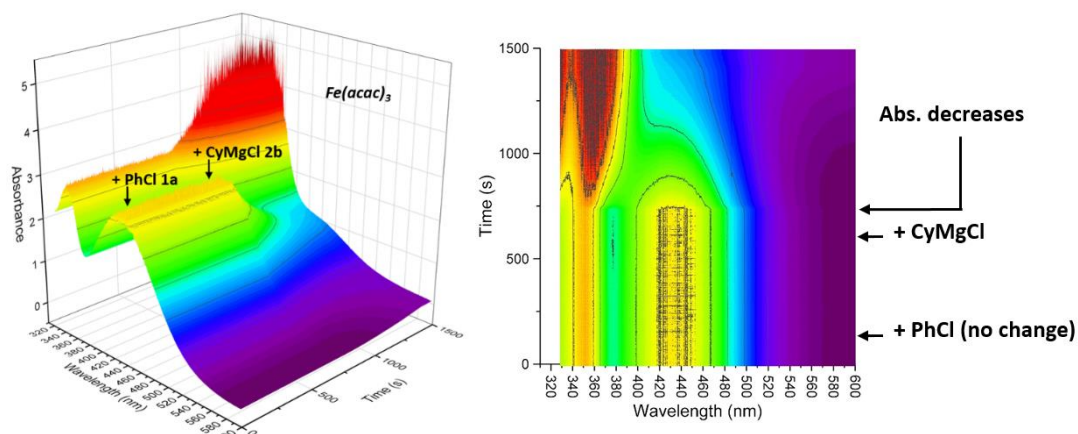
Figure 5.9: In-line UV-Vis measurements for the addition of chlorobenzene **1a** and cyclohexylmagnesium chloride **2b** to Fe(acac)$_3$
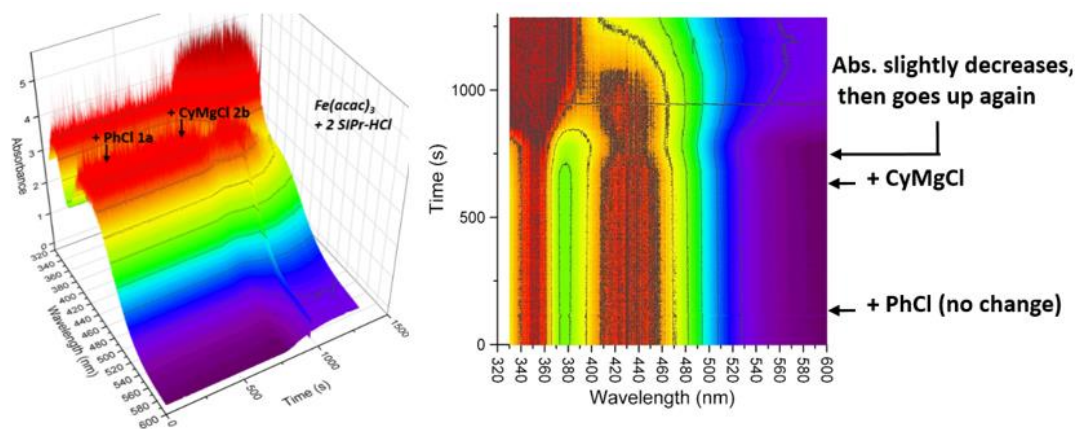
Figure 5.10: In-line UV-Vis measurements for the addition of chlorobenzene **1a** and cyclohexylmagnesium chloride **2b** to Fe(acac)$_3$/SIPr·HCl

General procedure for the inline UV analysis to test the first step of the catalytic reaction:

These experiments were performed to try to elucidate the role of light in the reaction. Due to its almost complete inertness in the absence of light (see manuscript), 5-chlorindole **1m** was used as reactant for these experiments. It is important to note that the concentration used for these experiments is much lower than the one used for the substrate scope or the kinetic profiles.

A solution of Fe(acac)$_3$ (3.5 mg, 0.01 mmol) and SIPr·HCl (8.5 mg, 0.02 mmol) in dry THF (20 mL) was charged into a reaction tube and stirred under Ar. The solution was continuously analyzed by in-line UV-Vis spectrophotometry (300-600 nm range), collecting one measurement per second. After about 5 minutes, cyclohexylmagnesium chloride **2b** (0.5 mL of 1.0 M solution in 2-MeTHF, 0.5 mmol) was added by syringe.

After other 5 minutes, 5-chloroindole **1m** (30.4 mg, 0.2 mmol in 0.5 mL THF) was added by syringe. This process was carried out in the preseance and in the absence of irradiation (18 W blue LED) for comparison.

Results:

THF solutions of Fe(acac)₃/SIPr·HCl show absorption maxima at around 350 and 450 nm. The absorption in the area between 400 and 500 nm decreases upon addition of cyclohexylmagnesium chloride and chloroindole. The decrease in absorbance in this range is almost instantaneous upon addition of the Grignard, and a little slower upon addition of the chloroindole. After a certain time (around 40 min) under stirring and irradiation, a broad band between 450 and 600 nm appears, and remains almost unaltered for the next 100 min. After this time, this band start disappearing.

During this whole time, no conversion was observed in GC-FID. We assume the excessive dilution of the reaction to be responsible for this. Based on this observation, we propose this absorption band to be related to an intermediate necessary before the catalytic cycle begins. DFT calculations suggest this band might be related to a Fe(I) intermediate, formed upon reduction of Fe(III) by the Grignard reagent.
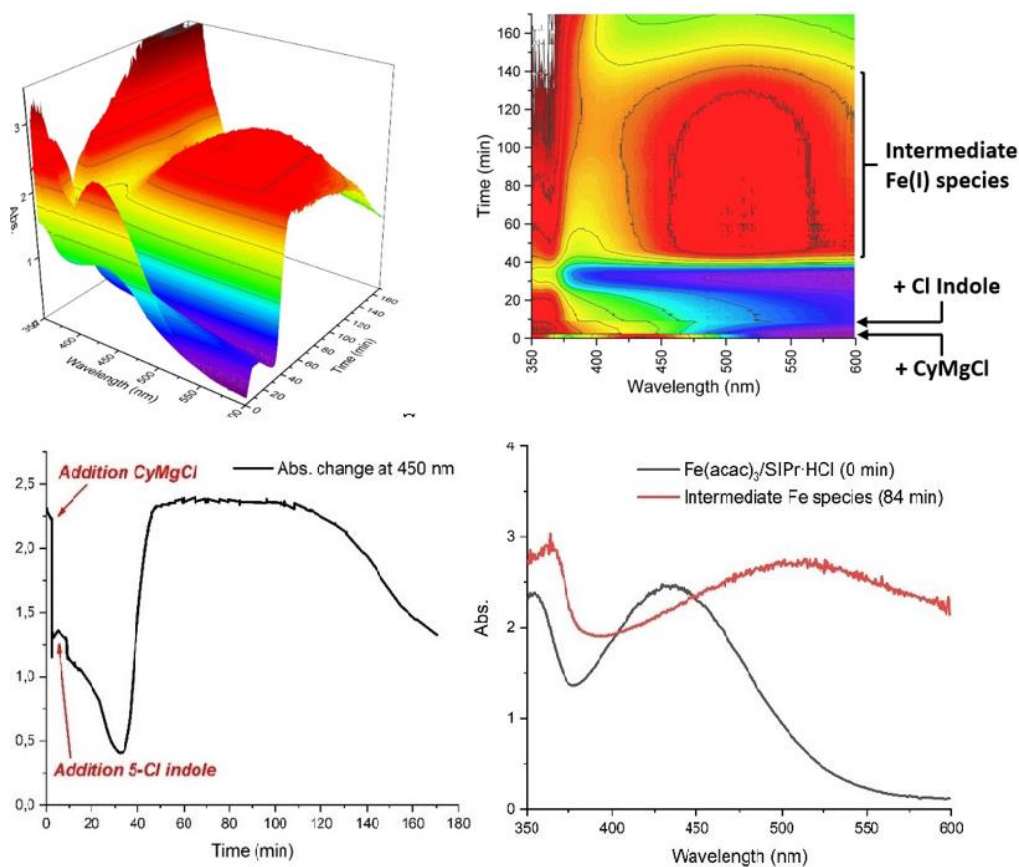
Figure 5.11: In-line UV-Vis with blue LED irradiation of the mixture
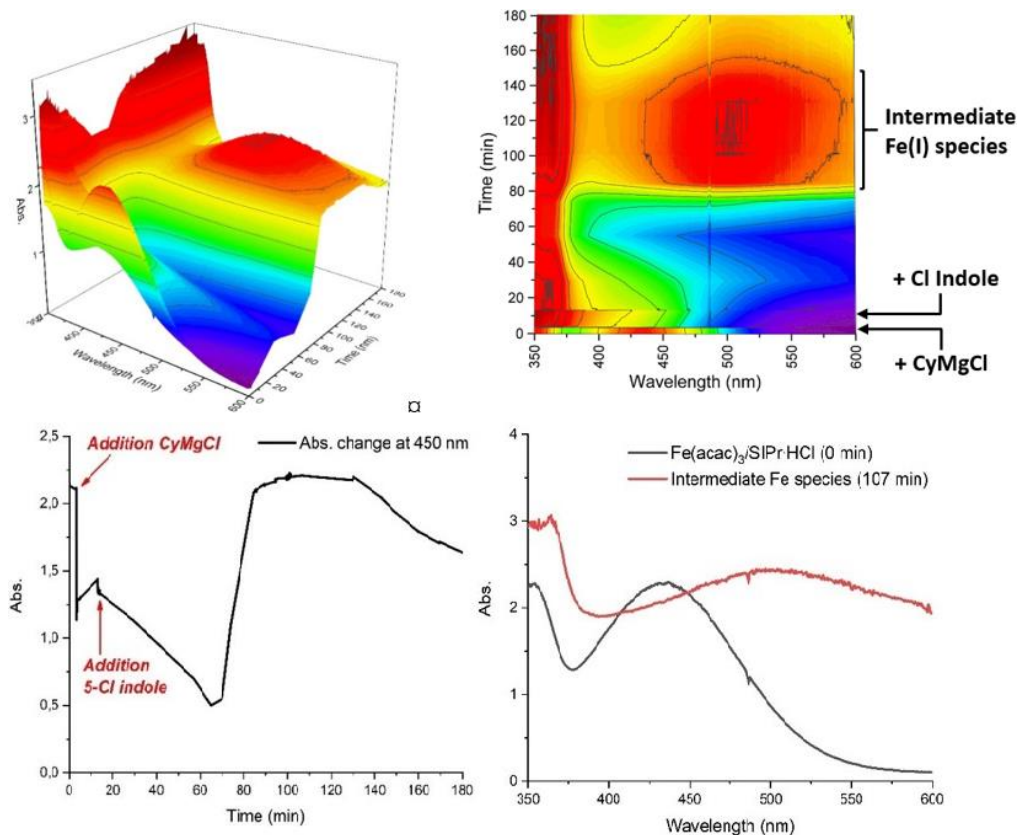
Figure 5.12: In-line UV-Vis without blue LED irradiation of the mixture

The process under irradiation (**Figure 5.11**) or in the dark (**Figure 5.12**) show only small differences (different timings for the appearance and disappearance of the broad band at 450-600 nm). The similarity of the two is clearly observed in the graphs reported in **Figures 5.11-5.12**, and suggests that the effect of light is not strong at this point of the reaction.

General procedure for the inline UV analysis with higher concentration:

UV-Vis analysis for more concentrated solutions were performed to gain insights under more realistic conditions.

SIPr·HCl (34.2 mg, 0.08 mmol, 4 mol%), cyclohexylmagnesium chloride **2b** (1.0 M in 2-MeTHF, 5.0 mL, 2.5 equiv.) and 10.0 mL dry THF were charged into a vial and stirred for 10 minutes under Ar. This solution was then added into a solution of Fe(acac)$_3$ (14.0 mg, 0.04 mmol, 2 mol%) and 5-chloroindole **1m** (303.8 mg, 2.0 mmol, 1 equiv) in 10.0 mL dry THF.

A modified flow sutup was designed to dilute the solution before analysis (**Figure 5.13**). The reaction mixture was pumped at 0.5 mL/min and diluted with dry THF (2.0 mL/min) via a T-mixer before UV-Vis flow cell. For the first 15 minutes, the reaction was performed without light irradiation, then the light was turned on.
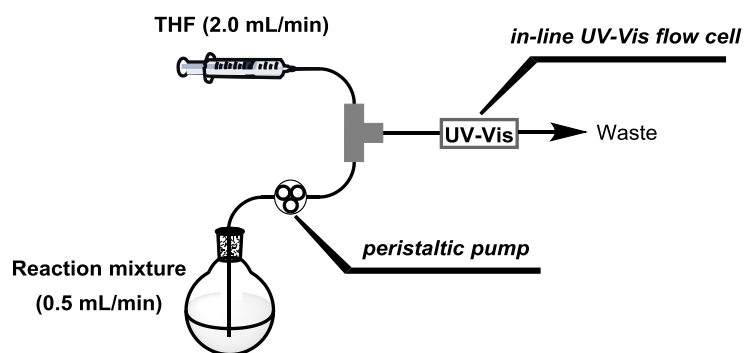
Figure 5.13: Modified flow setup for the analysis of concentrated reaction mixtures

Results:

Upon addition of the Grignard/NHC solution, the absorption band of Fe(acac)$_3$ at around 450 nm disappears quickly, and the concomitant appearance of the band at 450-600 nm is observed. This is similar with what we observed from the diluted solution. Under these concentrated conditions, however, this broad band disappears after about 2 minutes, after which almost no absorption in the range 350-600 is observed. At 7.5-8 minutes of reaction, a shoulder peak at 430-450 nm suddenly appears for a very short time. When the light was turned on at 15 minutes, the same peak, but much more intense, appeared and disappear immediately again (**Figure 5.14**). GC-FID measurements show almost complete conversion shortly after this point.

Based on DFT calculations and the fact that the UV absorption of the iron containing species is mainly influenced by the oxidative state of iron, we suggest the sudden shoulder peak appearing at 430-450 nm to be an Fe(III) species. The sudden formation and disappearance of this shoulder might be related to the formation of an Fe(III) species formed by oxidative addition of the aryl chloride. As the intensity of the peak was much higher under irradiation, we propose that irradiation strongly promotes the formation of this species. The acceleration of an oxidative addition step is in agreement with the strong effect of light on the coupling with electron-rich substrates, as demonstrated in the manuscript.
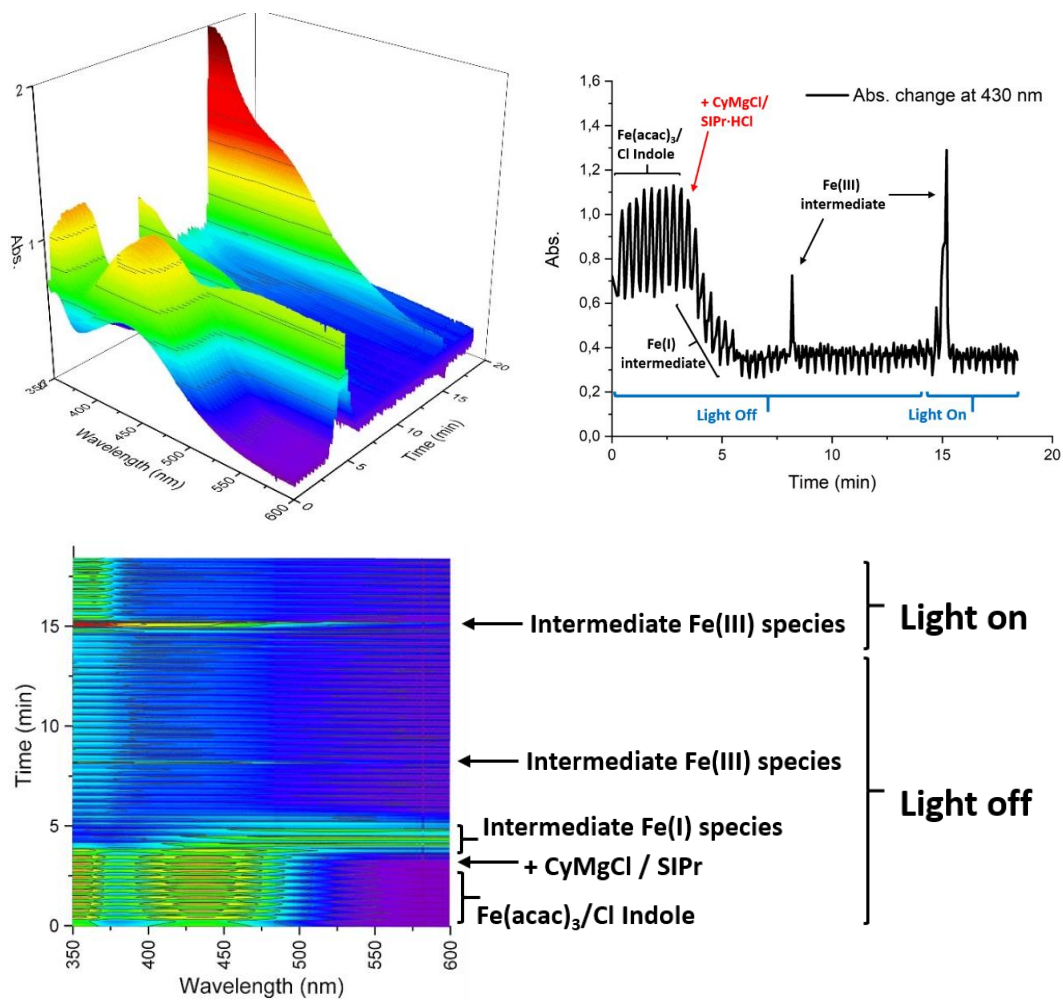
Figure 5.14: In-line UV-Vis at high concentration

Computational details

All calculations were performed with the Gaussian09, revision D.01 suite[27] employing the DFT method, the Becke three-parameter hybrid functional[28], and Lee-Yang-Parr's gradient-corrected correlation functional (B3LYP[29]) used in conjunction with Grimme's dispersion correction with Becke-Johnson damping[30]. The ground-state geometries of the complexes were first optimized in the gas-phase. Frequency calculations were performed to ensure that the optimized structures were true minima on the potential energy surface (PES). Singlet ground state geometry optimizations for $Fe(0)(acac)_3$ and $Fe(II)(acac)_3$ were carried out at the restricted spin condition, while the triplet and quintet ground state geometry optimizations for $Fe(0)(acac)_3$ and $Fe(II)(acac)_3$ and the doublet, quartet and sextet ground state geometry optimizations for $Fe(I)(acac)_3$ and $Fe(III)(acac)_3$ were carried out at the unrestricted spin condition. All elements except Iron were assigned the 6-311G(d, p) basis set[31]. The double-ζ quality SBKJC VDZ[32] ECP basis set with an effective core potential was employed for the Iron metal ion.

Vertical electronic excitations based on optimized geometries were computed for the lowest energy spin state of the 4 complexes using the TD-DFT[33] formalism in THF using the polarizable continuum model (PCM)[34]. *Gausssum 2.2*[35] was employed to visualize the absorption spectra (simulated with Gaussian distribution with a full-width at half maximum (fwhm) set to 3000 cm^{-1}.

Method: Ub3lyp-GD3BJ
Basis set: CHO 6-311G(d,p) Fe SBKJC VDZ ECP
Solvation: PCM=THF

——— Quartet
——— Doublet
——— Sixtet
——— Triplet
——— Singlet
——— Quintet

Fe(III)(acac)₃

Fe(II)(acac)₃

Fe(I)(acac)₃

————	51.1 kcal/mol
————	28.7 kcal/mol
————	28.4 kcal/mol

Fe(0)(acac)₃

————	168.7 kcal/mol
————	143.2 kcal/mol
————	143.1 kcal/mol
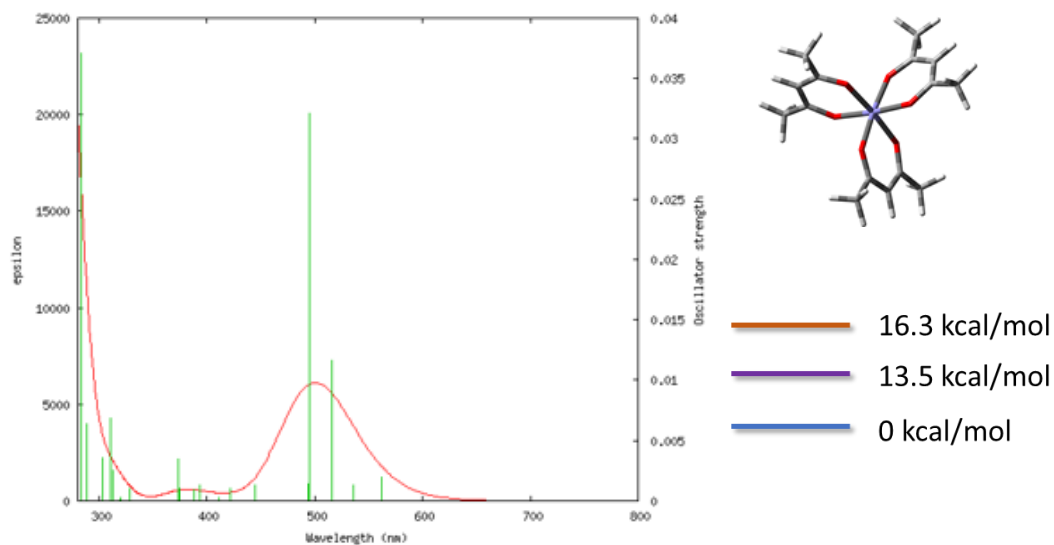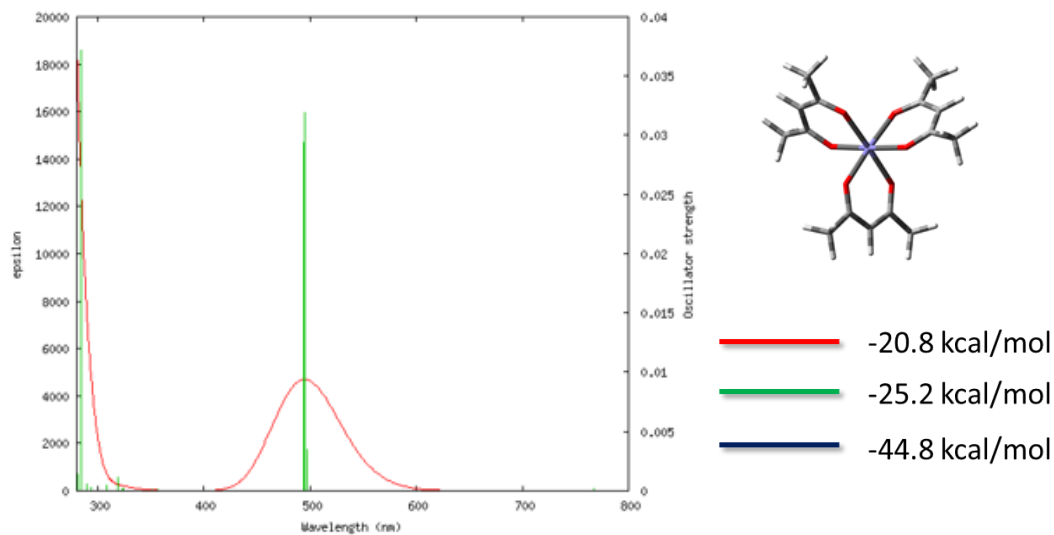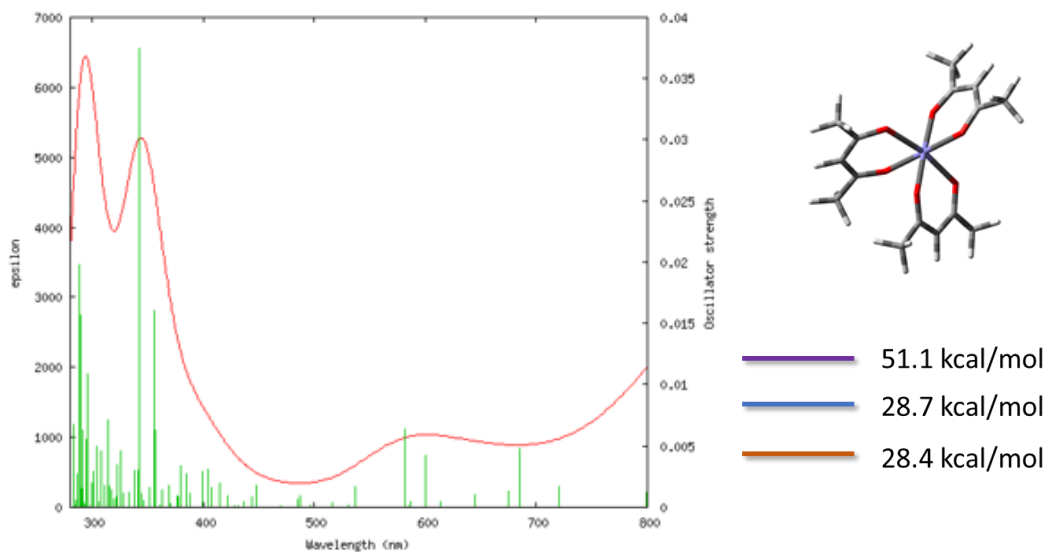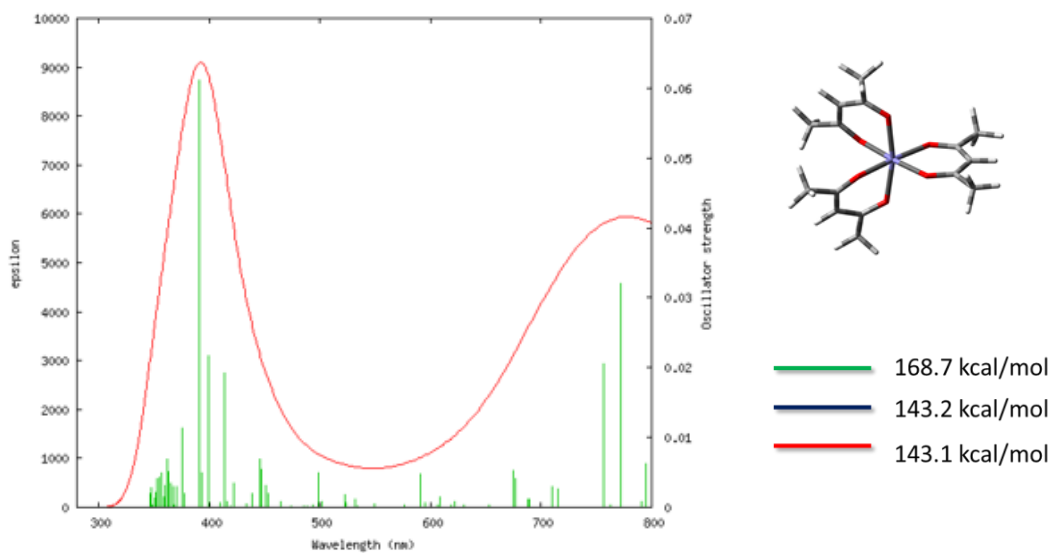
Figure 5.15: Predicted UV-Vis spectra of iron with different iron oxidative state, Oscillator strength and the molecular molecule images of selected electronic transitions

139
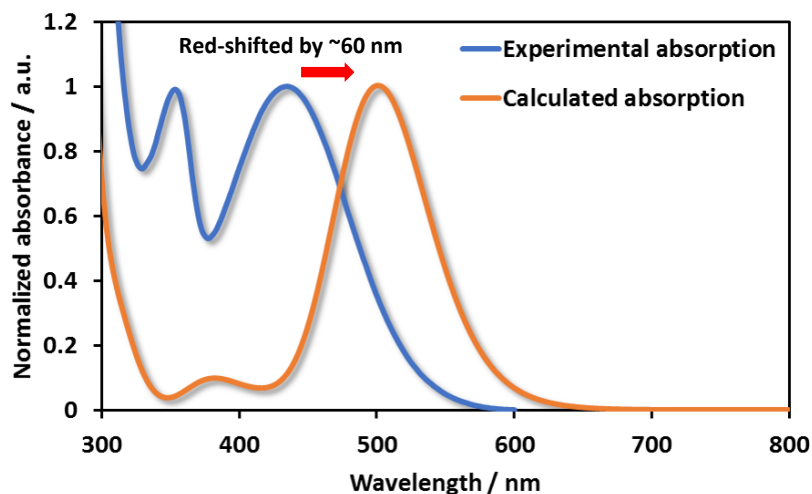
Figure 5.16: The calculated UV-Vis spectra and the experimental spectra of Fe(acac)₃

Table 5.2: Selected Transitions from TD-DFT calculations of Fe(acac)₃ in the Ground State (b3lyp/SBKJC-VDZ[Fe]6-311G**[C,H,O], PCM (THF)).

Oxidation state	Spin	State	λ/nm	f	Major transition(s)	Character
III	6	7	494.7	0.0321	H-2(B)->L+2(B) (37%) H-1(B)->L+1(B) (51%)	LMCT/LLCT
		21	373.7	0.0035	H-2(A)->L+2(A) (17%) H-1(A)->L+1(A) (14%) H(A)->L(A) (19%)	LMCT/LLCT
II	5	6	495.0	0.0319	H (B)->L (B) (81%) H (B)->L+4(B) (16%)	LMCT
		7	494.3	0.0294	H (B)->L+1(B) (65%) H (B)->L+2(B) (19%)	LMCT
I	4	16	685.3	0.0048	H (B)->L+8(B) (86%)	MC/LLCT
		23	581.1	0.0064	H (B)->L+14(B) (93%)	MLCT
0	3	28	771.6	0.0321	H-1(B)->L+9(B) (14%) H-1(B)->L+13(B) (18%)	MLCT/LC

					H (B)->L+17(B) (13%)	
		73	413.1	0.0193	H-2(B)->L+10(B) (16%)	MLCT
					H (B)->L+28(B) (46%)	
					H (B)->L+29(B) (15%)	
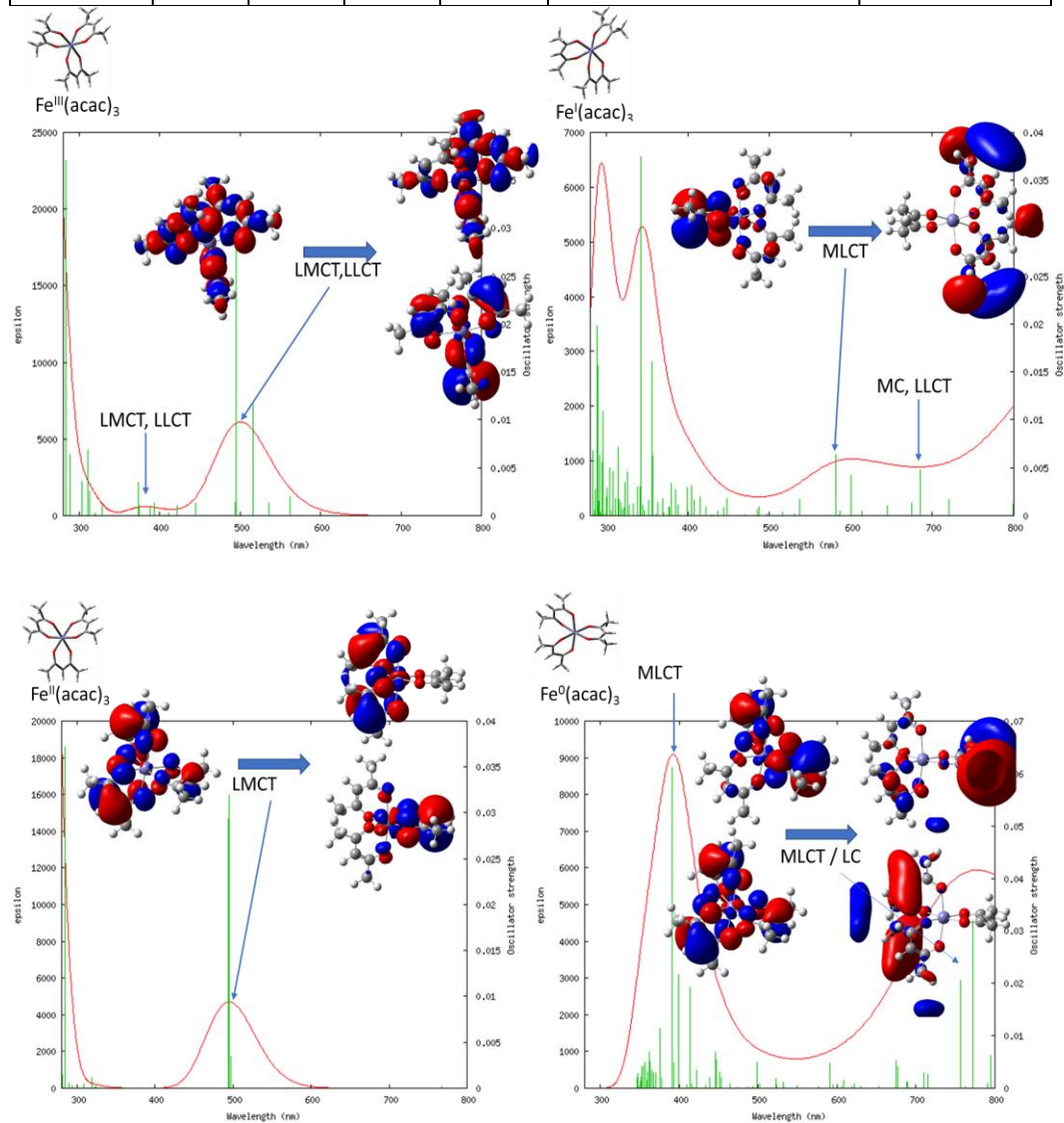
Figure 5.17: MOs related to the major electronic transitions of the related absorption bands.

Under the optimal reaction conditions, there are several possibilities of the combination of the intermediate $Fe(X)^{red}L_n$, (X = 0, I or II), L could be SIPr, acac, R and MgCl. Since many of the bands which gave the absorption at the visible region of iron centered complexes are d-d transition,

using an electronically similar ligand will gave the similar absorption when the number of electrons within d orbital is the same.[36] That means the UV-Vis absorption of the iron containing compound is mainly determined by the oxidative state of iron.

Figure 5.17 shows the comparison between the TD-DFT calculated UV-Vis spectra and the experimental one of Fe(acac)$_3$. The shape of the experimental spectra is similar with the calculated one but with a red shift of around 60 nm which is due to the error of TD-DFT calculations. **Figure 5.17** shows the TD-DFT predicted UV-Vis spectra of the Fe(0)(acac)$_3$, Fe(I)(acac)$_3$, Fe(II)(acac)$_3$, Fe(III)(acac)$_3$, the major transitions of related absorption bands is compiled in **Table 5.3**.

Both Fe(III)(acac)$_3$ and Fe(II)(acac)$_3$ show an similar intense charge transfer band at ~ 500 nm, which is assigned primarily to ligand-to-metal charge transfer (LMCT) and ligand-to-ligand charge transfer (LLCT), while the Fe(III)(acac)$_3$ has an absorption at ~ 370 nm also due to the LMCT/LLCT. The low energy CT bands of Fe(I)(acac)$_3$ and Fe(0)(acac)$_3$ red-shifted by ~80 and ~200 nm compared to Fe(III)(acac)$_3$, respectively, and the nature of the charge transfer excited states are metal-to-ligand charge transfer (MLCT), this is due to the electron richer low valent iron metal ion.

As shown in **Figure 5.14**, after the activation stage of the reaction, the 430 nm LMCT band of Fe(III) species disappeared and a broad absorption band (red-shifted by ~90 nm) showed increasing intensity. This is proposed to be the MLCT band of Fe(I) species.

Table 5.3: DFT optimized atomic coordinates of Fe(III)(acac)$_3$

_____

Center Number	Atomic Number	Forces (Hartrees/Bohr)		
		X	Y	Z

_____

Center Number	Atomic Number	X	Y	Z
1	6	0.000003976	−0.000001021	0.000003496
2	6	−0.000003224	−0.000000242	−0.000010716
3	6	0.000002078	−0.000001796	−0.000002993
4	6	−0.000004354	0.000005470	0.000010828
5	8	−0.000001851	−0.000003277	−0.000009861
6	6	0.000002240	0.000000144	−0.000007810
7	8	0.000002525	0.000004558	0.000003059
8	6	−0.000002217	−0.000005821	−0.000000190

9	6	0. 000002325	0. 000002164	0. 000009872
10	6	−0. 000003077	−0. 000001578	0. 000002042
11	6	0. 000009115	0. 000001488	0. 000000567
12	8	−0. 000003786	0. 000000490	0. 000004579
13	6	−0. 000003557	0. 000002605	0. 000006685
14	8	−0. 000003195	−0. 000000928	0. 000004233
15	6	−0. 000007603	0. 000000368	−0. 000002145
16	6	−0. 000000595	−0. 000008010	0. 000004914
17	6	−0. 000000222	0. 000002812	0. 000000724
18	6	0. 000002542	−0. 000000281	−0. 000008369
19	8	−0. 000011048	−0. 000003893	0. 000004004
20	6	0. 000007804	0. 000005264	−0. 000002064
21	8	0. 000003487	0. 000004979	−0. 000003193
22	26	0. 000010689	−0. 000002876	−0. 000004661
23	1	0. 000002231	0. 000001516	−0. 000002552
24	1	0. 000002741	0. 000001974	−0. 000000926
25	1	0. 000001728	0. 000001235	−0. 000001368
26	1	0. 000000563	−0. 000000213	−0. 000003378
27	1	−0. 000001501	−0. 000001590	−0. 000003999
28	1	−0. 000002256	−0. 000002772	−0. 000004379
29	1	−0. 000003338	−0. 000001625	−0. 000003782
30	1	−0. 000003197	−0. 000001890	0. 000002984
31	1	−0. 000001407	−0. 000001169	0. 000003717
32	1	−0. 000002186	−0. 000001158	0. 000005486
33	1	−0. 000000745	−0. 000000386	0. 000004502
34	1	0. 000001537	0. 000001010	0. 000004783
35	1	0. 000001589	0. 000002128	0. 000003906
36	1	0. 000003423	0. 000001881	0. 000003573
37	1	−0. 000001814	−0. 000000935	−0. 000000253
38	1	−0. 000002282	−0. 000001998	−0. 000000644
39	1	−0. 000002293	−0. 000002189	0. 000001223

40	1	−0. 000000316	0. 000000714	−0. 000002197
41	1	0. 000001650	0. 000002259	−0. 000002199
42	1	0. 000002319	0. 000000783	−0. 000003667
43	1	0. 000001500	0. 000001806	−0. 000003831

Table 5.4: DFT optimized atomic coordinates of Fe(II)(acac)$_3$

_____

| Center Number | Atomic Number | Forces (Hartrees/Bohr) | | |
		X	Y	Z
1	6	−0. 000000745	−0. 000000635	0. 000000793
2	6	−0. 000000154	0. 000000142	−0. 000003847
3	6	0. 000002043	−0. 000000121	−0. 000000957
4	6	−0. 000002398	0. 000001621	0. 000004532
5	8	−0. 000004281	−0. 000006246	−0. 000005781
6	6	−0. 000000662	0. 000000694	−0. 000000761
7	8	−0. 000007276	0. 000002657	0. 000007756
8	6	−0. 000000427	0. 000001894	−0. 000001056
9	6	−0. 000007161	−0. 000007441	−0. 000000867
10	6	0. 000001049	0. 000000252	0. 000005639
11	6	0. 000013274	−0. 000002712	0. 000002861
12	8	−0. 000005990	0. 000002121	−0. 000015026
13	6	−0. 000002483	−0. 000000652	0. 000000167
14	8	0. 000007666	0. 000006177	0. 000000867
15	6	0. 000000594	0. 000001775	0. 000002747
16	6	0. 000000626	−0. 000001915	−0. 000012176
17	6	0. 000002875	−0. 000000220	−0. 000003068
18	6	−0. 000003976	0. 000012450	0. 000003394
19	8	0. 000005727	−0. 000009777	−0. 000000760
20	6	−0. 000000736	−0. 000004450	0. 000000015
21	8	−0. 000000250	−0. 000002047	0. 000014662
22	26	0. 000004417	0. 000003103	−0. 000000031

23	1	0. 000000075	0. 000000121	0. 000000267
24	1	0. 000000406	0. 000000280	0. 000000020
25	1	−0. 000000284	0. 000000194	−0. 000000313
26	1	−0. 000000080	0. 000000127	−0. 000000002
27	1	0. 000000016	0. 000000180	−0. 000000267
28	1	−0. 000000056	0. 000000351	−0. 000000276
29	1	0. 000000077	0. 000000497	0. 000000103
30	1	0. 000000767	0. 000000250	−0. 000000642
31	1	0. 000000287	−0. 000000049	0. 000000433
32	1	−0. 000000939	0. 000000865	−0. 000001221
33	1	−0. 000000402	−0. 000000097	0. 000000511
34	1	−0. 000001623	−0. 000000245	−0. 000000336
35	1	0. 000000406	0. 000000421	0. 000001410
36	1	0. 000000013	0. 000000089	−0. 000000388
37	1	−0. 000000784	−0. 000000657	0. 000000288
38	1	−0. 000000143	0. 000000467	−0. 000000788
39	1	−0. 000000667	−0. 000000545	0. 000001661
40	1	0. 000000494	0. 000000385	−0. 000000343
41	1	−0. 000000105	0. 000000089	0. 000000336
42	1	−0. 000000058	0. 000000310	−0. 000000051
43	1	0. 000000872	0. 000000301	0. 000000495

Table 5.5: DFT optimized atomic coordinates of Fe(I)(acac)₃

Center Number	Atomic Number	Forces (Hartrees/Bohr)		
		X	Y	Z
1	6	0. 000001521	0. 000001563	−0. 000001009
2	6	−0. 000007289	0. 000000762	0. 000006616
3	6	−0. 000001402	0. 000002219	0. 000001969
4	6	0. 000001386	0. 000000214	−0. 000005318
5	8	−0. 000002585	−0. 000004706	0. 000007731

6	6	0. 000000141	0. 000000423	0. 000001763
7	8	0. 000007678	−0. 000002453	−0. 000011605
8	6	0. 000002898	0. 000000018	−0. 000004440
9	6	−0. 000001727	−0. 000004570	−0. 000002665
10	6	−0. 000001650	−0. 000000271	0. 000004224
11	6	0. 000005025	0. 000006500	−0. 000006930
12	8	−0. 000004762	−0. 000003123	0. 000006544
13	6	0. 000000316	−0. 000000479	−0. 000002904
14	8	0. 000005523	0. 000001729	−0. 000005567
15	6	0. 000001859	−0. 000001092	0. 000000660
16	6	−0. 000005266	0. 000001219	0. 000003984
17	6	0. 000000216	−0. 000002397	−0. 000000080
18	6	−0. 000004176	−0. 000001288	0. 000005593
19	8	0. 000009162	0. 000002602	−0. 000005821
20	6	−0. 000000621	−0. 000000541	0. 000003553
21	8	0. 000008901	−0. 000001631	−0. 000003740
22	26	−0. 000013022	0. 000004749	0. 000009013
23	1	−0. 000000010	0. 000002500	0. 000000014
24	1	−0. 000000249	0. 000003576	0. 000000119
25	1	−0. 000000613	0. 000002675	−0. 000000782
26	1	−0. 000000093	0. 000000826	0. 000000166
27	1	−0. 000000152	−0. 000000900	0. 000001255
28	1	0. 000000178	−0. 000002052	0. 000000503
29	1	−0. 000000579	−0. 000001718	0. 000002073
30	1	−0. 000000309	−0. 000002460	−0. 000001579
31	1	0. 000000180	0. 000000023	−0. 000002813
32	1	0. 000001065	−0. 000000260	−0. 000002295
33	1	0. 000000495	0. 000001017	−0. 000002302
34	1	−0. 000000005	0. 000000031	−0. 000001202
35	1	0. 000000437	0. 000001618	−0. 000001387
36	1	0. 000000005	−0. 000002024	0. 000000680

37	1	0. 000000719	−0. 000003497	−0. 000000285
38	1	−0. 000000801	−0. 000002011	−0. 000000615
39	1	−0. 000000145	−0. 000000483	0. 000001648
40	1	−0. 000000602	0. 000002377	0. 000002201
41	1	−0. 000001003	0. 000001610	0. 000003231
42	1	−0. 000000631	0. 000000953	0. 000002732
43	1	−0. 000000011	−0. 000001247	−0. 000002934

Table 5.6: DFT optimized atomic coordinates of Fe(0)(acac)$_3$

Center Number	Atomic Number	Forces (Hartrees/Bohr)		
		X	Y	Z
1	6	0. 000001254	−0. 000000455	−0. 000001402
2	6	0. 000001688	−0. 000002726	0. 000004795
3	6	0. 000000053	0. 000001549	−0. 000002791
4	6	−0. 000003386	0. 000002284	0. 000007280
5	8	0. 000005183	0. 000001335	−0. 000005545
6	6	−0. 000001388	0. 000000186	0. 000000394
7	8	0. 000005041	0. 000006651	−0. 000000523
8	6	0. 000001464	−0. 000000488	−0. 000002284
9	6	0. 000002541	−0. 000005162	−0. 000001258
10	6	−0. 000001144	0. 000003260	−0. 000000519
11	6	0. 000001975	−0. 000005940	0. 000004245
12	8	0. 000001414	0. 000004621	−0. 000002831
13	6	−0. 000001682	0. 000000655	−0. 000000767
14	8	−0. 000001957	0. 000000442	0. 000002236
15	6	−0. 000003807	−0. 000003432	−0. 000000600
16	6	−0. 000000566	0. 000005413	−0. 000005273
17	6	−0. 000002560	−0. 000002647	0. 000004311
18	6	0. 000004164	0. 000003501	−0. 000006527

19	8	−0. 000004612	−0. 000001274	0. 000002899
20	6	−0. 000000672	−0. 000001897	0. 000001942
21	8	0. 000002788	−0. 000003107	0. 000002155
22	26	−0. 000007570	−0. 000004066	−0. 000000966
23	1	0. 000001014	0. 000001300	0. 000001630
24	1	0. 000000881	0. 000000900	0. 000001465
25	1	0. 000000591	0. 000000930	0. 000001857
26	1	0. 000000197	0. 000000973	0. 000001413
27	1	−0. 000000588	0. 000000905	0. 000001271
28	1	−0. 000000414	0. 000000745	0. 000001437
29	1	−0. 000001407	0. 000000581	0. 000001144
30	1	−0. 000000900	−0. 000000319	0. 000000510
31	1	0. 000000643	0. 000001351	0. 000000557
32	1	0. 000000298	−0. 000000270	−0. 000000824
33	1	0. 000001145	−0. 000001169	−0. 000000963
34	1	0. 000001205	−0. 000001112	−0. 000001517
35	1	0. 000001423	−0. 000001583	−0. 000001038
36	1	−0. 000000564	−0. 000000210	−0. 000001253
37	1	−0. 000000391	0. 000000528	−0. 000000724
38	1	0. 000000584	−0. 000000476	−0. 000000598
39	1	−0. 000000901	−0. 000000581	−0. 000000989
40	1	−0. 000000529	−0. 000000254	−0. 000000570
41	1	−0. 000000606	−0. 000000190	−0. 000000917
42	1	−0. 000000354	−0. 000000792	−0. 000000662
43	1	0. 000000447	0. 000000037	−0. 000000199

_____

General procedure for the synthesis of Grignard reagents in flow (GP1)

Preparation of Mg column: a SolventPlusTM column (bore: 10 mm, length: 100 mm, AF; Omnifit, cat. no. 006EZS-10-10-AF) is filled with 4 g of magnesium (20-230 mesh, Sigma Aldrich Cat. NO.: 254126) weight in a beaker using a filter funnel. General flow procedure for magnesium activation and organomagnesium synthesis: 5 mL of DIBALH 1M in THF was passed through a 10 mm internal diameter Omni-fit column containing Mg (4 g) at 1 mL/min at room temperature. After that, a solution of TMSCl 2.0 M and 1-bromo-2-chloroethane 0.24

148

M in 10 mL THF was passed through the column at 1 mL/min at room temperature. After the activation, a solution of aliphatic bromide in THF was passed through the column at 0.5 mL/min and at 40 °C. The solution was collected in a sealed vial under nitrogen.
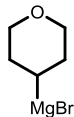
(tetrahydro-2H-pyran-4-yl)magnesium bromide: Prepared according to GP1 starting from 1.21 mL (10.8 mmol) of 4-bromotetrahydro-2H-pyran in 12 mL THF (0.83 M). Titration: An accurately weighed sample of benzoic acid and some crystal of 4-(phenylazo)diphenylamina are dissolved in 1 mL THF and stirred at rt under nitrogen while the Grignard reagent was added slowly. A yellow color formed initially, the end point being indicated by a change of this color to dark red. Concentration = 0.6 M.
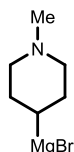
(1-methylpiperidin-4-yl)magnesium bromide: Prepared according to GP1 starting from 1.25 g (7 mmol) of 4-bromo-1-methylpiperidine in 8 mL THF (0.88 M). Titration: An accurately weighed sample of benzoic acid and some crystal of 4-(phenylazo)diphenylamina are dissolved in 1 mL THF and stirred at rt under nitrogen while the Grignard reagent was added slowly. A yellow color formed initially, the end point being indicated by a change of this color to dark red. Concentration = 0.7 M.

General procedure for the iron-catalyzed Kumada cross-coupling

General procedure for the Kumada cross-coupling reactions in flow (GP2)

SIPr-HCl (34.2 mg, 4 mol%), dry THF (2 mL), and 3 mL of Grignard reagent (1.5 equiv.) were charged into vial 1 under N_2. The solution was stirred for 10 minutes at rt. Fe(acac)$_3$ (14.1 mg, 2 mol%), chloroarene (2 mmol, 1 equiv), and dry THF (5 mL) were charged into vial 2 under N_2. The two solution were transferred into syringes (5 mL) and loaded onto a syringe pump. The reaction temperature was maintained at 25 °C by the gas flowing through a jar filling with dry ice with the control of the Vapourtec machine. After the reaction was completed (residence time = 5 min), the reaction mixture was collected, quenched with 20 mL 1.0 M HCl solution (for NH-containing substrates, basic NH_4/NH_3 aqueous solution was used to ensure efficient extraction), and extracted with pentane or DCM (3x20 mL), the organic fraction was washed with brine and evaporated. The crude residue was purified by silica gel column chromatography on Biotage with pentane/EtOAc to afford the pure product.

For reactions under irradiation Gen 1 type blue LED (450 nm, 24 W) were used; reactions without light were performed following the same procedure, and analyzed via GC or LC.

General procedure for the Kumada cross-coupling reactions in flow with *i*PrMgCl as additive (GP3)

SIPr-HCl (128.1 mg, 15 mol%), dry THF, and 0.3 mL isopropylmagnesium chloride (1.0 M in THF, 0.3 equiv.) were charged into vial 1 under N_2. The mixture was stirred until complete dissolution of the solid, then the Grignard reagent (1.5 or 2.5 equiv) was added. The solution was stirred for 10 minutes at rt. Fe(acac)$_3$ (35.3 mg, 5 mol%), chloroarene (2 mmol, 1 equiv), and dry THF (5 mL) were charged into vial 2 under N_2. The two solutions were transferred into syringes (5 mL) and loaded onto a syringe pump. The reaction temperature was maintained at 25 °C by the gas flowing through a jar filling with dry ice with the control of the Vapourtec

machine. After the reaction was completed (residence time = 20 min), the reaction mixture was collected, quenched with 20 mL 1.0 M HCl solution (for NH-containing substrates, basic NH_4/NH_3 aqueous solution was used to ensure efficient extraction), and extracted with pentane (3 x 20 mL), the organic fraction was washed with brine and evaporated. The crude residue was purified by silica gel column chromatography on Biotage with pentane/EtOAc to afford the pure product.

For reactions under irradiation Gen 1 type blue LED (450 nm, 24 W) were used; reactions without light were performed following the same procedure, and analyzed via LC.

General procedure for the Kumada cross-coupling reactions in batch (GP4)

SIPr-HCl (128.1 mg, 30 mol%), dry THF (2.5 mL), and 2.5 mL (trimethylsilyl)methylmagnesium chloride (1.0 M in diethyl ether, 2.5 equiv.) were charged into vial 1 under N_2. After stirring for several minutes, a lot of white solid was formed. Fe(acac)$_3$ (35.3 mg, 10 mol%), 1-chloro-4-methoxybenzene or 5-chloro-1H-indole (2 mmol, 1 equiv), and 5 mL THF were charged into vial 2 under N_2. As the mixture in vial 1 gave a lot of white solid upon stirring, flow experiments were not possible in these cases. The solution in vial 2 was therefore added into vial 1, which was placed in front of two 34 W blue LED. After 4 h irradiation, the reaction mixture was quenched with 20 mL 1.0 M HCl solution (for 1-chloro-4-methoxybenzene) or basic $NH_4Cl/NH_3.H_2O$ aqueous solution (for 5-chloro-1H-indole), and extracted with pentane or DCM (3x20 mL), the organic fraction was washed with brine and evaporated. The crude residue was purified by silica gel column chromatography on Biotage with pentane/EtOAc to afford the pure product.

For reactions under irradiation blue LED (450 nm, 34 W) were used; reactions without light were performed following the same procedure, and analyzed via GC or LC.

Characterization of the compounds

Cyclohexylbenzene (3ab):

The title compound was prepared according to general procedure **GP2**. Solution 1: chlorobenzene (225.1 mg, 2.0 mmol, 1.0 equiv), Fe(acac)$_3$ (14.2 mg, 2 mol%) in dry THF (5.0 mL); Solution 2: SIPr-HCl (34.2 mg, 4 mol%), cyclohexylmagnesium chloride (3.0 mL, 1.5 equiv.) in dry THF (2.0 mL) at 25 °C with 5 minutes residence time. Purification via chromatography (pentane, 100%) gave the desired product **3ab** as colorless oil in 91% yield (291.7 mg). **¹H NMR** (400 MHz, CDCl$_3$): δ (ppm) = δ 7.35-7.31(m, 2H), 7.26-7.21(m, 3H), 2.57-2.51(m, 1H), 1.95-1.85(m, 4H), 1.82-1.77(m, 1H), 1.54-1.28(m, 5H). **¹³C NMR** (101 MHz, CDCl$_3$): δ148.06, 128.24, 126.79, 125.73, 44.59, 34.36, 26.92, 26.17.

1-Cyclohexylnaphthalene (3bb):

The title compound was prepared according to general procedure **GP2**. Solution 1: 1-chloronaphthalene (324.0 mg, 2.0 mmol, 1.0 equiv), Fe(acac)$_3$ (14.2 mg, 2 mol%) in dry THF (5.0 mL); Solution 2: SIPr-HCl (34.2 mg, 4 mol%), cyclohexylmagnesium chloride (3.0 mL, 1.5 equiv.) in dry THF (2.0 mL) at 25 °C with 5 minutes residence time. Purification via chromatography (pentane, 100%) gave the desired product **3bb** as colorless oil in 83% yield (348.8 mg). **¹ H NMR** (400 MHz, CDCl$_3$): δ 8.19(d, *J* = 4.0 Hz, 1H), 7.91(d, *J* = 8.0 Hz, 1H), 7.76-7.74(m, 1H), 7.58-7.44 (m, 4H), 3.40-3.39(m, 1H), 2.12-2.09 (m, 2H), 2.01-1.97 (m, 2H), 1.93-1.89 (m, 1H), 1.63 (dd, *J* = 11.4, 8.4 Hz, 4H), 1.41 (tdt, *J* = 12.8, 9.2, 3.6 Hz, 1H). **¹³C NMR** (101 MHz, CDCl$_3$): δ143.78, 133.92, 131.34, 128.91, 128.89, 126.19, 125.63, 125.55, 123.18, 122.24, 39.28, 34.22, 27.29, 26.55.

4-Cyclohexyl-1,1'-biphenyl (3cb):

The title compound was prepared according to general procedure **GP2.** Solution 1: 4-chloro-1,1'-biphenyl (376.1 mg, 2.0 mmol, 1.0 equiv), Fe(acac)$_3$ (14.2 mg, 2 mol%) in dry THF (5.0 mL); Solution 2: SIPr-HCl (34.2 mg, 4 mol%), cyclohexylmagnesium chloride (3.0 mL, 1.5 equiv.) in dry THF (2.0 mL) at 25 °C with 5 minutes residence time. Purification via chromatography (pentane, 100%) gave the desired product **3cb** as white solid in 90% yield (425.1 mg). Melting point: 75.3 °C. **¹ H NMR** (400 MHz, CDCl$_3$): δ 7.61-7.58 (m, 2H), 7.55-7.53(m, 2H), 7.46-7.42(m, 2H), 7.35-7.31(m, 1H), 7.30-7.29(m, 2H), 2.59-2.53(m, 1H), 1.96-1.86(m, 4H), 1.81-1.76(m, 1H), 1.53-1.25 (m, 5H). **¹³C NMR** (101 MHz, CDCl$_3$): δ147.22, 141.18, 138.71, 128.66, 127.21, 127.02, 127.00, 126.91, 44.24, 34.47, 26.92, 26.17.

1-Cyclohexyl-3-fluorobenzene (3db):

The title compound was prepared according to general procedure **GP2.** Solution 1: 1-chloro-3-fluorobenzene (260.0 mg, 2.0 mmol, 1.0 equiv), Fe(acac)$_3$ (14.2 mg, 2 mol%) in dry THF (5.0 mL); Solution 2: SIPr-HCl (34.2 mg, 4 mol%), cyclohexylmagnesium chloride (3.0 mL, 1.5 equiv.) in dry THF (2.0 mL) at 25 °C with 5 minutes residence time. Purification via chromatography (pentane, 100%) gave the desired product **3db** as colorless oil in 88% yield (313.5 mg). **¹ H NMR** (400 MHz, CDCl$_3$): δ 7.32-7.29 (m, 1H), 7.04 (d, *J* = 4.0 Hz, 1H), 6.99-6.90 (m, 2H), 2.61-2.53 (m, 1H), 1.98-1.92 (m, 4H), 1.85- 1.78 (m, 1H), 1.49-1.27(m, 5H). **¹³C NMR** (101 MHz, CDCl$_3$): δ162.97 (d, *J* = 244.6 Hz), 150.74 (d, *J* = 6.7 Hz), 129.56 (d, *J* = 8.3 Hz), 122.48 (d, *J* = 2.6 Hz), 113.57

(d, $J = 20.9$ Hz), 112.49 (d, $J = 21.0$ Hz), 44.34 (d, $J = 1.7$ Hz), 34.29, 26.77, 26.07. **^{19}F NMR** (126 MHz, CDCl$_3$): -113.91.

1-Cyclohexyl-4-methylbenzene (3eb):

The title compound was prepared according to general procedure **GP2.** Solution 1: 1-chloro-4-methylbenzene (252.0 mg, 2.0 mmol, 1.0 equiv), Fe(acac)$_3$ (14.2 mg, 2 mol%) in dry THF (5.0 mL); Solution 2: SIPr-HCl (34.2 mg, 4 mol%), cyclohexylmagnesium chloride (3.0 mL, 1.5 equiv.) in dry THF (2.0 mL) at 25 °C with 5 minutes residence time. Purification via chromatography (pentane, 100%) gave the desired product **3eb** as colorless oil in 99% yield (344.8 mg). **^{1}H NMR** (400 MHz, CDCl$_3$, 300 K): δ 7.14 (s, 4H), 2.53 – 2.46 (m, 1H), 2.35(s, 3H), 1.94 – 1.84 (m, 4H), 1.79 – 1.75 (m, 1H), 1.54 – 0.89 (m, 5H). **^{13}C NMR** (101 MHz, CDCl3): δ 145.13, 135.14, 128.94, 126.66, 44.16, 34.58, 26.95, 26.19, 20.96.

1-Cyclohexyl-2-methoxybenzene (3fb):

The title compound was prepared according to general procedure **GP2.** Solution 1: 1-chloro-2-methoxybenzene (285.2 mg, 2.0 mmol, 1.0 equiv), Fe(acac)$_3$ (14.2 mg, 2 mol%) in dry THF (5.0 mL); Solution 2: SIPr-HCl (34.2 mg, 4 mol%), cyclohexylmagnesium chloride (3.0 mL, 1.5 equiv.) in dry THF (2.0 mL) at 25 °C with 5 minutes residence time. Purification via chromatography (pentane, 100%) gave the desired product **3fb** as colorless oil in 89% yield (338.4 mg). **[1] H NMR** (400 MHz, CDCl$_3$): δ 7.22-7.15 (m, 2H), 6.94(t, $J = 8.0$ Hz, 1H), 6.87(d, $J = 8.0$ Hz, 1H), 3.84(s, 3H), 3.01-2.95(m, 1H), 1.86-1.75(m, 5H), 1.47-1.25(m, 5H). **^{13}C NMR** (100 MHz, CDCl$_3$): δ 156.70, 136.25, 126.51, 126.42, 120.53, 110.35, 100.36, 55.37, 36.76, 33.22, 27.11, 26.45.

1-Cyclohexyl-3-methoxybenzene (3gb):

The title compound was prepared according to general procedure **GP2.** Solution 1: 1-chloro-3-methoxybenzene (285.2 mg, 2.0 mmol, 1.0 equiv), Fe(acac)$_3$ (14.2 mg, 2 mol%) in dry THF (5.0 mL); Solution 2: SIPr-HCl (34.2 mg, 4 mol%), cyclohexylmagnesium chloride (3.0 mL, 1.5 equiv.) in dry THF (2.0 mL) at 25 °C with 5 minutes residence time. Purification via chromatography (pentane, 100%) gave the desired product **3gb** as colorless oil in 85% yield (323.2 mg). **[1] H NMR** (400 MHz, CDCl$_3$): δ 7.22 (t, $J = 8.0$ Hz, 1H), 6.84 – 6.73 (m, 3H), 3.82 (s, 3H), 2.53 – 2.46 (m, 1H), 1.92 – 1.83 (m, 4H), 1.78 – 1.74 (m, 1H), 1.45 – 1.24 (m, 5H). **^{13}C NMR** (101 MHz, CDCl$_3$): δ159.58, 149.84, 129.16, 129.29, 112.79, 110.82, 55.11, 44.67, 34.41, 26.89, 26.17.

1-Cyclohexyl-4-methoxybenzene (3hb):

The title compound was prepared according to general procedure **GP2.** Solution 1: 1-chloro-4-methoxybenzene (285.2 mg, 2.0 mmol, 1.0 equiv), Fe(acac)$_3$ (14.2 mg, 2 mol%) in dry THF (5.0 mL); Solution 2: SIPr-HCl (34.2 mg, 4 mol%), cyclohexylmagnesium chloride (3.0 mL, 1.5 equiv.) in dry THF (2.0 mL) at 25 °C with 5 minutes residence time. Purification via chromatography (pentane, 100%) gave the desired product **3hb** as white solid in 93% yield (353.7 mg). Melting point: 58.5 °C. **[1] H NMR** (400 MHz, CDCl$_3$): δ 7.14 (d, $J = 8.0$ Hz, 2H), 6.85 (d, $J = 8.0$ Hz, 2H), 3.80 (s, 3H), 2.50 – 2.42 (m, 1H), 1.89 – 1.83 (m, 4H), 1.78 – 1.72 (m, 1H), 1.46 – 1.22 (m, 5H). **^{13}C NMR** (101 MHz, CDCl$_3$): δ157.63, 140.37, 127.60, 113.64, 103.38, 55.23, 43.68, 34.72, 26.96, 26.18.

1-Cyclohexyl-3,5-dimethoxybenzene (3ib):

The title compound was prepared according to general procedure **GP2.** Solution 1: 1-chloro-3,5-dimethoxybenzene (344.0 mg, 2.0 mmol, 1.0 equiv), Fe(acac)$_3$ (35.3 mg, 5 mol%) in dry THF (5.0 mL); Solution 2: SIPr-HCl (85.4 mg, 10 mol%), cyclohexylmagnesium chloride (3.0 mL, 1.5 equiv.) in dry THF (2.0 mL) at 25 °C with 20 minutes residence time. Purification via chromatography (pentane, 100%) gave the desired product **3ib** as colorless oil in 71% yield (312.2 mg). **¹ H NMR** (400 MHz, CDCl$_3$): δ 6.44 (d, *J* = 2.3 Hz, 2H), 6.35 (d, *J* = 2.3 Hz, 1H), 3.82 (s, 6H), 2.49(m, 1H), 1.95-1.87(m, 4H), 1.82-1.76(m, 1H), 1.51-1.27 (m, 5H). **¹³C NMR** (101 MHz, CDCl$_3$): δ 160.63, 150.57, 104.94, 97.57, 55.08, 44.93, 34.30, 26.82, 26.11. **HRMS** (ESI) (m/z): [M+Na]$^+$ calcd. for C$_{14}$H$_{20}$NaO$_2$: 243.1361, found: 243.1365**.**

4-Cyclohexyl-1,2-dimethoxybenzene(3jb):

The title compound was prepared according to general procedure **GP2.** Solution 1: 4-chloro-1,2-dimethoxybenzene (344.0 mg, 2.0 mmol, 1.0 equiv), Fe(acac)$_3$ (35.3 mg, 5 mol%) in dry THF (5.0 mL); Solution 2: SIPr-HCl (85.4 mg, 10 mol%), cyclohexylmagnesium chloride (3.0 mL, 1.5 equiv.) in dry THF (2.0 mL) at 25 °C with 20 minutes residence time. Purification via chromatography (pentane, 100%) gave the desired product **3jb** as colorless oil in 61% yield (268.5 mg). **¹ H NMR** (400 MHz, CDCl$_3$): δ 6.83-6.81 (m, 1H), 6.77-6.76 (m, 2H), 3.90 (s, 3H), 3.87 (s, 3H), 2.50-2.43(m, 1H), 1.91-1.84 (m, 4H), 1.79-1.74(m, 1H), 1.47-1.25 (m, 5H). **¹³C NMR** (101 MHz, CDCl$_3$): δ 148.56, 146.90, 140.77, 118.17, 111.03, 110.22, 55.70, 55.59, 44.02, 34.56, 26.78, 26.01.

3-Cyclohexyl-N,N-dimethylaniline (3kb):

The title compound was prepared according to general procedure **GP2.** Solution 1: 3-chloro-N,N-dimethylaniline (310.1 mg, 2.0 mmol, 1.0 equiv), Fe(acac)$_3$ (14.2 mg, 2 mol%) in dry THF (5.0 mL); Solution 2: SIPr-HCl (34.2 mg, 4 mol%), cyclohexylmagnesium chloride (3.0 mL, 1.5 equiv.) in dry THF (2.0 mL) at 25 °C with 5 minutes residence time. Purification via chromatography (pentane/EtOAc 2-5%) gave the desired product **3kb** as colorless oil in 96% yield (390.1 mg). **¹ H NMR** (400 MHz, CDCl$_3$): δ 7.22 (t, *J* = 7.9 Hz, 1H), 6.67 – 6.62 (m, 3H), 2.99 (s, 6H), 2.54 – 2.47 (m, 1H), 1.97 – 1.92 (m, 4H), 1.82 – 1.77 (m, 1H), 1.55 – 1.38 (m, 5H). **¹³C NMR** (101 MHz, CDCl$_3$): δ150.71, 149.02, 128.89, 115.33, 111.50, 110.38, 45.19, 40.72, 34.53, 29.02, 27.01, 26.25.

4-Cyclohexyl-N-methylaniline (3lb):

The title compound was prepared according to general procedure **GP2.** Solution 1: 4-chloro-N-methylaniline (282.1 mg, 2.0 mmol, 1.0 equiv), Fe(acac)$_3$ (35.3 mg, 5 mol%) in dry THF (5.0 mL); Solution 2: SIPr-HCl (85.4 mg, 10 mol%), cyclohexylmagnesium chloride (5.0 mL, 2.5 equiv.) at 25 °C with 20 minutes residence time. Purification via chromatography (pentane, 100%) gave the desired product **3lb** as colorless oil in 82% yield (310.1 mg). **¹ H NMR** (400 MHz, CDCl$_3$): δ 7.08 (d, *J* = 8.0 Hz, 2H), 6.60 (d, *J* = 8.0 Hz, 2H), 3.60 (brs, 1H), 2.85(s, 3H), 2.46 – 2.39 (m, 1H), 1.90 – 1.83 (m, 4H), 1.78 – 1.73 (m, 1H), 1.46 – 1.24 (m, 5H). **¹³C NMR** (101 MHz, CDCl$_3$): δ147.39, 137.16, 127.39, 112.45, 43.60, 34.76, 30.98, 27.01, 26.22.

5-Cyclohexyl-1H-indole (3mb):

The title compound was prepared according to general procedure **GP2.** Solution 1: 5-chloro-1H-indole (302.0 mg, 2.0 mmol, 1.0 equiv), Fe(acac)$_3$ (7.1 mg, 2 mol%) in dry THF (5.0 mL); Solution 2: SIPr-HCl (17.1 mg, 4

mol%), cyclohexylmagnesium chloride (5.0 mL, 2.5 equiv.) at 25 °C with 5 minutes residence time. Purification via chromatography (pentane/EtOAc, 90%) gave the desired product **3mb** as white solid with 91% yield (362.4mg). Melting point: 91.1 °C. **^{1}H NMR** (400 MHz, CDCl$_3$): δ 8.05(brs, 1H), 7.50-7.49(m, 1H), 7.33 (d, J = 8.0 Hz, 1H), 7.19-7.18(m, 1H), 7.10(dd, J = 8.0, 4.0 Hz, 1H), 6.53-6.51(m, 1H), 2.65-2.57(m, 1H), 1.98-1.84(m, 4H), 1.81-1.75(m, 1H), 1.56-1.25(m, 5H). **^{13}C NMR** (101 MHz, CDCl$_3$): δ 139.81, 134.37, 127.96, 124.17, 121.73, 117.97, 110.64, 102.41, 44.69, 35.19, 27.15, 26.32.

5-Cyclohexyl-1H-pyrrolo[2,3-b]pyridine (3nb):

The title compound was prepared according to general procedure **GP2**. Solution 1: 5-chloro-1H-pyrrolo[2,3-b]pyridine (304.0 mg, 2.0 mmol, 1.0 equiv), Fe(acac)$_3$ (14.2 mg, 2 mol%) in dry THF (5.0 mL); Solution 2: SIPr-HCl (34.2 mg, 4 mol%), cyclohexylmagnesium chloride (5.0 mL, 2.5 equiv.) at 25 °C with 5 minutes residence time. Purification via chromatography (pentane/EtOAc, 90%) gave the desired product **3nb** as white solid in 91% yield (362.4mg). **^{1}H NMR** (400 MHz, CDCl$_3$): δ 11.81(s, 1H), 8.28-8.27(m, 1H), 7.84(s, 1H), 7.41(s, 1H), 6.49(s, 1H), 2.71-2.64(m, 1H), 2.00-1.89(m, 4H), 1.84-1.79(m, 1H), 1.60-1.31(m, 5H). **^{13}C NMR** (101 MHz, CDCl$_3$): δ147.83, 142.10, 135.09, 126.58, 125.41, 120.35, 100.03, 42.25, 35.07, 26.98, 26.11.

6-Cyclohexyl-2-methylquinoline (3ob):

The title compound was prepared according to general procedure **GP2** with solution 1: 6-chloro-2-methylquinoline (354.0 mg, 2.0 mmol, 1.0 equiv), Fe(acac)$_3$ (14.2 mg, 2 mol%) in dry THF (5.0 mL); Solution 2: SIPr-HCl (34.2 mg, 4 mol%), cyclohexylmagnesium chloride (3.0 mL, 1.5 equiv.) in 2.0 mL THF at 25 °C with 5 minutes residence time. Purification via chromatography (pentane/EtOAc, 90%) gave the desired product **3ob** as colorless oil in 68% yield (306.2 mg). **^{1}H NMR** (400 MHz, CDCl$_3$): δ 7.95 (dd, J = 8.4, 3.9 Hz, 2H), 7.58 - 7.50 (m, 2H), 7.21 (d, J = 8.4 Hz, 1 H), 2.71(s, 3H), 2.66 - 2.61(m, 1H), 1.97 - 1.84(m, 4H), 1.79 - 1.75(m, 1H), 1.54 - 1.25(m, 5H). **^{13}C NMR** (101 MHz, CDCl$_3$): δ157.88, 146.64, 145.32, 135.79, 129.58, 128.22, 126.41, 123.91, 121.72, 44.28, 34.31, 26.78, 25.12.

3-Cyclohexyl-2-methoxypyridine (3pb):

The title compound was prepared according to general procedure **GP2**. Solution 1: 3-chloro-2-methoxypyridine(286.0 mg, 2.0 mmol, 1.0 equiv), Fe(acac)$_3$ (7.1 mg, 2 mol%) in dry THF (5.0 mL); Solution 2: SIPr-HCl (17.1 mg, 4 mol%), cyclohexylmagnesium chloride (3.0 mL, 1.5 equiv.) in 2.0 mL THF at 25 °C with 15 minutes residence time. Purification via chromatography (pentane/EtOAc, 90%) gave the desired product **3pb** as colorless oil in 45% yield (172.0 mg). **^{1}H NMR** (400 MHz, CDCl$_3$): δ 7.99 (dd, J = 5.0, 1.9 Hz, 1H), 7.41 (dd, J = 7.3, 1.9 Hz, 1H), 6.83 (dd, J = 7.3, 5.0 Hz, 1H), 3.95 (s, 3H), 2.81(tt, J = 11.6, 3.1 Hz, 1H), 1.89 - 1.81 (m, 4H), 1.79 - 1.73 (m, 1H), 1.49-1.20(m, 5H). **^{13}C NMR** (100 MHz, CDCl$_3$): δ 161.47, 143.52, 134.49, 130.15, 116.76, 53.16, 36.92, 32.57, 26.85, 26.29. **HRMS** (ESI) (m/z): [M+H]$^+$ calcd. for C$_{12}$H$_{18}$NO: 192.1388, found: 192.1393.

5-Cyclohexyl-2-(methylthio)pyrimidine (3qb):

The title compound was prepared according to general procedure **GP2**. Solution 1: 5-chloro-2-(methylthio)pyrimidine (320.0 mg, 2.0 mmol, 1.0 equiv), Fe(acac)$_3$ (7.1 mg, 2 mol%) in dry THF (5.0 mL); Solution 2: SIPr-HCl (17.1 mg, 4 mol%), cyclohexylmagnesium chloride (3.0 mL, 1.5 equiv.) in 2.0 mL THF at

25 °C with 1 minutes residence time. Purification via chromatography (pentane/EtOAc, 90%) gave the desired product **3qb** as colorless oil in 84% yield (349.6 mg). **¹ H NMR** (400 MHz, CDCl₃): δ 8.38(s, 2H), 2.55(s, 3H), 2.49-2.41(m, 1H), 1.89-1.82(m, 4H), 1.79-1.73(m, 1H), 1.45-1.22(m, 5H). **¹³C NMR** (101 MHz, CDCl₃): δ169.85, 155.96, 134.91, 39.27, 33.76, 26.46, 25.67, 14.03. **HRMS** (ESI) (m/z): [M+Na]⁺ calcd. for C₁₁H₁₆N₂NaS: 231.0932, found: 231.0940**.**

2-Cyclohexylbenzofuran (3rb):

The title compound was prepared according to general procedure **GP2.** Solution 1: 2-chlorobenzofuran (152.0 mg, 1.0 mmol, 1.0 equiv), Fe(acac)₃ (17.7 mg, 5 mol%) in dry THF (2.5 mL); Solution 2: cyclohexylmagnesium chloride (1.5 mL, 1.5 equiv.), SIPr-HCl (42.7mg, 10 mol%), in dry THF (1.0 mL) at 25 °C with the residence time of 20 minutes. Purification via chromatography (pentane, 100%) gave the desired product **3rb** as colorless oil in 75% yield (150.0 mg). **¹H NMR** (400 MHz, Chloroform-*d*) δ δ 7.51-7.42(m, 2H), 7.20(td, J = 6.8, 1.6 Hz), 6.36(s, 1H), 2.78 (tt, *J* = 11.2, 3.6 Hz, 1H), 2.17 − 2.07 (m, 2H), 1.86 (dt, *J* = 12.3, 3.5 Hz, 2H), 1.79-1.73(m, 1H), 1.56 − 1.33 (m, 4H), 1.32 (ddt, *J* = 15.6, 12.1, 5.6 Hz, 1H). **¹³C NMR** (101 MHz, CDCl₃): δ 164.05, 154.37, 128.87, 122.96, 122.26, 120.24, 110.70, 99.75, 37.58, 31.32, 26.08, 25.92.

1-Methoxy-4-propylbenzene (3ha):

The title compound was prepared according to general procedure **GP2.** Solution 1: 1-chloro-4-methoxybenzene (285.2 mg, 2.0 mmol, 1.0 equiv), Fe(acac)₃ (14.2 mg, 2 mol%) in dry THF (5.0 mL); Solution 2: SIPr-HCl (34.2 mg, 4 mol%), propylmagnesium bromide (2.0 M in Et₂O solution), (1.5 mL, 1.5 equiv.) in 3.5 mL THF at 25 °C with 20 minutes residence time. Purification via chromatography (pentane, 100%) gave the desired product **3ha** as colorless oil in 95% yield (285.0 mg). **¹ H NMR** (400 MHz, CDCl₃): δ 7.12 (d, *J* = 8.0 Hz, 2H), 6.85 (d, *J* = 8.0 Hz, 2H), 3.81 (s, 3H), 2.56 (t, *J* = 8.0 Hz, 2H), 1.67-1.58 (m, 2H), 0.98-0.90 (m, 3H). **¹³C NMR** (101 MHz, CDCl₃): δ157.63, 134.79, 129.28, 113.61, 55.21, 37.14, 24.78, 13.76.

2-Propylbenzo[d]thiazole (3ra):

The title compound was prepared according to general procedure **GP2.** Solution 1: 2-chlorobenzo[d]thiazole (378.0 mg, 2.0 mmol, 1.0 equiv), Fe(acac)₃ (35.3 mg, 5 mol%) in dry THF (5.0 mL); Solution 2: SIPr-HCl (128.1 mg, 15 mol%), propylmagnesium bromide (2.0 M in Et₂O solution) (1.5 mL, 1.5 equiv.) in 3.5 mL THF at 25 °C with 20 minutes residence time. Purification via chromatography (pentane/EtOAc, 90%) gave the desired product **3ra** as colorless oil in 55% yield (194.8mg). **¹ H NMR** (400 MHz, CDCl₃): δ 7.98 (d, *J* = 8.0 Hz, 1H), 7.85 (d, *J* = 8.0, Hz, 1H), 7.46 (ddd, *J* = 8.2, 7.2, 1.3 Hz, 1H), 7.35 (ddd, *J* = 8.3, 7.2, 1.2 Hz, 1H), 3.11 (dd, *J* = 8.0, 7.2 Hz, 2H), 1.93 (h, *J* = 7.4 Hz, 2H), 1.07 (t, *J* = 7.4 Hz, 3H). **¹³C NMR** (101 MHz, CDCl₃): δ172.16, 153.25, 135.14, 125.83, 124.59, 122.49, 121.45, 36.24, 23.08, 13.70.

(4-Methoxybenzyl)trimethylsilane (3hc):

The title compound was prepared according to general procedure **GP4.** 1-Chloro-4-methoxybenzene (142.6 mg, 1.0 mmol, 1.0 equiv), (Trimethylsilyl)methylmagnesium chloride solution (1.0 M in diethyl ether)(1.5 mL, 1.5 equiv.), SIPr-HCl (128.1mg, 30 mol%), Fe(acac)₃ (35.3mg, 10 mol%) in dry THF (5 mL) at the irradiation of blue LED in batch for 4 hours. Purification via chromatography (pentane, 100%) gave the desired product **3hc** as colorless oil in 73% yield (142.0 mg). **¹ H NMR** (400 MHz, CDCl₃): δ 6.93 (d, *J* = 4.0 Hz, 2H), 6.79 (d, *J* =

155

8.0 Hz, 2H), 3.79 (s, 3H), 2.02(s, 2H), 0.01 (s, 9H). **¹³C NMR** (101 MHz, CDCl₃): δ156.49, 132.33, 128.78, 113.64, 55.23, 25.49, -1.94.

5-((Trimethylsilyl)methyl)-1H-indole (3nc):

The title compound was prepared according to general procedure **GP4.** 5-Chloro-1H-indole (151.0 mg, 1.0 mmol, 1.0 equiv), (trimethylsilyl)methylmagnesium chloride solution (1.0 M in diethyl ether) (2.5 mL, 2.5 equiv.), SIPr-HCl (128.1mg, 30 mol%), Fe(acac)₃ (35.3mg, 10 mol%) in dry THF (2.5 mL) at the irradiation of blue LED in batch for 4 hours. Purification via chromatography (pentane/EtOAc, 90%) gave the desired product **3nc** as colorless oil in 75% yield (152.3 mg). **¹H NMR** (400 MHz, CDCl₃): δ 7.88 (brs, 1H), 7.26-7.23 (m, 1H), 7.20 (d, *J* = 8.0 Hz, 1H), 7.08 (s, 1H), 6.87-6.84 (m, 1H), 6.44-6.42 (m, 1H), 2.16 (d, *J* = 4.0 Hz, 2H), 0.00 (s, 9H). **¹³C NMR** (101 MHz, CDCl₃): δ 133.43, 131.41, 128. 17, 123.96, 123.93, 123.19, 119.01, 110.50, 110.47, 101.88, 26.54, -1.81.

4-(4-Methoxyphenyl)tetrahydro-2H-pyran (3hd):

The title compound was prepared according to general procedure **GP2.** Solution 1: 1-chloro-4-methoxybenzene (284.0 mg, 2.0 mmol, 1.0 equiv), Fe(acac)₃ (35.3 mg, 5 mol%) in dry THF (5.0 mL); Solution 2: (tetrahydro-2H-pyran-4-yl)magnesium bromide (5.0 mL, 1.5 equiv.), SIPr-HCl (128.1 mg, 15 mol%) at 25 °C at the residence time of 20 minutes. Purification via chromatography (pentane, 100%) gave the desired product **3hd** as colorless oil in 70% yield (268.9 mg). **¹H NMR** (400 MHz, CDCl₃): δ 7.18-7.14 (m, 2H), 6.90-6.86(m, 2H), 4.11-4.06 (m, 2H), 3.09 (s, 3H), 3.57-3.50 (m, 2H), 2.72 (tt, *J* = 10.9, 4.9 Hz, 1H), 1.83–1.74 (m, 4H). **¹³C NMR** (101 MHz, CDCl₃): δ158.00, 138.07, 127.54, 113.84, 68.40, 55.21, 40.66, 34.17.

5-(Tetrahydro-2H-pyran-4-yl)-1H-indole (3nd):

The title compound was prepared according to general procedure **GP2.** Solution 1: 5-chloro-1H-indole (151.0 mg, 1.0 mmol, 1.0 equiv), Fe(acac)₃ (17.7 mg, 5 mol%) in dry THF (3.4 mL); Solution 2: (tetrahydro-2H-pyran-4-yl)magnesium bromide (3.4 mL, 2.0 equiv.), SIPr-HCl (64.0 mg, 15 mol%), at 40 °C at the residence time of 20 minutes. Purification via chromatography (pentane/EtOAc, 90%) gave the desired product **3nd** as white solid in 70% yield (141.0 mg). Melting point: 122.0 ºC. **¹H NMR** (400 MHz, CDCl₃): δ 8.17 (brs, 1H), 7.52 (d, *J* = 1.6 Hz, 1H), 7.36 (d, *J* = 8.4 Hz, 1H), 7.21 (t, *J* = 2.8 Hz, 1H), 7.11 (dd, *J* = 8.4, 1.7 Hz, 1H), 6.56 – 6.50 (m, 1H), 4.18 – 4.09 (m, 2H), 3.59 (td, *J* = 11.6, 2.4 Hz, 2H), 2.92 – 2.76 (m, 1H), 2.06 – 1.76 (m, 4H). **¹³C NMR** (101 MHz, CDCl₃): δ137.52, 134.58, 128.03, 124.47, 121.37, 118.07, 110.94, 102.40, 68.63, 41.68, 34.68.

5-(Tetrahydro-2H-pyran-4-yl)-1H-indole (4od):

The title compound was prepared according to general procedure **GP3.** Solution 1: 5-chloro-1H-pyrrolo[2,3-b]pyridine (152.0 mg, 1.0 mmol, 1.0 equiv), Fe(acac)₃ (17.7 mg, 5 mol%) in dry THF (4.2 mL); Solution 2: (tetrahydro-2H-pyran-4-yl)magnesium bromide(4.2 mL, 2.5 equiv.), isopropylmagnesium chloride (1.0 M in THF) (0.3 mL, 0.3 equiv.), SIPr-HCl (128.1 mg, 15 mol%), at 25 °C at the residence time of 20 minutes. Purification via chromatography (pentane/EtOAc, 90%) gave the desired product **4od** as colorless oil in 78% yield (315.3 mg). **¹H NMR** (500 MHz, CDCl₃) δ 10.93 (s, 1H), 8.26 (d, *J* = 2.1 Hz, 1H), 7.83 (d, *J* = 2.0 Hz, 1H), 7.38 (dd, *J* = 3.6, 1.4 Hz, 1H), 6.49 (dd, *J* = 3.5, 0.9 Hz, 1H), 4.13 (dd, *J* = 11.6, 4.4, Hz, 2H), 3.59 (td, *J* = 11.8,

2.2 Hz, 2H), 2.91 (tt, J = 12.0, 4.0 Hz, 1H), 1.97-1.91 (m, 2H), 1.86 – 1.82 (m, 2H). **¹³C NMR** (126 MHz, CDCl₃) δ 147.90, 142.22, 133.21, 126.57, 125.52, 120.29, 100.40, 68.44, 39.36, 34.53, 34.51.

3-(Tetrahydro-2H-pyran-4-yl)pyridine (3sd):

The title compound was prepared according to general procedure **GP3.** Solution 1: 5-chloro-1H-pyrrolo[2,3-b]pyridine (226.0 mg, 2.0 mmol, 1.0 equiv), Fe(acac)₃ (35.3 mg, 5 mol%) in dry THF (5.0 mL); Solution 2: (tetrahydro-2H-pyran-4-yl)magnesium bromide (0.6 M in THF) (5.0 mL, 1.5 equiv.), SIPr-HCl (128.1 mg, 15 mol%) at 25 °C at the residence time of 20 minutes. Purification via chromatography (DCM) gave the desired product **3sd** as colorless oil in 95% yield (309.9 mg). **¹H NMR** (400 MHz, CDCl₃) δ 8.51 (d, J = 2.3 Hz, 1H), 8.48 (dd, J = 4.8, 1.6 Hz, 1H), 7.54 (dt, J = 7.9, 2.0 Hz, 1H), 7.27 – 7.19 (m, 1H), 4.14 – 4.07 (m, 2H), 3.55 (td, J = 11.5, 2.8 Hz, 2H), 2.85 – 2.74 (m, 1H), 1.97 – 1.72 (m, 4H) .**¹³C NMR** (101 MHz, CDCl₃): δ148.87, 147.90, 133.98, 123.47, 68.15, 39.12, 33.54.

4-(4-Methoxyphenyl)-1-methylpiperidine (3he):

The title compound was prepared according to general procedure **GP3.** Solution 1: 1-chloro-4methoxybenzene (284.0 mg, 2.0 mmol, 1.0 equiv), Fe(acac)₃ (35.3 mg, 5 mol%) in dry THF (5.0 mL); Solution 2: (1-methylpiperidin-4-yl)magnesium bromide (4.3 mL, 1.5 equiv.), isopropylmagnesium chloride (1.0 M in THF) (0.3 mL, 0.3 equiv.), SIPr-HCl (128.1 mg, 15 mol%), in dry THF (0.7 mL) at 25 °C with the residence time of 20 minutes. Purification via chromatography (pentane/EtOAc, 90%) gave the desired product **3he** as colorless oil in 85% yield (348.8 mg). **¹H NMR** (400 MHz, CDCl₃) δ 7.15 (d, J = 7.1 Hz, 2H), 6.85(d, J = 7.1 Hz, 2H), 3.79 (s, 3H), 2.99-2.96 (m, 2H), 2.46-2.39 (m, 1H), 2.33 (d, J = 1.9 Hz, 3H), 2.05 (td, J = 12.2, 3.1 Hz, 2H), 1.84–1.76 (m, 4H). **¹³C NMR** (101 MHz, CDCl₃): δ157.87, 138.44, 127.65, 113.76, 56.39, 55.20, 46.44, 41.13, 33.69.

Associated Content

The *Supporting Information* for this article is available free of charge on the Willey Publications website at https://doi.org/10.1002/anie.201906462

Reference:

(1) Busch, M.; Wodrich, M. D.; Corminboeuf, C. *ACS Catal.* **2017**, *7*, 5643-5653.

(2) Johansson Seechurn, C. C. C.; Kitching, M. O.; Colacot, T. J.; Snieckus, V. *Angew. Chem. Int. Ed.* **2012**, *51*, 5062-5085.

(3) Tasker, S. Z.; Standley, E. A.; Jamison, T. F. *Nature* **2014**, *509*, 299.

(4) (a)Corriu, R. J. P.; Masse, J. P. *J. Chem. Soc., Chem. Commun.* **1972**, 10.1039/C3972000144A, 144a-144a; (b)Tamao, K.; Sumitani, K.; Kumada, M. *J. Am. Chem. Soc.* **1972**, *94*, 4374-4376.

(5) Hockin, B. M.; Li, C.; Robertson, N.; Zysman-Colman, E. *Catal. Sci. Technol.* **2019**, *9*, 889-915.

(6) (a)Gopalaiah, K. *Chem. Rev.* **2013**, *113*, 3248-3296; (b)Jia, F.; Li, Z. *Org. Chem. Front.* **2014**, *1*, 194-214; (c)Bauer, I.; Knölker, H.-J. *Chem. Rev.* **2015**, *115*, 3170-3387; (d)Fürstner, A. *ACS Cent. Sci.* **2016**, *2*, 778-789.

(7) (a)Kuzmina, O. M.; Steib, A. K.; Moyeux, A.; Cahiez, G.; Knochel, P. *Synthesis* **2015**, *47*, 1696-1705; (b)Guérinot, A.; Cossy, J. *Top. Curr. Chem.* **2016**, *374*, 49; (c)Piontek, A.; Bisz, E.; Szostak, M. *Angew. Chem. Int. Ed.* **2018**, *57*, 11116-11128.

(8) Kharasch, M. S.; Tawney, P. O. *J. Am. Chem. Soc.* **1941**, *63*, 2308-2316.

(9) (a)Kwan, C. L.; Kochi, J. K. *J. Am. Chem. Soc.* **1976**, *98*, 4903-4912; (b)Smith, R. S.; Kochi, J. K. *J. Org. Chem.* **1976**, *41*, 502-509; (c)Tamura, M.; Kochi, J. K. *J. Am. Chem. Soc.* **1971**, *93*, 1487-1489.

(10) (a)Cahiez, G.; Avedissian, H. *Synthesis* **1998**, *1998*, 1199-1205; (b)Dohle, W.; Kopp, F.; Cahiez, G.; Knochel, P. *Synlett* **2001**, *2001*, 1901-1904.

(11) (a)Fürstner, A.; Leitner, A. *Angew. Chem. Int. Ed.* **2002**, *41*, 609-612; (b)Fürstner, A.; Leitner, A.; Méndez, M.; Krause, H. *J. Am. Chem. Soc.* **2002**, *124*, 13856-13863.

(12) Tatsuo, K.; Masayuki, U. *Chem. Lett.* **1991**, *20*, 2073-2076.

(13) (a)Rushworth, P. J.; Hulcoop, D. G.; Fox, D. J. *J. Org. Chem.* **2013**, *78*, 9517-9521; (b)Cahiez, G.; Lefèvre, G.; Moyeux, A.; Guerret, O.; Gayon, E.; Guillonneau, L.; Lefèvre, N.; Gu, Q.; Zhou, E. *Org. Lett.* **2019**, *21*, 2679-2683.

(14) (a)Perry, M. C.; Gillett, A. N.; Law, T. C. *Tetrahedron Lett.* **2012**, *53*, 4436-4439; (b)Agata, R.; Iwamoto, T.; Nakagawa, N.; Isozaki, K.; Hatakeyama, T.; Takaya, H.; Nakamura, M. *Synthesis* **2015**,

47, 1733-1740; (c)Agata, R.; Takaya, H.; Matsuda, H.; Nakatani, N.; Takeuchi, K.; Iwamoto, T.; Hatakeyama, T.; Nakamura, M. *Bull. Chem. Soc. Jpn.* **2019**, *92*, 381-390.

(15) (a)O'Brien, H. M.; Manzotti, M.; Abrams, R. D.; Elorriaga, D.; Sparkes, H. A.; Davis, S. A.; Bedford, R. B. *Nature Catalysis* **2018**, *1*, 429-437; (b)Jin, M.; Adak, L.; Nakamura, M. *J. Am. Chem. Soc.* **2015**, *137*, 7128-7134; (c)Bedford, R. B.; Carter, E.; Cogswell, P. M.; Gower, N. J.; Haddow, M. F.; Harvey, J. N.; Murphy, D. M.; Neeve, E. C.; Nunn, J. *Angew. Chem. Int. Ed.* **2013**, *52*, 1285-1288; (d)Guisán-Ceinos, M.; Tato, F.; Buñuel, E.; Calle, P.; Cárdenas, D. J. *Chem. Sci.* **2013**, *4*, 1098-1104; (e)Adams, C. J.; Bedford, R. B.; Carter, E.; Gower, N. J.; Haddow, M. F.; Harvey, J. N.; Huwe, M.; Cartes, M. Á.; Mansell, S. M.; Mendoza, C.; Murphy, D. M.; Neeve, E. C.; Nunn, J. *J. Am. Chem. Soc.* **2012**, *134*, 10333-10336; (f)Hatakeyama, T.; Okada, Y.; Yoshimoto, Y.; Nakamura, M. *Angew. Chem. Int. Ed.* **2011**, *50*, 10973-10976; (g)Hatakeyama, T.; Hashimoto, T.; Kondo, Y.; Fujiwara, Y.; Seike, H.; Takaya, H.; Tamada, Y.; Ono, T.; Nakamura, M. *J. Am. Chem. Soc.* **2010**, *132*, 10674-10676; (h)Hatakeyama, T.; Hashimoto, S.; Ishizuka, K.; Nakamura, M. *J. Am. Chem. Soc.* **2009**, *131*, 11949-11963.

(16) (a)Abdiaj, I.; Fontana, A.; Gomez, M. V.; de la Hoz, A.; Alcázar, J. *Angew. Chem. Int. Ed.* **2018**, *57*, 8473-8477; (b)Abdiaj, I.; Huck, L.; Mateo, J. M.; de la Hoz, A.; Gomez, M. V.; Díaz-Ortiz, A.; Alcázar, J. *Angew. Chem. Int. Ed.* **2018**, *57*, 13231-13236.

(17) (a)Casnati, A.; Gemoets, H. P. L.; Motti, E.; Della Ca', N.; Noël, T. *Chem. Eur. J.* **2018**, *24*, 14079-14083; (b)Gemoets, H. P. L.; Laudadio, G.; Verstraete, K.; Hessel, V.; Noël, T. *Angew. Chem. Int. Ed.* **2017**, *56*, 7161-7165; (c)Sharma, U. K.; Gemoets, H. P. L.; Schröder, F.; Noël, T.; Van der Eycken, E. V. *ACS Catalysis* **2017**, *7*, 3818-3823; (d)Gemoets, H. P. L.; Hessel, V.; Noël, T. *Org. Lett.* **2014**, *16*, 5800-5803; (e)Noël, T.; Kuhn, S.; Musacchio, A. J.; Jensen, K. F.; Buchwald, S. L. *Angew. Chem. Int. Ed.* **2011**, *50*, 5943-5946; (f)Noël, T.; Naber, J. R.; Hartman, R. L.; McMullen, J. P.; Jensen, K. F.; Buchwald, S. L. *Chem. Sci.* **2011**, *2*, 287-290.

(18) (a)Noël, T.; Buchwald, S. L. *Chem. Soc. Rev.* **2011**, *40*, 5010-5029; (b)Cantillo, D.; Kappe, C. O. *ChemCatChem* **2014**, *6*, 3286-3305.

(19) (a)Nakamura, M.; Ito, S.; Matsuo, K.; Nakamura, E. *Synlett* **2005**, *2005*, 1794-1798; (b)Bedford, R. B.; Huwe, M.; Wilkinson, M. C. *Chem. Comm.* **2009**, 10.1039/B818961G, 600-602.

(20) (a)Campbell, P. S.; Jamieson, C.; Simpson, I.; Watson, A. J. B. *Chem. Comm.* **2018**, *54*, 46-49; (b)Mayol-Llinàs, J.; Farnaby, W.; Nelson, A. *Chem. Comm.* **2017**, *53*, 12345-12348.

(21) Huck, L.; de la Hoz, A.; Díaz-Ortiz, A.; Alcázar, J. *Org. Lett.* **2017**, *19*, 3747-3750.

(22) For compounds **3od-3he** the addition of 0.3 equiv. of *i*PrMgBr at the beginning of the reaction was found to be beneficial. We believe this acts as a base to deprotonate the NHC precursor.

(23) (a)Cassani, C.; Bergonzini, G.; Wallentin, C.-J. *ACS Catal.* **2016**, *6*, 1640-1648; (b)Parchomyk, T.; Koszinowski, K. *Synthesis* **2017**, *49*, 3269-3280; (c)Sears, J. D.; Neate, P. G. N.; Neidig, M. L. *J. Am. Chem. Soc.* **2018**, *140*, 11872-11883; (d)Bedford, R. B. *Acc. Chem. Res.* **2015**, *48*, 1485-1493.

(24) Fürstner, A.; Martin, R.; Krause, H.; Seidel, G.; Goddard, R.; Lehmann, C. W. *J. Am. Chem. Soc.* **2008**, *130*, 8773-8787.

(25) (a)Kleimark, J.; Hedström, A.; Larsson, P.-F.; Johansson, C.; Norrby, P.-O. *ChemCatChem* **2009**, *1*, 152-161; (b)Kleimark, J.; Larsson, P.-F.; Emamy, P.; Hedström, A.; Norrby, P.-O. *Adv. Synth. Catal.* **2012**, *354*, 448-456.

(26) As the spectroscopic studies could not be accurately performed under the typical reaction conditions, and no well-defined Fe species were employed for such investigations (reaction components were reacted in-situwith the catalyst precursor), the proposed catalytic cycle is not certain. Under such conditions, a variety of Fe species might be present in solution with different coordination, ligand environment and/or oxidation state, likely very dynamic under the reaction conditions. Different mechanistic pathways might also be possible, such as for example the excitation of a Fe species, which then acts as a photoredox catalyst; see: R. Kancherla, K. Muralirajan, A. Sagadevan, M. Rueping, *Trends Chem.*, 10.1016/j.trechm.2019.03.012

(27). Frisch, M. J. *et al*. Gaussian 09, Revision D.01 (Gaussian Inc., Wallingford, CT, 2013).

(28) Becke, A. D. *J. Chem. Phys.* **1993**, *98*, 5648-5652.

(29) Lee, C. W. Yang, R. G. Parr, *Phys. Rev. B* **1988**, *37*, 785-789.

(30) Grimme, S.; Ehrlich, S.; Goerigk, L. *J. Comp. Chem* **2011**, *32*, 1456-1465.

(31) Krishnan, R.; Binkley, J. S.; Seeger, R.; Pople, J. A. *J. Chem. Phys.* **1980**, *72*, 650-654.

(32) Stevens, W. J.; Krauss, M.; Basch, H.; Jasien, P. G. *Can. J. Chem.* **1992**, *70*, 612-630.

(33) (a) Casida, M. E.; Jamorski, C.; Casida, K. C.; Salahub, D. R. *J. Chem. Phys.* **1998**, *108*, 4439-4449; (b) Stratmann, R. E.; Scuseria, G. E.; Frisch, M. J. *J. Chem. Phys.* **1998**, *109*, 8218-8224.

(34) (a) Cossi, M.; Barone, V. *J. Chem. Phys.* **2001**, *115*, 4708-4717; (b) Barone, V.; Cossi, M. *J. Phys. Chem. A* **1998**, *102*, 1995-2001; (c) Tomasi, J.; Mennucci, B.; Cammi, R. *Chem, Rev.* **2005**, *105*, 2999-3094.

(35) O'boyle, N. M.; Tenderholt, A. L.; Langner, K. M. *J. Comp. Chem* **2008**, *29*, 839-845.

160

(36) Reddy, S. L.; Endo, T.; Reddy, G. S. Advanced Aspects of Spectroscopy, Chapter 1, **2012** http://dx.doi.org/10.5772/50128

.

Chapter 6:

Iron-Catalyzed Cross-Coupling of Alkynyl and Styrenyl Chlorides with Alkyl Grignard Reagents in Batch and Flow

Abstract

Transition-metal-catalyzed cross-coupling chemistry can be regarded as one of the most powerful protocols to construct carbon-carbon bonds. While the field is still dominated by palladium catalysis, there is an increasing interest to develop protocols which utilize cheaper and more sustainable metal sources. Herein, we report a selective, practical and fast iron-based cross-coupling reaction which enables the formation of Csp–Csp^3 and Csp^2–Csp^3 bonds. In a telescoped flow process, the reaction can be combined with the Grignard reagent synthesis. Moreover, flow allows to avoid the use of a supporting ligand without eroding the reaction selectivity.

Introduction

Transition-metal-catalyzed cross-coupling reactions serve as one of the most powerful protocols to construct carbon-carbon and carbon-heteroatom bonds in a variety of biologically active molecules,[1] natural products[2] and functional materials.[3] To date, the workhorse of cross-coupling chemistry has been palladium, which in combination with suitable ligands allowed to enact high catalytic efficiency for a wide variety of electrophile-nucleophile combinations.[4] However, due to the scarcity and increasing cost of palladium and the stringent heavy metal regulations in the pharmaceutical industry, alternatives for palladium are currently of high interest.[5] Amongst potential candidates, earth-abundant first row transition metals provide arguably the highest likelihood to replace palladium due to their reduced cost and low toxicity.[6] In this regard, iron has received substantial attention as it is a metal with minimum safety concern and it provides many catalytic options as its oxidation states range from –II to +VI.[7] However, despite the great potential to cover essentially all relevant catalytic transformations in organic synthesis, reality is different and iron proves to be notorious to tame, hindering its widespread adoption.[8]

While the classical Sonogashira reaction enables the efficient coupling between aryl halides and terminal alkynes,[9] metal-catalyzed Csp–Csp^3 couplings are very rare (**Scheme 6.1**). Cahiez *et al.* found that alkyl-alkynyl cross-coupling can be achieved using copper catalysis and slow addition of the Grignard coupling partner.[10] A cobalt-enabled coupling between bromoalkynes and organozinc halide nucleophiles was described by Gosmini and coworkers. The groups of Nakamura[11] and Hu[12] developed iron-catalyzed protocols to couple alkyl bromides and iodides with alkynyl Grignard reagents.[13] In search of synthetically useful Fe-catalyzed cross-coupling reactions,[14] we describe herein our efforts to develop a robust protocol to cross-couple both styrenyl and alkynyl chlorides with alkyl Grignard reagents using an Fe catalyst and an NHC ligand.[15] This method provides a set of conditions which are both practical and widely applicable in Csp–Csp^3 and Csp^2–Csp^3 bond forming reactions. Interestingly, the Fe-based coupling reaction could be translated to flow and was combined with an inline generation of Grignard reagents. Furthermore, the flow strategy allowed to carry out the reaction at mild conditions and to avoid the use of an NHC ligand, thus simplifying the overall process.

Copper catalysis (Cahiez et al.)

R─≡─Br + XMg─R' →(CuCl₂ / N-methylpyrrolidinone / THF, 0 °C)→ R─≡─R'

R = Alkyl, Aryl   R' = Alkyl, Aryl

$CuCl_2$
N-methylpyrrolidinone
THF, 0 °C
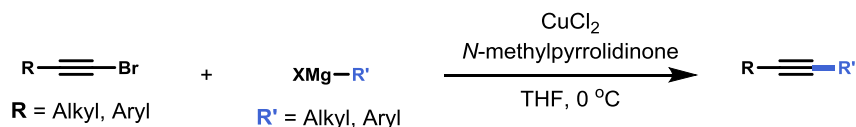
Cobalt catalysis (Gosmini et al.)

R─≡─Br + XZn─R' →→ R─≡─R'

R = Alkyl, Aryl   R' = Aryl

$CoBr_2$
PPh_3 or phenanthroline
CH_3CN, 0 °C
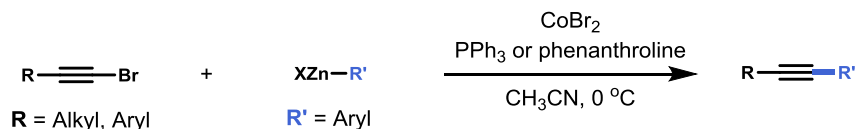
Iron catalysis (Nakamura *et al.*; Hu *et al.*)

R─≡─MgBr + X─R' →→ R─≡─R'

R = Alkyl, Aryl   R' = Alkyl
X = Br, I

$FeCl_2$(bisphosphine)
$FeBr_2$ (Hu)
THF/NMP, rt - 60 °C
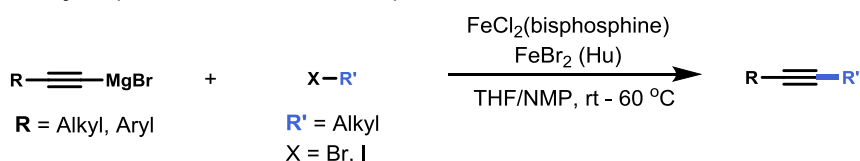
This work: Iron-catalyzed Csp-Csp³ and Csp²-Csp³ cross-coupling

R─≡─Cl
or
R─CH=CH─Cl

+ XMg─R'

R' = Alkyl, Aryl

Fe(acac)₃ (1 mol%)
SIPr·HCl (2 mol%)
THF, 0 °C - RT, 3 min

→ R─≡─R'
or
R─CH=CH─R'

R = Aryl
chlorinated starting materials

- convenient Fe source
- broad scope
- high selectivity
- mild reaction conditions
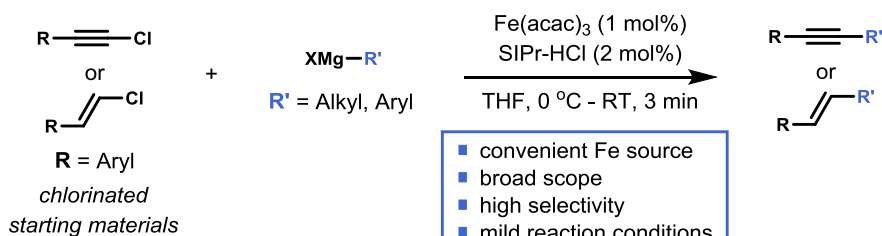
Scheme 6.1. Established metal-catalyzed C*sp*–C*sp³* coupling reactions and reaction design of an Fe-based protocol to enable the C*sp*–C*sp³* and C*sp²*–C*sp³* coupling.

Experimental Section

Initial cross-coupling experiments started with 1-chloro-2-phenylacetylene as a benchmark substrate and cyclohexyl-magnesium chloride in ethereal solvents at 0°C (**Table 6.1**). With $FeCl_3·6H_2O$ as the iron source, the use of THF as a solvent was preferred over Et_2O (**Table 6.1**, Entries 1 and 2). In both cases, substantial amounts of byproducts were observed resulting from homocoupling (**2a'**) and reduction (**2a''**). Switching to an $FeCl_2·4H_2O$ catalyst resulted in a diminished reactivity (**Table 6.1**, Entry 3). A higher selectivity and reactivity for the desired cross-coupled product (**2a**) was observed using Fe(acac)₃ (**Table 6.1**, Entry 4). However, the highest selectivities were obtained when catalyst complexes arising from Fe(acac)₃ and NHC ligands were used, with the SIPr ligand providing the best results in terms of reaction efficiency and selectivity. (**Table 6.1**, Entries 5-6). A lower selectivity was observed when the reaction temperature was raised to room temperature (**Table 6.1**, Entry 7).
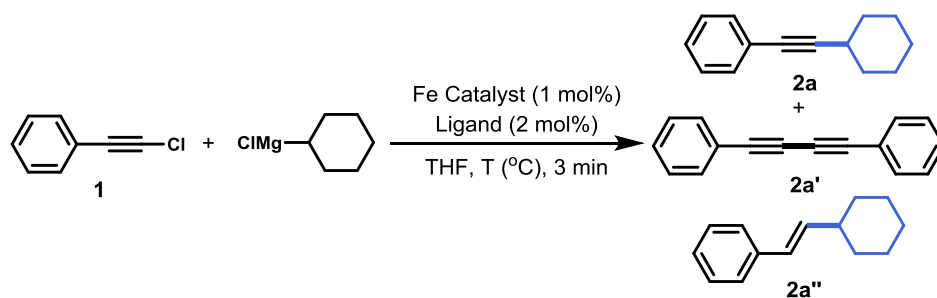
Entry	Catalyst	Ligand	T ($^\circ$C)	Conv.(%)	2a (%)	2a' (%)	2a'' (%)
1[a]	FeCl$_3$·6H$_2$O	--	0 $^\circ$C	88%	66%	5%	18%
2	FeCl$_3$·6H$_2$O	--	0 $^\circ$C	100%	80%	12%	8%
3	FeCl$_2$·4H$_2$O	--	0 $^\circ$C	32%	27%	1%	4%
4	Fe(acac)$_3$	--	0 $^\circ$C	90%	77%	3%	10%
5	Fe(acac)$_3$	L1	0 $^\circ$C	71%	69%	--	2%
6	Fe(acac)$_3$	L2	0 $^\circ$C	100%	97%	1%	2%
7	Fe(acac)$_3$	L2	r.t.	100%	91%	6%	3%
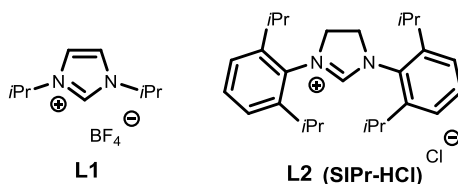
Table 6.1. Optimization of the reaction conditions for the iron-catalyzed cross-coupling between alkynyl chlorides and alkyl Grignard reagents. Standard reaction condition: **1** (0.5 mmol), cyclohexylmagnesium chloride (1.0 M in THF, 0.6 mmol), THF (1.9 mL, 0.2 M), Fe catalyst (1 mol%) and SIPr-HCl (2 mol%). [a]Et$_2$O instead of THF.

With optimal conditions in hand, we probed the generality of his protocol for the coupling of alkynyl chlorides with Grignard reagents (**Figure 6.1**). Various alkynyl chlorides with electron-neutral (**2a**, **2c**, **2d**), electron-withdrawing (**2b**) and electron-donating (**2e**) underwent efficient cross coupling with cyclohexylmagnesium chloride (89-96% yield). 1-chloro-2-phenylacetylene could be efficiently coupled with a diverse set of aliphatic Grignard reagents, including phenylmagnesium chloride (**2f**), propylmagnesium chloride (**2g**), methylmagnesium chloride (**2h**), (trimethylsilyl)methylmagnesium chloride (**2i**), cyclopentyl magnesium chloride (**2j**) (81-93% yield). Also Grignard reagents decorated with medicinally important scaffolds, such as *N*-methylpiperidine

(**2k**), can be tolerated (99% yield). Finally, also aromatic Grignard reagents (**2l**) can be engaged in this protocol furnishing the targeted product in 87% isolated yield.
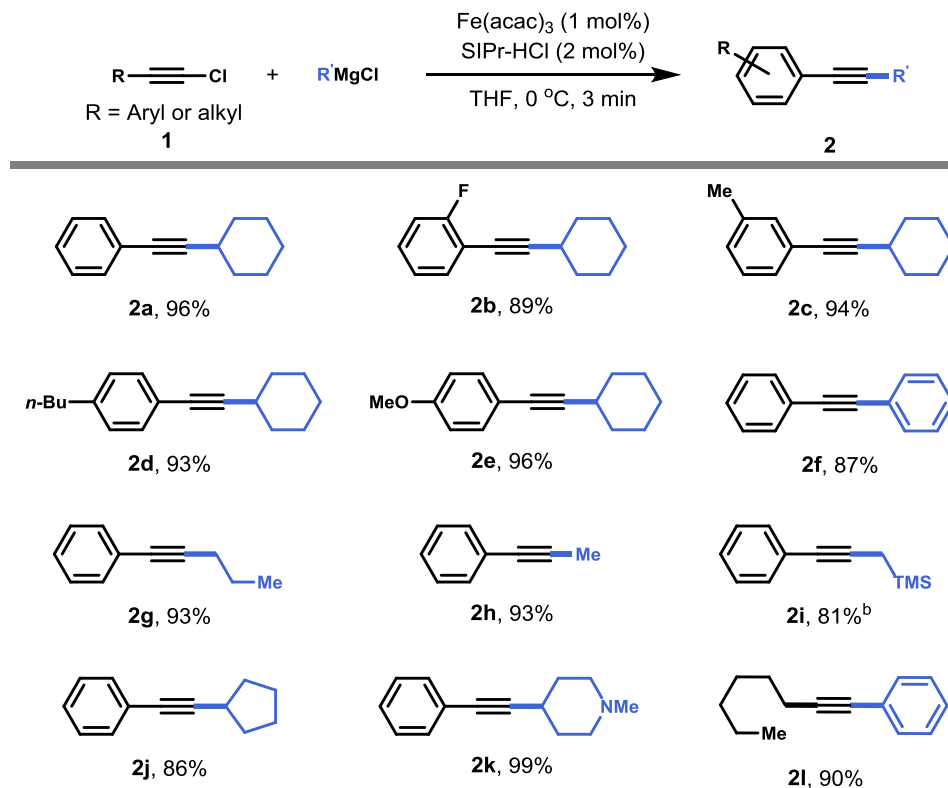
Figure 6.1. Scope of the iron-catalyzed cross-coupling between alkynyl chlorides and alkyl Grignard reagents. Reaction conditions: 0.5 mmol **1**, 0.6 mmol R'MgCl, 1 mol% Fe(acac)$_3$, 2 mol% SIPr-HCl in 2.5 mL THF at 0 °C; [b] 2 mol% Fe(acac)$_3$ and 4 mol% SIPr-HCl.

Expanding the substrate scope to involve styrenyl chlorides in this Fe-catalyzed cross-coupling protocol permitted us to forge Csp^2–Csp^3 bonds as well (**Figure 6.2**). Interestingly, for most substrates, the reaction could be completed at room temperature without adding any supporting ligand. *β*-Chlorostyrene can be rapidly and efficiently coupled with assorted aliphatic (**4a-g**, 90-96% yield) and aromatic (**4h**) (97% yield) Grignard nucleophiles. The protocol is easily scalable without reduced efficiency (**4f**, 8 mmol, 90% yield). *β*-Chlorostyrenes bearing electron-neutral (**4i-l**), electron-donating (**4m-q**) and electron-withdrawing (**4r**) at the ortho, meta and para positions are readily tolerated (89-97% yield). The reaction does not display a great sensitivity to steric hindrance, as both naphthyl substrates (**4s-t**, 91-94% yield) and α-substituted *β*-chlorostyrenes (**4u-v**, 94% yield) were efficiently coupled with cyclohexylmagnesium chloride. Double functionalization was also possible, albeit at a slightly diminished yield (**4w**, 57% yield). The reaction was stereoselective in all

cases and even (*Z*)-*β*-Chlorostyrene was obtained in good yield and with retained stereoselectivity (**4x**, 93% yield).

4a, 90%   **4b**, 97%   **4c**, 96%   **4d**, 93%

4e, 90%[a]   **4f**, 90% (90%)[b]   **4g**, 96%

4h, 97%   **4i**, 97%   **4j**, 93%

4k, 97%   **4l**, 95%   **4m**, 94%

4n, 91%   **4o**, 94%   **4p**, 89%

4q, 90%   **4r**, 91%   **4s**, 91%

4t, 94%   **4u**, 94%   **4v**, 94%

4w, 57% (49%)[c]   **4x**, 93%[d]
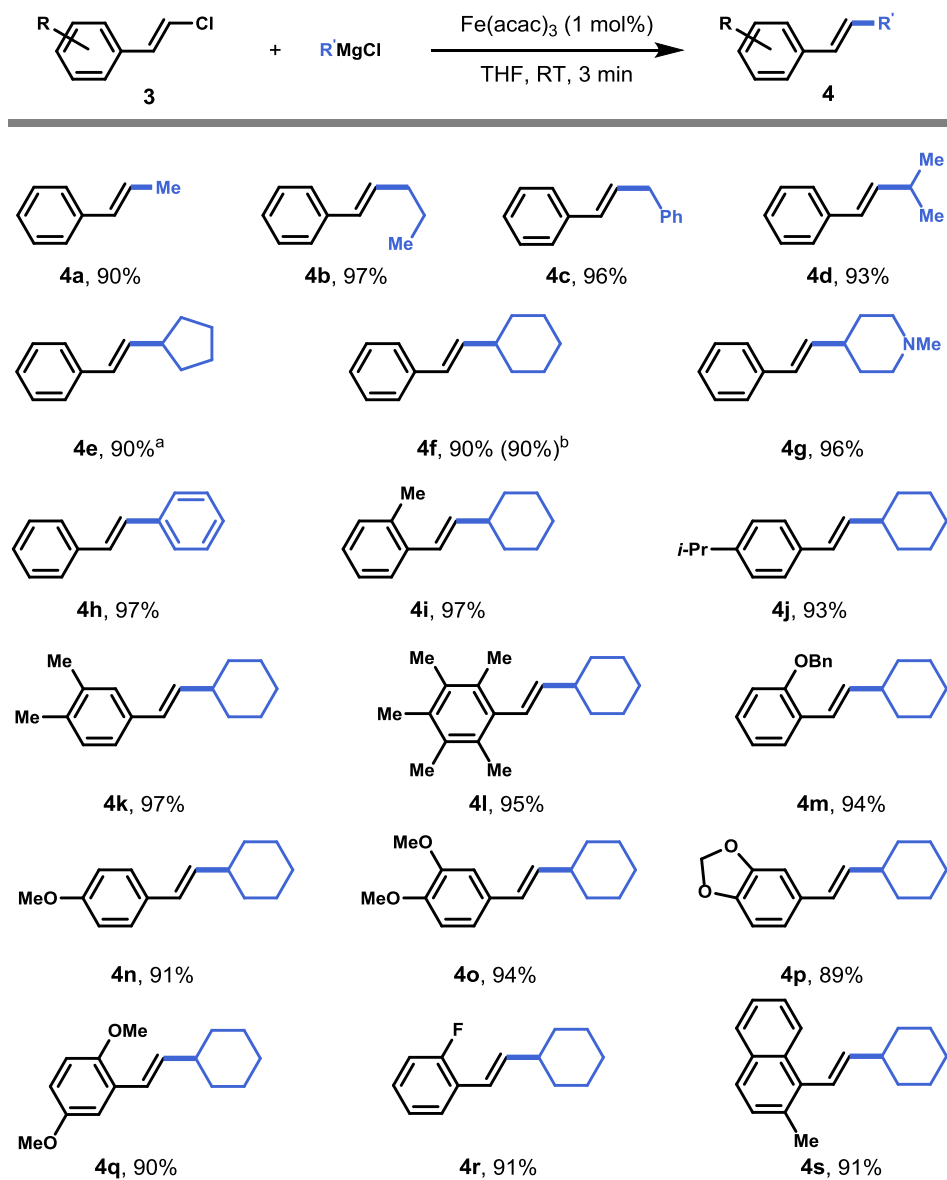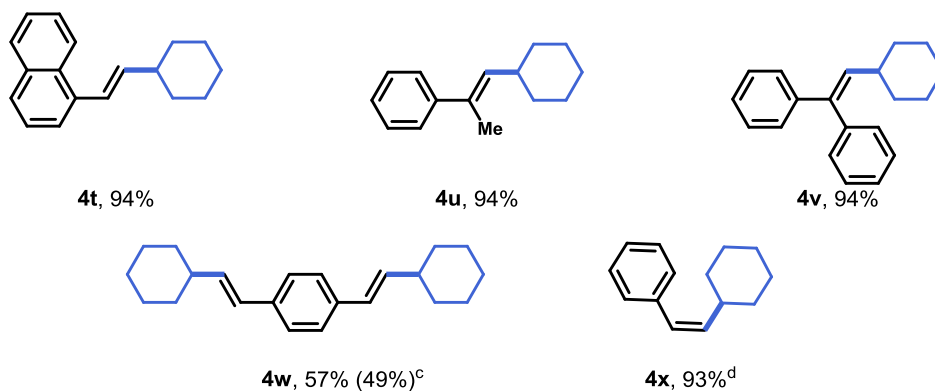
Figure 6.2. Scope of the iron-catalyzed cross-coupling between styrenyl chlorides and alkyl Grignard reagents. Reaction conditions: 0.5 mmol **3**, 0.6 mmol R'MgCl, 1 mol% Fe(acac)$_3$, in 2.5 mL THF at Room Temperature; [a]3 mol% Fe(acac)$_3$ and 6 mol% SIPr-HCl was added. [b]Scale-up experiment on an 8 mmol scale. [c]Scale-up experiment on an 4.7 mmol scale. [d]The *Z/E* ratio of starting material **3x** was 91:9 and of product **4x** was 88:12.

Next, we investigated the possibility to telescope both the Grignard reagent synthesis and the iron-catalyzed cross-coupling transformation in a single, streamlined continuous-flow process. The combination of these two individual steps allows to safely control the exotherm of the Grignard reagent synthesis,[16] to keep the total inventory of potentially hazardous Grignard reagents low and to use cheap organohalides as starting materials.[17] For the preparation of the Grignard reagent, we filled an open column with magnesium according to the procedure reported by Alcazar *et al*[18]. Over this magnesium packed-bed reactor, a solution of alkyl bromide was directed and the generated Grignard reagent was merged with the reagents required for the Fe-catalyzed cross coupling transformation (**Table 6.2**).[19] The combined reaction mixture was fed to a capillary microreactor (perfluoroalkoxy alkane, PFA; 750 μm ID). The coupling between *β*-chlorostyrene and *n*-pentylmagnesium bromide resulted in the formation of the corresponding cross-coupled product in 95% isolated yield, requiring only 30 s residence time (**Table 6.2**, Entry 1). Next, *β*-chlorostyrene and 1-chloro-2-phenylacetylene can be reacted with *in situ*-generated 3-butenylmagnesium bromide (**Table 6.2**, Entries 2-3). Interestingly, the yield and selectivity in flow was systematically higher due a better dissipation of the reaction exotherm, which can be attributed to the increased surface-to-volume ratio, and to the enhanced mixing efficiency in the microreactor setup (**Table 6.2**, Entry 3-5).[20] Furthermore, this feature allowed to avoid the addition of a supporting NHC ligand without deterioration of the selectivity of the transformation.
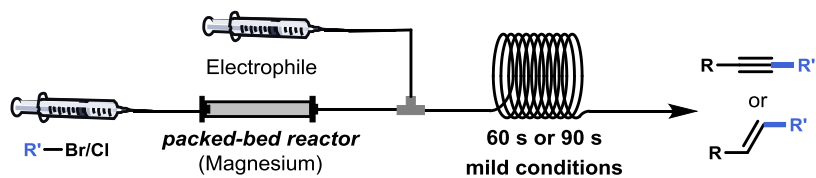
Entry	R—Br	Electrophile	Residence Time[e]	Product [f]
1[a]		3a	30 s	5a Flow: 95% (5a) + 3% homocoupling
2[b]		3a	90 s	5b Flow: 91% (5b) + 5% homocoupling
3[c]		1a	60 s	5c Flow: 95% (5c) + 3% homocoupling Batch: 50% (5c) + 49% homocoupling
4[d]		1a	60 s	5d Flow: 96% (5d) + 2% homocoupling
5[d]		1a	60 s	5e Flow: 94% (5e) + 3% homocoupling
6[d]		1a	60 s	5f Flow: 94% (5f) + 3% homocoupling
7[d]		1a	60 s	5g Flow: 98% (5g) + 1% homocoupling
8[d]		1a	60 s	5h Flow: 97% (5h) + 2% homocoupling

9^d · **1a** · **60 s**

5i
Flow: 94% (**5i**) + 2% homocoupling

10^d · **1a** · **60 s**

Me

5j
Flow: 95% (**5j**) + 3% homocoupling

11^d · **1a** · **60 s**

CF$_3$

5k
Flow: 97% (**5k**) + 1% homocoupling
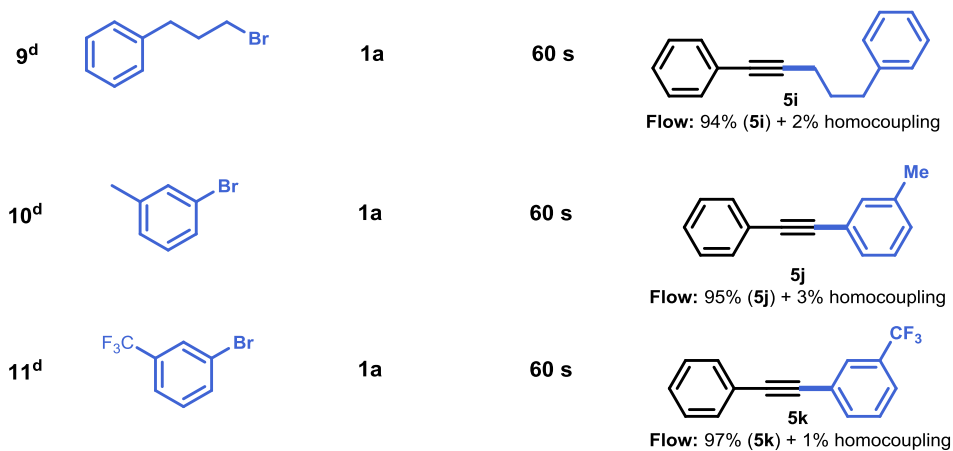
Table 6.2. Telescoped organomagnesium bromide synthesis and iron-catalyzed cross-coupling in flow. ^{a}Fe(acac)$_3$ (1 mol%), electrophile (0.31 M), room temperature. ^{b}Fe(acac)$_3$ (2 mol%), electrophile (0.33 M), room temperature. ^{c}Fe(acac)$_3$ (2 mol%), electrophile (0.33 M), 0 °C. ^{d}Fe(acac)$_3$ (1 mol%), electrophile (1 equiv., based on the concentration of the Grignard reagent), 0 °C. ^{e}Residence time denotes the time spent in the capillary microreactor. ^{f}Homocoupling compound was determined by GCMS analysis.

Conclusion

We have developed a practical and mild iron-catalyzed cross-coupling method to establish Csp–Csp^3 and Csp^2–Csp^3 linkages. The protocol utilizes an NHC ligand to efficiently couple alkynyl chlorides and alkyl Grignard reagents, while no supporting ligand is needed for the functionalization of styrenyl chlorides. Interestingly, the Fe-based cross-coupling reaction can be translated to flow and be combined with the synthesis of Grignard reagents in a single, uninterrupted continuous process. Salient feature of the flow protocol is that the use of an NHC ligand can be avoided for the Csp–Csp^3 coupling without compromising the reaction selectivity, which is attributed to the improved temperature control in a microreactor.

Experimental section

General procedure for the synthesis of 1-chloroalkynes GP1

In a dry flask, K_2CO_3 (1 mmol), *N*-Chlorosuccinimide (4 mmol) and Ag_2CO_3 (0.2 mmol) was added under argon atmosphere. Then 4 mL n-propanol and 2 mmol terminal alkyne was added to the reaction system, and the reaction mixture was stirred at 50 °C for 5 hours. After that, the mixture was allowed to cool to room temperature, 10 mL of brine was added to the mixture at 0 °C. The resulting mixture was extracted by ethyl ether for three times (20 mL × 3), the combined organic phase was washed with water (150 mL × 3) to remove the n-propanol, then dried over sodium sulfate. The solvent was removed by rotary evaporation and purified by column chromatography on silica gel to give the final product.
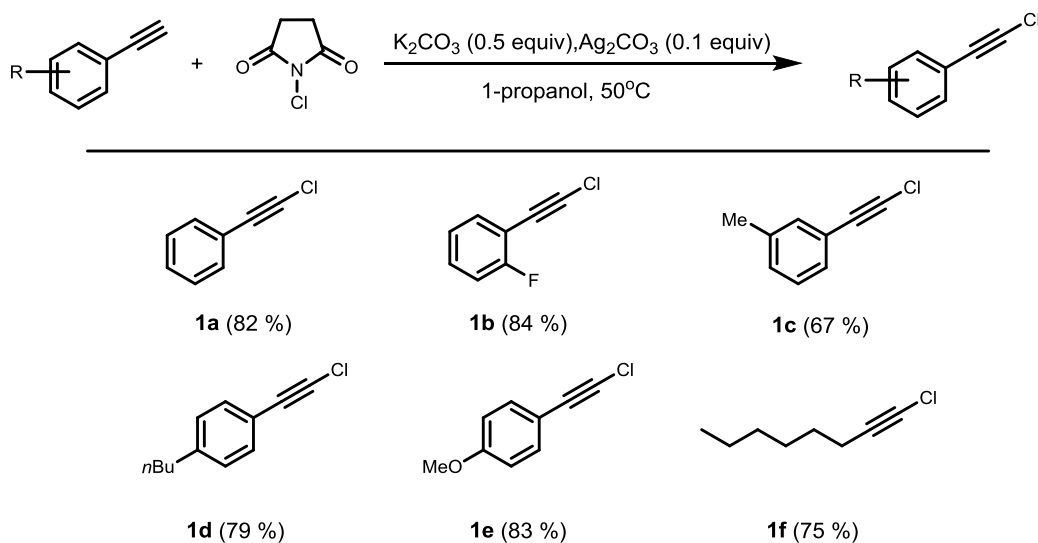
Scheme 6.2 Synthesis of 1-chloroalkynes.

2.2 General procedure for the synthesis of styrenyl chlorides GP2

Li_2CO_3 (1.25 mmol) was added to a mixture of cinnamic acid (5 mmol) and *N*-Chlorosuccinimide (10 mmol) in 30 mL acetonitrile/water (7:1 v/v) solution under argon. After stirring for 6 h at 60 °C, the mixture was cool to room temperature, 5 mL of water was added, the aqueous phase was extracted with ethyl acetate (20 mL × 3), and the combined organic layer was washed with brine (50 mL). The organic part was combined and dried over anhydrous $MgSO_4$. After evaporation, the mixture was subjected to column chromatography (silica gel, ethyl acetate/cyclohexane) to afford the desired product.

In the synthesis of the styryl chlorides, the reaction conditions was optimized with different lithium salt as additive, compared with LiOAc, LiCl, $LiBF_4$, $LiCO_3$ shows good yield in MeCN/H_2O solution, when the temperature was increased to 60 °C, 99% of compound was obtained.

Then the reaction scope was expanded under the standard reaction conditions, various styryl chlorides were prepared from the corresponding cinnamic acid. The yield gave in the parentheses was isolated yield.
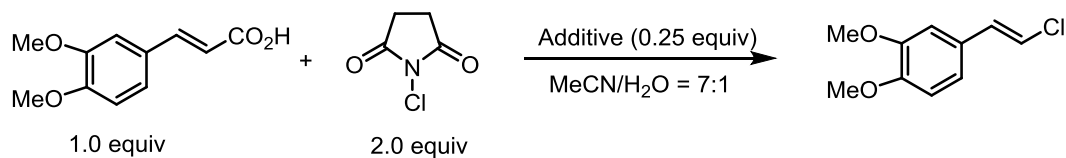
Entry	Additive	Solvent	T/^{o}C	Yield% [a]
1	LiOAc	MeCN/H$_2$O	20	53%
2	Li$_2$CO$_3$	MeCN/H$_2$O	20	70%
3	LiCl	MeCN/H$_2$O	20	60%
4	LiBF$_4$	MeCN/H$_2$O	20	26%
5	Li$_2$CO$_3$ 1.2 equiv	MeCN/H$_2$O	20	20%
6	Li$_2$CO$_3$ 1.2 equiv	MeCN	20	not observed
7	Li$_2$CO$_3$	MeCN	20	not observed
8	Li$_2$CO$_3$	MeCN/H$_2$O	60	99%

Scheme 6.3 Synthesis of styryl halides. [a]Yield determined by GCMS analysis.

Scheme 6.4 Synthesis of styryl halides. [a] LiOAc was used instead of Li₂CO₃.

General procedure for the synthesis of *(Z)*-(2-chlorovinyl)benzene GP3

(2, 2, 2-Trichloroethyl)benzene (1.0 mmol) was dissolved in THF (4 mL) and H₂O (1.0 mmol), which was added to a stirring suspension of anhyd CrCl₂ (1.0 mmol, 1 equiv; Sigma-Aldrich 99.9%) and Fe(0) powder (3.0 mmol, 3 equiv; Sigma-Aldrich 97%, 325 mesh) in THF (15 mL) under argon atmosphere. The reaction mixture was stirred at 50 °C for 18 h, then cooled to room temperature. Then the suspension was filtered through a short pad of silica gel, the filter cake was washed with ethyl ether. The combined filtrates were evaporated in vacuo and the residue was purified by column chromatography on silica gel to give the *(Z)*-(2-chlorovinyl)benzene (*cis:tans* = 91:9, 201 mg, 73 % yield).
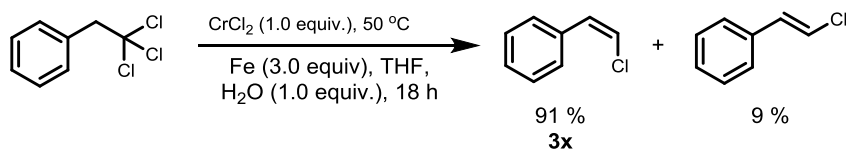
General procedure for the coupling of alkynyl chlorides with Grignard reagent in batch (GP4)

SIPr-HCl (4.3 mg, 2 mol%) was added to vial 1 containing a stirring bar, which is filled with argon and fitted with a septum. 0.6 mL of dry THF was added to the vial, organomagnesium reagent solution (1.2 equiv.) was added to this vial. Vial 1 was left for stirring for 10 minutes. Fe(acac)$_3$ (1.7 mg, 1 mol%) and 1-chloroalkynes or styryl chlorides (0.5 mmol, 1 equiv) was added in vial 2. The vial was filled with N$_2$ and fitted with septum, afterwards 1.2 mL of THF was added. The solution in vial 2 was transferred to vial 1 at 0 °C and the mixed solution in vial 1 turned black. After stirring for 3 minutes at 0 °C, the mixture was was quenched with a 1.0 M aqueous HCl solution and extracted with ethyl acetate. The organic layer was separated, washed with water and dried over anhydrous MgSO$_4$. After evaporation of solvent, the mixture was subjected to column chromatography (silica gel, ethyl acetate/cyclohexane) to afford pure product.

General procedure the coupling of alkenyl chlorides with Grignard reagent in batch (GP5).

Fe(acac)$_3$ (1.7 mg, 1 mol%) and styryl chlorides (0.5 mmol, 1 equiv) was added to vial containing a stirring bar. The vial was filled with argon and fitted with septum, afterwards 2.0 mL of THF was added. The organomagnesium reagent solution (1.2 equiv.) was added to this vial and the mixed solution turned black and the reaction mixture get warm immediately. After stirring for 3 minutes at room temperature, the mixture was was quenched with a 1.0 M aqueous HCl solution and extracted with ethyl acetate. The organic layer was separated, washed with water and dried over anhydrous MgSO$_4$. After evaporation of solvent, the mixture was subjected to column chromatography (silica gel, ethyl acetate/cyclohexane) to afford pure product.
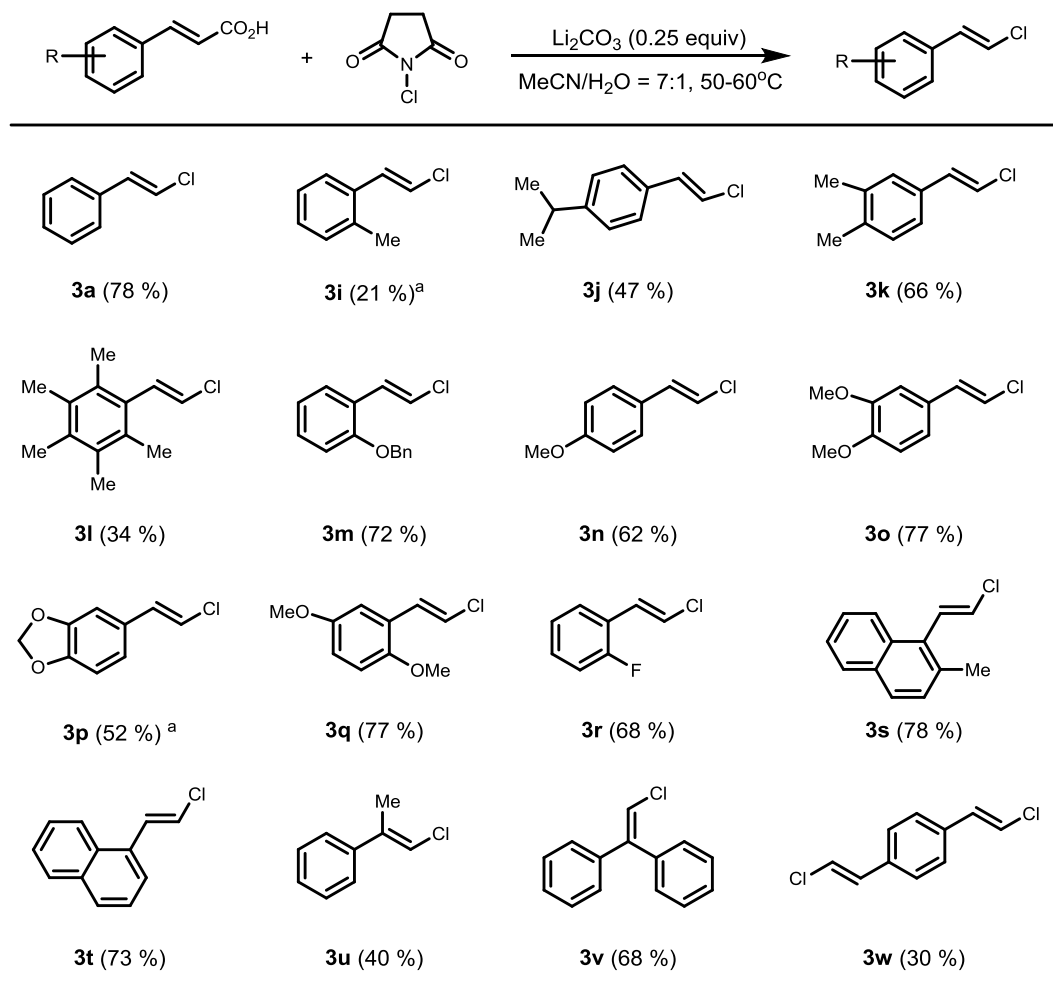
General procedure for the synthesis of organomagnesium reagent in flow (GP6).

Preparation of Mg column: a SolventPlusTM column (bore: 10 mm, length: 100 mm, AF; Omnifit, cat. no.006EZS-10-10-AF) is filled with 4g of magnesium (20-230 mesh, Sigma Aldrich Cat. No.: 254126) weight in a beaker using a filter funnel. General flow procedure for magnesium activation and organomagnesium synthesis: 5 mL of DIBAL-H 1M in THF was passed through a 10 mm internal diameter Omni-fit column containing Mg (4 g) at 1 mL/min. After that, 5 mL solution of TMSCl 2.0 M and 1-bromo-2-chloroethane 0.24 M in 10 mL THF was passed through the column at 1 mL/min at room temperature. After the activation, a solution of aliphatic bromide in THF was passed through the column at 0.5 mL/min and at 40 °C. The solution was collected in a sealed vial under argon. Titration: An accurately weighed sample of 2-Hydroxybenzaldehyde phenylhydrazone (around 25 mg) is dissolved in 0.5 mL of THF under nitrogen, then the Grignard reagent is added drop by drop until the color of the solution turned dark red from pale yellow.

Pentylmagnesium bromide: Prepared according to GP6 starting from 0.93 mL (7.5 mmol) of 1-bromopentane in 15 mL THF (0.47 M). The calculated concentration of the organomagnesium reagent was 0.37 M.

Benzylmagnesium bromide: Prepared according to GP6 starting from 0.6 mL (5 mmol) of benzyl bromide in 10 mL THF (0.47 M). The calculated concentration of the organomagnesium reagent was 0.40 M.

(but-3-en-1-yl)magnesium bromide: Prepared according to GP6 starting from 0.7 mL (7 mmol) of 4-bromobut-1-ene in 10 mL THF (0.65 M). The calculated concentration of the organomagnesium reagent was 0.42 M.

(1-methylpiperidin-4-yl)magnesium chloride: Prepared according to GP6 starting from 1.0 mL (8 mmol) of 4-chloro-1-methylpiperidine in 10 mL THF (0.73 M). The calculated concentration of the organomagnesium reagent was 0.50 M.

Cyclohexylmagnesium chloride: Prepared according to GP6 starting from 0.9 mL (7.5 mmol) of chlorocyclohexane in 15 mL THF (0.5 M). The calculated concentration of the organomagnesium reagent was 0.45 M.

Propylmagnesium bromide: Prepared according to GP6 starting from 0.68 mL (7.5 mmol) of 1-bromopropane in 15 mL THF (0.48 M). Titration: An accurately weighed sample of 2-Hydroxybenzaldehyde phenylhydrazone (around 25 mg) is dissolved in 0.5 mL of THF under nitrogen, then the Grignard reagent is added drop by drop until the color of the solution turned dark red from pale yellow. The calculated concentration of the organomagnesium reagent was 0.39 M.

Isopropylmagnesium bromide: Prepared according to GP6 starting from 0.70 mL (7.5 mmol) of 2-bromopropane in 15 mL THF (0.48 M). Titration: An accurately weighed sample of 2-Hydroxybenzaldehyde phenylhydrazone (around 25 mg) is dissolved in 0.5 mL of THF under nitrogen, then the Grignard reagent is added drop by drop until the color of the solution turned dark red from pale yellow. The calculated concentration of the organomagnesium reagent was 0.36 M.

Butylmagnesium iodide: Prepared according to GP6 starting from 0.85 mL (7.5 mmol) of 1-iodobutane in 15 mL THF (0.47 M). Titration: An accurately weighed sample of 2-Hydroxybenzaldehyde phenylhydrazone (around 25 mg) is dissolved in 0.5 mL of THF under nitrogen, then the Grignard reagent is added drop by drop until the color of the solution turned dark red from pale yellow. The calculated concentration of the organomagnesium reagent was 0.46 M.

(3,3,3-trifluoropropyl)magnesium iodide: Prepared according to GP6 starting from 0.85 mL (7.5 mmol) of 1,1,1-trifluoro-3-iodopropane in 15 mL THF (0.47 M). Titration: An accurately weighed sample of 2-Hydroxybenzaldehyde phenylhydrazone (around 25 mg) is dissolved in 0.5 mL of THF under nitrogen, then the Grignard reagent is added drop by drop until the color of the solution turned dark red from pale yellow. The calculated concentration of the organomagnesium reagent was 0.44 M.

(3-phenylpropyl)magnesium bromide: Prepared according to GP6 starting from 1.1 mL (7.5 mmol) of (3-bromopropyl)benzene in 15 mL THF (0.47 M). Titration: An accurately weighed sample of 2-Hydroxybenzaldehyde phenylhydrazone (around 25 mg) is dissolved in 0.5 mL of THF under nitrogen, then the Grignard reagent is added drop by drop until the color of the solution turned dark red from pale yellow. The calculated concentration of the organomagnesium reagent was 0.29 M.

_m_-tolylmagnesium bromide: Prepared according to GP6 starting from 0.91 mL (7.5 mmol) of 1-bromo-3-methylbenzene in 15 mL THF (0.47 M). Titration: An accurately weighed sample of 2-Hydroxybenzaldehyde phenylhydrazone (around 25 mg) is dissolved in 0.5 mL of THF under nitrogen, then the Grignard reagent is added drop by drop until the color of the solution turned dark red from pale yellow. The calculated concentration of the organomagnesium reagent was 0.39 M.

(3-(trifluoromethyl)phenyl)magnesium bromide: Prepared according to GP6 starting from 1.0 mL (7.5 mmol) of 1-bromo-3-(trifluoromethyl)benzene in 15 mL THF (0.47 M). Titration: An accurately weighed sample of 2-Hydroxybenzaldehyde phenylhydrazone (around 25 mg) is dissolved in 0.5 mL of THF under nitrogen, then the Grignard reagent is added drop by drop until the color of the solution turned dark red from pale yellow. The calculated concentration of the organomagnesium reagent was 0.41 M.

General procedure for telescope reactions

The Grignard reagent was prepared following **GP6**, 5 mL of DIBAL-H 1M in THF was passed through a 10 mm internal diameter Omni-fit column containing Mg (4 g) at 1 mL/min at 40 °C. After that, 5 mL solution of TMSCl 2.0 M and 1-bromo-2-chloroethane 0.24 M in THF was passed through the column at 1 mL/min. After the activation step, a solution of aliphatic bromide/chloride in THF was passed through the column at 0.5 mL/min. A solution of the alkyl bromide/chloride (7.5 mmol) in 15 mL THF (0.5 M) was passed through the column at 40 °C at the flowrate of 0.5 mL/min. The first 3 mL of Grignard reagent was collected and titrate with 2-Hydroxybenzaldehyde phenylhydrazone. Based on the concentration of the Grignard reagent, THF was added to the vial of vinyl or alkynl chloride ($C_{Grignard\ reagent} = 1.2\ C_{Sub}$) with Fe(acac)$_3$ (1.7 mg, 1 mol%). The solution of the substrate and Fe(acac)$_3$ was charged to a syringe pump and mixed with Grignard reagent with T-mixture, the combined solution was passed through a PFA (I.D. 0.75 mm) reactor at room temperature or ice-water bath. The outcome mixture was quenched with 3.0 mL 1.0 M HCl solution and extracted with ethyl acetate (10 mL × 3). The organic layer was combined, washed with brine (30 mL) and dried over anhydrous MgSO$_4$. After evaporation, the crude was isolated with chromatography (silica gel, 100 % cyclohexane) to afford the desired product.

Set up for the telescope reactions

Flow reactions were carried out in an Omnifit column fixed on a R2/R4 Vapourtec equipment. All microfluidic fittings were purchased from IDEX Health and Science. The syringes were connected to the capillary using 1/16 flat-bottom flangeless fittings. Syringe pump (Fusion 200 Classic) equipped with a 10 or 5 mL syringe was used to infuse the liquid reagents into a reactor coil fabricated from a high purity perfluoroalkoxyalkane (PFA) capillary tubing (1.0 mL, ID = 750 μm). The outlet of the microreactor led to the collection vial under argon. The detail of the assembling the reactor is shown in **Figure 6.3-6.4**.
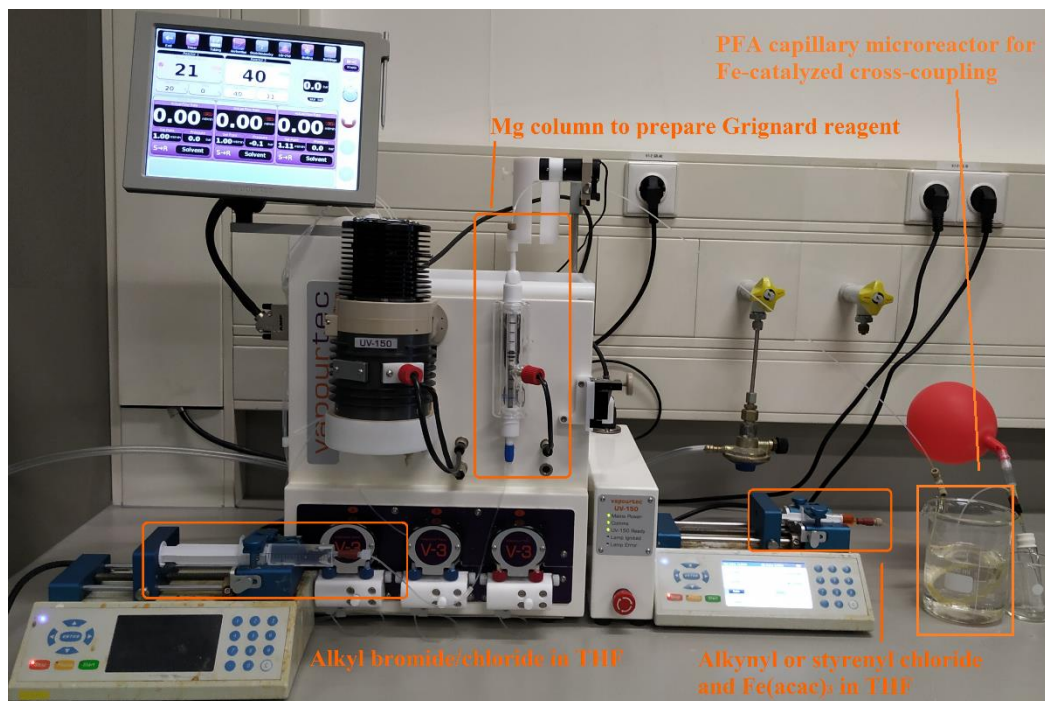
Figure 6.3: The overview of the set-up for telescope
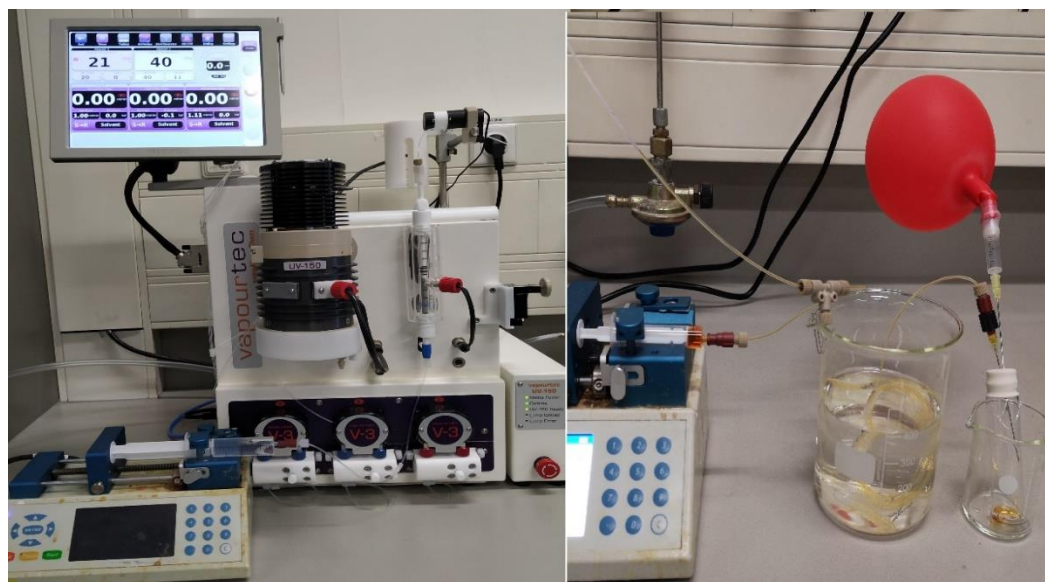
Figure 6.4: The details of the telescope reaction

Preliminary mechanistic study

To test whether this iron-catalyzed cross-coupling reaction is proceeding through a radical pathway, some preliminary mechanism was studied and all the data was collected by GC-MS. Firstly, 1 equivalent of TEMPO was added to the reaction mixture of (2-chlorovinyl)benzene and cyclohexylmagnisum chloride under standard reaction condition, the product was observed with 18% of yield from GC. When the amount of TEMPO was decreased to 0.2 equivalent, the product was detected with 71% yield. In both cases, the adduct of TEMPO-Cyhexyl was detected with GC-MS. However, when we tried the reaction of TEMPO with the (2-chlorovinyl)benzene and cyclohexylmagnisum chloride separately. It shows that the substrate can not react with TEMPO, but Grignard reagent and TEMPO could be coupled directly without iron catalyst. These results didn't necessarily indicated the radical pathway is involved in the reaction. The addition of TEMPO to the reaction of (chloroethynyl)benzene shows the same result.
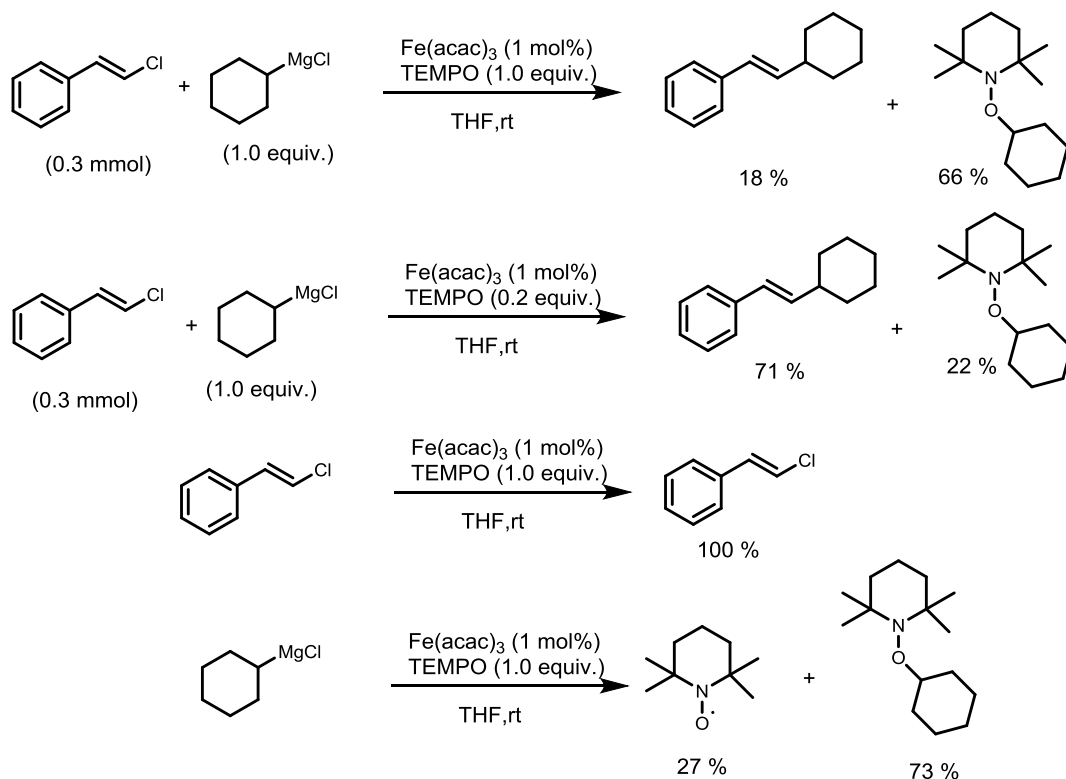
Scheme 6.5 Control experiments with TEMPO.

We observed that the *Z*-configuration substrate *(Z)*-(2-chlorovinyl)benzene (*cis:trans* = 91:9) could remain the configuration when conducted under the standard reaction condition, the ratio of the isomer is *cis:trans* = 88:12 compared with 91:9 (**Scheme 6.6**). This evidence demonstrated that radical pathways were not likely involved in the main pathway of the reaction.
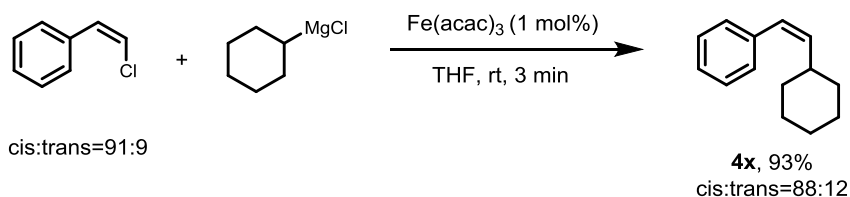
Scheme 6.6 Reaction of Z-configuration substrate.

Characterization of the compounds

(cyclohexylethynyl)benzene (2a): 0.5 mmol (68 mg) **1a** was employed with general procedure GP4 and 88 mg (96 % yield) **2a** was obtained as pale yellow oil using column chromatography (eluent: 100% cyclohexane). **^{1}H NMR** (400 MHz, CDCl$_3$) δ 7.42 – 7.39 (m, 2H), 7.31 – 7.27 (m, 3H), 2.63 – 2.57 (m, 1H), 1.91 – 1.88 (m, 2H), 1.79 – 1.74 (m, 2H), 1.59 – 1.51 (m, 3H), 1.39 –1.39 (m, 3H). **^{13}C NMR** (101 MHz, CDCl$_3$) δ 131.55, 128.12, 127.37, 124.12, 94.45, 80.48, 32.71, 29.66, 25.93, 24.91.

1-(cyclohexylethynyl)-2-fluorobenzene (2b): 0.5 mmol (77 mg) **1b** was employed with general procedure GP4 and 90 mg (89 % yield) **2b** was obtained as pale yellow oil using column chromatography (eluent: 100% cyclohexane). **^{1}H NMR** (400 MHz, CDCl$_3$) δ 7.39 (td, J = 7.6, 1.8 Hz, 1H), 7.24 – 7.24 (m, 1H), 7.08 – 7.00 (m, 2H), 2.68 – 2.61 (m, 1H), 1.91 – 1.86 (m, 2H), 1.82 – 1.71 (m, 2H), 1.61 – 1.54 (m, 3H), 1.38 – 1.32 (m, 3H). **^{13}C NMR** (101 MHz, CDCl$_3$) δ 162.74 (d, J_{C-F} = 251.0 Hz), 133.52 (d, J_{C-F} = 1.5 Hz), 129.97 (d, J_{C-F} = 7.9 Hz), 123.69 (d, J_{C-F} = 3.8 Hz), 115.28 (d, J_{C-F} = 21.3 Hz), 112.57 (d, J_{C-F} = 15.9 Hz), 99.90 (d, J_{C-F} = 3.2 Hz), 73.82, 32.52, 29.79, 25.91, 24.78. **^{19}F NMR** (376 MHz, CDCl$_3$) δ -111.78 (q, J = 7.7, 7.2 Hz).

1-(cyclohexylethynyl)-3-methylbenzene (2c): 0.5 mmol (75 mg) **1c** was employed with general procedure GP4 and 93 mg (94 % yield) **2c** was obtained as pale yellow oil using column chromatography (eluent: 100% cyclohexane). **^{1}H NMR** (400 MHz, CDCl$_3$) δ 7.23 – 7.14 (m, 3H), 7.07 (d, J = 7.4 Hz, 1H), 2.58 (tt, J = 9.0, 3.6 Hz, 1H), 2.31 (s, 3H), 1.88 – 1.84 (m, 2H), 1.78 – 1.73 (m, 2H), 1.58 – 1.49 (m, 3H), 1.38 – 1.32 (m, 3H). **^{13}C NMR** (101 MHz, CDCl$_3$) δ 137.74, 132.18, 128.58, 128.26, 128.02, 123.89, 94.06, 80.60, 32.74, 30.92, 29.64, 25.94, 24.90, 21.18.

1-butyl-4-(cyclohexylethynyl)benzene (2d): 0.5 mmol (96 mg) **1d** was employed with general procedure GP4 and 112 mg (93 % yield) **2d** was obtained as pale yellow oil using column chromatography (eluent: 100% cyclohexane). **^{1}H NMR** (400 MHz, CDCl$_3$) δ 7.30 (d, J = 8.1 Hz, 2H), 7.08 (d, J = 8.2 Hz, 2H), 2.64 – 2.55 (m, 3H), 1.89 – 1.85 (m, 2H), 1.77 – 1.72 (m, 2H), 1.61 – 1.51 (m, 5H), 1.36 – 1.30 (m, 5H), 0.91 (t, J = 7.3 Hz, 3H). **^{13}C NMR** (101 MHz, CDCl$_3$) δ 142.34, 131.41, 128.24, 121.20, 93.64, 80.52, 35.48, 33.43, 32.77, 30.92, 29.66, 25.94, 24.90, 22.25, 13.91.

1-(cyclohexylethynyl)-4-methoxybenzene (2e): 0.5 mmol (83 mg) **1e** was employed with general procedure GP4 and 103 mg (96 % yield) **2e** was obtained as pale yellow oil using column chromatography (eluent: 100% cyclohexane). **^{1}H NMR** (400 MHz, CDCl$_3$) δ 7.35 – 7.30 (m, 2H), 6.83 – 6.78 (m, 2H), 3.80 (s, 3H), 2.59 – 2.53

(m, 1H), 1.92 – 1.83 (m, 2H), 1.78 – 1.73 (m, 2H), 1.58 – 1.49 (m, 3H), 1.37 – 1.31 (m, 3H). **^{13}C NMR** (101 MHz, CDCl$_3$) δ 158.91, 132.85, 116.28, 113.73, 92.83, 80.12, 55.23, 32.83, 30.91, 29.68, 25.94, 24.95.

1,2-diphenylethyne (2f): 0.5 mmol (68 mg) **1a** was employed with general procedure GP4 and 77 mg (87 % yield) **2l** was obtained as white solid using column chromatography (eluent: 100% cyclohexane). Melting point: 53.9 °C. **^{1}H NMR** (400 MHz, CDCl$_3$) δ 7.57 – 7.51 (m, 4H), 7.38 – 7.31 (m, 6H). **^{13}C NMR** (101 MHz, CDCl$_3$) δ 131.59, 128.32, 128.23, 123.26, 89.35.

pent-1-yn-1-ylbenzene (2g): 0.5 mmol (68 mg) **1a** was employed with general procedure GP4 and 67 mg (93 % yield) **2g** was obtained as colorless oil using column chromatography (eluent: 100% cyclohexane). **^{1}H NMR** (400 MHz, CDCl$_3$) δ 7.43 – 7.38 (m, 2H), 7.30 – 7.25 (m, 3H), 2.40 (t, J = 7.0 Hz, 2H), 1.65 (h, J = 7.3 Hz, 3H), 1.06 (t, J = 7.4 Hz, 3H). **^{13}C NMR** (101 MHz, CDCl$_3$) δ 131.52, 128.15, 127.44, 124.07, 90.24, 80.68, 22.22, 21.39, 13.54.

prop-1-yn-1-ylbenzene (2h): 0.5 mmol (68 mg) **1a** was employed with general procedure GP4 and 54 mg (93 % yield) **2h** was obtained as colorless oil using column chromatography (eluent: 100% cyclohexane). **^{1}H NMR** (400 MHz, CDCl$_3$) δ 7.42 – 7.39 (m, 2H), 7.31 – 7.26 (m, 3H), 2.06 (s, 3H). **^{13}C NMR** (101 MHz, CDCl$_3$) δ 131.46, 128.17, 127.48, 124.00, 85.77, 79.70, 4.29.

trimethyl(3-phenylprop-2-yn-1-yl)silane (2i): 0.5 mmol (68 mg) **1a** was employed with general procedure GP4 and 76 mg (81 % yield) **2i** was obtained as colorless oil using column chromatography (eluent: 100% cyclohexane). **^{1}H NMR** (400 MHz, CDCl$_3$) δ 7.37 – 7.03 (m, 5H), 1.61 (s, 2H), 0.08 (s, 9H). **^{13}C NMR** (101 MHz, CDCl$_3$) δ 131.40, 128.12, 126.99, 124.83, 88.44, 79.58, 7.96, -1.96.

(cyclopentylethynyl)benzene (2j): 0.5 mmol (68 mg) **1a** was employed with general procedure GP4 and 73 mg (86 % yield) **2j** was obtained as colorless oil using column chromatography (eluent: 100% cyclohexane). **^{1}H NMR** (400 MHz, CDCl$_3$) δ 7.40 – 7.37 (m, 2H), 7.27 – 7.24 (m, 3H), 2.82 (p, J = 7.5 Hz, 1H), 2.04 – 1.96 (m, 2H), 1.80 – 1.67 (m, 4H), 1.62 – 1.57 (m, 2H). **^{13}C NMR** (101 MHz, CDCl$_3$) δ 131.51, 128.12, 127.35, 124.14, 94.59, 80.03, 33.92, 30.78, 25.05.

1-methyl-4-(phenylethynyl)piperidine (2k): 0.5 mmol (69 mg) **1a** was employed with general procedure GP4. The reaction mixture was quenched with 3.0 mL 1.0 M aqueous HCl solution. The acidic aqueous layer was basified with saturated K$_2$CO$_3$ aqueous solution and extracted with diethyl ether, and the combined organic layers were dried (anhydrous MgSO$_4$). After filtration, the solvent was evaporated in vacuo and 99 mg (99 % yield) **2k** was obtained as orange oil. **^{1}H NMR** (400 MHz, CDCl$_3$) δ 7.43 – 7.38 (m, 2H), 7.31 – 7.24 (m, 3H), 2.79 – 2.66 (m, 2H), 2.66 – 2.54 (m, 1H), 2.29 (s, 3H), 2.25 – 2.14 (m, 2H), 1.99 – 1.89 (m, 2H), 1.83 – 1.72 (m, 2H). **^{13}C NMR** (101 MHz, CDCl$_3$) δ 131.55, 128.16, 127.59, 123.78, 92.74, 81.42, 81.35, 54.21, 46.52, 31.81, 27.03. **HRMS** (ESI) calcd for C$_{14}$H$_{17}$NH [M]$^+$: 200.1434; found: 200.1447.

oct-1-yn-1-ylbenzene (2l): 0.5 mmol (72 mg) **1f** was employed with general procedure GP4 and 84 mg (90 % yield) **2f** was obtained as pale yellow oil using column chromatography (eluent: 100% cyclohexane). **^{1}H NMR** (400 MHz, CDCl$_3$) δ 7.42 – 7.36 (m, 2H), 7.31 – 7.26 (m, 3H), 2.40 (t, J = 7.1 Hz, 2H), 1.64 – 1.57 (m, 2H),

1.49 − 1.42 (m, 2H), 1.34 − 1.30 (m, 4H), 0.91 (t, J = 6.9 Hz, 3H). **¹³C NMR** (101 MHz, CDCl₃) δ 131.52, 128.15, 127.42, 124.09, 90.47, 80.52, 31.37, 28.73, 28.60, 22.57, 19.41, 14.06, 1.02.

(E)-prop-1-en-1-ylbenzene (4a): 0.5 mmol (69 mg) **3a** was employed with general procedure GP5 and 53 mg (90 % yield) **4a** was obtained as colorless oil using column chromatography (eluent: 100% cyclohexane). **¹H NMR** (400 MHz, CDCl₃) δ 7.34 − 7.27 (m, 4H), 7.22 − 7.16 (m, 1H), 6.42 (dd, J = 15.7, 1.4 Hz, 1H), 6.24 (dq, J = 15.7, 6.5 Hz, 1H), 1.89 (dd, J = 6.5, 1.5 Hz, 3H). **¹³C NMR** (101 MHz, CDCl₃) δ 137.92, 131.00, 128.45, 126.71, 125.79, 125.68, 18.48.

(E)-pent-1-en-1-ylbenzene (4b): 0.5 mmol (69 mg) **3a** was employed with general procedure GP5 and 71 mg (97 % yield) **4b** was obtained as colorless oil using column chromatography (eluent: 100% cyclohexane). **¹H NMR** (400 MHz, CDCl₃) δ 7.39 − 7.30 (m, 4H), 7.24 − 7.20 (m, 1H), 6.42 (d, J = 15.8 Hz, 1H), 6.26 (dt, J = 15.8, 6.9 Hz, 1H), 2.25 − 2.20 (m, 2H), 1.58 − 1.47 (m, 2H), 0.99 (t, J = 7.4 Hz, 3H). **¹³C NMR** (101 MHz, CDCl₃) δ 137.92, 130.94, 129.87, 128.43, 126.72, 125.89, 35.11, 22.54, 13.73.

(E)-prop-1-ene-1,3-diyldibenzene (4c): 0.5 mmol (69 mg) **3a** was employed with general procedure GP5 and 93 mg (96 % yield) **4c** was obtained as colorless oil using column chromatography (eluent: 100% cyclohexane). **¹H NMR** (400 MHz, CDCl₃) δ 7.38 − 7.26 (m, 7H), 7.25 − 7.19 (m, 3H), 6.47 (d, J = 15.8 Hz, 1H), 6.37 (dt, J = 15.7, 6.6 Hz, 1H), 3.57 (d, J = 6.6 Hz, 2H). **¹³C NMR** (101 MHz, CDCl₃) δ 140.15, 137.46, 131.05, 129.21, 128.65, 128.48, 127.08, 126.16, 126.10, 39.34.

(E)-(3-methylbut-1-en-1-yl)benzene (4d): 0.5 mmol (69 mg) **3a** was employed with general procedure GP5 and 68 mg (b:l = 94:6, 93 % yield) **4d** was obtained as colorless oil using column chromatography (eluent: 100% cyclohexane). **¹H NMR** (400 MHz, CDCl₃) δ 7.36 (d, J = 7.3 Hz, 2H), 7.29 (t, J = 7.6 Hz, 2H), 7.19 (t, J = 7.2 Hz, 1H), 6.35 (d, J = 16.1 Hz, 1H), 6.20 (dd, J = 15.9, 6.7 Hz, 1H), 2.52 − 2.43 (m, 1H), 1.10 (d, J = 6.7 Hz, 6H). **¹³C NMR** (101 MHz, CDCl₃) δ 138.00, 137.94, 128.44, 126.80, 126.73, 125.94, 31.52, 22.44.

(E)-(2-cyclopentylvinyl)benzene (4e): 0.5 mmol (69 mg) **3a** was employed with general procedure GP4 and 77 mg (90 % yield) **4e** was obtained as colorless oil using column chromatography (eluent: 100% cyclohexane). **¹H NMR** (400 MHz, CDCl₃) δ 7.36 (d, J = 7.3 Hz, 2H), 7.29 (t, J = 7.6 Hz, 2H), 7.19 (t, J = 7.2 Hz, 1H), 6.38 (d, J = 15.8 Hz, 1H), 6.22 (dd, J = 15.8, 7.7 Hz, 1H), 2.56 − 2.66 (m, 1H), 1.91 − 1.84 (m, 2H), 1.76 − 1.61 (m, 4H), 1.45 − 1.37 (m, 2H). **¹³C NMR** (101 MHz, CDCl₃) δ 137.92, 135.69, 128.43, 127.82, 126.68, 125.89, 43.80, 33.21, 25.23.

(E)-(2-cyclohexylvinyl)benzene (4f): 0.5 mmol (69 mg) **3a** was employed with general procedure GP5 and 84 mg (90 % yield) **4f** was obtained as colorless oil using column chromatography (eluent: 100% cyclohexane). **¹H NMR** (400 MHz, CDCl₃) δ 7.34 (d, J = 7.2 Hz, 2H), 7.29 (d, J = 7.4 Hz, 2H), 7.18 (t, J = 7.2, 1H), 6.35 (d, J = 16.0 Hz, 1H), 6.18 (dd, J = 16.0, 6.9 Hz, 1H), 2.16 − 2.10 (m, 1H), 1.83 − 1.67 (m, 5H), 1.37 − 1.14 (m, 5H). **¹³C NMR** (101 MHz, CDCl₃) δ 138.11, 136.87, 128.49, 127.29, 126.77, 125.99, 41.23, 33.03, 26.25, 26.13.

(E)-1-methyl-4-styrylpiperidine (4g): 0.5 mmol (69 mg) **3a** was employed with general procedure GP5. The reaction mixture was quenched with 3.0 mL 1.0 M aqueous HCl solution. The acidic aqueous layer was basified with saturated K₂CO₃ aqueous solution and extracted with diethyl ether, and the combined organic layers were

dried (anhydrous MgSO$_4$). After filtration, the solvent was evaporated in vacuo and 97 mg (96 % yield) **4g** was obtained as orange oil. **^{1}H NMR** (400 MHz, CDCl$_3$) δ 7.39 – 7.32 (m, 2H), 7.31 – 7.26 (m, 2H), 7.16 – 7.22 (m, 1H), 6.38 (d, *J* = 16.0 Hz, 1H), 6.17 (dd, *J* = 16.0, 6.9 Hz, 1H), 2.95 – 2.86 (m, 1H), 2.31 (s, 3H), 2.14 – 2.07 (m, 1H), 2.07 – 1.97 (m, 2H), 1.82 – 1.74 (m, 2H), 1.57 (qd, *J* = 12.9, 12.4, 3.7 Hz, 2H). **^{13}C NMR** (101 MHz, CDCl$_3$) δ 137.64, 134.95, 128.47, 128.23, 126.96, 125.98, 55.57, 46.40, 38.66, 32.02.

***(E)*-1,2-diphenylethene (4h)**: 0.5 mmol (69 mg) **3a** was employed with general procedure GP5 and 87 mg (97 % yield) **4h** was obtained as colorless oil using column chromatography (eluent: 100% cyclohexane). **^{1}H NMR** (400 MHz, CDCl$_3$) δ 7.57 – 7.55 (m, 4H), 7.42 – 7.39 (m, 4H), 7.34 – 7.27 (m, 2H), 7.16 (s, 2H). **^{13}C NMR** (101 MHz, CDCl$_3$) δ 137.29, 128.66, 128.64, 127.58, 126.48.

***(E)*-1-(2-cyclohexylvinyl)-2-methylbenzene (4i)**: 0.5 mmol (76 mg) **3i** was employed with general procedure GP5 and 97 mg (97 % yield) **4i** was obtained as colorless oil using column chromatography (eluent: 100% cyclohexane). **^{1}H NMR** (400 MHz, CDCl$_3$) δ 7.46 (d, *J* = 7.0 Hz, 1H), 7.21 – 7.13 (m, 3H), 6.59 (d, *J* = 15.8 Hz, 1H), 6.09 (dd, *J* = 15.8, 7.0 Hz, 1H), 2.38 (s, 3H), 2.24 – 2.17 (m, 1H), 1.89 – 1.72 (m, 5H), 1.43 – 1.20 (m, 5H). **^{13}C NMR** (101 MHz, CDCl$_3$) δ 138.22, 137.12, 134.91, 130.09, 126.65, 125.95, 125.31, 125.01, 41.45, 33.09, 26.18, 26.05, 19.80.

***(E)*-1-(2-cyclohexylvinyl)-4-isopropylbenzene (4j)**: 0.5 mmol (90 mg) **3j** was employed with general procedure GP5 and 106 mg (93 % yield) **4j** was obtained as colorless oil using column chromatography (eluent: 100% cyclohexane). **^{1}H NMR** (400 MHz, CDCl$_3$) δ 7.34 (d, *J* = 8.1 Hz, 2H), 7.21 (d, *J* = 8.1 Hz, 2H), 6.38 (d, *J* = 16.0 Hz, 1H), 6.19 (dd, *J* = 16.0, 7.0 Hz, 1H), 2.97 – 2.90 (m, 1H), 2.21 – 2.14 (m, 1H), 1.87 – 1.72 (m, 5H), 1.36 – 1.24 (m, 11H). **^{13}C NMR** (101 MHz, CDCl$_3$) δ 147.49, 135.99, 135.69, 127.00, 126.49, 125.86, 41.16, 33.81, 33.03, 26.19, 26.06, 23.98.

***(E)*-4-(2-cyclohexylvinyl)-1,2-dimethylbenzene (4k)**: 0.5 mmol (83 mg) **3k** was employed with general procedure GP5 and 104 mg (97 % yield) **4k** was obtained as colorless oil using column chromatography (eluent: 100% cyclohexane). **^{1}H NMR** (400 MHz, CDCl$_3$) δ 7.20 (s, 1H), 7.13 (q, *J* = 7.8 Hz, 2H), 6.36 (d, *J* = 16.0 Hz, 1H), 6.18 (dd, *J* = 16.0, 6.9 Hz, 1H), 2.31 (s, 3H), 2.30 (s, 3H), 2.21 – 2.14 (m, 1H), 1.88 – 1.73 (m, 5H), 1.44 – 1.20 (m, 5H). **^{13}C NMR** (101 MHz, CDCl$_3$) δ 136.39, 135.70, 135.62, 135.01, 129.69, 127.15, 127.08, 123.39, 41.13, 33.03, 26.20, 26.07, 19.74, 19.40. **MS (EI, 70 ev)**: *m/z* (relative intensity) = 214 (M$^{+\bullet}$, 81), 199 (28), 171 (14), 157 (35), 143 (24), 132 (100), 119 (38), 108 (13), 91 (12), 41 (6).

***(E)*-1-(2-cyclohexylvinyl)-2,3,4,5,6-pentamethylbenzene (4l)**: 0.5 mmol (104 mg) **3l** was employed with general procedure GP5 and 122 mg (95 % yield) **4l** was obtained as white solid using column chromatography (eluent: 100% cyclohexane). Melting point: 89.6 ºC. **^{1}H NMR** (400 MHz, CDCl$_3$) δ 6.31 (d, *J* = 16.3 Hz, 1H), 5.43 (dd, *J* = 16.3, 6.9 Hz, 1H), 2.25 – 2.17 (m, 15H), 1.87 – 1.67 (m, 5H), 1.40 – 1.17 (m, 5H). **^{13}C NMR** (101 MHz, CDCl$_3$) δ 141.14, 136.15, 133.04, 132.19, 131.50, 126.72, 41.38, 33.02, 26.25, 26.04, 17.83, 16.71, 16.59. **MS (EI, 70 ev)**: *m/z* (relative intensity) = 256 (M$^{+\bullet}$, 93), 241 (100), 185 (25), 173 (38), 160 (54), 148 (56), 133 (17), 107 (10), 79 (8), 55 (6), 41 (7).

(E)-1-(benzyloxy)-2-(2-cyclohexylvinyl)benzene (4m): 0.5 mmol (122 mg) **3m** was employed with general procedure GP5 and 137 mg (94 % yield) **4m** was obtained as pale yellow oil using column chromatography (eluent: 100% cyclohexane). **^{1}H NMR** (400 MHz, CDCl$_3$) δ 7.53 – 7.49 (m, 3H), 7.44 (t, J = 7.4 Hz, 2H), 7.37 (t, J = 7.2 Hz, 1H), 7.21 – 7.17 (m, 1H), 6.99 – 6.93 (m, 2H), 6.83 (d, J = 16.1 Hz, 1H), 6.25 (dd, J = 16.1, 7.1 Hz, 1H), 5.14 (s, 2H), 2.24 – 2.17 (m, 1H), 1.88 – 1.71 (m, 5H), 1.42 – 1.20 (m, 5H). **^{13}C NMR** (101 MHz, CDCl$_3$) δ 155.46, 137.53, 137.35, 128.45, 127.69, 127.62, 127.54, 127.15, 126.30, 121.82, 120.97, 112.59, 70.28, 41.54, 33.05, 26.18, 26.02. **HRMS** (ESI) calcd for C$_{21}$H$_{24}$ONa [M]$^+$: 315.1719; found: 315.1718.

(E)-1-(2-cyclohexylvinyl)-4-methoxybenzene (4n): 0.5 mmol (84 mg) **3n** was employed with general procedure GP5 and 98 mg (91 % yield) **4n** was obtained as pale yellow oil using column chromatography (eluent: ethyl acetate/cyclohexane = 1:20). **^{1}H NMR** (400 MHz, CDCl$_3$) δ 7.28 (d, J = 8.7 Hz, 2H), 6.83 (d, J = 8.7 Hz, 2H), 6.29 (d, J = 16.0 Hz, 1H), 6.04 (dd, J = 16.0, 7.0 Hz, 1H), 3.80 (s, 3H), 2.14 – 2.06 (m, 1H), 1.81 – 1.66 (m, 5H), 1.36 – 1.12 (m, 5H). **^{13}C NMR** (101 MHz, CDCl$_3$) δ 158.57, 134.78, 130.87, 126.96, 126.50, 113.87, 55.28, 41.11, 33.08, 26.19, 26.08.

(E)-4-(2-cyclohexylvinyl)-1,2-dimethoxybenzene (4o): 0.5 mmol (99 mg) **3o** was employed with general procedure GP5 and 116 mg (94 % yield) **4o** was obtained as pale yellow oil using column chromatography (eluent: ethyl acetate/cyclohexane = 1:20). **^{1}H NMR** (400 MHz, CDCl$_3$) δ 6.92 – 6.78 (m, 3H), 6.28 (d, J = 15.9 Hz, 1H), 6.04 (dd, J = 15.9, 6.9 Hz, 1H), 3.90 (s, 3H), 3.86 (s, 3H), 2.14-2.07 (m, 1H), 1.86 – 1.67 (m, 5H), 1.37 – 1.14 (m, 5H). **^{13}C NMR** (101 MHz, CDCl$_3$) δ 148.92, 148.11, 134.93, 131.14, 126.78, 118.78, 111.11, 108.40, 55.86, 55.72, 41.06, 33.03, 26.14, 26.03.

(E)-5-(2-cyclohexylvinyl)benzo[d][1,3]dioxole (4p): 0.5 mmol (91 mg) **3p** was employed with general procedure GP5 and 102 mg (89 % yield) **4p** was obtained as pale yellow oil using column chromatography (eluent: ethyl acetate/cyclohexane = 1:20). **^{1}H NMR** (400 MHz, CDCl$_3$) δ 6.95 – 6.90 (m, 1H), 6.81 – 6.72 (m, 2H), 6.27 (d, J = 15.9 Hz, 1H), 6.02 (dd, J = 15.9, 7.0 Hz, 1H), 5.93 (s, 2H), 2.15 – 2.07 (m, 1H), 1.82 – 1.68 (m, 5H), 1.38 – 1.14 (m, 5H). **^{13}C NMR** (101 MHz, CDCl$_3$) δ 147.87, 146.45, 135.10, 132.56, 126.74, 120.19, 108.13, 105.34, 100.83, 41.01, 33.00, 26.14, 26.03.

(E)-2-(2-cyclohexylvinyl)-1,4-dimethoxybenzene (4q): 0.5 mmol (99 mg) **3q** was employed with general procedure GP5 and 111 mg (90 % yield) **4q** was obtained as pale yellow oil using column chromatography (eluent: ethyl acetate/cyclohexane = 1:20). **^{1}H NMR** (400 MHz, CDCl$_3$) δ 7.01 (d, J = 2.9 Hz, 1H), 6.79 (d, J = 8.9 Hz, 1H), 6.73 (dd, J = 8.9, 2.9 Hz, 1H), 6.67 (d, J = 16.1 Hz, 1H), 6.16 (dd, J = 16.1, 7.0 Hz, 1H), 3.80 (s, 3H), 3.79 (s, 3H), 2.16 (m, 1H), 1.85 – 1.70 (m, 5H), 1.38 – 1.16 (m, 5H). **^{13}C NMR** (101 MHz, CDCl$_3$) δ 153.71, 150.81, 137.69, 127.98, 121.55, 112.61, 112.19, 111.61, 56.22, 55.70, 41.49, 33.00, 26.17, 26.05. **HRMS** (ESI) calcd for C$_{16}$H$_{22}$O$_2$Na [M]$^+$: 269.1512; found: 269.1529.

(E)-1-(2-cyclohexylvinyl)-2-fluorobenzene (4r): 0.5 mmol (78 mg) **3r** was employed with general procedure GP5 and 93 mg (91 % yield) **4r** was obtained as colorless oil using column chromatography (eluent: 100% cyclohexane). **^{1}H NMR** (400 MHz, CDCl$_3$) δ 7.44 (td, J = 7.7, 1.7 Hz, 1H), 7.19 – 7.11 (m, 1H), 7.10 – 6.96 (m, 2H), 6.51 (d, J = 16.2 Hz, 1H), 6.25 (dd, J = 16.1, 7.0 Hz, 1H), 2.20 – 2.12 (m, 1H), 1.87 – 1.64 (m, 5H), 1.39 –

1.13 (m, 5H). **¹³C NMR** (101 MHz, CDCl₃) δ 169.96 (d, J_{C-F} = 248.8 Hz), 139.34 (d, J_{C-F} = 4.1 Hz), 127.85 (d, J_{C-F} = 8.3 Hz), 126.84 (d, J_{C-F} = 4.1 Hz), 125.74 (d, J_{C-F} = 12.4 Hz), 123.90 (d, J_{C-F} = 3.5 Hz), 119.54 (d, J_{C-F} = 3.9 Hz), 115.55 (d, J_{C-F} = 22.3 Hz), 41.53, 32.84, 26.14, 26.00. **¹⁹F NMR** (376 MHz, CDCl₃) δ -119.08 (ddd, J = 10.9, 7.7, 5.2 Hz).

(E)-1-(2-cyclohexylvinyl)-2-methylnaphthalene (4s): 0.5 mmol (101 mg) **3s** was employed with general procedure GP5 and 114 mg (91 % yield) **4s** was obtained as colorless oil using column chromatography (eluent: 100% cyclohexane). **¹H NMR** (400 MHz, CDCl₃) δ 8.11 – 8.09 (m, 1H), 7.80 – 7.77 (m, 1H), 7.64 (d, J = 8.4 Hz, 1H), 7.45 – 7.37 (m, 2H), 7.32 (d, J = 8.4 Hz, 1H), 6.61 (d, J = 16.3 Hz, 1H), 5.79 (dd, J = 16.3, 6.9 Hz, 1H), 2.46 (s, 3H), 2.36 – 2.28 (m, 1H), 1.97 – 1.93 (m, 2H), 1.85 – 1.80 (m, 2H), 1.75– 1.70 (m, 1H), 1.45 – 1.26 (m, 5H). **¹³C NMR** (101 MHz, CDCl₃) δ 143.35, 134.53, 132.66, 132.25, 132.17, 128.81, 127.97, 126.28, 125.54, 125.35, 124.57, 123.51, 41.68, 33.12, 26.23, 26.07, 20.87. **MS (EI, 70 ev)**: *m/z* (relative intensity) = 250 (M⁺•, 82), 235 (23), 207 (18), 193 (19), 179 (54), 167 (100), 153 (40), 143 (18), 115 (6), 89 (5), 55 (4), 41 (5).

(E)-1-(2-cyclohexylvinyl)naphthalene (4t): 0.5 mmol (94 mg) **3t** was employed with general procedure GP5 and 111 mg (94 % yield) **4t** was obtained as colorless oil using column chromatography (eluent: 100% cyclohexane). **¹H NMR** (400 MHz, CDCl₃) δ 8.08 (d, J = 7.7 Hz, 1H), 7.80 – 7.77 (m, 1H), 7.68 (d, J = 8.1 Hz, 1H), 7.51 – 7.36 (m, 4H), 7.21 (s, 1H), 7.03 (d, J = 15.7 Hz, 1H), 6.15 (dd, J = 15.7, 6.9 Hz, 1H), 2.25 – 2.18 (m, 1H), 1.88 – 1.65 (m, 5H), 1.38 – 1.21 (m, 5H). **¹³C NMR** (101 MHz, CDCl₃) δ 140.21, 135.89, 133.61, 131.19, 128.43, 127.11, 125.69, 125.64, 125.56, 124.34, 123.94, 123.40, 41.53, 33.05, 26.21, 26.07.

(E)-(1-cyclohexylprop-1-en-2-yl)benzene (4u): 0.5 mmol (76 mg) **3u** was employed with general procedure GP5 and 94 mg (94 % yield) **4u** was obtained as colorless oil using column chromatography (eluent: 100% cyclohexane). **¹H NMR** (400 MHz, CDCl₃) δ 7.39 (d, J = 7.7 Hz, 2H), 7.30 (t, J = 7.6 Hz, 2H), 7.21 (t, J = 7.2 Hz, 1H), 5.64 (d, J = 8.9 Hz, 1H), 2.41 – 2.31 (m, 1H), 2.05 (d, J = 1.0 Hz, 3H), 1.77 – 1.67 (m, 5H), 1.39 – 1.12 (m, 5H). **¹³C NMR** (101 MHz, CDCl₃) δ 144.03, 134.57, 132.72, 128.08, 126.39, 125.60, 37.75, 33.06, 26.12, 26.01, 15.80.

(2-cyclohexylethene-1,1-diyl)dibenzene (4v): 0.5 mmol (107 mg) **3v** was employed with general procedure GP5 and 128 mg (98 % yield) **4v** was obtained as colorless oil using column chromatography (eluent: 100% cyclohexane). **¹H NMR** (400 MHz, CDCl₃) δ 7.35 – 7.26 (m, 3H), 7.25 – 7.14 (m, 7H), 5.87 (d, J = 10.0 Hz, 1H), 2.13 – 2.06 (m, 1H), 1.66 – 1.56 (m, 5H), 1.21 – 1.10 (m, 5H). **¹³C NMR** (101 MHz, CDCl₃) δ 142.91, 140.56, 139.57, 135.94, 129.76, 128.10, 128.00, 127.17, 126.74, 126.68, 38.29, 33.32, 25.98, 25.58.

1,4-bis((E)-2-cyclohexylvinyl)benzene (4w): 4.7 mmol (930 mg) **3w** was employed with general procedure GP5 and 1389 mg (49 % yield) **4w** was obtained as white solid using column chromatography (eluent: 100% cyclohexane). Melting point: 93.1 ºC. **¹H NMR** (400 MHz, CDCl₃) δ 7.29 (s, 4H), 6.33 (dd, J = 16.0, 1.0 Hz, 2H), 6.17 (dd, J = 16.0, 6.9 Hz, 2H), 2.14 (ddp, J = 10.2, 6.7, 3.6, 3.1 Hz, 2H), 1.88 – 1.66 (m, 10H), 1.41 – 1.28 (m, 5H), 1.26 – 1.15 (m, 5H). **¹³C NMR** (101 MHz, CDCl₃) δ 136.56, 136.28, 126.97, 126.02, 41.18, 32.97, 26.18, 26.06.

(Z)-(2-cyclohexylvinyl)benzene (4x): 0.5 mmol (69 mg) **3x** was employed with general procedure GP5 and 86 mg (cis: trans = 88:12, 93 % yield) **4x** was obtained as colorless oil using column chromatography (eluent: 100% cyclohexane). **¹H NMR** (400 MHz, CDCl₃) δ 7.37 – 7.22 (m, 5H), 6.33 (d, *J* = 11.7 Hz, 1H), 5.51 (dd, *J* = 11.6, 10.2 Hz, 1H), 2.65 – 2.56 (m, 1H), 1.82 – 1.67 (m, 5H), 1.38 – 1.27 (m, 3H), 1.22 – 1.13 (m, 2H). **¹³C NMR** (101 MHz, CDCl₃) δ 138.99, 137.95, 128.58, 128.15, 126.80, 126.39, 36.89, 33.26, 26.03, 25.67.

(E)-hept-1-en-1-ylbenzene (5a): The Grignard reagent was prepared according to GP6 starting from 0.93 mL (7.5 mmol) of 1-bromopentane in 15 mL THF (0.47 M). Titration: C = 0.37 M. Based on the concentration of the Grignard reagent, 6.5 mL THF was added to the vial of *(E)*-(2-chlorovinyl)benzene (**3a**, 2 mmol, 276 mg, 0.31 M) (C$_{Grignard\ reagent}$ = 1.2 C$_{Sub}$) with Fe(acac)₃ (7.0 mg, 1 mol%). Prepared according to general procedure GP7, the solution of the substrate was charged to a syringe pump and mixed with Grignard reagent pumped with T-mixture, the combined solution was passed through a 0.5 mL PFA (I.D. 0.75 mm) reactor at room temperature (Rt = 30 s). 165 mg (95 % yield, took 6.5 mL mixture after reaction containing 1.0 mmol *(E)*-(2-chlorovinyl)benzene for isolation) **5a** was obtained as colorless oil using column chromatography (eluent: 100% cyclohexane). **¹H NMR** (400 MHz, CDCl₃) δ 7.37 – 7.33 (m, 2H), 7.32 – 7.28 (m, 2H), 7.22 – 7.18 (m, 1H), 6.39 (d, *J* = 15.8 Hz, 1H), 6.24 (dt, *J* = 15.8, 6.8 Hz, 1H), 2.25 – 2.19 (m, 2H), 1.53 – 1.45 (m, 2H), 1.38 – 1.30 (m, 4H), 0.92 (t, *J* = 7.0 Hz, 3H). **¹³C NMR** (101 MHz, CDCl₃) δ 137.94, 131.24, 129.66, 128.44, 126.71, 125.88, 33.01, 31.44, 29.06, 22.56, 14.06.

(E)-hexa-1,5-dien-1-ylbenzene (5b): The Grignard reagent was prepared according to GP6 starting from 0.7 mL (7 mmol) of 4-bromobut-1-ene in 10 mL THF (0.65 M). Titration: C = 0.42 M. Based on the concentration of the Grignard reagent, 3 mL THF was added to the vial of *(E)*-(2-chlorovinyl)benzene (**3a**, 1 mmol, 138 mg, 0.33 M) (C$_{Grignard\ reagent}$ = 1.2 C$_{Sub}$) with Fe(acac)₃ (7.0 mg, 2 mol%). Prepared according to general procedure GP7, the solution of the substrate was charged to a syringe pump and mixed with Grignard reagent pumped with T-mixture, the combined solution was passed through a 1.5 mL PFA (I.D. 0.75 mm) reactor at room temperature (Rt = 90 s). 144 mg (91 % yield, took all mixture after reaction containing 1.0 mmol *(E)*-(2-chlorovinyl)benzene for isolation) **5b** was obtained as colorless oil using column chromatography (eluent: 100% cyclohexane). **¹H NMR** (400 MHz, CDCl₃) δ 7.37 – 7.27 (m, 4H), 7.22 – 7.17 (m, 1H), 6.41 (d, *J* = 15.9 Hz, 1H), 6.23 (dt, *J* = 15.8, 6.6 Hz, 1H), 5.87 (ddt, *J* = 16.7, 10.2, 6.4 Hz, 1H), 5.11 – 4.96 (m, 2H), 2.36 – 2.30 (m, 2H), 2.28 – 2.21 (m, 2H). **¹³C NMR** (101 MHz, CDCl₃) δ 138.09, 137.74, 130.17, 130.11, 128.46, 126.86, 125.94, 114.90, 33.54, 32.42.

hex-5-en-1-yn-1-ylbenzene (5c): The Grignard reagent was prepared according to GP7 starting from 0.7 mL (7 mmol) of 4-bromobut-1-ene in 10 mL THF (0.65 M). Titration: C = 0.42 M. Based on the concentration of the Grignard reagent, 3 mL THF was added to the vial of (chloroethynyl)benzene (**1a**, 1 mmol, 136 mg, 0.33 M) (C$_{Grignard\ reagent}$ = 1.2 C$_{Sub}$) with Fe(acac)₃ (7.0 mg, 2 mol%). Prepared according to general procedure GP7, the solution of the substrate was charged to a syringe pump and mixed with Grignard reagent pumped with T-mixture, the combined solution was passed through a 1.0 mL PFA (I.D. 0.75 mm) reactor at 0 ºC (Rt = 60 s). 145 mg (93 % yield, took all mixture after reaction containing 1.0 mmol (chloroethynyl)benzene for isolation) **5c** was obtained as colorless oil using column chromatography (eluent: 100% cyclohexane). **¹H NMR** (400 MHz,

CDCl$_3$) δ 7.43 – 7.38 (m, 2H), 7.32 – 7.24 (m, 3H), 5.94 (ddt, J = 16.9, 10.2, 6.6 Hz, 1H), 5.14 (dq, J = 17.1, 1.6 Hz, 1H), 5.07 (dd, J = 10.2, 1.6 Hz, 1H), 2.51 (t, J = 7.3 Hz, 2H), 2.40 – 2.30 (m, 2H). **^{13}C NMR** (101 MHz, CDCl$_3$) δ 136.94, 131.54, 128.16, 128.08, 127.55, 123.89, 115.68, 89.48, 81.00, 32.95, 19.26.

(cyclohexylethynyl)benzene (5d): The Grignard reagent was prepared according to GP7 starting from 0.9 mL (7.5 mmol) of chlorocyclohexane in 15 mL THF (0.47 M). Titration: C = 0.45 M. Based on the concentration of the Grignard reagent, 2.7 mL THF was added to the vial of (chloroethynyl)benzene (**1a**, 1 mmol, 136 mg, 0.37 M) (C$_{Grignard\ reagent}$ = 1.2 C$_{Sub}$) with Fe(acac)$_3$ (3.5 mg, 1 mol%). Prepared according to general procedure GP7, the solution of the substrate was charged to a syringe pump and mixed with Grignard reagent pumped with T-mixture, the combined solution was passed through a 1.0 mL PFA (I.D. 0.75 mm) reactor at 0 ºC (Rt = 60 s). 110 mg (96 % yield, took 3 mL mixture after reaction containing 0.625 mmol (chloroethynyl)benzene for isolation) **5d** was obtained as colorless oil using column chromatography (eluent: 100% cyclohexane). **^{1}H NMR** (400 MHz, CDCl$_3$) δ 7.42 – 7.39 (m, 2H), 7.31 – 7.27 (m, 3H), 2.63 – 2.57 (m, 1H), 1.91 – 1.88 (m, 2H), 1.79 – 1.74 (m, 2H), 1.59 – 1.51 (m, 3H), 1.39 –1.39 (m, 3H). **^{13}C NMR** (101 MHz, CDCl$_3$) δ 131.55, 128.12, 127.37, 124.12, 94.45, 80.48, 32.71, 29.66, 25.93, 24.91.

pent-1-yn-1-ylbenzene (5e): The Grignard reagent was prepared according to GP7 starting from 0.68 mL (7.5 mmol) of 1-bromopropane in 15 mL THF (0.48 M). Titration: C = 0.39 M. Based on the concentration of the Grignard reagent, 3.1 mL THF was added to the vial of (chloroethynyl)benzene (**1a**, 1 mmol, 136 mg, 0.32 M) (C$_{Grignard\ reagent}$ = 1.2 C$_{Sub}$) with Fe(acac)$_3$ (3.5 mg, 1 mol%). Prepared according to general procedure GP7, the solution of the substrate was charged to a syringe pump and mixed with Grignard reagent pumped with T-mixture, the combined solution was passed through a 1.0 mL PFA (I.D. 0.75 mm) reactor at 0 ºC (Rt = 60 s). 136 mg (94 % yield, took all mixture after reaction containing 1.0 mmol (chloroethynyl)benzene for isolation) **5e** was obtained as colorless oil using column chromatography (eluent: 100% cyclohexane). **^{1}H NMR** (400 MHz, CDCl$_3$) δ 7.43 – 7.38 (m, 2H), 7.30 – 7.25 (m, 3H), 2.40 (t, J = 7.0 Hz, 2H), 1.65 (h, J = 7.3 Hz, 3H), 1.06 (t, J = 7.4 Hz, 3H). **^{13}C NMR** (101 MHz, CDCl$_3$) δ 131.52, 128.15, 127.44, 124.07, 90.24, 80.68, 22.22, 21.39, 13.54.

(3-methylbut-1-yn-1-yl)benzene (5f): The Grignard reagent was prepared according to GP7 starting from 0.70 mL (7.5 mmol) of 2-bromopropane in 15 mL THF (0.48 M). Titration: C = 0.36 M. Based on the concentration of the Grignard reagent, 3.3 mL THF was added to the vial of (chloroethynyl)benzene (**1a**, 1 mmol, 136 mg, 0.30 M) (C$_{Grignard\ reagent}$ = 1.2 C$_{Sub}$) with Fe(acac)$_3$ (3.5 mg, 1 mol%). Prepared according to general procedure GP7, the solution of the substrate was charged to a syringe pump and mixed with Grignard reagent pumped with T-mixture, the combined solution was passed through a 1.0 mL PFA (I.D. 0.75 mm) reactor at 0 ºC (Rt = 60 s). 68 mg (94 % yield, took 3.3 mL mixture after reaction containing 0.5 mmol (chloroethynyl)benzene for isolation) **5f** was obtained as colorless oil using column chromatography (eluent: 100% cyclohexane). **^{1}H NMR** (400 MHz, CDCl$_3$) δ 7.42 – 7.36 (m, 2H), 7.30 – 7.26 (m, 3H), 2.78 (hept, J = 6.9 Hz, 1H), 1.28 (s, 3H), 1.26 (s, 3H). **^{13}C NMR** (101 MHz, CDCl$_3$) δ 131.52, 128.12, 127.42, 124.00, 95.75, 79.69, 23.03, 21.11.

hex-1-yn-1-ylbenzene (5g): The Grignard reagent was prepared according to GP7 starting from 0.85 mL (7.5 mmol) of 1-iodobutane in 15 mL THF (0.47 M). Titration: C = 0.46 M. Based on the concentration of the

Grignard reagent, 2.6 mL THF was added to the vial of (chloroethynyl)benzene (**1a**, 1 mmol, 136 mg, 0.37 M) ($C_{\text{Grignard reagent}}$ = 1.2 C_{Sub}) with Fe(acac)$_3$ (3.5 mg, 1 mol%). Prepared according to general procedure GP7, the solution of the substrate was charged to a syringe pump and mixed with Grignard reagent pumped with T-mixture, the combined solution was passed through a 1.0 mL PFA (I.D. 0.75 mm) reactor at 0 °C (Rt = 60 s). 155 mg (98 % yield, took all mixture after reaction containing 0.5 mmol (chloroethynyl)benzene for isolation) **5g** was obtained as colorless oil using column chromatography (eluent: 100% cyclohexane). **^{1}H NMR** (400 MHz, CDCl$_3$) δ 7.43 – 7.36 (m, 2H), 7.31 – 7.26 (m, 3H), 2.41 (t, *J* = 7.0 Hz, 2H), 1.65 – 1.56 (m, 2H), 1.52 – 1.43 (m, 2H), 0.96 (t, *J* = 7.3 Hz, 3H). **^{13}C NMR** (101 MHz, CDCl3) δ 131.51, 128.15, 127.42, 124.08, 90.40, 80.52, 30.84, 22.01, 19.09, 13.64.

(5,5,5-trifluoropent-1-yn-1-yl)benzene (5h): The Grignard reagent was prepared according to GP7 starting from 0.85 mL (7.5 mmol) of 1,1,1-trifluoro-3-iodopropane in 15 mL THF (0.47 M). Titration: C = 0.44 M. Based on the concentration of the Grignard reagent, 2.7 mL THF was added to the vial of (chloroethynyl)benzene (**1a**, 1 mmol, 136 mg, 0.37 M) ($C_{\text{Grignard reagent}}$ = 1.2 C_{Sub}) with Fe(acac)$_3$ (3.5 mg, 1 mol%). Prepared according to general procedure GP7, the solution of the substrate was charged to a syringe pump and mixed with Grignard reagent pumped with T-mixture, the combined solution was passed through a 1.0 mL PFA (I.D. 0.75 mm) reactor at 0 °C (Rt = 60 s). 96 mg (97 % yield, took 2.7 mL mixture after reaction containing 0.5 mmol (chloroethynyl)benzene for isolation) **5h** was obtained as colorless oil using column chromatography (eluent: 100% cyclohexane). **^{1}H NMR** (400 MHz, CDCl$_3$) δ 7.43 – 7.37 (m, 2H), 7.35 – 7.27 (m, 3H), 2.78 – 2.63 (m, 2H), 2.53 – 2.36 (m, 2H). **^{13}C NMR** (101 MHz, CDCl$_3$) δ 131.56, 128.26, 128.04, 123.13, 86.07, 81.64, 33.44 (q, *J* $_{C-F}$ = 29.1 Hz), 13.06 (q, *J* $_{C-F}$ = 4.2 Hz). **^{19}F NMR** (376 MHz, CDCl3) δ -66.97 (t, *J* = 10.4 Hz).

pent-1-yne-1,5-diyldibenzene (5i): The Grignard reagent was prepared according to GP7 starting from 1.1 mL (7.5 mmol) of (3-bromopropyl)benzene in 15 mL THF (0.47 M). Titration: C = 0.29 M. Based on the concentration of the Grignard reagent, 4.1 mL THF was added to the vial of (chloroethynyl)benzene (**1a**, 1 mmol, 136 mg, 0.24 M) ($C_{\text{Grignard reagent}}$ = 1.2 C_{Sub}) with Fe(acac)$_3$ (3.5 mg, 1 mol%). Prepared according to general procedure GP7, the solution of the substrate was charged to a syringe pump and mixed with Grignard reagent pumped with T-mixture, the combined solution was passed through a 1.0 mL PFA (I.D. 0.75 mm) reactor at 0 °C (Rt = 60 s). 207 mg (94 % yield, took all mixture after reaction containing 1.0 mmol (chloroethynyl)benzene for isolation) **5i** was obtained as colorless oil using column chromatography (eluent: 100% cyclohexane). **^{1}H NMR** (400 MHz, CDCl$_3$) δ 7.46 – 7.39 (m, 2H), 7.35 – 7.27 (m, 5H), 7.22 (dd, *J* = 15.4, 7.1 Hz, 3H), 2.88 – 2.74 (m, 2H), 2.44 (t, *J* = 7.0 Hz, 2H), 1.94 (p, *J* = 7.1 Hz, 2H). **^{13}C NMR** (101 MHz, CDCl$_3$) δ 141.62, 131.54, 128.55, 128.35, 128.19, 127.54, 125.88, 123.96, 89.81, 81.13, 34.83, 30.31, 18.82.

1-methyl-3-(phenylethynyl)benzene (5j): The Grignard reagent was prepared according to GP7 starting from 0.91 mL (7.5 mmol) of 1-bromo-3-methylbenzene in 15 mL THF (0.47 M). Titration: C = 0.39 M. Based on the concentration of the Grignard reagent, 3.1 mL THF was added to the vial of (chloroethynyl)benzene (**1a**, 1 mmol, 136 mg, 0.32 M) ($C_{\text{Grignard reagent}}$ = 1.2 C_{Sub}) with Fe(acac)$_3$ (3.5 mg, 1 mol%). Prepared according to general procedure GP7, the solution of the substrate was charged to a syringe pump and mixed with Grignard reagent pumped with T-mixture, the combined solution was passed through a 1.0 mL PFA (I.D. 0.75 mm) reactor at 0

189

°C (Rt = 60 s). 183 mg (95 % yield, took all mixture after reaction containing 1.0 mmol (chloroethynyl)benzene for isolation) **5j** was obtained as colorless oil using column chromatography (eluent: 100% cyclohexane). **¹H NMR** (400 MHz, CDCl₃) δ 7.56 – 7.49 (m, 2H), 7.39 – 7.31 (m, 5H), 7.27 – 7.21 (m, 1H), 7.17 – 7.12 (m, 1H), 2.36 (s, 3H). **¹³C NMR** (101 MHz, CDCl₃) δ 137.99, 132.17, 131.58, 129.14, 128.67, 128.30, 128.22, 128.15, 123.36, 123.05, 89.54, 89.01, 21.23.

1-(phenylethynyl)-3-(trifluoromethyl)benzene (5k): The Grignard reagent was prepared according to GP7 starting from 1.0 mL (7.5 mmol) of 1-bromo-3-(trifluoromethyl)benzene in 15 mL THF (0.47 M). Titration: C = 0.41 M. Based on the concentration of the Grignard reagent, 2.9 mL THF was added to the vial of (chloroethynyl)benzene (**1a**, 1 mmol, 136 mg, 0.34 M) ($C_{Grignard\ reagent}$ = 1.2 C_{Sub}) with Fe(acac)₃ (3.5 mg, 1 mol%). Prepared according to general procedure GP7, the solution of the substrate was charged to a syringe pump and mixed with Grignard reagent pumped with T-mixture, the combined solution was passed through a 1.0 mL PFA (I.D. 0.75 mm) reactor at 0 °C (Rt = 60 s). 239 mg (97 % yield, took all mixture after reaction containing 1.0 mmol (chloroethynyl)benzene for isolation) **5k** was obtained as colorless oil using column chromatography (eluent: 100% cyclohexane). **¹H NMR** (400 MHz, CDCl₃) δ 7.81 (s, 1H), 7.70 (d, J = 7.7 Hz, 1H), 7.61 – 7.53 (m, 3H), 7.48 (t, J = 7.8 Hz, 1H), 7.41 – 7.35 (m, 3H). **¹³C NMR** (101 MHz, CDCl₃) δ 134.63, 131.69, 130.81 (q, $J_{C\text{-}F}$ = 32.8 Hz), 128.85, 128.74, 128.43, 128.36 (q, $J_{C\text{-}F}$ = 3.9 Hz), 124.73 (q, $J_{C\text{-}F}$ = 3.8 Hz), 124.25, 123.9 (q, $J_{C\text{-}F}$ = 272.7 Hz), 122.59, 90.89, 87.77. **¹⁹F NMR** (376 MHz, CDCl3) δ -62.94.

References:

(1) Brown, D. G.; Boström, J. *J. Med. Chem.* **2016**, *59*, 4443-4458.

(2) Nicolaou, K. C.; Bulger, P. G.; Sarlah, D. *Angew. Chem. Int. Ed.* **2005**, *44*, 4442-4489.

(3) (a)Johansson Seechurn, C. C. C.; Kitching, M. O.; Colacot, T. J.; Snieckus, V. *Angew. Chem. Int. Ed.* **2012**, *51*, 5062-5085; (b)Choi, J.; Fu, G. C. *Science* **2017**, *356*, eaaf7230; (c)Xu, S.; Kim, E. H.; Wei, A.; Negishi, E.-i. *Sci. Technol. Adv. Mater.* **2014**, *15*, 044201.

(4) (a)Roy, D.; Uozumi, Y. *Adv. Synth. Catal.* **2018**, *360*, 602-625; (b)Biffis, A.; Centomo, P.; Del Zotto, A.; Zecca, M. *Chem. Rev.* **2018**, *118*, 2249-2295; (c)Ingoglia, B. T.; Wagen, C. C.; Buchwald, S. L. *Tetrahcdron* **2019**, https://doi.org/10.1016/j.tet.2019.05.003.

(5) Ludwig, J. R.; Schindler, C. S. *Chem* **2017**, *2*, 313-316.

(6) (a)Tasker, S. Z.; Standley, E. A.; Jamison, T. F. *Nature* **2014**, *509*, 299; (b)Cahiez, G.; Moyeux, A.; Cossy, J. *Adv. Synth. Catal.* **2015**, *357*, 1983-1989; (c)Zweig, J. E.; Kim, D. E.; Newhouse, T. R. *Chem. Rev.* **2017**, *117*, 11680-11752; (d)Gandeepan, P.; Müller, T.; Zell, D.; Cera, G.; Warratz, S.; Ackermann, L. *Chem. Rev.* **2019**, *119*, 2192-2452; (e)Beaumier, E. P.; Pearce, A. J.; See, X. Y.; Tonks, I. A. *Nat. Rev. Chem.* **2019**, *3*, 15-34; (f)Wenger, O. S. *J. Am. Chem. Soc.* **2018**, *140*, 13522-13533.

(7) (a)Bauer, I.; Knölker, H.-J. *Chem. Rev.* **2015**, *115*, 3170-3387; (b)Legros, J.; Figadère, B. *Nat. Prod. Rep.* **2015**, *32*, 1541-1555; (c)Guérinot, A.; Cossy, J. *Top. Curr. Chem.* **2016**, *374*, 49; (d)Mako, T. L.; Byers, J. A. *Inorg. Chem. Front.* **2016**, *3*, 766-790.

(8) Fürstner, A. *ACS Cent. Sci.* **2016**, *2*, 778-789.

(9) (a)Chinchilla, R.; Nájera, C. *Chem. Soc. Rev.* **2011**, *40*, 5084-5121; (b)Chinchilla, R.; Nájera, C. *Chem. Rev.* **2007**, *107*, 874-922; (c)Sonogashira, K. *J. Organomet. Chem.* **2002**, *653*, 46-49.

(10) Cahiez, G.; Gager, O.; Buendia, J. *Angew. Chem. Int. Ed.* **2010**, *49*, 1278-1281.

(11) Hatakeyama, T.; Okada, Y.; Yoshimoto, Y.; Nakamura, M. *Angew. Chem. Int. Ed.* **2011**, *50*, 10973-10976.

(12) Cheung, C. W.; Ren, P.; Hu, X. *Org. Lett.* **2014**, *16*, 2566-2569.

(13) Kneebone, J. L.; Brennessel, W. W.; Neidig, M. L. *J. Am. Chem. Soc.* **2017**, *139*, 6988-7003.

(14) Wei, X.-J.; Abdiaj, I.; Sambiagio, C.; Li, C.; Zysman-Colman, E.; Alcazar, J.; Noel, T. *Angew. Chem. Int. Ed.*, **2019**, DOI: 10.1002/anie.201906462.

(15) Castagnolo, D.; Botta, M. *Eur. J. Org. Chem.* **2010**, *2010*, 4732-4732.

(16) (a)Gutmann, B.; Kappe, C. O. *J. Flow Chem.* **2017**, *7*, 65-71; (b)Kockmann, N.; Thenée, P.; Fleischer-Trebes, C.; Laudadio, G.; Noël, T. *React. Chem. Eng* **2017**, *2*, 258-280; (c)Gutmann, B.; Cantillo, D.; Kappe, C. O. *Angew. Chem. Int. Ed.* **2015**, *54*, 6688-6728.

(17) (a)Pieber, B.; Gilmore, K.; Seeberger, P. H. *J. Flow Chem.* **2017**, *7*, 129-136; (b)Hessel, V.; Kralisch, D.; Kockmann, N.; Noël, T.; Wang, Q. *ChemSusChem* **2013**, *6*, 746-789; (c)Webb, D.; Jamison, T. F. *Chem. Sci.* **2010**, *1*, 675-680.

(18) Huck, L.; de la Hoz, A.; Díaz-Ortiz, A.; Alcázar, J. *Org. Lett.* **2017**, *19*, 3747-3750.

(19) (a)Noël, T.; Buchwald, S. L. *Chem. Soc. Rev.* **2011**, *40*, 5010-5029; (b)Cantillo, D.; Kappe, C. O. *ChemCatChem* **2014**, *6*, 3286-3305.

(20) Noël, T.; Su, Y.; Hessel, V. *Top. Organomet. Chem.* **2016**, *57*, 1-41.

Chapter 7

Summary

In this thesis, the development of new methodologies in continuous flow using visible light photocatalysis were presented, including the use of a traditional iridium catalyst, an olefin-disulfide charge-transfer complex and earth-abundant metal iron catalysis.

In **Chapter 2**, a simple yet effective photocatalytic stereoselective decarboxylative protocol to prepare difluoromethylated styrenes and phenylacetylenes was presented. In contrast to previously described methods, this procedure does not require additional metal catalysts or hypervalent iodine reagents to facilitate CO_2 extrusion. The generality of this protocol is demonstrated by the broad substrate scope. *Meta* and *para-* substituted cinnamic acids provide the expected *E*-isomer. In contrast, *ortho*-substituted cinnamic acids yield selectively less stable *Z*-product, whereas the *E*-isomer can be obtained via continuous-flow processing through accurate control of the reaction time. The different stereoselectivity of *ortho*-substituted cinnamic acids can be attributed to the high triplet energy of the catalyst. In batch, with prolonged visible light irradiation (14 hours), the *E*-isomer can be obtained in high selectivity. In flow, within 15 minutes residence time, the *E*-isomer can be obtained selectively. This phenomenon was due to the energy transfer of *fac*-Ir(ppy)$_3$, as the triplet energy of the catalyst is higher than the *E*-isomer of the product. In batch, the catalyst had sufficient time to convert the resulting *E*-isomer into the *Z* configuration, while in flow, the *E*-isomer is the only isomer formed due to the short reaction time. In this case, continuous-flow technology has proven to be powerful not only in improving the reaction efficiency, but also tuning the stereoselectivity.

In **Chapter 3**, the development of a novel photocatalytic 1, 2-heterocycle migration method was presented. This protocol allows the preparation of heterocycles with a *sp^3*-enriched character. A variety of synthetically useful *β*-difluorinated *α*-aryl heterocyclic ketones can be easily prepared under mild reaction conditions with excellent regioselectivity. The application of continuous flow allows to reduce the reaction time (from 6 hours to 10 minutes), provides higher reaction selectivity and displays potential for scaling the chemistry. Interesting also the allylic alcohol substrates were prepared in flow via a classical Grignard reaction. The flow method enables safe handling of the reaction exotherm and allows to prepare sufficient quantities of starting material for the consecutive migration chemistry.

With the successful implemention of a difluoromethylated group into organic molecules with photocatalyst *fac*-Ir(ppy)$_3$, we turned our attention to other organic complexes that can absorb light, which is more cost efficient. The olefin-disulfide charge-transfer complex was developed for the aerobic oxidative cleavage the C=C bond under visible-light at room temperature, this project was presented in **Chapter 4**. Bis(4-methoxyphenyl) disulfide was employed and typical monosubstituted as well as 1,1- and 1,2-disubstituted aromatic alkenes could be converted to corresponding aldehydes and ketones. Interestingly, the mechanistic study using NMR and DFT calculations shows that the

coordinating effect between thiols and olefins might also exist between certain disulfides and olefins. The unconventional homolysis of the aromatic S–S bond by visible-light was rationalized by the olefin-disulfide charge-transfer complex.

Next, the cost-efficient earth abundant transition metal iron was successfully employed in visible light photocatalytic process, which is presented in **Chapter 5**. The visible light promoted iron catalyzed continuous-flow protocol was designed to overcome the limitations of Kumada-Corriu cross-couplings. The use of blue light was demonstrated to considerably accelerate the coupling reaction, and allowed the use of mild conditions at very short reaction times even for previously very stubborn substrates, which makes it a competitive alternative to the commonly used Pd or Ni catalysts for this transformation. Under visible light irradiation, unreactive aryl chlorides including electron-rich aryl chlorides and unreactive heterocycles including pyridine and benzofuran, can be coupled with alkylmagnesium compounds successfully. Moreover, the scale up of the reaction was conducted on an unprotected indole: within 2.5 hours, 11.4 grams of product could be obtained in 95% isolated yield. Preliminary mechanistic studies were done including inline UV analysis and DFT calculation. The intramolecular radical clock reaction indicated both cross coupling and radical process could be involved in this process. Light on/off reaction shos light is needed in the entire catalytic process. Inline UV-VIS analysis and DFT calculations suggested an Fe(I)/Fe(III) catalytic cycle. The precatalyst Fe(acac)$_3$ is first reduced by Grignard reagent to produce the Fe(I) intermediate, following a classical cross coupling cycle with the oxidative addition of the aryl chloride forming the Fe(III) species, then transmetalation and reductive elimination to regenerate the Fe(I) species and to yield to targeted product.

During those investigation, we also found that iron catalysis can be useful in the coupling of α, β-unsaturated aromatic chlorides with Grignard reagents, which is presented in **Chapter 6**. The aromatic alkyne chlorides and aromatic vinyl chlorides proved to be reactive within this reaction system: a variety of internal alkynes and alkenes were prepared with this practical and efficient method, providing a procedure that was never realized before. The chemistry could also be translated to flow. The telescoped process was developed which combines both Grignard reagent synthesis and the Fe-based cross coupling reaction, in this proess the use of NHC ligand can be avoided for the Csp-Csp^3 coupling without compromising the reaction selectiviy. The chemistry displayed a broad substrate scope (> 35 examples) and scale up experiments show the potential for applications in both medicinal chemistry as synthetic organic chemistry in general.

List of abbreviations

2-MeTHF	2-Methyltetrahydrofuran
Ac	Acetyl
AIBN	Azobisisobutyronitrile
BHT	2,6-Di-*tert*-butyl-4-methylphenol
Bn	Benzyl
Bu$_3$SnH	Tributylammonium iodide
Cy	Cyclohexyl
DABCO	1,4-Diazabicyclo[2.2.2]octane
DBU	1,8-Diazabicyclo[5.4.0]undec-7-ene
EPR	Electron paramagnetic resonance
ESI-MS	Electrospray ionization mass spectrometry
Et$_3$N	Triethylamine
fac-Ir(ppy)$_3$	Tris[2-phenylpyridinato-C2,N]iridium(III)
Fe(acac)$_3$	Tris(acetylacetonato) iron(III)
FDA	Food and drug administration
GC-FID	Gas Chromatography with flame-ionization detection
GC-MS	Gas chromatography–mass spectrometry
HOMO	Highest occupied molecule orbital
HRMS	High-resolution mass spectrometry
*i*Pr$_2$NEt	*N*, *N*-Diisopropylethylamine
ID	Internal diameter
IR	Infrared
ISC	Inter system crossing

LED	Light emitting diode
LOMO	Lowest unoccupied molecular orbital
MCD	Magnetic circular dichroism
m-CPBA	*meta*-Chloroperoxybenzoic acid
MeCN	Acetonitrile
MLCT	Metal to ligand charge transfer
NEt$_3$	Triethylamine
N.D.	Not detected
NHPI	*N*-Hydroxyphthalimide
NMP	*N*-Methyl-2-pyrrolidone
NMR	Nuclear magnetic resonance
OTf	Trifluoromethanesulfonate
PC	photocatalyst
PFA	Perfluoroalkoxy alkanes
R.T.	Residence time
Ru(bpy)$_3$Cl$_2$	Tris(bipyridine)ruthenium(II)chloride
SI	Supporting Information
TEMPO	2,2,6,6-Tetramethyl-1-piperidinyloxy
THF	Tetrahydrofuran
TLC	Thin layer chromatography
UV	Ultraviolet

Publication List

Yuchao Deng†, **<u>Xiao-Jing Wei</u>**†, Xiao Wang, Yuhan Sun and Timothy Noël, Iron-Catalyzed Cross-Coupling of Alkynyl and Styrenyl Chlorides with Alkyl Grignard Reagents in Batch and Flow. *Submitted*, **2019** (†Equal contribution).

<u>Xiao-Jing Wei</u>, Irini Abdiaj, Carlo Sambiagio, Chenfei Li, Eli Zysman-Colman, Jesus Alcázar and Timothy Noël, Visible-Light-Promoted Iron-Catalyzed Csp^2-Csp^3 Kumada Cross-Coupling in Flow. *Angew. Chem. Int. Ed.* **2019**, 58, 13030-13034.

<u>Xiao-Jing Wei</u>, and Timothy Noël, Visible-light Photocatalytic Difluoroalkylation-induced 1, 2-Heteroarene Migration of Allylic Alcohols in Batch and Flow. *J. Org. Chem.* **2018**, *83*, 11377–11384.

<u>Xiao-Jing Wei</u>, Wout Boon, Volker Hessel and Timothy Noël, Visible-light Photocatalytic Decarboxylation of *α*, *β*-Unsaturated Carboxylic Acids: Facile Access to Stereoselective Difluoromethylated Styrene in Batch and Flow. *ACS Catal*. **2017**, *7*, 7136–7140.

Yuchao Deng, **<u>Xiao-Jing Wei</u>**, Hui Wang, Yuhan Sun, Timothy Noël and Xiao Wang, Disulfide-Catalyzed Visible-Light-Mediated Oxidative Cleavage of C= C Bonds and Evidence of an Olefin–Disulfide Charge-Transfer Complex. *Angew. Chem. Int. Ed.* **2017**, *56*, 832-836.

Out of the thesis:

Cecilia Bottecchia†, **<u>Xiao-Jing Wei</u>**†, Koen Kuijpers, Volker Hessel, Timothy Noël, Visible light-induced Trifluoromethylation and Perfluoroalkylation of Cysteine Residues in Batch and Continuous Flow. *J. Org. Chem.* **2016**, *81*, 7301-7307 († Equal contribution).

<u>Xiao-Jing Wei</u>, Lin Wang, Shao-Fu Du and Qiang Liu, Visible-Light Photoredox Intramolecular Difluoroacetamidation: Facile Synthesis of 3, 3-Difluoro-2-Oxindoles from Bromodifluoroacetamides. *Org. Biomol. Chem.* **2016**, *14*, 2195-2199.

<u>Xiao-Jing Wei</u>, Lin Wang, Wen-Liang Jia, Shao-Fu Du, Li-Zhu Wu and Qiang Liu, Metal-Free-Mediated Oxidation Aromatization of 1,4-Dihydropyridines to Pyridines Using Visible Light and Air, *Chin. J. Chem.* **2014**, 1245-1250.

<u>Xiao-Jing Wei</u>, Deng-Tao Yang, Lin Wang, Tao Song, Li-Zhu Wu and Qiang Liu, A Novel Intermolecular Synthesis of γ-Lactones via Visible Light Photoredox Catalysis, *Org. Lett.* **2013**, *15*, 6054-6057.

Lin Wang, **<u>Xiao-Jing Wei</u>**, Wen-Liang Jia, Jian-Ji Zhong, Li-Zhu Wu and Qiang Liu, Visible-Light-Driven Difluoroacetamidation of Unactive Arene and Heteroarenes by Direct C−H Functionalization at Room Temperature, *Org. Lett.* **2014**, *16*, 5842-5845.

Lin Wang, Zhi-Gang Ma, **Xiao-Jing Wei**, Qing-Yuan Meng, Deng-Tao Yang, Shao-Fu Du, Zi-Fei Chen and Qiang Liu, Synthesis of 2-subsituted Pyrimidines and Benzoxazoles via a Visible-light-driven Organocatalytic Aerobic Oxidation: Enhancement of Reaction Rate and Selectivity by a Base, *Green Chem.* **2014**, *16*, 3752-3757.

Lin Wang, **Xiao-Jing Wei**, Wen-Long Lei, Han Chen, Li-Zhu Wu and Qiang Liu, Direct C−H Difluoromethylenephosphonation of Arenes and Heteroarenes with Bromodifluoromethyl phosphonate via Visible-Light Photocatalysis, *Chem. Commun.* **2014**, *50*, 15916-15919.

Qiang Liu, Lin Wang, **Xiao-Jing Wei**, Yan-Fei Gu, Song-Po Guo, Method for Synthesis of 4-(4-Fluorophenyl)-6-isopropyl-2-thiopyrimidine-5-formate, *China Patents* **2014**, CN 201410190730.2.

Conference participations

Oral

Xiao-Jing Wei, Timothy Noël, 'Difluoromethylation via Photochemistry in Continuous-Flow' *Photo4Future winter school,* 12-13th November **2018**, Eindhoven, Netherlands

Xiao-Jing Wei, Timothy Noël, 'Visible-light photocatalytic difluoroalkylation induced 1, 2-heteroarene migration of allylic alcohols in batch and flow' *Photo4Future winter school,* 11-14th December **2017**, Toledo, Spain

Xiao-Jing Wei, Timothy Noël, 'Visible-light photocatalytic decarboxylation of α, β-unsaturated carboxylic acids', *Photo4Future summer school,* 12-15th Jun **2017**, Bordeaux, France

Xiao-Jing Wei, Timothy Noël, 'Disulfide- Catalyzed Visible- Light- Mediated Oxidative Cleavage of C=C Bonds' *Photo4Future winter school,* 8-11th November **2016**, Cordoba, Spain

Xiao-Jing Wei, Timothy Noël, 'Visible light-induced trifluoromethylation and perfluoroalkylation of cysteine residues in batch and continuous flow', *Photo4Future summer school,* 6-9th Jun **2016**, Leuven, Belgium

Xiao-Jing Wei, Timothy Noël, 'Photocatalytic perfluoroalkylation of biomolerclues' *Photo4Future winter school,* 7-10th December **2015**, Leipzig, Germany

Xiao-Jing Wei, Timothy Noël, 'Photocatalytic fluorination of indole in continuous-flow'*, Photo4Future Summer School*, 8-11th September **2015**, Eindhoven, Netherlands

Poster

Xiao-Jing Wei, Timothy Noël, Visible-light photocatalytic decarboxylation of α, β-unsaturated carboxylic acids, *Flow Chemistry Europe* 7-8th February **2018**, Cambridge, UK.

Acknowledgements

Firstly, I would like to express my sincere gratitude to my promotor, Prof. Timothy Noël, for providing me the precious opportunity to pursue my ph.D. research under his supervision. Appreciation goes for him for his constant support, encouragement and motivations during the past four years. He taught me the value of flow chemistry and gave me the freedom to discover more in this field. He was always accessible and quick to respond to my questions throughtout my doctoral studies, his solid knowledge and passion on chemistry always inspired me a lot. His guidance helped me in all the time of research, not only in chemistry. Moreover, he is willing to give suggestions on how to face the frustrations in my life. He is my supervisor, also my trustworthy friend I will always think of when I need advice.

I also want to thank my supervisor in Johnson & Johnson Pharmaceuticals, Dr. Jesús Alcázar. During my secondment in Toledo (Spain), I got the hornor to work in a true Med Chem Lab. I am so impressed with your extensive knowledge and experience in medicinal chemistry, I learned a lot from our fruitful discussions and the lab training in your smart but warm team. I will thank Irini for the great help and company during my stay in Toledo.

I would like also thank the funding from the European Union, as part of the Marie Skłodowska-Curie Innovative Training Network (ITN) Photo4future (Grant No. 641861). Within this generous financial support, we are able to finsh my phD project and have chance to travel to different universities, insititutes and share our research results at the winter and summer schools with all the members from Photo4future network. The training programmes we received always let me understand more about the world and gave me a lot of courage for the future. I will also thank all the photo4future members for all the nice and happy time we have been together. The encounters provided me with a greater undersdanding in the different European clutures.

It has been more than 4 years since the first time I came to the Netherland, great thanks to our awesome team: Noel Research Group. Thank you so much for helping me adapt to the European culture in the

beginning, thank you for the fruitful discussions about projects and help in sloving a lot of setup and experiment issues in the lab. Without all your support and help, the work described in the thesis will not be possible. I will always remember all the happy times we have spent together.

It is my great privilege to be a member in the Micro Flow Chemistry & Synthetic Methodology group, and I would like to thank all the awesome collegues for the friendly and open environment. A special appreaction goes to our disguished stuff members, thank you so much for the assistance from which we can work with high efficiency. I would like to express my gratitude to all the people in SPE group.

I am grateful to all my friends in Netherlands, we have shared a lot of unforgettable moments at weekends and Chinese fesivals together, thank you so much for all the help, company and suggestions.

I will express my deep gratitude to my family, especially my parents and sister for the unconditional love and support during the past years, I feel so lucky to have you all being my families. Finally, I will thank my husband Lin. Thank you so much for always being around, always being patient and always give me inspiration for the future.

Xiaojing

20-09-2019

About the author

Xiao-Jing Wei was born in 1989 in Henan province in China. She studied photochemistry at the State Key Laboratory of Applied Organic Chemistry at Lanzhou University (China), where she obtained her M.Sc. degree in 2015. Her M.Sc. dissertation focused on the topic of photochemistry under the supervision of prof. Qiang Liu. Afterwards, she started Ph.D. study in the Micro Flow Chemistry and Synthetic Methodology group under the supervision of dr. Timothy Noël at the Eindhoven University of Technology. Her Ph.D. research focuses on the photocatalytic difluoromethylation and light induced iron cross-coupling in continuous flow. Her research was funded by the European Union as part of the MSCA Innovative Training Network (ITN) Photo4Future. The results of the studies are presented in this dissertation.